INSTITUTE OF SEISMOLOGY
UNIVERSITY OF HELSINKI

REPORT S-72

LITHOSPHERE 2022

TWELFTH SYMPOSIUM ON THE STRUCTURE, COMPOSITION AND EVOLUTION OF THE LITHOSPHERE

Åbo Akademi University, Turku, Finland
November 15-17, 2022

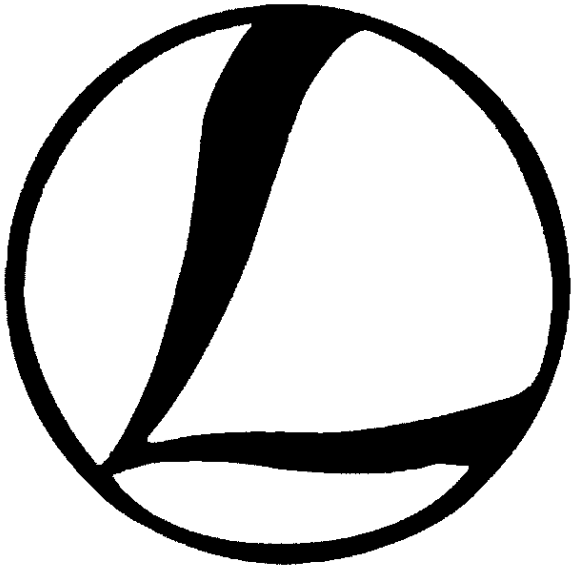

PROGRAMME AND EXTENDED ABSTRACTS

edited by

Pietari Skyttä, Kaisa Nikkilä, Esa Heilimo, Ilmo Kukkonen, Toni Veikkolainen, Fredrik Karell, Elena Kozlovskaya, Arto Luttinen, Vesa Nykänen, Markku Poutanen, Eija Tanskanen and Timo Tiira

---

Turku 2022

INSTITUTE OF SEISMOLOGY
UNIVERSITY OF HELSINKI
REPORT S-72

LITHOSPHERE 2022

TWELFTH SYMPOSIUM ON THE STRUCTURE, COMPOSITION AND EVOLUTION OF THE LITHOSPHERE

PROGRAMME AND EXTENDED ABSTRACTS

Edited by

Pietari Skyttä, Kaisa Nikkilä, Esa Heilimo, Ilmo Kukkonen, Toni Veikkolainen, Fredrik Karell, Elena Kozlovskaya, Arto Luttinen, Vesa Nykänen, Markku Poutanen, Eija Tanskanen and Timo Tiira

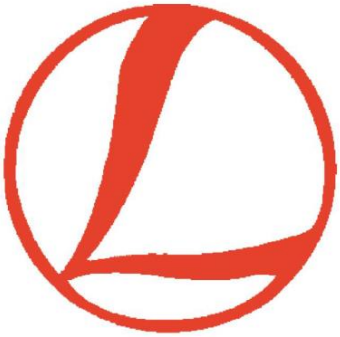

Åbo Akademi University, Turku Finland
November 15 – 17, 2022

Series Editor-in-Chief: Timo Tiira

Guest Editors: Pietari Skyttä, Kaisa Nikkilä, Esa Heilimo, Ilmo Kukkonen, Toni Veikkolainen, Fredrik Karell, Elena Kozlovskaya, Arto Luttinen, Vesa Nykänen, Markku Poutanen and Eija Tanskanen

Publisher: Institute of Seismology
P.O. Box 68
FI-00014 University of Helsinki
Finland
Phone: +358-294-1911 (switchboard)
Email: seismo@helsinki.fi
https://www.seismo.helsinki.fi

ISSN 0357-3060
ISBN 978-952-10-9610-5 (Paperback)
Grano Print
Turku 2022
ISBN 978-952-10-9611-2 (PDF)

LITHOSPHERE 2022

TWELFTH SYMPOSIUM ON THE STRUCTURE, COMPOSITION AND EVOLUTION OF THE LITHOSPHERE

PROGRAMME AND EXTENDED ABSTRACTS

Åbo Akademi University, Turku, Finland
November 15 – 17, 2022

CONTRIBUTING ORGANIZATIONS

Finnish National Committee of the International Lithosphere Programme (ILP)
University of Turku
Åbo Akademi University
Geological Survey of Finland (GTK)
National Land Survey of Finland, Finnish Geospatial Research Institute (FGI)
University of Oulu
University of Helsinki

ORGANIZING COMMITTEE AND EDITORS

Pietari Skyttä	University of Turku (pimisk@utu.fi)
Kaisa Nikkilä	Åbo Akademi University (kaisa.nikkila@abo.fi)
Esa Heilimo	University of Turku (esa.heilimo@utu.fi)
Ilmo Kukkonen	University of Helsinki (ilmo.kukkonen@helsinki.fi)
Toni Veikkolainen	University of Helsinki (toni.veikkolainen@helsinki.fi)
Fredrik Karell	Geological Survey of Finland (fredrik.karell@gtk.fi)
Elena Kozlovskaya	University of Oulu (elena.kozlovskaya@oulu.fi)
Arto Luttinen	University of Helsinki (arto.luttinen@helsinki.fi)
Vesa Nykänen	Geological Survey of Finland (vesa.nykanen@gtk.fi)
Markku Poutanen	Finnish Geospatial Research Institute FGI (markku.poutanen@nls.fi)
Eija Tanskanen	University of Oulu (eija.tanskanen@oulu.fi)
Timo Tiira	University of Helsinki (timo.tiira@helsinki.fi)

References of Lithosphere Symposia Publications

Pesonen, L.J., Korja, A. and Hjelt, S.-E., 2000 (Eds.). Lithosphere 2000 - A Symposium on the Structure, Composition and Evolution of the Lithosphere in Finland. Programme and Extended Abstracts, Espoo, Finland, October 4-5, 2000. Institute of Seismology, University of Helsinki, Report S-41, 192 pages.

Lahtinen, R., Korja, A., Arhe, K., Eklund, O., Hjelt, S.-E. and Pesonen, L.J., 2002 (Eds.). Lithosphere 2002 – Second Symposium on the Structure, Composition and Evolution of the Lithosphere in Finland. Programme and Extended Abstracts, Espoo, Finland, November 12-13, 2002. Institute of Seismology, University of Helsinki, Report S-42, 146 pages.

Ehlers, C., Korja A., Kruuna, A., Lahtinen, R. and Pesonen, L.J., 2004 (Eds.). Lithosphere 2004 – Third Symposium on the Structure, Composition and Evolution of the Lithosphere in Finland. Programme and Extended Abstracts, November 10-11, 2004, Turku, Finland. Institute of Seismology, University of Helsinki, Report S-45, 131 pages.

Kukkonen, I.T., Eklund, O., Korja, A., Korja, T., Pesonen, L.J. and Poutanen, M., 2006 (Eds.). Lithosphere 2006 – Fourth Symposium on the Structure, Composition and Evolution of the Lithosphere in Finland. Programme and Extended Abstracts, Espoo, Finland, November 9-10, 2006. Institute of Seismology, University of Helsinki, Report S-46, 233 pages.

Korja, T., Arhe, K., Kaikkonen, P., Korja, A., Lahtinen, R. and Lunkka, J.P., 2008 (Eds.). Lithosphere 2008 – Fifth Symposium on the Structure, Composition and Evolution of the Lithosphere in Finland. Programme and Extended Abstracts, Oulu, Finland, November 5-6, 2008. Institute of Seismology, University of Helsinki, Report S-53, 132 pages.

Heikkinen, P., Arhe, K., Korja, T., Lahtinen, R., Pesonen, L.J. and Rämö, T., 2010 (Eds.). Lithosphere 2010 – Sixth Symposium on the Structure, Composition and Evolution of the Lithosphere in Finland. Programme and Extended Abstracts, Helsinki, Finland, October 27-28, 2010. Institute of Seismology, University of Helsinki, Report S-55, 154 pages.

Kukkonen, I.T., Kosonen, E., Oinonen, K., Eklund, O., Korja, A., Korja, T., Lahtinen, R., Lunkka, J.P. and Poutanen, M., 2012 (Eds.). Lithosphere 2012 – Seventh Symposium on the Structure, Composition and Evolution of the Lithosphere in Finland. Programme and Extended Abstracts, Espoo, Finland, November 6-8, 2012. Institute of Seismology, University of Helsinki, University of Helsinki, S-56, 116 pages.

Eklund, O., Kukkonen, I.T., Skyttä, P., Sonck-Koota, P., Väisänen, M. and Whipp, D., 2014 (Eds.). Lithosphere 2014 – Eighth Symposium on the Structure, Composition and Evolution of the Lithosphere in Finland. Programme and Extended Abstracts, Turku, Finland, November 4-6, 2014. Institute of Seismology, University of Helsinki, S-62, 126 pages.

Kukkonen, I.T., Heinonen, S., Oinonen, K., Arhe, K., Eklund, O., Karell, F., Kozlovskaya, E., Luttinen, A., Lahtinen, R., Lunkka, J., Nykänen, V., Poutanen, M., Tanskanen, E. and Tiira T. (Eds.), 2016. Lithosphere 2016 – Ninth Symposium on the Structure, Composition and Evolution of the Lithosphere in Finland. Programme and Extended Abstracts, Espoo, Finland, November 9-11, 2016. Institute of Seismology, University of Helsinki, Report S-65, 156 pages.

Kukkonen, I.T., Heinonen, S., Silvennoinen, H., Karell, Kozlovskaya, E., Luttinen, A., Nikkilä, K., Nykänen, V., Poutanen, M., Skyttä, P., Tanskanen, E., Tiira, T. and Oinonen, K. (Eds.), 2018. Lithosphere 2018 – Tenth Symposium on the Structure, Composition and Evolution of the Lithosphere. Programme and Extended Abstracts, Oulu, Finland, November 14-16, 2018. Institute of Seismology, University of Helsinki, Report S-67, 134 pages.

Kukkonen, I.T., Veikkolainen, T., Heinonen, S., Karell, F., Kozlovskaya, E., Luttinen, A., Nikkilä, K., Nykänen, V., Poutanen, M., Skyttä, P., Tanskanen, E. and Tiira, T. (Eds.), 2021. Lithosphere 2021 – Eleventh Symposium on the Structure, Composition and Evolution of the Lithosphere in Finland. Programme and Extended Abstracts, January 19-20, 2021. Institute of Seismology, University of Helsinki, Report S-71, 164 pages (pdf).

Skyttä, P., Nikkilä, K., Heilimo, E., Kukkonen, I.T., Veikkolainen, T., Karell, F., Kozlovskaya, E., Luttinen, A., Nykänen, V., Poutanen, M., Tanskanen, E., and Tiira, T. (Eds.), 2022. Lithosphere 2022 – Twelfth Symposium on the Structure, Composition and Evolution of the Lithosphere. Programme

and Extended Abstracts, November 15-17, 2022. Institute of Seismology, University of Helsinki, Report S-72, 200 pages.

Keywords (GeoRef Thesaurus, AGI): lithosphere, crust, upper mantle, Fennoscandia, Finland, Precambrian, Baltic Shield, symposia

TABLE OF CONTENTS

PREFACE

The Finnish National committee of the International Lithosphere Programme (ILP) is responsible for organizing the biannual LITHOSPHERE symposium, which provides a forum for lithosphere researchers to present results and reviews as well as to inspire interdisciplinary discussions.

The twelfth symposium - LITHOSPHERE 2022 - comprises 56 presentations. The extended abstracts (in this volume) provide a good overview on current research focusing on the structure and processes of solid Earth.

The three-day symposium is hosted by the Abo Akademi University, with contributions from the University of Turku, and it will take place in the Armfelt Auditorium, Åbo Akademi University, Turku in November 15-17, 2022.

The participants will present their results in oral and poster sessions. Posters prepared by graduate and postgraduate students will be evaluated and the best one will be awarded. The keynote talk is given by Prof. Atle Rotevatn, University of Bergen, Norway.

This special volume “LITHOSPHERE 2022” contains the programme and extended abstracts of the symposium in alphabetical order.

Turku, October 28, 2022

Pietari Skyttä, Kaisa Nikkilä, Esa Heilimo, Ilmo Kukkonen, Toni Veikkolainen, Fredrik Karell, Elena Kozlovskaya, Arto Luttinen, Vesa Nykänen, Markku Poutanen, Eija Tanskanen and Timo Tiira

Lithosphere 2022 Organizing Committee

LITHOSPHERE 2022 Symposium
Programme

Tuesday, Nov 15

09:00 - 10:00 Registration and hanging up posters at the entrance hall of Arken, Åbo Akademi University

10:00 - 10:15 Opening and greetings

10:00 - 10:05 **Pietari Skyttä**, Dept. Geography and Geology, University of Turku
10:05 - 10:10 **Patrik Henelius**, Dean of the Faculty of Science and Engineering, Åbo Akademi
10:10 - 10:15 **Hans Thybo**, President of the International Lithosphere Program (ILP)

10:15 - 12:05 Session 1: Lithosphere structure and evolution from upper crust to asthenosphere
Chair: Pietari Skyttä

10:15 - 10:50 **M. Malinowski, S. Mazur and M. Mężyk [Invited]**
Exploring East European Craton crust in Poland using state-of-the-art deep reflection seismic profiling
10:50 - 11:15 **M. Cyz, M. Malinowski, T. Linqvist, E. Virta, S. Heinonen, T. Arola, J.Riissanen, S. Mustonen, J. Hietava and P. Skyttä**
Seismic recognition of the faults for geothermal exploration in crystalline rocks: results from the pilot survey in Helsinki
11:15 - 11:40 **J.D. Solano-Acosta, A. Soesoo and R. Hints**
New insights of the crustal structure across Estonia using satellite potential fields derived from WGM-2012 gravity data and EMAG2v3 magnetic data
11:40 - 12.05 **M. Nousiainen, S. Heinonen and T. Karinen**
Petrophysics of the Koillismaa drill hole

12:05 - 13:00 Lunch

13:00 - 15:10 Session 2: Earth Resources and sustainability
Chair: Esa Heilimo

13:00 - 13:25 **A. Soesoo**
Critical Earth Resources: an Estonian Contribution
13:25 - 13:50 **A. Bischoff, J. Kuva, M. J. Heap, E. Jolis, T. Reuschlé, J. Engström, J. Salminen and T. Karinen**
Chasing Deep Geothermal Resources in Crystalline Cratons
13:50 - 14:15 **K. Piipponen and A. Martinkauppi**
A thermogeological analysis of medium-deep borehole heat exchangers in low-enthalpy crystalline rocks

14:15 - 14:45 Coffee/Tea

14:45 - 15:10 **P. Eilu**
Critical mineral raw material potential in the Nordic countries

15:10 - 16:50 Session 3: Lithosphere evolution and structures
Chair: Fredrik Karell

15:10 - 15:35 **A. Amer**
Offshore Cyrenaica New Bathymetry Using World War II Data, Implications on the Central Mediterranean Plate Boundaries

15:35 - 16:00 **J. Kohonen, J. Jäsberg, J. Laitala and J. Luukas**
Basement tectonics along the margins of the Jormua-Outokumpu suture zone

16:00 - 16:25 **J. Engström, N. Ovaskainen, M. Markovaara-Koivisto and N. Nordbäck**
Integrated lineament interpretation

16:25 - 16:50 **N. Ovaskainen, N. Nordbäck and P. Skyttä**
Brittle structural characterization of the Åland rapakivi

17:00 - 20:00 Session 4: Posters and networking with refreshments (Ice breaker), including short posters introductions
Chair: Esa Heilimo

POSTERS

P01. K. Ahlqvist, N. Anttila, P. Skyttä and A. Ojala
3D bedrock topography model of City of Turku using geotechnical soundings

P02. K. Cutts, P. Hölttä and R. Lahtinen
Paleoproterozoic metamorphism of Peräpohja and Kuusamo Belts: a combined U-Pb monazite, apatite and garnet study

P03. T. Gråsten, E. Heilimo and T. Halkoaho
Nickel remobilisation in Sika-aho, Kuhmo greenstone belt

P04. P. Haapanala, A. Korja and FIN-EPOS community
Solid Earth Science RI collaboration in Finland

P05. M. Holma, J. Korteniemi, G. Casini, E. Saura, F. Šumanovac, J. Kapuralić and F. Tornos
Agile Exploration and Geo-modelling for European Critical Raw Materials – Introduction to the AGEMERA project

P06. H. Höytiä, P. Peltonen, P. Lamberg and T. Halkoaho
Lithogeochemical approach to constrain Ni-Cu-PGE fertility of Paleoproterozoic ultramafic rocks in Northern Fennoscandia

P07. S.R. Islam, E. Heilimo and K. Cutts
Determining the age and metamorphic evolution of the Pyhäsalmi region, Central Finland: relationship between metamorphism, ore genesis and evolution

P08. P. Jänkävaara, J. Konnuaho and E. Heilimo
Petrographic and micro-XRF studies of Co-Cu mineralized Tanhua mafic intrusion

P09. N. Junno, L. Fülöp, K. Oinonen, P. Mäntyniemi, A. Korja and SEISMIC RISK working group
SEISMIC RISK – Mitigation of induced seismic risk in urban environment

P010. J. Kara, M. Väisänen and H. O'Brien
Zircon U-Pb age of the Haveri basalt and felsic dyke

P011. T. Kauti, P. Skyttä and E. Heilimo
Structural evolution of the Archaean Siilinjärvi carbonatite complex

P012. L. Kotomaa, M. Väisänen, E. Mäkilä, H. O'Brien and P. Kokko
Lieksa-4: a P-rich iron meteorite from Lieksa

P013. V. Laakso, S. Heinonen, E. Koskela and M. Malinowski
Reflection seismic profiling in the Kevitsa Ni-Cu-PGE mining area for mineral exploration

P014. N. Lindén, A. Saukko, M. Kurhila and O. Eklund
Sm-Nd and Lu-Hf isotopes in the Svecofennian rocks of southernmost Finland

P015. T. Lindqvist, E. Ruuska, E. Kosonen, N. Hornborg, P. Skyttä and N. Putkinen
Integrated modelling of bedrock surface and bedrock deformation zones for induced seismic risk assessments – improved constraints for thickness of sedimentary cover

P016. T. Luhta and J. Hällsten
Åland seismic network

P017. M. Malinowski, B. Brodic, I. Martinkauppi, E. Koskela and V. Laakso
Distributed acoustic sensing walkaway vertical seismic profiling in Koillismaa deep drillhole

P018. M. Rydberg, M. Kurhila and K. Nikkilä
Classification of mafic dikes in the Hanko-Inkoo archipelago

P019. A. Savakko, P. Mikkola and E. Heilimo
Geochemical features of the felsic and intermediate igneous rocks in Pasalanmäki area in Archean Proterozoic boundary

P020. L. Tuikka, B. Cateland, D. M. Whipp and M. Häkkinen
Exploring the effects of continental collision obliquity and temperature on orogeny evolution and P-T-t paths

P021. M. Tuppurainen, P. Mikkola and M. Kurhila
New U-Pb Age Data from Pasalanmäki In Leppävirta, Central Finland – Older Svecofennian Magmatism Or Not?

P022. E. Virta, T. Lindqvist, P. Skyttä and S. Mustonen
Correlation of bedrock outcrop structures with subsurface data – with emphasis on the need of geoenergy research

P023. D. Whipp and D. Kellett
Quantifying crustal evolution using low-temperature thermochronology and numerical modelling

Wednesday, Nov 16

09:00 - 10:35 Session 5: Crustal structures and mineral resources
Chair: Ilmo Kukkonen

09:00 - 09:45 **A. Rotevatn [Keynote]**
Hard breakup - the rifted margin of western Fennoscandia

09:45 - 10:10 **S. Géhin and A. J. Miles**
Mineralogical and geochemical characteristics of the red 'Rektor Porphyry' associated with the Per Geijer AIO ore, Northern Sweden

10:10 - 10:35 **P. Lupoli, L. Lobo, O. Katai, R. Prata, C. Santana, L. Gerlach, C. Benedicto, S. Johansson, M.-L. Friedländer, M. Martins and P. Biedzio**
Proximal hydrothermal alteration assemblages in the Kiruna deposit – a preliminary petrographic study

10:35 - 11:00 Coffee/Tea

11:00 - 12:05 Session 6: Archaean and Proterozoic lithosphere evolution
Chair: Kaisa Nikkilä

11:00 - 11:25 **J. Kara, M. Väisänen, J.S. Heinonen and H. O'Brien**
Arclogite formation beneath the Svecofennian orogen

11:25 - 11:50 **A.E. Johnson and O. Eklund**
Intraorogenic mafic magmatism in Nagu, SW Finland

11:50 - 12:05 **M. Seitsamo-Ryynänen and M. Kotilainen**
Plans and Actions with FIN-GEO

12:05 - 13:45 Lunch, poster viewing and FIN-GEO open discussion

13:45 - 17:10 Session 7: Archaean and Proterozoic lithosphere evolution (cont.)
Chair: Suvi Heinonen

13:45 - 14:10 **P. Mikkola, J. Jäsberg, J. Luukas and M. Kurhila**
Lithological units and geological evolution of Outokumpu allochthon's western parts, update based on recent studies

14:10 - 14:35 **O. Teräs, K. Nikkilä and O. Eklund**
Relation between rare element pegmatites and post-collisional magmatism in the Svecofennian domain

14:35 - 15:00 **A. Saukko, K. Nikkilä, S. Fröjdö, O. Eklund and M. Väisänen**
Magmas, metasomatism, and melting – the Svecofennian orogeny in southernmost Finland

15:00 - 15:30 Coffee/Tea

15:30 - 15:55 **P. Skyttä, E. Ruuska, T. Lindqvist and K. Ahlqvist**
Fracture-controlled glacial erosion - using outcrops analogues to model the erosional signature of unexposed faults

15:55 - 16:20 **T. Luoto, J. Salminen, S. Mertanen, S.-Å. Elming and L. J. Pesonen**
New reliable ~1885 Ma paleomagnetic pole from Svecofennian gabbro intrusions, central Finland

16:20 - 17:10 **I.T. Kukkonen [Invited]**
Evolution, structure and fluids of lithosphere in Finland

17:10 - 17:20 **National Lithosphere Committee**
Honouring Ilmo Kukkonen for his work in lithospheric research

19:00 - Conference Dinner, Café Pegasus, Aboa Vetus & Ars Nova

Thursday, Nov 17

9:30 - 10:30 Session 8: Crustal structures and mineral resources (cont. from Session 5)
Chair: Olav Eklund

9:30 - 10:05 **J. Kamm [invited]**
Studying the crust and its mineral systems with deep electromagnetic induction

10:05 - 10:30 **S. Aatos**
Constraining serpentinite-related pseudo-lithological entities in western boundaries of Outokumpu allochthon

10:30 - 11:00 Coffee/Tea

11:00 - 14:10 Session 9: Short communications and project presentations
Chair: Toni Veikkolainen

11:00 - 11:15 **E. Salin**
Lunar regolith as an archive of Solar System history

11:15 - 11:30 **I. Aaltonen, H. Reijonen and T. Bornhorst**
Michigan International Copper Analogue (MICA) project

11:30 - 11:45 **S. Heinonen, J. Kamm, M. Malinowski and the SEEMS DEEP Working Group**
SEEMS DEEP – combining seismic and electromagnetic methods for deep bedrock imaging

11:45 - 12:00 **K. Loukola-Ruskeeniemi, E. Hyvönen, J. Lerssi, H. Arkimaa, M.-L. Airo, J. Vanne, S. Vuoriainen, R. Turunen and J. Eskelinen**
The Black Shale Database of Finland: Precambrian metasedimentary rocks rich in graphite and sulphides

12:00 - 13:00 Lunch

13:00 - 13:15 **A. Korja and P. Haapanala**
Introduction to EPOS outreach videos

13:15 - 13:30 **I. Kukkonen, G. Hillers, P. Haapanala and the FLEX-EPOS team**
Finnish Seismic Instrument Pool

13:30 - 13:45 **S. Yang, E. Kozlovskaya and SEMACRET consortium**
Introduction to project SEMACRET: Sustainable exploration for orthomagmatic (critical) raw materials in the EU: Charting the road to the green energy transition

13:45-14:00 **D. Whipp and K. Cutts**
Tektonika: A new diamond open-access journal for the structural geology and tectonics community

14:00-14:30 Poster Award; Forthcoming Meetings; Closing of Symposium
Chair: Pietari Skyttä

EXTENDED ABSTRACTS

The publication is electronically available at https://www.seismo.helsinki.fi/ilp/lito2022/.

Michigan International Copper Analogue (MICA) project

I. Aaltonen[1], H. Reijonen[1] and T. Bornhorst[2]

[1]Geological Survey of Finland (GTK), Vuorimiehentie 5 02151, Finland
[2]Department of Geological and Mining Engineering and Sciences, Michigan Tech, USA
E-mail: Ismo.Aaltonen@gtk.fi

One of the key requirements for the geological disposal of high-level radioactive waste (HLW) is the assessment of long-term performance of waste canisters. An elemental copper coated canister is used in many disposal concepts, e.g., in Sweden, Finland and Canada, and therefore its stability is of particular interest in assessing long-term performance of deep geological HLW repositories. Studying natural analogues over geological time scales can be an important way of obtaining a better understanding the stability of elemental copper in the natural environment of the disposal facility. Here we give a status report on Michigan International Copper Analogue (MICA) project.

Keywords: Keweenaw Peninsula, Michigan USA, native copper, natural analogue, safety case, nuclear waste management

1. Background

Research on corrosion of natural native copper in combination with interpretation of their past geologic history is relevant for predicting the stability of elemental copper in the repository system. The stability of engineered barrier system (EBS) materials, such as elemental copper, is based on relatively short-term investigations, such as laboratory experiments. Elemental copper is an important part of many waste packaging and disposal concepts, e.g., KBS-3 developed in Sweden and Finland and Mark II developed in Canada (Figure 1). Waste management organisations have also reviewed native copper analogues because of their potential to supplement and improve our understanding of copper corrosion. The Michigan International Copper Analogue (MICA) project focuses on the general stability of native copper in the world's largest native copper dominated deposits of the Keweenaw Peninsula native copper district in Michigan USA. The ultimate objective for the partners[1], five radioactive waste management organisations, is to better understand the future behaviour of waste containers with an outer layer of elemental through the study of the natural geologic processes.

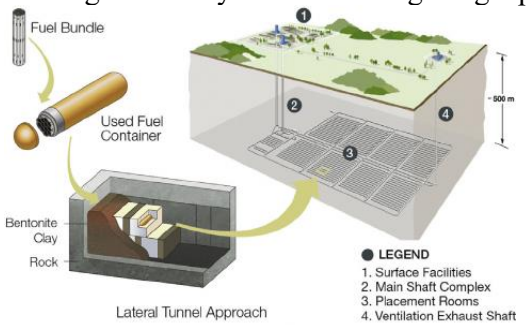

Figure 1. Mark II concept (Boyle and Meguid, 2015) utilizes copper-coated containers.

[1] Nuclear Waste Management Organization, NWMO, Canada; Radioactive Waste Management Limited, RWM, UK; Svensk Kärnbränslehantering AB, SKB, Sweden; Bundesgesellschaft für Endlagerung mbH, BGE, Germany; National Cooperative for the Disposal of Radioactive Waste, Nagra, Switzerland

2. Natural Analogue

One of the key requirements for the deep geological disposal of high-level nuclear waste is the assessment of its long-term performance and safety for 1 million years. Natural analogues provide a way of evaluating potential repository system behaviour. Observations made from the geological systems can be utilized in the safety case and in some cases providing information on times far beyond 1 million years. Both, natural and archaeological, analogue studies are reported in the literature and extensively reviewed by various authors (e.g., Miller et al., 2000) and in safety case projects (e.g., Reijonen et al., 2015). So far, only a few studies have focussed on the stability of native copper within its natural media (e.g., Milodowski et al., 2000; Marcos, 2002). The goal of the MICA Project is to provide a unique complementary data source to estimate processes governing long-term corrosion behaviour of elemental copper used in waste canisters and to support disposal safety cases as well as stakeholder communication.

3. Keweenaw Peninsula native copper

The Keweenaw Peninsula native copper district occurs within the ca. 1.1 Ga North American Midcontinent Rift system (MCR). The host rocks of native copper deposits are rift-filling subaerial basaltic lava flows (Figure 2) with minor interbedded clastic sedimentary rocks (Bornhorst and Lankton, 2009). Metamorphogenic ore-forming hydrothermal fluids moved upward from the source zone in the rift into the zone of precipitation of native copper and associated minerals in primary and secondary open spaces at about 1.04 to 1.07 Ga (Bodden et al., 2022; Bornhorst et al., 1988). Subsequent erosion during the Precambrian likely exposed the deposits at the land surface and this Precambrian erosional surface was covered by Paleozoic sedimentary rocks of the Michigan Basin (Bornhorst and Lankton, 2009). Quaternary glaciations stripped away almost all the Paleozoic rocks of the Keweenaw Peninsula and once again exposed the native copper deposits at the surface (Bornhorst and Lankton, 2009).

Keweenaw native copper occurrences (Upper Peninsula, Michigan, USA) have been mentioned as a qualitative source of information to support the use of elemental copper as part of waste containers, e.g., in Miller et al. (2000). However, data on corrosion of native copper for geological disposal process-based safety assessments is lacking. The Keweenawan deposits were commercially mined from 1845 to 1968. The combination of geologic setting and geologic and environment history is used to group natural native copper occurrences into several different potential analogues.

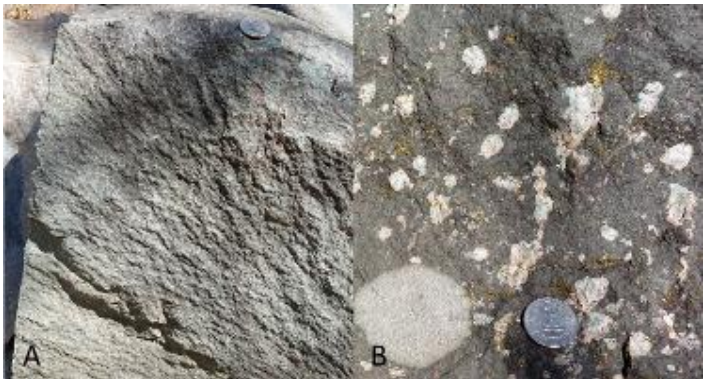

Figure 2. A) A massive vesicle-free interior of a subaerial basaltic lava flow. B) A lava flow top with vesicles filled with secondary hydrothermal minerals. The gray spot in the lower left corner is lichen. Pictures from South Range quarry (Bornhorst and Rose, 1994).

4. Phase I

Phase I of the MICA Project consists of developing an overview relevant to all potential Keweenawan natural native copper corrosion analogues. For each potential analogue, the geologic history, environment type, length of exposure, and uncertainties were described based on existing data. The feasibility of obtaining sufficient representative existing or new samples with a reasonably high potential for being exposed to water were assessed for each analogue. Water is an essential component to facilitate corrosion of native copper as illustrated by native copper inclusions encased in calcite which do not show visible corrosion (Wilson and Dyl, 1992). Availability of supportive information such as estimates of water composition was also evaluated. All these data were reviewed against disposal concepts and processes.

5. Relevant natural analogues

While all the analogues have the potential to provide insight into corrosion of elemental copper, some of the analogues are ranked to have higher potential than others.

Native copper encased in bedrock or minerals, such as in basalt or calcite, with limited to no exposure to waters provides a baseline analogue or background level of corrosion. A few of the corrosion analogues identified as the most promising are:

1. *Bedrock native copper – cumulative corrosion over time frames of up to 100s of millions of years and more and at depths up to 2 km.* Bedrock native copper has potential to corrode while under different probable conditions: anoxic to oxic and variable water compositions of brines, groundwater, and glacial/modern lake water.
2. *Bedrock native copper formed in situ in hydrothermal fracture-filling clay – cumulative corrosion under conditions described for bedrock native copper*.
3. *Bedrock native copper effected by sulfur-bearing waters – cumulative corrosion under conditions described for bedrock native copper with addition of corrosion by sulfur-bearing waters*.

Figure 3. Native copper and calcite crystals in a cavity from the Adventure Mine. The native copper was exposed to oxic conditions at shallow depths resulting in formation of tenorite (black).

6. Conclusions

The results from Phase I of the MICA project provides a context and a starting point for the detailed study of natural corrosion of native copper during Phase II. There is a wealth of established geological context useful for planning and implementing Phase II.

References:

Bodden, T.J., Bornhorst, T.J., Bégué, F., Deering, C., 2022. Sources of Hydrothermal Fluids Inferred from Oxygen and Carbon Isotope Composition of Calcite, Keweenaw Peninsula Native Copper District, Michigan, USA. Minerals 2022, 12, 474.

Boyle, C.H., Meguid, S.A., 2015. Mechanical performance of integrally bonded copper coatings for the long term disposal of used nuclear fuel. Nuclear Engineering and Design, Volume 293, pp 403–412.

Bornhorst, T.J., Lankton, L.D., 2009. Copper mining: A billion years of geologic and human history. In Michigan Geography and Geology; Schaetzl, R., Darden, J., Brandt, D., Eds.; Pearson Custom Publishing: New York, NY, USA, 2009; pp. 150–173.

Bornhorst, T.J., Rose, W.I., 1994. Self-guided geological field trip to the Keweenaw Peninsula, Michigan. Institute on Lake Superior Geology, United States.

Butler, B.S., Burbank, W.S., 1929. The Copper Deposits of Michigan. U.S. Geological Survey Professional Paper 144. Washington, DC.

Milodowski, A. E., Styles, M. T., Hards, V. L., 2000. A natural analogue for copper waste canisters: The copper-uranium mineralised concretions in the Permian mudrocks of south Devon, United Kingdom. Technical Report TR-00-11, Stockholm, 40 Sweden: Swedish Nuclear Fuel and Waste Management Co. (SKB) 84 pages.

Marcos, N., 2002. Lessons from nature. The behaviour of technical and natural barriers in the geological disposal of spent nuclear fuel. Acta Polytechnica Scandinavica, Civil Engineering and Building Construction Series No. 124, Espoo, Finland: Finnish Academy of Technology.

Miller, W.M., Alexander, W.R., Chapman, N.A., McKinley, I. G., Smellie, J.A.T., 2000. The geological disposal of 45 radioactive wastes and natural analogues: Lessons from nature and archaeology. Waste management series Vol. 2, Oxford, UK: Elsevier Science Ltd. Pergamon, 332 pages.

Reijonen, H., Alexander, W.R., Marcos, N., Lehtinen, A., 2015. Complementary considerations in the safety case for the deep repository at Olkiluoto, Finland: support from natural analogues. Swiss Journal of Geosciences. 108 (1) pp. 111-120.

Wilson, M.L., Dyl II, S.J., 1992. The Michigan Copper Country: The Mineralogical Record, Tucson, Arizona, 104 p.

Constraining serpentinite-related pseudo-lithological entities in western boundaries of Outokumpu allochthon

S. Aatos[1]

[1]Geological Survey of Finland, P.O. Box 1237, 70211 Kuopio, Finland
E-mail: Soile.Aatos@gtk.fi

Exploratory data analysis with multivariate statistical and GIS tools and integrated use of aerogeophysical and lithogeochemical data can be used to extract so called pseudo-lithological entities to help interpretating regional bedrock geology and related zones that may have mineral potential. In this paper, unsupervised clustering tools were used to identify model classes that could be preliminary interpreted to originate from Outokumpu type serpentinites or Outokumpu assemblage rocks in western boundaries of Outokumpu allochthon. Consequently, the results can be further applied to develop computation-aided interpretation of large multivariate data of crystalline bedrock regions for bedrock geological and mineral potential mapping purposes.

Keywords: pseudo-lithology, lithogeochemistry, bedrock unit, nickel, Northern Karelia, Outokumpu, Finland

1. Introduction

Mikkola et al. (2022) used exploratory data analysis methods to delineate areas potentially hosting rocks with Outokumpu assemblage type mineral potential in western boundaries of Outokumpu allochthon, Central Finland. The preliminary results of Mikkola et al. (2022) suggested that computed pseudo-lithological entities based on multivariate approach combining aerogeophysical and lithogeochemical data may be used as a labelling aid in geological interpretation of rock samples from the study area.

2. Pseudo-lithology of Outokumpu assemblage rocks and enrichment of nickel

A set of previously clustered apparent resistivity-magnetic aerogeophysical GIS raster model data pixels with labelled bedrock type information and lithogeochemical data (Mikkola et al. 2022) was selected for this study (Table 1). The selected raster model clusters exemplify clusters that include observations of serpentinite, which is a characteristic member of the Outokumpu assemblage (Table 1).

Pseudo-lithological clusters and lithogeochemistry of the rock samples (Table 1) were used to describe the enrichment of Ni in rocks constraining Outokumpu assemblage type rock units (Figure 1). Statistical receiver operating characteristic (ROC) analysis of Ni, compared to Co, Cu and S concentrations, and values of a lithogeochemical exploration index of nickel "NiMgOresidual" (Brand, 2004) of resisivity-magnetic model cluster number 3 were used to evaluate modelling results of this study. Evaluation was done first using all the project's lithogeochemical data with Ni determined (n=791) and then with Ni ≥ 100 ppm (n=243 Figures 2 and 3).

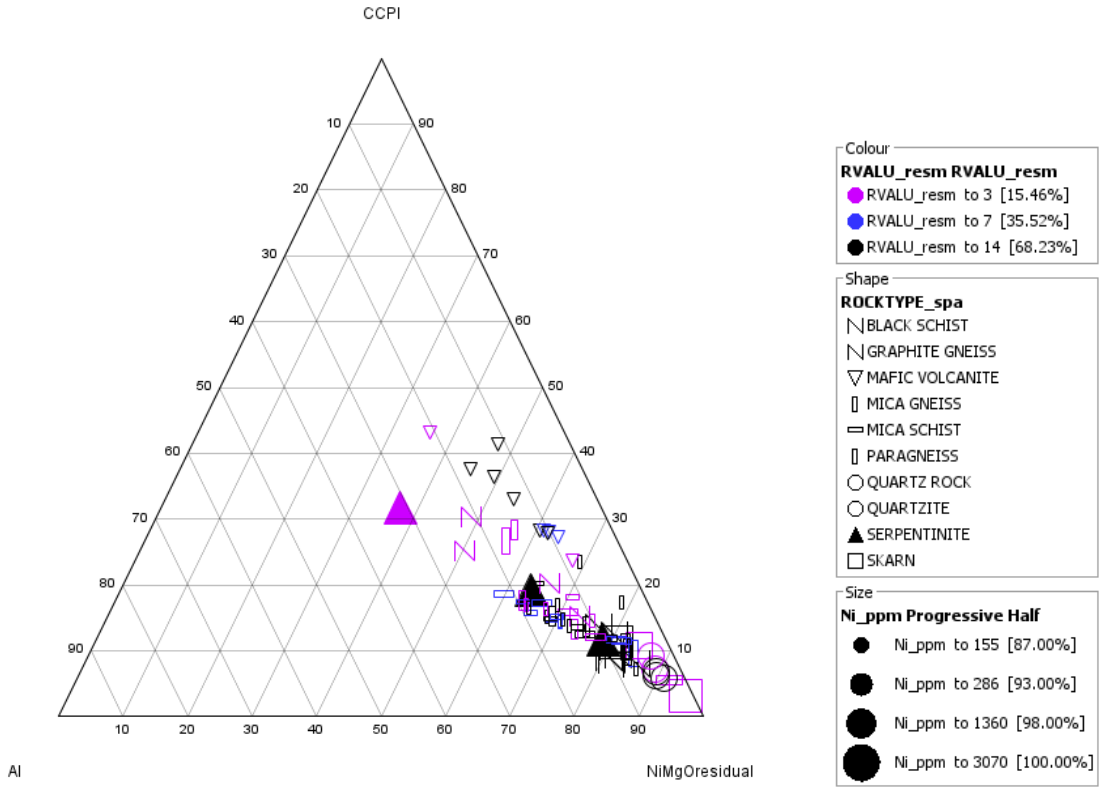

Figure 1. The Ni-bearing population of selected resistivity-magnetic raster model clusters (Table 1) containing 82 % of the serpentinite observations (colour of symbols) on ternary plot of alteration indices Ishikawa Alteration Index (AI) (Ishikawa et al., 1976), Chlorite-Carbonate-Pyrite Index (CCPI) (Total Fe) (Gemmel, 2007), and Ni – MgO residual "NiMgOresidual" (Brand 2004). Shape of symbols is based on dominant bedrock type labels of model clusters (Table 1). Treshold of Ni = concentration > 92 ppm (75%) (size of symbols). N of samples = 103. Some of the serpentinite samples don't have alteration index values due to missing analytical chemical determinations of main element compounds or negative index values.

The general qualitative measure of model quality for the overall model (cluster number = 3) was good (model value above 0.5) for Ni and S, but near random for model with elevated Ni concentrations (Figures 2 and 3). A model value less than 0.5 indicates the model is no better than random prediction. The enrichment of Ni and S may be related to Outokumpu type metal sulphide anomalies of pseudo-lithological clusters resembling metasedimentary rock units including serpentinite bodies. The random or poor values of a lithogeochemical exploration index of nickel "NiMgOresidual" (Brand, 2004) suggest scattered mineralization intensity of Ni over various rock types in the sample data, possible source being Outokumpu type rock assemblage (Table 1, Figures 1-3).

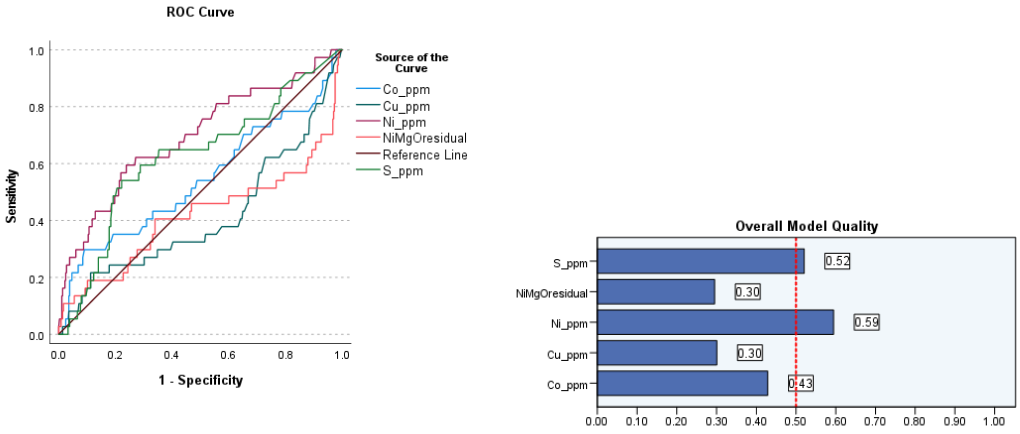

Figure 2. Statistical ROC analysis of Ni concentrations in comparison with Co, Cu, and S concentrations (ppm), and values of a lithogeochemical exploration index of nickel "NiMgOresidual" (Brand, 2004) of resisivity-magnetic model cluster number 3 (n of samples = 791).

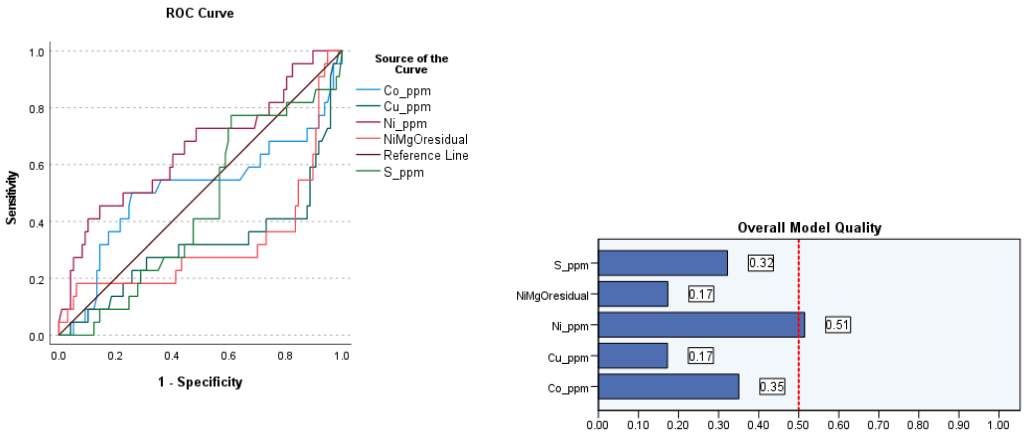

Figure 3. Statistical ROC analysis of elevated Ni concentrations (Ni ≥ 100 ppm, n of samples = 243), in comparison with Co, Cu, and S concentrations (ppm), and values of a lithogeochemical exploration index of nickel "NiMgOresidual" (Brand, 2004) of resisivity-magnetic model cluster number 3.

References:

Brand, N.W. 2004. Geochemical Expressions of Nickel Sulphide Deposits. AIG Seminar, Advances and Innovations in the exploration for Nickel Sulphide Deposits, Perth WA, 12 November 2004.

Gemmel, J.B. 2007. Hydrothermal Alteration Associated with the Gosowong Epithermal Au-Ag Deposit, Halmahera, Indonesia: Mineralogy, Geochemistry, and Exploration Implications, Economic Geology, v. 102, pp. 893–922

Ishikawa, Y, Sawaguchi, T., Iwaya, S. and Horiuchi, M. 1976. Delineation of prospecting targets for Kuroko deposits based on modes of volcanism of underlying dacite and alteration halos. Mining Geology 26: 105 to 117.

Mikkola, P., Aatos, S., Halkoaho, T., Heinonen, S., Hietava, J., Hietala, S., Kurhila, M., Jäsberg, J., Laine, E.-L., Luukas, J., Niskanen, M., Nousiainen, M., Nygård, H., Piispanen, A., Pirinen, H., Rantanen, H. & Romu, I. 2022. Geological evolution and structure along thewestern boundary of the Outokumpu allochthon. Geological Survey of Finland, Open File Research Report 23/2022, 117 p.

Table 1. Statistics of three computationally combined aerogeophysical resistivity-magnetic raster model clusters (original n of clusters = 31) of the study area as in Mikkola et al. (2022). Model cluster number 3 was selected for further evaluation of enrichment of Ni based on computed and observed lithologies. The selection was based on presence of serpentinite with other typical bedrock types related to Outokumpu assemblage.

Rocktype	**RVALU_resm = 3**	**RVALU_resm = 7**	**RVALU_resm = 14**	**RVALU_resm = Other**	**Total**
Black schist, graphite gneiss	4	0	3	9	16
Mafic volcanite	2	2	0	8	12
Mica gneiss, paragneiss	7	6	14	30	57
Mica schist	4	9	10	17	40
Quartz rock, quartzite	2	0	7	2	11
Serpentinite	7	5	2	3	17
Skarn	3	1	4	0	8
Other	6	3	7	66	82
Total	35	26	47	135	243

3D bedrock topography model of City of Turku using geotechnical soundings

K. Ahlqvist[1], N. Anttila[1], P. Skyttä[1] and A. Ojala[1]

[1]University of Turku
E-mail: kati.m.ahlqvist@utu.fi

Urban areas could benefit from 3D bedrock models, and geotechnical soundings are easily available input data for modelling in these areas. This data have uncertainties especially in the areas where is thick overburden. In this study we evaluate geotechnical soundings usability and produce a digital elevation model of City of Turku. We use bedrock verified soundings, controlling soundings, and digital elevation model data from the outcrops. The bedrock of Turku has a several narrow and long valley-like linking structures and the elevation difference across the structures can be over 100 m. The east-west structures are more straightforward and crosscutting ones form more step-like structures.

Keywords: geotechnical soundings, bedrock topography, 3D model

1. Introduction

Geological properties of the bedrock and overlying sedimentary deposits are among the most important factors in terms of construction of the infrastructure and its cost. Urban planning and cost control may be facilitated with sufficient 3D models of the subsurface, including bedrock composition and structure, bedrock surface topography and the composition and thickness of the overburden.

Geotechnical soundings have been carried out by larger cities for decades during their progressive construction phases, resulting in comprehensive datasets which can be used for further investigations. This data comprise e. g. verified bedrock height, bore ending method and types of superficial deposits, and is a valuable, quick, and cost-effective input for bedrock topography modelling.

The bedrock verification in the sounding process is always the drillers interpretation and it is dependent on his experience (SGY, 1986). The deeper the sounding progresses, the more difficult it is to interpret the surface of the bedrock (SGY, 1986). According to Tanttu (2015) the misinterpretation is usually deeper than reality. Especially very tight moraine layer is difficult to separate from soft bedrock (SGY, 1986) The sounding data, especially the older soundings done without GPS and advanced equipment, always include errors in coordinates or other data. The placement of soundings in relation to geological structures is important factor. The placement is dependent on infrastructure, and in modelling crosscutting sounding lines are more useful and gives more information about bedrock topography.

In this study we i) evaluate how the point density and their spatial distribution effects the modelling ii) evaluate the usability of different sounding methods to determine the bedrock height and their reliability, iii) produce a digital elevation model of City of Turku and compare the model to bedrock structures. This work is a part of Turku 3D project where we are producing integrated models of bedrock and sedimentary deposits in, and special attention is paid to their interactions. We acknowledge Finnish Cultural Foundation for funding and Turku City for data and collaboration.

2. Methods

In determining the elevation of bedrock surface, we used two types of soundings: i) bedrock verified soundings (n=6425) and ii) soundings whose termination method is wedging, boulder or unverified bedrock (n=29 763). The later one was used to control the modelling, and their bore end height was lowered 2 m. To produce outcrop data, we used digital elevation model (DEM 2 m and 10 m; NLS, 2022a, b), superficial deposits map (1:20 000; GTK, 2021) and clay observation points from earlier studies (Pirilä, 2016). The outcrop data were processed in four phases: i) digitalization of the outcrop border with polylines and projecting the polylines to DEM, ii) converting DEM to point data, iii) clipping the DEM point data with polylines and iiii) converting the polylines to points. The final point data of the outcrops included 468 095 DEM points and 94 848 points from polyline data. We did the interpolation with Kriging interpolation tool (Move®).

3. The 3D model of bedrock

Turku area has based on DEM and bedrock model several faults that forms narrow and long topographic valleys in both the land and bedrock surface topography. (Figure 1). In the produced 3D model, the bedrock elevation varies between -56.4 m and 67.6 m and the maximum elevation contrast across the topographic depressions into the surrounding exposed outcrops of the hill areas can exceed 100 m. The dominant trends of the bedrock depressions are ENE-WSW, which coincides with the ductile structural grain of the regional as defined by the main foliation, migmatite banding and the trend of major lithological contacts. In addition to the ENE-WSW set, a few distinct NNW-SSE depressions occur as well. The ENE-WSW zones are linear and continuous, while the NNW-SSE ones are shorter and display some step-like structures.

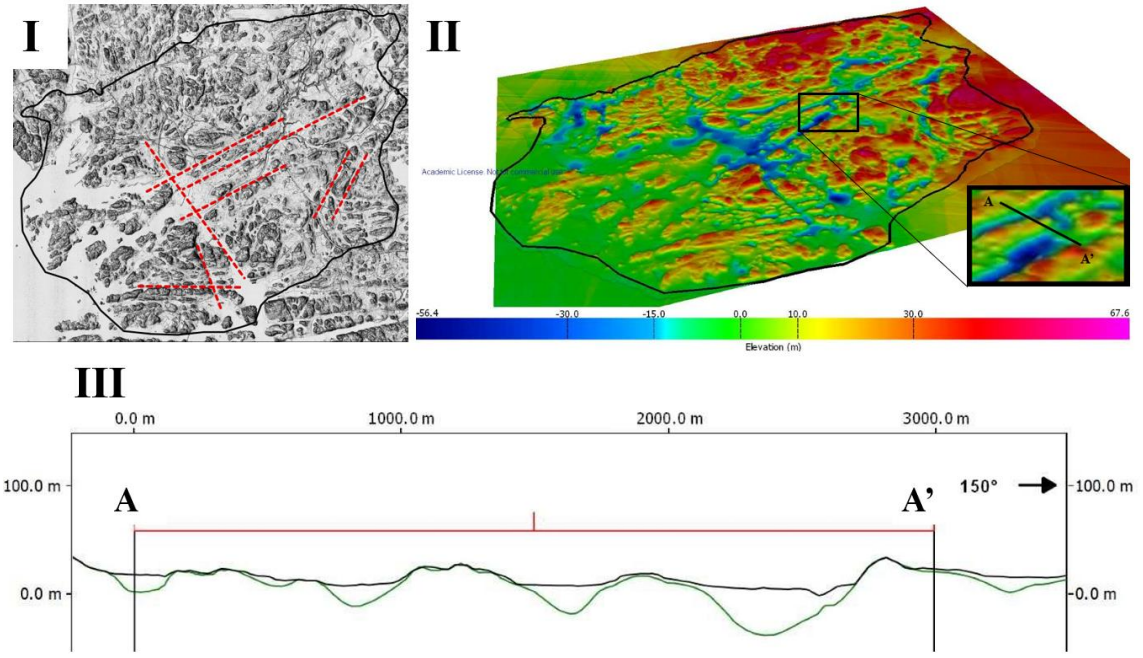

Figure 1. I) Lineament interpretation from DEM (2 m) (NLS, 2022a), II) The 3D model of the bedrock surface and III) A Cross section (black line = DEM (2 m), green line = 3D model of the bedrock surface (NLS, 2022a).

Regarding the reliability of the elevation point data from the geotechnical drillings, the closer the bedrock DEM is to the surface, the more reliable the model is, because of the possible misinterpretation of the bedrock surface in sounding process. The topographic depressions have thick overburden, and the model is probably not fully reliable in these areas. The controlling soundings improve the reliability of the model in the thick overburden areas, because with those soundings the bedrock elevation is it not possible to interpret too deep.

References:

SGY, 1986. Finnish Geotechnical Society (. Kairausopas V, porakonekairaus. 9 p.

GTK, 2022. Geological Survey of Finland (GTK). Superficial depostits 1:20 000/1:50 000. 8.5.2022. https://hakku.gtk.fi/fi/locations/search

NLS, 2022a. National Land Survey of Finland. Elevation model (2 m). 8.5.2022. https://www.maanmittauslaitos.fi/kartat-ja-paikkatieto/asiantuntevalle-kayttajalle/tuotekuvaukset/korkeusmalli-2-m

NLS, 2022b. National Land Survey of Finland. Elevation model (10 m). 8.5.2022. https://www.maanmittauslaitos.fi/kartat-ja-paikkatieto/asiantuntevalle-kayttajalle/tuotekuvaukset/korkeusmalli-10-m

Pirilä, L., 2016. Savikerrostumien syntyhistoria, niiden paksuus- ja ominaisuusvaihtelut sekä vaikutukset yhdyskuntatekniikkaan Turun alueella. Master thesis, University of Turku. 135 s.

Tanttu, K., 2015. Kalliopintamallin luotettavuuden analysointi porakonekairausten määrän ja laadun perusteella. Liikenneviraston tutkimuksia ja selvityksiä, 27/2015. 67 p.

Offshore Cyrenaica New Bathymetry Using World War II Data, Implications on the Central Mediterranean Plate Boundaries

A. Amer[1]

[1]Department of Geography and Geology, University of Turku, Turku, Finland
E-mail: aamer@slb.com

The offshore area of northeast Libya is only vaguely known because of the limited offshore hydrocarbon exploration and literature. The topographic high onshore the northeast flank of the country, is known as Al-Jabal Al-Akhadar (The Green Mountain) and is composed of carbonate formations ranging in age from Cretaceous up to late Miocene.

The lack in knowledge of the offshore area led to the search in public and private domains in order to have a better understanding on the tectonic nature of the offshore area and attempt to link its kinematics to the onshore structural features. The data collected and processed in this study, utilizes sonar data collected from the 40s during the second World War by US and British naval war ships.

This data was compiled with the help of different software packages to produce a detailed 3D bathymetric map, leading to the discovery of a submarine subduction zone. This abstract will demonstrate how this data was interpreted and will highlight discrepancies in the current plate tectonic understanding of the region. In conclusion, we propose an alternative kinematic model that is consistent with the onshore and offshore newly revealed structures.

Keywords: Al-Jabal Al-Akhadar, subduction zone, Cyrenaica trench, oblique convergences

1. Introduction

The Cyrenaica platform reside at an area of 160,000 km^2, stretching from the city of Benghazi to the border with Egypt to the east, and from the northeastern coast of Libya to the north bank of the Hameimat Trough to the south. The Al-Jabal Al-Akhdar anticlinorium consists primarily of shoaling upward carbonate successions with a maximum elevation of 867 m above sea level.

The area was first studied by Gregory (1911), where he identified the general geological architecture of the Cyrenaican formations. This work was followed by numerous studies such as Amrouni et al. (2016), El-Hawat and Salem (1987), Marinelli (1920) and Silvestri et al. (1929). The University of Benghazi Earth Science Department continues to study the area in addition to other universities around the world.

The interest of studying such area intensified following the offshore production of oil and gas from the offshore western region of Libya. The Libyan National Oil Corporation (N.O.C.) announced new concessions offshore Al-Jabal Al-Akhdar area making this area a zone of interest for investors. However, limited data is available on the tectonic kinematics, which resulted in several hypotheses that are largely controversial.

The main issue in the current interpretations is centred around the structural lineament offshore Cyrenaica (central Mediterranean). In some cases, it is interpreted as a fault plane named the Offshore Cyrenaica Fault, and in other cases it is interpreted as a subduction zone, where some authors favour a northern subduction and other a southern subduction. Such vocal discrepancy in interpretation would benefit from a detailed review, potentially using old data with new techniques. In this extended abstract, I attempt to propose a new theory based on sonar data that was collected during the second World War and processed with state-of-the-art software technology.

2. Methodology

The goal of this work was to produce a bathymetry map from old sonar data using several new techniques. The dataset was first collected from NASA's Earth Observatory Blue Marble Next Generation database, which consisted of sonar survey sweeps collected by the US and British Navy's in the second Word War during their hunt for German U-boats. This data were later loaded into Petrel software package and processed to produce a 3D bathymetry map. The mineralogical composition of key elevated areas was identified using core analysis obtained from the Deep Sea Drilling Project (DSDP) public database. This was followed by a detailed structural mapping and analysis of the Al-Jabal Al-Akhdar mountain, using satellite imagery terrain analysis with the objective of mapping faults and structural lineaments.

3. Results

The processing of the sonar data resulted in a detailed 3D bathymetry map that covered the offshore area of Cyrenaica and the central Mediterranean region. This map revealed a submarine trench that exhibits an average depth of -3100 mss and a maximum depth of -4096 mss 152 km north of the city of Benghazi. The trench is found to extend from Egypt in the east to Italy in the north. Other features that have been observed are volcanic bodies, submarine canyons, and a sea floor plateau (Figure 1). The areal extent of the volcanic bodies have been mapped using sonar data over the sea floor, whereas the composition was adopted from core data from Bellon and Letouzey (1977).

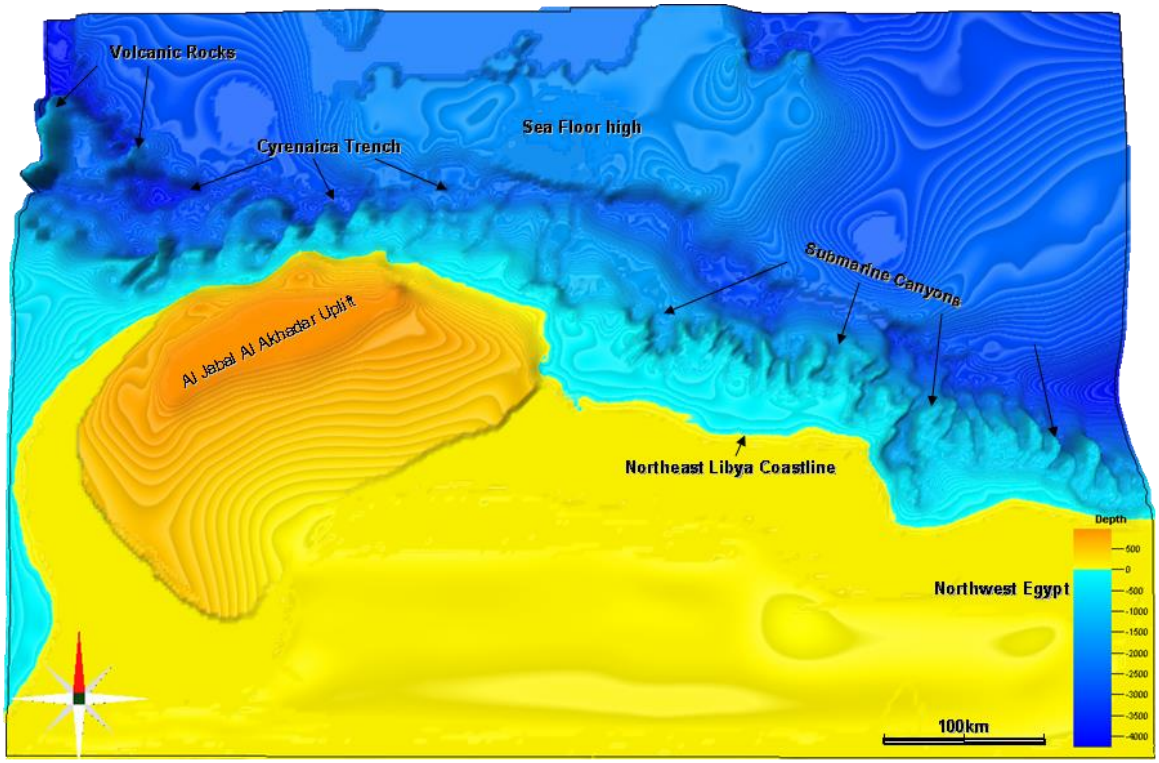

Figure 1. High resolution 3D bathymetry produced for the offshore Cyrenaica area from sonar data collected during the World War II.

The fault patterns observed over the Al-Jabal Al-Akhdar, are steeply inclined and are dominated by strike-slip movement. This fault system is linear to curvilinear in plain view, and possess a principal displacement zone (PDZ) along a WNW-ESE orientation. It has been found that south of the city of Tubruq, the area is characterized by pull-apart basins resulting from fault bending. The area is also characterized by *en-echelon* folding, faulting, and fracturing along the Marmarica Basin in the east and fades away towards the Al-Jabal Al-Akhdar western escarpments (Figure 2).

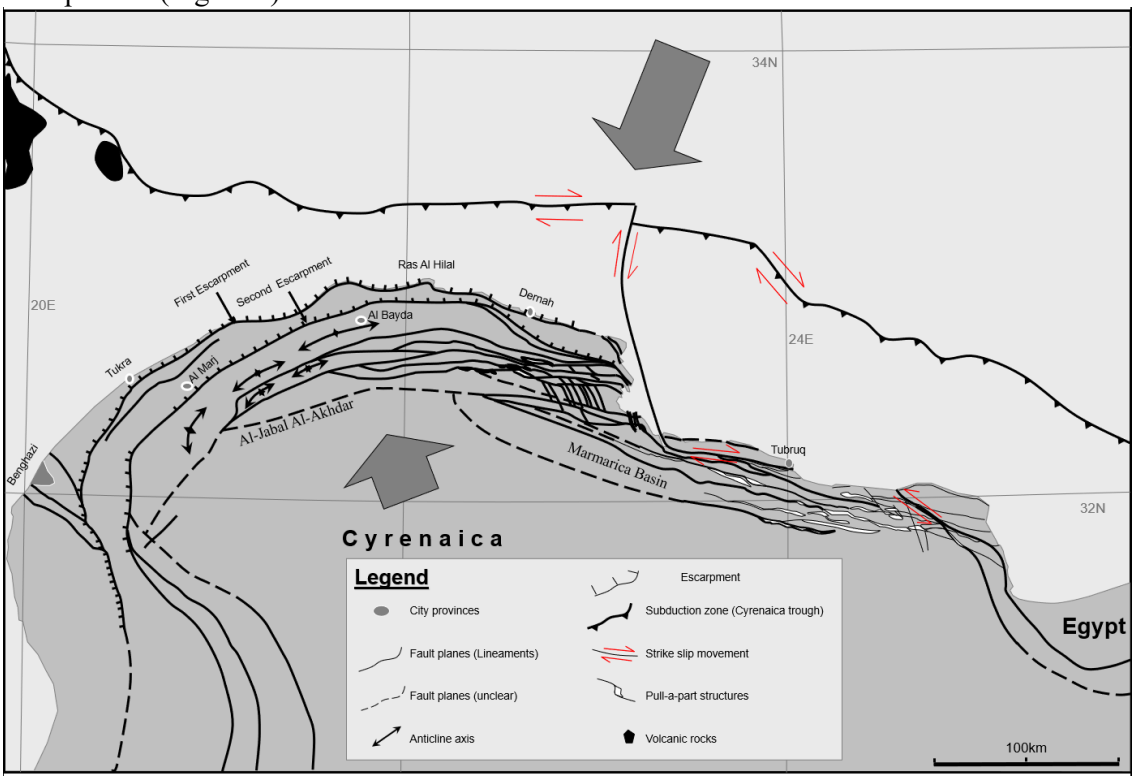

Figure 2. The main structural elements of the onshore and offshore area of Al-Jabal Al-Akhdar.

4. Discussion and Conclusions

The development of the high-resolution 3D bathymetry map of the offshore area of Cyrenaica revealed a submarine trench, volcanic bodies, submarine canyons, and a sea floor plateau (Figure 1). The focus of this extended abstract will be on the submarine trench that extends from Egypt in the east to the Apennines thrust belt in Italy to the north. Nevertheless, the observed volcanic bodies are found to be linked to the trench, and it is proposed that such features can assist in identifying the polarity of this subduction zone, especially in the absence of deep tomography measurements. The volcanic bodies are located towards the south of the identified trench, consequently, such observation supports the southern polarity of the identified plate boundary. The presence of the volcanic bodies also assist in identifying the subduction plunge angle, where volcanic bodies indicate a deep angle subduction, and the absence of volcanic bodies suggest a shallow angle subduction. Such postulation is supported by earthquake epicentre depths documented in the region by Thornes and Wainwright, (2004).

Surface geology mapping of the Al-Jabal Al-Akhdar revealed that the first and second escarpments (Figure 2) coincides with a PDZ interpretation with a horsetail splay, present at both ends, south of Benghazi city and Marmarica Basin. The kinematics of this fault system is characterized by transtensional faults. As a result of the onshore structural analysis, it is

postulated that the submarine trench kinematics are dominated by a dextral transform faulting combined with subduction, indicating an oblique convergences plate boundary system. It is suggested in this extended abstract, to name this subduction zone the Cyrenaica Trench, due to its proximity to the Cyrenaican region, and it is recommended to run deep tomography services in the area to evaluate this complex area of the Mediterranean Sea (Figure 3).

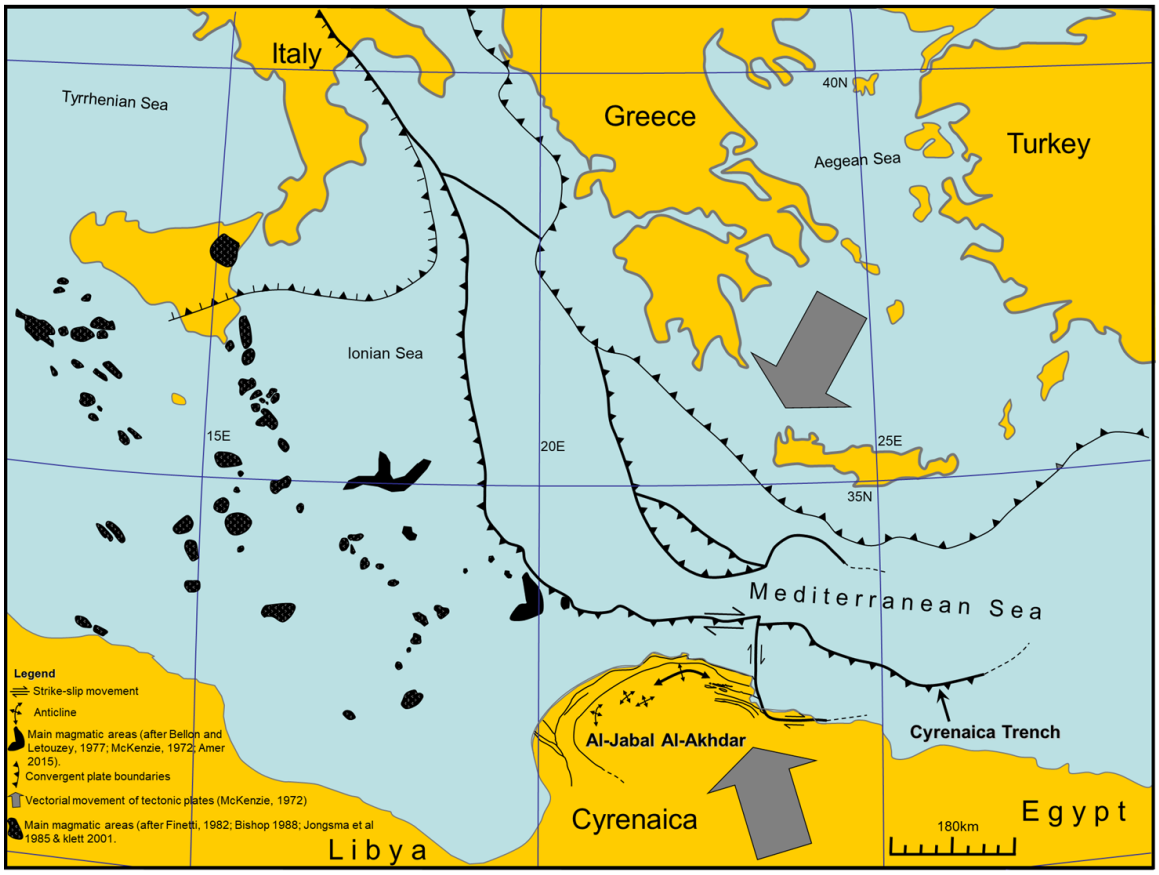

Figure 3. Central Mediterranean tectonic elements along with the newly interpreted Cyrenaica Trench.

5. References

Amrouni, K., Pope, M., El-Hawat, A., Obeidi, A., Amer, A., Elbileikia, E., Elbargathi, H., El-Gahmi, M., Mustafa, K., Al-Alwani, A., 2016. Distribution of Fault Controlled, Wave-Tide Dominated, Prograding Oolitic Shoals of the Miocene Carbonate-Evaporite Successions of Ar-Rajmah Group.

Bellon, H., Letouzey, J., 1977. Volcanism related to plate tectonics in the western and eastern Mediterranean. Structural History of the Mediterranean Basins. Paris: Technip, 165–184.

El-Hawat, A., Salem, M., 1987. A case study of the stratigraphic subdivision of Ar-Rajmah Formation and its implication on the Miocene of northern Libya: Ann. Inst. Geol. Publ. Hung, 70, 173–183.

Gregory, J.W., 1911. The geology of Cyrenaica. Quarterly Journal of the Geological Society, 67, 572–615.

Marinelli, O., 1920. Sulla morfologia della Cirenaica. Riv. Geogr. Ital, 27, 7.

Silvestri, A., Desio, A., Zuffardi-Comerci, R., 1929. Resultati Scientifici della Missione alla Oasi di Giarabub (1926-1927): La paleontologia.

Thornes, J.B., Wainwright, J., 2004. Environmental issues in the Mediterranean: processes and perspectives from the past and present. Routledge.

Chasing Deep Geothermal Resources in Crystalline Cratons

A. Bischoff[1], J. Kuva[1], M.J. Heap[2], E. Jolis[1], T. Reuschlé[2], J. Engström[1], J. Salminen[1] and T. Karinen[1]

[1]Geological Survey of Finland, Finland
[2] Université de Strasbourg, France
E-mail: alan.bischoff@gtk.fi

Discovering deep geothermal resources in crystalline rocks beyond high-temperature volcanic and rifting areas is pivotal to enable a rapid global transition towards clean and reliable energy sources. Therefore, a detailed assessment of the petrophysical and thermal properties of deep crystalline rocks is necessary to comprehend heat generation, transfer and storage at low-enthalpy conditions. With a total depth of 1724 m, the so-called Koillismaa Deep Drillhole, Eastern Finland, penetrated a series of highly fractured and altered mafic-ultramafic layered intrusions and coeval granitic rocks that offer a rare opportunity to evaluate the geothermal potential of the deeper Fennoscandia crystalline crust. The Geological Survey of Finland in collaboration with national and international research institutions is presently developing a series of novel studies combining large-scale geophysical data, borehole and field information, and pore-scale microscopic observations to assess the geothermal potential of the rocks perforated by the Koillismaa Deep Drillhole. Insights from these studies will help in defining deep crystalline rock targets and de-risking geothermal exploration in stable cratonic settings – key to upscale geothermal energy production and increase the uptake of sustainable energy sources globally.

Keywords: crystalline reservoirs, geothermal energy, petrophysics, stable Cratons

1. Introduction

The rapid displacement of fossil fuels by sustainable and affordable energy sources will require novel technologies that can meet large-scale commercial demands. Increasing the uptake of deep geothermal resources beyond hot volcanic and rifting areas offers near-unlimited energy for multiple spheres of our society, including direct heating and electricity generation. However, finding these resources is a global challenge that will require new understanding of how heat flows and accumulates at lower-temperature conditions.

Large-scale (>1MW) geothermal production relies on two critical factors: *heat and permeability*. Finding Earth's heat is reasonably straightforward. As an empirical rule, the deeper you drill, the hotter it gets, making geothermal energy a nearly limitless natural resource still largely untapped (e.g. Arnórsson et al., 2015; Jolie et al., 2021). To illustrate, the crystalline bedrock beneath Finland is estimated to *store nearly 4 000 000 TWh of power* at a depth interval of four to seven kilometres, sufficient to *supply the country's current district heating demands for over 100 000 years* (GTK, 2022).

Although we can reach the Earth's "deep heat" with modern drilling technology, our capacity to harvest this power is limited by the rate that heat dissipates from its source, which is primarily a function of the fluid and thermal flow properties of rocks (Duwiquet et al., 2021; Piipponen et al., 2022). Consequently, an accurate understanding of the parameters that control heat migration and storage, including porosity, permeability, pore connectivity, heat capacity, and thermal conductivity, is necessary to assess the potential of deep crystalline reservoirs and propose realistic geothermal exploration models.

2. Scientific and Technological Challenges

Presently, three (global) issues make the utilisation of deep geothermal heat in low-enthalpy crystalline settings challenging:

i. Substantial temperatures are achieved much deeper than in active volcanic or rifting areas (e.g. ca 100°C at 6 km in Finland; Kukkonen, 2000);
ii. With progressive depths, large (>1 km^3) permeable structures become scarce and harder to detect based on our current exploration geophysics knowledge (Kukkonen, 2000);
iii. The depth and low permeability combination lead to drilling and reservoir engineering complexity (Heap and Kennedy., 2016; Villeneuve et al., 2018; Jolie et al., 2021).

Specifically in the Fennoscandian Shield, numerous permeable zones have been drilled in the uppermost 500 m of the crust (Kukkonen et al., 2000). At deeper levels, boreholes are rare (only ~10 have reached depths >1 km in Finland) and cannot represent the diversity of the deeper Fennoscandian crust. Where data are available, bacterial communities and saline brines indicate little groundwater movement, suggesting that *permeability is too low or there is no hydro-or thermodynamic force driving deep fluid flow circulation* (Purkamo et al., 2016).

3. Novel Science and Understanding

It is broadly accepted that processes like rock fracturing and mineral alteration are key for defining the fluid and thermal flow properties of *higher-enthalpy geothermal reservoirs* (Duwiquet et al., 2021; Figure 1). Conversely, fundamental knowledge of how these processes are likely to affect deep crystalline reservoir formation at *lower-enthalpy conditions is lacking*. Therefore, new research is necessary to understand variables such as:

i. The relationships between fracturing, faulting and mineral alteration;
ii. The thermal conductivity and geomechanical strength of fractured and altered rocks;
iii. The pore-space morphology and connectivity of complex crystalline reservoirs;
iv. The permeability ratio between stable crustal fault zones and their host rocks;
v. The size and geometry of fracture networks near ancient igneous intrusions;
vi. The ability of geophysical methods to detect discrete fracture networks.

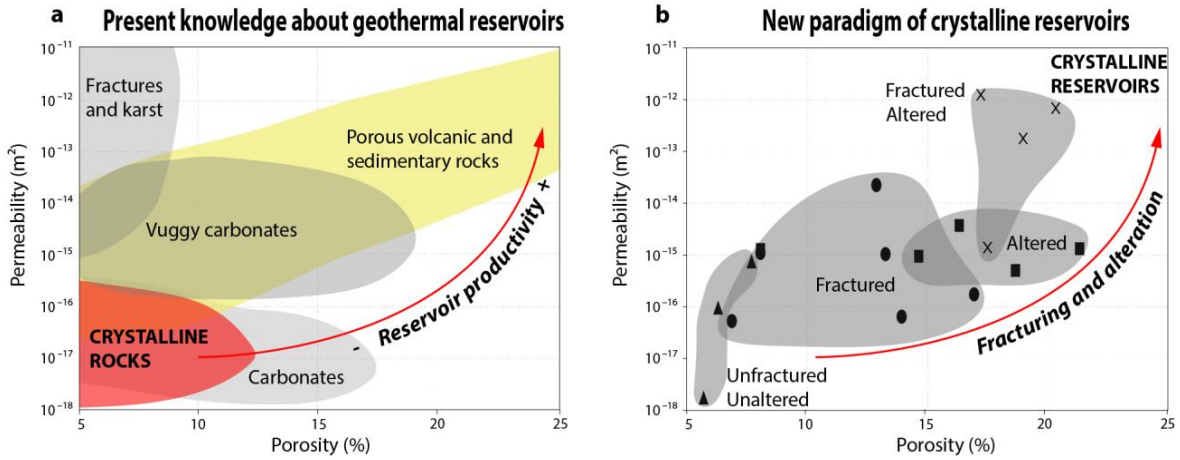

Figure 1. Typical porosity and permeability plots of diverse rock types adapted from (a) Jolie et al., (2021) and (b) Duwiquet et al., (2021).

4. Our New Endeavor

In 2020-2021, the Geological Survey of Finland perforated a new deep drillhole to test a large geophysical anomaly that connects the Paleoproterozoic Koillismaa-Näränkävaara layered igneous complexes, which outcrop in the Central Karelian Province, Eastern Finland. Particularly towards the drillhole bottom (ca 1-1.7 km deep), the broad occurrence of highly

fractured mafic-ultramafic and coeval granitic rocks provides a rare opportunity to evaluate the reservoir and thermal properties of crystalline rocks located in deep cratonic settings away from active volcanic or rifting areas.

We performed a detailed petrographic description of the lowest 700 m of the Koillismaa Deep Drillhole (~1000-1724 m) and conducted a suite of laboratory experiments on selected rocks, including petrophysical (density, porosity, permeability, elastic wave velocity), thermal (conductivity, diffusivity, specific heat capacity), and analytical tests (3D computed tomography scanning and micro XRF spectrometry) to investigate the processes that form deep geothermal targets in relatively low-enthalpy (<150 °C) crystalline settings.

Our results indicate that the geothermal properties of the bedrock penetrated by the Koillismaa Deep Drillhole are primarily controlled by fracturing and mineral alteration, and secondarily by their mineral composition (Figure 2). Open fractures with apertures up to 20 mm typically occur within granitic rocks and near lithological contacts or fault zones characterized by slickenlines and a cataclastic texture, the latter associated with intergranular porosity. Mafic-ultramafic rocks are usually fragile and desegregate in contact with water, thus, we could not assess the impact of their fracture networks on reservoir formation.

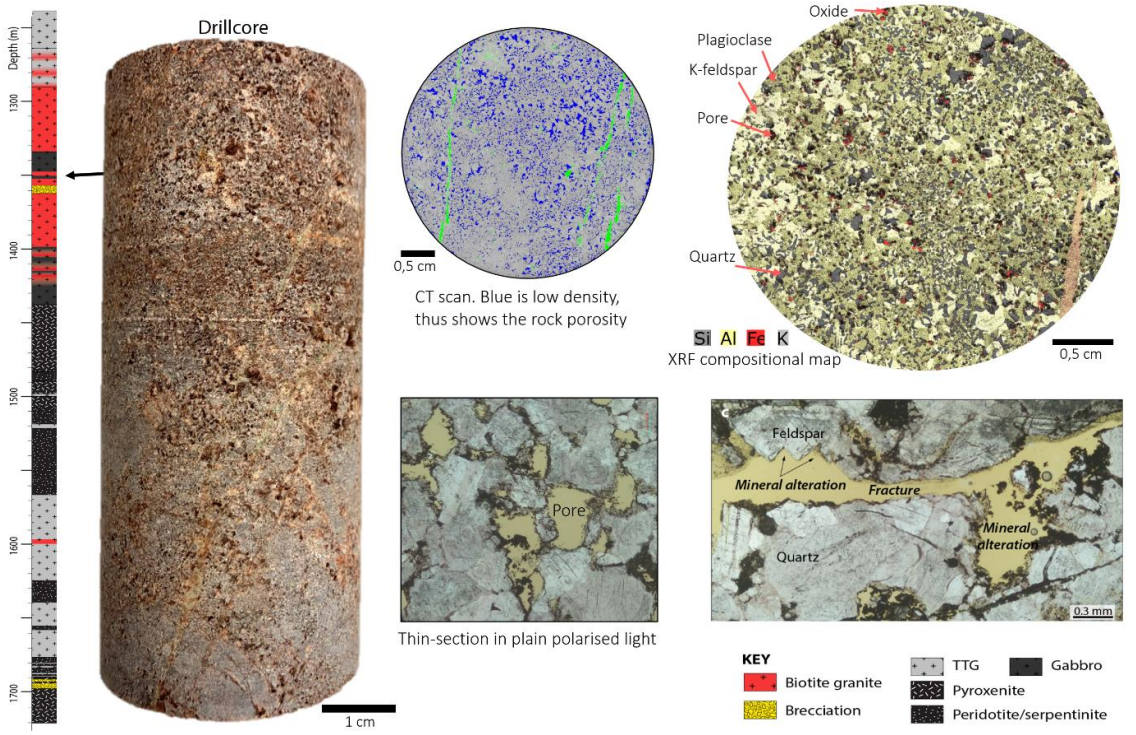

Figure 2. Drillcore photograph, CT scan image, XRF compositional map, and thin-section photographs showing pores and minerals within the altered and fractured biotite granite recovered from 1351 m deep.

Mafic-ultramafic lithologies typically have low thermal conductivity (<2.90 W/mK), high specific heat capacity (681 J/kgK), low porosity (<2%), and are commonly associated with widespread chlorite, epidote, and serpentine precipitation that infill any pre-existing porosity. Altered granitic rocks show pervasive moldic porosity (up to 17%) with pore diameters up to 3 mm formed by partial or total dissolution of mafic minerals, mainly biotite. These altered granitic rocks have the lowest thermal conductivity and highest specificity heat capacity (1.75 W/mK and 794 J/kgK, respectively) whereas unaltered end-members show an inversely proportional trend (up to 3.27 W/mK and down to 505 J/kgK, respectively).

Collectively, these results indicate that altered granitic rocks may constitute potential targets for geothermal production, while the mafic-ultramafic lithologies more likely act as an insulator body with high thermal mass capacity and thus could constitute a heat source.

5. Conclusions and further work

Unlocking the full potential of deep geothermal resources in crystalline settings beyond volcanic and rifting areas will require novel research and significant technological innovation. Crystalline rocks characteristically have low matrix porosity and low matrix permeability. However, substantially large (>1 km^3) geological structures such as *crustal fault zones and the contact zone of ancient igneous intrusions may host prolific crystalline reservoirs at depths >1 km,* as suggested by the Koillismaa Deep Drillhole.

In both cases, novel research from active geothermal areas and our preliminary observations in the Fennoscandian Shield suggest that (i) these structures form connected fracture networks that can create pathways for deep groundwater circulation, which (ii) induces mineral alteration and dissolution, (iii) enlarges the fracture size and aperture, (iv) increases pore-throat radius, (v) reduces fluid flow tortuosity, and (vi) expands the reservoir volume – all critical factors that enhance the performance of geothermal reservoirs.

Determining these variables (particularly the effects of fracturing and mineral dissolution) is still in its infancy and is critical in defining a new paradigm of crystalline reservoir formation in low-enthalpy settings. In addition, further research should focus on improving geophysical methods to identify subsurface fractured and altered zones.

6. Acknowledgements

Several people have been involved in characterising the Koillismaa Deep Drillhole rocks and we much appreciate their efforts and contribution. In particular, we thank Arto Peltola for the outstanding quality of thin-section, Satu Vuoriainen for the diligently work with our challenging fractured and altered rocks, and Teppo Arola for the fruitful discussions.

7. References:

Arnórsson, S., Thórhallsson, S., Stefánsson, A., 2015. Utilization of geothermal resources. In: The Encyclopedia of Volcanoes. https://doi.org/10.1016/B978-0-12-385938-9.00071-7

Duwiquet, H., Guillou-Frottier, L., Arbaret, L., Bellanger, M., Guillon, T., Heap, M.J., 2021 Crustal Fault Zones (CFZ) as Geothermal Power Systems: A Preliminary 3D THM Model Constrained by a Multidisciplinary Approach, Geofluids, Article ID 8855632, 24 pages. https://doi.org/10.1155/2021/8855632

Geological Survey of Finland. 2022. Unpublished numerical models based on the Deep Geothermal Energy Potential Maps of Finland. https://hakku.gtk.fi/en/locations/ search?location_id=194

Heap, M.J., Kennedy, B.M., 2016. Exploring the scale-dependent permeability of fractured andesite: Earth and Planetary Science Letters, 447, 139-150. doi:10.1016/j.epsl.2016.05.004.

Jolie, E., Scott, S., Faulds, J., et al., 2021. Geological controls on geothermal resources for power generation. Nat Rev Earth Environ 2, 324–339. https://doi.org/10.1038/s43017-021-00154-y

Kukkonen, I.T., 2000. Geothermal energy in Finland. Proceedings World Geothermal Congress, Japan. https://www.geothermal-energy.org/pdf/IGAstandard/WGC/2000/R0778.PDF

Piipponen, K., Martinkauppi, A., Korhonen, K., Vallin, S., Arola, Teppo., Bischoff, A., Leppäharju, N., 2022. The deeper the better? A thermogeological analysis of medium-deep borehole heat exchangers in low-enthalpy crystalline rocks. Geotherm Energy, 10, 12. https://doi.org/10.1186/s40517-022-00221-7

Purkamo, L., Bomberg, M., Kietäväinen, R., Salavirta, H., Nyyssonen, M., Nuppunen-Puputti, M., Ahonen, L., Kukkonen, I., Itävaara, M., 2016, Microbial co-occurrence patterns in deep Precambrian bedrock fracture fluids, Biogeosciences, vol. 13, no. 10, pp. 3091-3108. https://doi.org/10.5194/bg-13-3091-2016

Villeneuve, M.C., Heap, M.J., Kushnir, A.R.L. et al. 2018. Estimating in situ rock mass strength and elastic modulus of granite from the Soultz-sous-Forêts geothermal reservoir (France). Geotherm Energy 6, 11. https://doi.org/10.1186/s40517-018-0096-1

Paleoproterozoic metamorphism of Peräpohja and Kuusamo Belts: a combined U-Pb monazite, apatite and garnet study

K. Cutts[1], P. Hölttä[1] and R. Lahtinen[1]

[1]Geological Survey of Finland, P.O. Box 96, FI-02151 Espoo, Finland
E-mail: kathryn.cutts@gtk.fi

In this article we utilize petrochronological methods to investigate the Palaeoproterozoic metamorphism occurring in the Peräpohja and Kuusamo Belts. These rocks are polydeformed during the Svecofennian Orogeny (1.91-1.78 Ga). We are using a novel U-Pb garnet dating approach in combination with in situ monazite and apatite dating.

Keywords: lithosphere, crust, upper mantle, Fennoscandia, Helsinki

1. General

The Central Lapland terrain consist of the Central Lapland Granitoid Complex (CLGC) which is bordered by 2.5-1.9 Ga metasedimentary successions that have been polydeformed and metamorphosed at amphibolite to local greenschist facies between 1.91 and 1.78 Ga (Fig. 1). This study utilises petrochronological methods on three broad regions within the Central Lapland terrain in order to unravel the P-T-t evolution of each region, their relationship with each other, and the plate tectonic processes that caused this deformation. Rocks of the east-west trending Peräpohja Belt contain chlorite-muscovite-biotite to cordierite-andalusite in the south. In the north of the belt the rocks are garnet migmatites overprinted by staurolite-kyanite assemblages, which are in turn overprinted by late cordierite-andalusite. To the southeast, the ENE-WSW trending Kuusamo Belt contains garnet-staurolite assemblages with early coarse biotite and fine-grained garnet, and late coarse staurolite. P-T modelling for this sample indicate early garnet growth conditions of 4 kbar and 550 °C, reaching peak metamorphic conditions of 8 kbar and 650 °C. The northernmost belt, the Central Lapland Belt contains coarse kyanite-biotite assemblages overprinted by cordierite and sillimanite, while further north, andalusite-chlorite-muscovite-chloritoid schists increase in grade to andalusite-kyanite gneisses overprinted by kyanite-staurolite. Most monazite U-Pb age data from the metasedimentary rocks yield ages of 1.75-1.81 Ga (Höltta et al., 2019). In contrast, most dated samples from the CLGC give ages of ca. 1.87-1.92 Ga. Younger ages of 1.76 -1.78 Ga are also obtained from late intrusive veins in the central Lapland area (Höltta et al., 2019). Lahtinen et al. (2015) suggested that Central Lapland was affected by three metamorphic events at 1.92-1.90 Ga, 1.86-1.85 Ga and 1.83-1.77 Ga. The spread of ages obtained from the CLGC is attributed to the crust remaining at elevated temperature for 120-100 Ma (Lahtinen et al., 2018). The first metamorphic event results from east-vergent thrusting and stacking, whereas younger events are related to far-field collisional effects due to the Svecofennian orogeny.

2. Age results so far

At present, we have only the monazite data collected and processed. For Kuusamo the monazite data has peaks at ca. 1790 Ma with some minor older analyses. In Perapohja, rocks with garnet-kyanite associations overprinted by cordierite preserve older monazite ages of ca. 1880, while low grade garnet-cordierite-andalusite schists only have the younger age population of 1790-1770 Ma. Apatite and garnet dating is planned to gain more insight into the prograde evolution (using garnet ages) and retrograde evolution (using apatite).

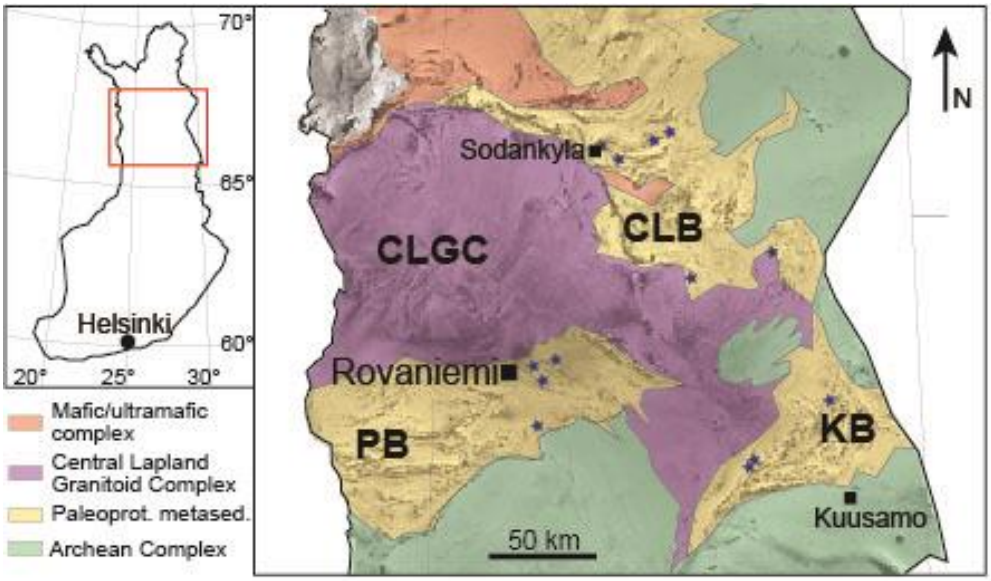

Figure 1. Simplified geological map of the Central Lapland Area overlayed on the total magnetic intensity of Finland. Map area is indicated by the red box on the map of Finland. KB-Kuusamo Belt, PB- Peräpohja Belt, CLB-Central Lapland Belt, CLGC-Central Lapland Granitoid Complex. Blue stars indicate sample locations.

3. Conclusions

While preliminary, the results indicate that it should be possible to tie ages with the metamorphic evolution and also deformation events for the Svecofennian orogenic event in Lapland.

References:

Höltta, P., Huhma, H., Lahaye, Y., Mänttäri, I., Lukkari, S., O'Brien, H., 2019. Paleoproterozoic metamorphism in the northern Fennoscandian Shield: age constraints revealed by monazite. International Geology Review, 62, 360-387.

Lahtinen, R., Huhma, H., Lahaye, Y., Jonsson, E., Manninen, T., Lauri, L.S., Bergman, S., Hellström, F., Niiranen, T., Nironen, M., 2015. New geochronological and Sm–Nd constraints across the Pajala shear zone of northern Fennoscandia: Reactivation of a Paleoproterozoic suture. Precambrian Research, 256, 102–119.

Lahtinen, R., Huhma, H., Sayab, M., Lauri, L.S., Hölttä, P., 2018. Age and structural constraints on the tectonic evolution of the Paleoproterozoic Central Lapland Granitoid Complex in the Fennoscandian Shield. Tectonophysics, 305–325.

Seismic recognition of the faults for geothermal exploration in crystalline rocks: results from the pilot survey in Helsinki

M. Cyz[1], M. Malinowski[1], T. Linqvist[1], E. Virta[2], S. Heinonen[1], T. Arola[1], J. Riissanen[3], S. Mustonen[3], J. Hietava[1] and P. Skyttä[2]

[1]Geological Survey of Finland, FI-02151 Espoo, Finland
[2] Department of Geography and Geology, University of Turku, FI-20014 Turku, Finland
[3] Helen Ltd, 00090 Helen, Finland
E-mail: marta.cyz@gtk.fi

In geothermal resource studies, the recognition of faults and fractures is one of the key components for building hydrogeothermal models and reducing the risk and cost of drilling production wells. The large-scale faults and sets of fractures can be identified with the help of seismic data analysis, especially throughout using seismic interpretation techniques measuring the geometrical components of the features. This study presents the preliminary results of the seismic-based fault detection study conducted in a challenging geothermal site in the Helsinki city area, characterized by geological complexity and operational restrictions.

Keywords: seismic, faults, geothermal, seismic modelling, Helsinki

1. Introduction

Geothermal energy exploitation is of growing interest worldwide, especially in those societally unstable times, the carbon-neutral alternatives to energy resources are in high demand. The same applies to the city of Helsinki, where geothermal energy has been identified as a potential sustainable energy source to generate district heating (Helsingin geoenergiapotentiaali report 2019). In the recognition of the geothermal resources, seismic data analysis can mitigate the exploration risk and cost (e.g. Krawczyk et al., 2019; Siler et al., 2019; Schmelzbach et al., 2016; Alerdi et al., 2015; Hloušek et al., 2015) as it contributes to the building of the 3D geomodels and characterization of the faults and fractures within the reservoirs. One of the basic tools to map large-scale faults and fracture networks from seismic data are seismic attributes, especially those geometry based (for example curvature, azimuth, dip, semblance, similarity) that can highlight the desired features within the reservoir (Chopra and Marfurt, 2007). Even though seismic attributes have been commonly used in various studies, their potential for geothermal exploration in general, and particularly within crystalline rocks is yet to be explored. This study presents preliminary results of the seismic data analysis for the structural interpretation of a planned geothermal well site in the city of Helsinki.

2. Data and methods

The employment of the seismic method for the imaging of crystalline basement is an ambitious task, because of the method's limitations multiplied by crystalline rock specification e.g. high velocities of the rocks, small impedance contrast between the intervals, low signal-to-noise ratio and usually steeply dipping structures diffracting the energy. Additionally, data acquisition in Helsinki city is strongly limited in terms of source accessibility and power, survey design, and the high noise level of the urban environment.

Despite that, 2D/semi-3D seismic data was acquired in the urban environment of Helsinki Central Park (Keskuspuisto; Figure 1) in 2019, using Vibroseis sources (2 x 9.5 t INOVA UniVibe trucks) and a wireless acquisition system (750 channels). The acquisition consisted of one main, approximately 5 km long profile with 10 m receiver spacing, and two shorter, perpendicular lines with 20 m receiver spacing (Figure 1).

The different approaches to seismic data processing were tested, including the processing techniques able to overcome the challenges caused by crystalline rock environment (e.g. dip move-out [DMO] corrections, depth migration application) and recover the steeply dipping features. The final version of the seismic sections, used in this study, was obtained by processing the data in a 3D manner and application of pre-stack depth migration (PSDM) using the velocity model built from first-arrival tomography. The different approaches to seismic data processing were tested, including the processing techniques able to overcome the challenges caused by crystalline rock environment (e.g. dip move-out [DMO] corrections, depth migration application) and recover the steeply dipping features. The final version of the seismic sections, used in this study, was obtained by processing the data in a 3D manner and application of pre-stack depth migration (PSDM) using the velocity model built from first-arrival tomography.

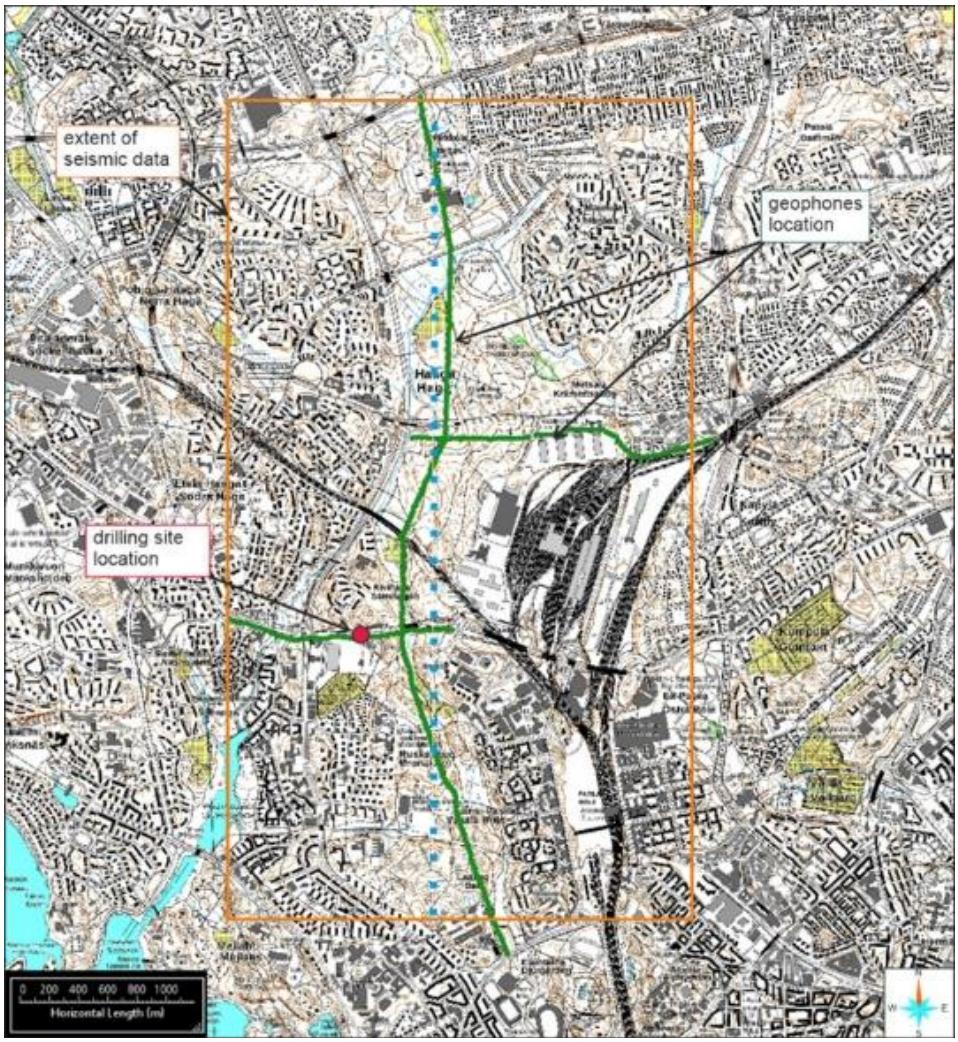

Figure 1. Location of Keskuspuisto semi-3D seismic survey overlaid on the Helsinki city map (map source: National Land Survey of Finland). The green lines mark the locations of geophones; the orange rectangle is the extent of the seismic data; the red dot points to the Ruskeasuo drilling site. The dotted blue line marks the seismic cross-section shown in Figure 2.

Partially based on the seismic data, Helsinki's first medium-depth geothermal well was drilled in the Ruskeasuo area. The planned depth of the well was about 2.5 km with an expected temperature of 40 degrees. Unfortunately, the drilling was stopped at the depth of ~850 m, where a major fracture zone disabled further drilling. Full waveform sonic logging was performed in the well, resulting in information about the P- and S-wave velocities down to 600 m depth, showing the typical values for granitic rock without many changes within the interval. Furthermore, the rock cuttings from drilling are being analyzed for lithological and mineralogical content. Recently, also the surface geological mapping of the Ruskeasuo area has been performed to better understand the geology, including faults and fracture systems of the surrounding, manifesting mostly the steeply dipping structures along the ground surface. Such mapping can be somewhat extrapolated towards depth and further corroborated with the seismic data, especially focused on the recognition of larger-scale faults.

3. Initial results and discussion

A number of seismic attributes has been calculated from the depth-migrated 3D seismic volume, including the geometrical attributes highlighting faults and aiming stratigraphic recognition such as, among others, curvature (min, max, most-positive, most-negative), semblance, dip and azimuth or similarity-based fault-likelihood. Some of those, standalone does not bring reasonable results, but should be combined and superimposed to emphasize the desired features. On the other hand, some, such as fault likelihood are able itself to point out the possible steeply dipping structures/faults. Figure 2 present an example cross-section through the major profile (see the location on the map on the Figure 1) and corresponding thinned fault likelihood.

Special attention in the analysis of the seismic data was paid to the Ruskeasuo drilling site and the fracture zone encountered during drilling. The initial result from the analysis indicated possible correlation of the fault observed on the surface, seen on the seismic attributes sections, and reached while drilling.

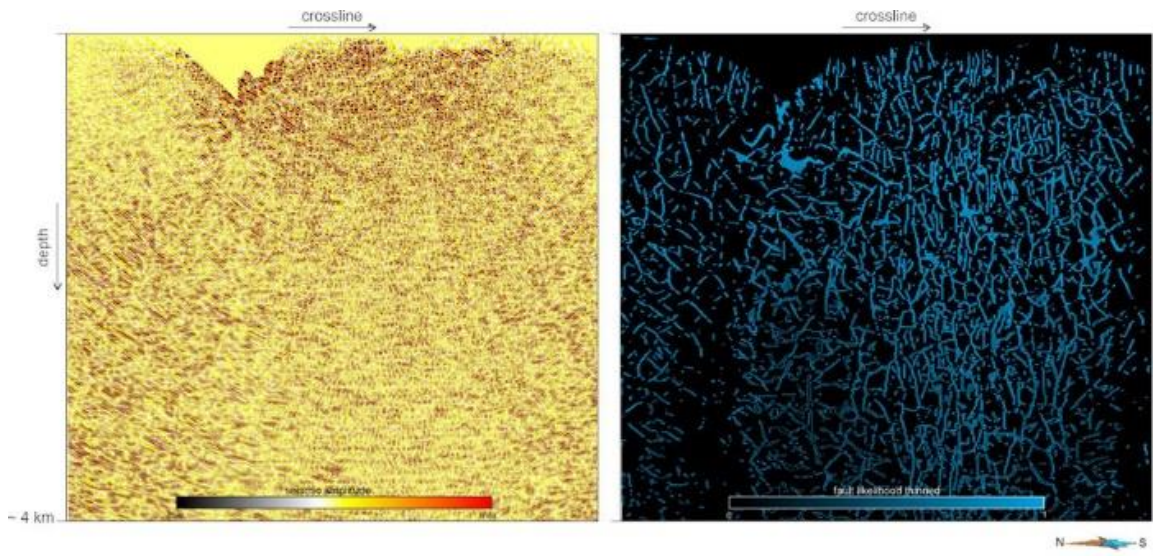

Figure 2. Example cross-section through the migrated seismic data close to the major acquisition line and corresponding seismic attribute of thinned fault likelihood.

Further analysis will include the extended analysis of the correlation between the seismic data and results from the surface geological mapping. Also, seismic forward modelling is in progress to better understand seismic imaging in terms of the recognition of the steeply dipping faults in the hardrock bedrock and the complexness of the Keskuspuisto/Ruskeasuo site. The obtained synthetic seismic data will provide the basis for the seismic-based faults and fractures prediction using both seismic attributes and more advanced AI/Machine Learning techniques.

References:

Aleardi, M., Mazzotti, A., Tognarelli, A., Ciuffi, S., Casini, M., 2015. Seismic and well log characterization of fractures for geothermal exploration in hard rocks. Geophysical Journal International, 203(1), pp.270-283.

Chopra, S., Marfurt, K., 2007, Seismic curvature attributes for mapping faults/fractures, and other stratigraphic. CSEG-Recorder, VOL. 32 NO. 09.

Helsingin geoenergiapotentiaali, 2019. https://www.hel.fi/kaupunkiymparisto/fi/julkaisut-ja-aineistot/julkaisuja-sarja (In Finnish)

Hloušek, F., Hellwig, O., Buske, S., 2015. Three-dimensional focused seismic imaging for geothermal exploration in crystalline rock near Schneeberg, Germany. Geophysical Prospecting, 63(4-Hard Rock Seismic imaging), pp. 999-1014.

Krawczyk, C.M., Stiller, M., Bauer, K., Norden, B., Henninges, J., Ivanova, A., Huenges, E., 2019. 3-D seismic exploration across the deep geothermal research platform Groß Schönebeck north of Berlin/Germany. Geothermal Energy, 7 (1), pp.1-18.

Schmelzbach, C., Greenhalgh, S., Reiser, F., Girard, J.F., Bretaudeau, F., Capar, L., Bitri, A., 2016. Advanced seismic processing/imaging techniques and their potential for geothermal exploration. Interpretation, 4 (4), pp.SR1-SR18.

Siler, D.L., Faulds, J.E., Hinz, N.H., Dering, G.M., Edwards, J.H., Mayhew, B., 2019. Three-dimensional geologic mapping to assess geothermal potential: examples from Nevada and Oregon. Geothermal Energy, 7 (1), pp.1-32.

Critical mineral raw material potential in the Nordic countries

P. Eilu[1]

[1]Geological Survey of Finland, Espoo, Finland
E-mail: pasi.eilu@gtk.fi

Finland, Norway, Sweden, and the ice-free part of Greenland jointly contain a large resource base of an extensive set of mineral commodities essential and critical for the economy of both the Nordic countries and the entire Europe. For some commodities, the volume of known and assumed resources is significant even in the global scale. The main reason for the Nordic resource richness is the diversified geology covering nearly all major orogenic events from the Palaeoarchaean to the Holocene. These events can be linked to nearly all post-Archaean major stages of supercontinent evolution of the Earth. In the Archaean, the relationship is with superplume(?), rifting, and Neoarchaean supercontinent evolution.

Keywords: critical minerals, mineral resources, metallogeny, plate tectonics, Finland, Sweden, Norway, Greenland

1. Introduction

Since the early 2000s, all major mineral-consuming countries and the EU have been assessing the access to raw materials essential for their industries. Critical raw materials (CRM) are defined as being of high importance to the economy and having major risks of supply (e.g., Blengini et al., 2020; Lee & Cha, 2021). The latest CRM list for the EU contains 28 mineral/metal entries, of which three are metal groups (HREEs, LREEs and PGMs). The number of mineral commodities listed as critical just keeps increasing. This is because 1) increasing global demand of manufactured products, 2) increasing range and complexity of modern technologies, and 3) the acute need towards a low-carbon society to mitigate climate change (IEA, 2021; Marscheider-Weidemann et al., 2021). Also affecting are the facts that, for all of the CRMs, there are no indications that the demand from almost any industrial sector is significantly decreasing, and that even the most effective recycling will not cover more than 10–25 % of the increasing demand of the metals and minerals (Hund et al., 2020; IEA, 2021). On top of these factors, we now have another, extremely acute issue: the war in Ukraine which has an immediate effect on global supply of not just fossil energy and foodstuffs, but also on the metals and minerals that Russia, Ukraine and/or Belarus have had a large share in the international trade (BGS, 2022). There currently are no major indications that any of these issues would go away in short nor medium term. These developments mean that probably more commodities will be added into the near-future CRM lists, especially for Europe.

2. Nordic CRM resources

The land area of Finland, Norway, Sweden, and the ice-free part of Greenland forms perhaps the most significant domain of the CRM mine production, resource base, and potential in Europe. This is essentially grounded in that: 1) the bedrock is a product of multiple orogenic and non-orogenic events covering a very extensive part of the crustal history of the Earth, 2) it is, hence, similar to major mineral-rich terrains globally but uniquely for Europe, 3) the Nordic countries jointly comprise a land area (1.5 million km^2) similar in size to the most mineral-rich parts of Canada, USA, Australia, South Africa, or Brazil, 4) a continuous presence of modern mining, and 5) abundant locally developed leading-edge mineral exploration, mining and ore processing technology (e.g., Eilu, 2012; Boyd et al., 2016; Kolb et al., 2016; Eilu et al., 2021).

The currently available, harmonised, information of CRMs in the Nordic countries (end-

2020 data) shows that, for the EU, EAA, and EU-member candidate countries (excluding Turkey), the only mine production of Co and phosphate is from *Finland*, and of Ti from *Norway*. Also, *Finnish* mines produce 95 % of the PGEs and 60 % of Cr, *Norwegian* mines 90 % of flake graphite, and *Swedish* mines 90 % of Te in Europe (Zhou & Damm 2020, BGS 2022). For CRM resources, commodity-specific, selected data are listed in Table 1, based on national mineral deposit databases and on European and global demand data (Eilu et al. 2021 and references therein, and BGS, 2022; USGS 2022).

Table 1. Nordic CRM potential in European and global context (end-2020 data). Large Nordic resources in the European annual demand context in bold.

	Global demand (t)	European demand 2020 (t)	Nordic (t)		European mine production (t)	Nordic prod. of European demand **(%)**	Nordic resources ***years*** of European demand	Nordic resources ***years*** of Global demand
			Mine production	Known resources				
Be	242	60	0	989	0	0	16	4.1
Co	131,500	28,600#	1,454	502,818*	1,454	5	18	3.8
Cr	20,000,000	630,000	321,996	**43,830,000***	321,996	51	70	2.2
Ga	600	30	0	**21,300**	0	0	710	36
Graphite (flake)	1,000,000	120,000#	16,000	**10,500,000**	17,000	13	88	11
Hf	80	36	0	**1,107,000**	36	0	30,700	13,800
Li	83,000	4,322#	0	78,240*	835	0	18	0.9
Nb	75,000	NA	0	**6,645,000**	0	0	NA	89
Ni	2,375,000	250,200#	41,429	7,930,000*	49,539	17	32	3.3
Phos-phate	78,000,000	1,183,000	182,600	**322,985,000**	182,600	15	273	4.1
Pt + Pd	520	122	2.14	1,150*	2.27	2	9	2.2
REE	206,400	4,500#	0	**36,139,000***	0	0	8,000	175
Sb	110,000	1,500	0	26,219	0	0	17	0.2
Sc	25	7	0	**2,180**	0	0	311	87
Silicon metal	2,500,000	435,000	240,000	**31,600,000**	302,000	55	73	13
Sr	167,013	50,000	0	**12,500,000**	71,577	0	250	75
Ta	2,100	400	0	**1,100,000**	13	0	2750	524
Te	562	NA	42	1,053	45	NA	NA	1.9
Ti	2,400,000	1,500,000	189,000	**180,200,000***	189,000	13	120	75
V	105,000	12,000	0	**6,914,000***	0	0	576	66
W	78,400	2,200	0	7,514*	0	0	3	0.1
Zr	888	NA	0	**30,208,000**	0	0	NA	34,000

* Additional *assumed* ("undiscovered") resources, Finland: 108,000 t Co, 350 Mt Cr, 510,000 t Li, 5.9 Mt Ni, 17,600 t Pd+Pt, 2.7 Mt REE, 380 Mt Ti, 13 Mt V; Greenland: 3.8 Mt Ni, 65 Mt Ti, 500,000 t W. If realised, these would also bring the Nordic Li, Ni, PGE, and W resources large in the European context.
# Assumed to be in strong growth due to increasing demand in climate change mitigation.

3. Nordic metallogeny events

This large resource base and potential is directly related to the geology of the Nordic bedrock and cover units, combined with the extensive exploration, bedrock geology investigations, and metallogeny and mineral potential assessments done in the region (e.g., Henriksen et al., 2009; Eilu, 2012; Boyd et al., 2016; Kolb et al., 2016; Rasilainen et al., 2017). Essentially, there are rocks and mineral deposits from nearly all major orogenic events since the Palaeoarchaean, as summarised in Table 2.

Table 2. Significant Nordic CRM metallogeny events in plate-tectonic context.

Age (Ga)	(Plate-)tectonic setting	Major CRM deposit types		CRMs in the deposits	
		Fennoscandia	Greenland	Fennoscandia	Greenland
3.6–2.75	Rifting, superplume events, collision?	Komatiitic Ni; Mafic-ultramafic intrusion Ni-PGE	Komatiitic Ni; Mafic-ultramafic intrusion Ni-PGE; Layered intrusion Cr, Ti-V	Co, Ni, PGE	Co, Cr, Ni, PGE, Ti, V
2.75–2.6	Kenorland assembly	LCT-pegmatites; Carbonatite P	?	Be, Li, P, Ta (Hf+Zr?)	
2.50–2.44	Kenorland initial break up	Layered intrusion Cr, PGE(-Ni-Cu), Ti-V	?	Co, Cr, Ni, PGE, Ti, V	
2.2–1.95	Supercontinent break up	Komatiitic Ni; Mafic-ultramafic intrusion Ni-PGE; Alkaline–peralkaline intrusions; Mafic intrusion Ti-V; Soapstones	?	Co, Hf, Mg(?), Nb, Ni, PGE, REE, Ta, Ti, V, Zr	
2.0?–1.94	Passive margins	Black shale polymetallic	?	Co, Ni, V	
1.93–1.48	Columbia assembly	VMS; Skarn W; Orogenic Sb-Au; Orogenic intrusion Ni; Alkaline intrusion Sc; LCT & NYF pegmatites; Quartz veins; Alkaline–peralkaline & carbonatite intrusions; Graphitic mica gneiss; Mafic intrusion Ti-V; Kiruna Fe; IOCG	Orogenic intrusion Ni-PGE; Graphitic mica gneiss; VMS; Peralkaline hydrothermal/intrusive	Be, Bi, Co, Grf, Hf, Li, Ni, P, REE, Sb, Sc, Si, Ta, Te, Ti, V, W, Y, Zr	Bi(?), Co, Grf, Ni, PGE, REE, Sb
1.25–1.14	Columbia break up	Mafic intrusion Ti-V	Alkaline–peralkaline intrusions; Mafic intrusion Ti-V; Mafic-ultramafic intrusion Ni	Ti, V	Be, Co, Hf, Ni, Nb, P, PGE, REE, Sc, Ta, Ti, V, Zr
1.10–0.92	Rodinia assembly	Quartz veins; Mafic intrusion Ti; Orogenic intrusion Ni	?	Co, Ni, Si, Ti	
0.82–0.54?	Rodinia break up	Alkaline–peralkaline & carbonatite intrusions	Alkaline–peralkaline & carbonatite intrusions	P, REE, Nb, Ta, Hf, Zr	P, REE, Nb, Ta, Hf, Zr
0.60–0.43	Passive margins	Alum shale; Phosphorite	SEDEX	Co, Mo, Ni, P, V	Ge(?), Te(?)
0.43–0.39	Pangaea assembly	VMS; Orogenic intrusion Ni; Quartz veins; Skarn W; Mafic intrusion Ti; Eclogite	Magmatic-hydrothermal W-Sb; Orogenic Au-Sb; MVT	Bi, Co, Ni, Sb, Si, Te(?), Ti, W	Ge(?), Sb, W
0.38–0.24	Pangaea rifting	Alkaline–peralkaline & carbonatite intrusions; Vein Ag; porphyry Mo	Evaporite	Co, Hf, Mo, Nb, P, REE, Sr, Ta, Zr	Sr
0.16–0.05	Pangaea break up	?	Alkaline–peralkaline & carbonatite intrusions; Mafic-ultramafic intrusions; Porphyry Mo-W		Co, Ga, Hf, Mo, Nb, P, PGE, REE, Sr, Ta, Ti, V, W, Zr
0.02–	Passive margins	?	Heavy mineral sands		Hf, REE(?), Ti, Zr

4. Conclusions

Finland, Greenland, Norway, and Sweden jointly form one of the most significant mining regions in Europe with, probably, the largest critical mineral raw material potential. Ongoing and, especially, the planned global climate mitigation efforts require very large volumes of mining of a large set of metals and minerals. For this "Green Energy Transition", and for other technological developments, the Nordic countries provide a major sustainable European

resource base. This resource potential directly reflects the large land area and the very extensive geological history, from the Archaean to the Recent, with all supercontinent assembly and break up stages of the Earth.

Acknowledgements
This review is largely based on joint work between GEUS, GTK, NGU, SGU, MMR (Govt. Greenland), Reykjavik University, and the National Energy Authority of Iceland – people crucial in the work are the authors of the report by Eilu et al. (2021), and in a two-decade long work in the FODD Project. The opinions expressed here are those of this author.

References:

BGS, 2022. World mineral production 2016−2020. British Geological Survey, Nottingham. 88 p. https://www2.bgs.ac.uk/mineralsuk/download/world_statistics/2010s/WMP_2016_2020.pdf

Blengini, G.A., Latunussa, C.E.L., Eynard, U., Torres de Matos, C., Wittmer, D., Georgitzikis, K., Pavel, C., Carrara, S., Mancini, L., Unguru, M., Blagoeva, D., Mathieux, F., Pennington, D., 2020. Study on the EU's list of Critical Raw Materials, Final Report. 152 p. doi:10.2873/11619

Boyd, R., Bjerkgård, T., Nordahl, B., Schiellerup, H., (eds.) 2016. Mineral resources in the Arctic. Geol. Surv. Norway, Special Publ., 483 p. https://www.ngu.no/en/publikasjon/mineral-resources-arctic

Eilu, P., (Ed.) 2012. Mineral deposits and metallogeny of Fennoscandia. Geol. Surv. Finland, Special Paper 53. 401 p. https://tupa.gtk.fi/julkaisu/specialpaper/sp_053.pdf

Eilu, P., Bjerkgård, T., Franzson, H., Gautneb, H., Häkkinen, T., Jonsson, E., Keiding, J.K., Pokki, J., Raaness, A., Reginiussen, H., Róbertsdóttir, B.G., Rosa, D., Sadeghi, M., Sandstad, J.S., Stendal, H., Þórhallsson, E.R., Törmänen T., 2022. The Nordic supply potential of critical metals and minerals for a Green Energy Transition. Nordic Innovation Report, 93 p. https://norden.diva-portal.org/smash/get/diva2:1593571/FULLTEXT02

Henriksen, N., Higgins, A.K., Kalsbeek, F., Pulvertaft, T.C.R., 2009. Greenland from Archaean to Quaternary. Descriptive text to the 1995 Geological map of Greenland, 1:2 500 000. 2nd edition. Geol. Surv. Denmark and Greenland, Bull. 18, 126 p. https://geusbulletin.org/index.php/geusb/article/view/4993

Hund, K., La Porta, D., Fabregas, T.P., Laing, T., Drexhage, J., 2020. Minerals for Climate Action: The Mineral Intensity of the Clean Energy Transition. International Bank for Reconstruction and Development/The World Bank. 110 p. https://pubdocs.worldbank.org/en/961711588875536384/Minerals-for-Climate-Action-The-Mineral-Intensity-of-the-Clean-Energy-Transition.pdf

IEA, 2021. The role of critical minerals in clean energy transitions.IEA, Paris, 283 p. www.iea.org/reports/the-role-of-critical-minerals-in-clean-energy-transitions

Kolb, J., Keiding, J.K., Steenfeldt, A., Secher, K., Keulen, N., Rosa, D., Stensgaard, B.M., 2016. Metallogeny of Greenland. Ore Geol. Rev. 78, 493–555. https://doi.org/10.1016/j.oregeorev.2016.03.006

Lee, K., Cha, J., 2021. Towards improved circular economy and resource security in South Korea. Sustainability 13, 17. http://dx.doi.org/10.3390/su13010017

Marscheider-Weidemann, F., Langkau, S., Baur, S.-J., Billaud, M., Deubzer, O., Eberling, E., Erdmann, L., Haendel, M., Krail, M., Loibl, A., Maisel, F., Marwede, M., Neef, C., Neuwirth, M., Rostek, L., Rückschloss, J., Shirinzadeh, S., Stijepic, D., Tercero Espinoza, L., Tippner, M., 2021. Rohstoffe für Zukunftstechnologien 2021. DERA Rohstoffinformationen 50. 370 p. https://www.deutsche-rohstoffagentur.de/DE/Gemeinsames/Produkte/Downloads/DERA_Rohstoffinformationen/rohstoffinformationen-50-en.pdf?__blob=publicationFile&v=2

Rasilainen, K., Eilu, P., Halkoaho, T., Heino, T., Huovinen, I., Iljina, M., Juopperi, H., Karinen, T., Kärkkäinen, N., Karvinen, A., Kontinen, A., Kontoniemi, O., Kousa, J., Lauri, L.S., Lepistö, K., Luukas, J., Makkonen, H., Manninen, T., Niiranen, T., Nikander, J., Pietikäinen, K., Räsänen, J., Sipilä, P., Sorjonen-Ward, P., Tiainen, M., Tontti, M., Törmänen, T., Västi, K., 2017. Assessment of undiscovered metal resources in Finland. Ore Geology Reviews, 86, 896–923. https://doi.org/10.1016/j.oregeorev.2016.09.031

USGS 2022. Mineral commodity summaries 2022. U.S. Geological Survey. 202 p. https://doi.org/10.3133/mcs2022.

Zhou, Q., Damm, S., 2020. Supply and demand of natural graphite. DERA Rohstoffinformationen 43, 36 p. https://www.deutsche-rohstoffagentur.de/DERA/DE/Downloads/Studie%20Graphite%20eng%202020.pdf?__blob=PublicationFile&v=3

Integrated lineament interpretation

J. Engström[1], N. Ovaskainen[1], M. Markovaara-Koivisto[1] and N. Nordbäck[1]

[1]Geological Survey of Finland, P.O. Box 96, 02151 Espoo, Finland
E-mail: jon.engstrom@gtk.fi

During the recent years the number of infrastructure and geothermal projects has been increasing, which also increases the demand on knowledge and research about brittle structures of the bedrock, such as fractures and faults. Therefore, the Geological Survey of Finland has produced a new country-wide lineament interpretation from the whole of Finland. This resulted in four new lineament datasets: a magnetic lineament interpretation, an electromagnetic interpretation, a LiDAR interpretation, and a joint integration of all the three datasets.

Keywords: lineament, LiDAR, magnetic, electromagnetic, brittle structures

1. Introduction

The initial method for lineament interpretation utilized topographical maps of the Earth's surface. The topographical highs and depressions such as valleys and slopes often form linear continuities along which an interpreter could place an interpreted continuous semi-linear one-dimensional line, a lineament (Hobbs, 1904, 1911). Today, lineament interpretations are based on photographs, topographical and geophysical sources. These are e.g., aerial photos, elevation data, multi-spectral sensing, laser, radar, and airborne geophysical data comprising magnetic, electromagnetic, radiation measurements, and gravimetric measurements.

The understanding of the subsurface brittle bedrock structures is essential in several aspects such as groundwater movement, underground construction and seismic hazards. As the typical first step to map potential underground structures is to identify those that are visible on the surface. Motivation for a new lineament interpretation was further caused by the release of the new country-wide high resolution Light Detection and Ranging (LiDAR) -data (2008-2019; 0.5 points per square meter) from the National Land Survey of Finland which substantially increased the accuracy of the Digital Elevation Model (DEM), the primary dataset used for lineament interpretation. The accuracy of the new digital elevation model also allows interpretations in multiple scales, as the accuracy of the model is no longer the limiting factor in interpretation, rather the time-investment required for the interpretation.

2. Study method and data utilized for the interpretation

The new country-wide lineament interpretation, performed in the scale of 1:500 000, started in 2019 and was finished in 2021. Several geologists and researchers at Geological Survey of Finland (GTK) were involved in the work as interpreters of the lineaments using multiple datasets. The primary dataset utilized in the interpretation was the recently surveyed low-altitude airborne LiDAR-based topographical digital elevation model, produced by GTK. This new accurate airborne LiDAR-based dataset is exceptional for the purpose of accurate topographic lineament interpretation. The high-resolution LiDAR point cloud data, collected by the National Land Survey of Finland, was processed at GTK into a digital elevation model which represents the bare earth surface. We used the procedure described by Palmu et al. (2015), with the standardized visualization that consists of the 2-meter grid DEM (point density for the cloud point data is 0.5 points per square meter and elevation accuracy 0.3 meters) with the height colour classification set to calculate statistics from the current extent of the display. The interpretation was continued into the sea areas with the aid of the sea-bottom topography,

referred to as bathymetry, that was acquired from the European Emodnet bathymetry website (https://www.emodnet-bathymetry.eu/). The remote-sensing data sources used in the new interpretation are low-altitude airborne geophysical data that comprise magnetic and electromagnetic measurements, that are available in the GTK's database as geophysical maps. The magnetic maps used were shaded magnetic anomaly grayscale, tilt derivative and filtered magnetic grayscale, in which the lineaments were interpreted to the minima, maxima and discontinuity features. The electromagnetic maps were interpreted based on the minima of the airborne electromagnetic dataset with 3 kHz quadrature component grayscale.

3. Results

The lineaments were first interpreted using the three separate datasets (topographic, magnetic and electromagnetic) and were later integrated into a single integrated lineament interpretation map where lineaments interpreted from the separate datasets were combined. The LiDAR lineaments were digitized with a multidirectional, oblique-weighted hillshade layered on top of the digital elevation model and 1 579 lineaments were identified (Figure 1A). The 1 244 electromagnetic lineaments were interpreted from single grayscale map (Figure 1B), while magnetic interpretation utilized 3 different magnetic raster maps to compile a magnetic lineament map with 983 lineaments (Figure 1C).

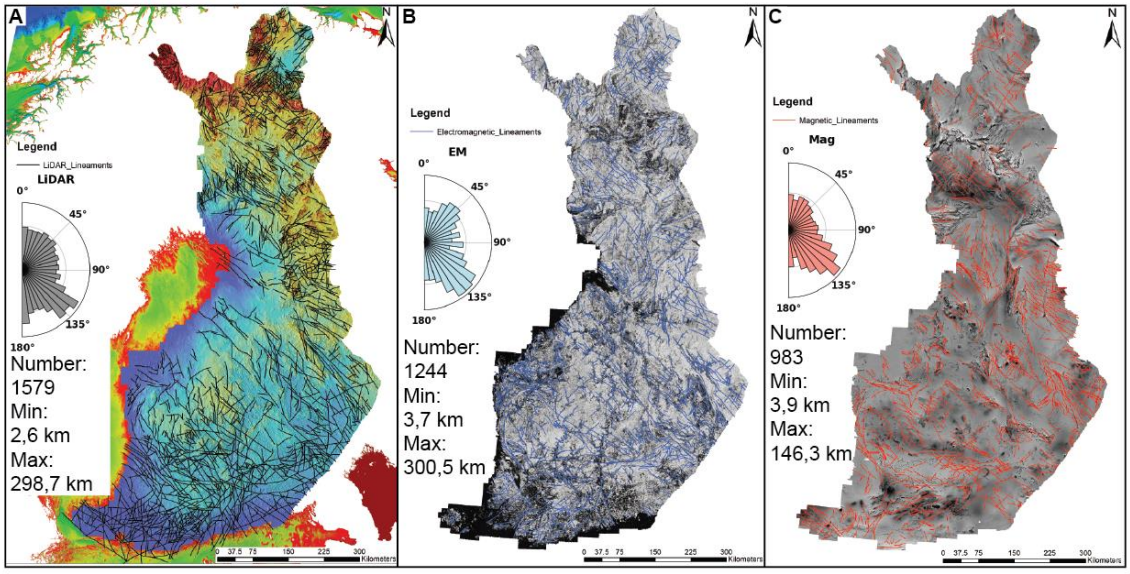

Figure 1. The lineaments in 1:500 000 scale. A) LiDAR lineaments on the topographical digital elevation map. The rose plot shows the orientation of the lineaments. B) Electromagnetic lineaments on a 3 kHz quadrature component grayscale map. The rose plot shows the orientation of the lineaments. C) Magnetic lineaments on a shaded magnetic anomaly grayscale map. The rose plot shows the orientation of the lineaments.

The final interpretation step was to integrate the three LiDAR, Electromagnetic (EM) and Magnetic (MAG) lineament datasets into one final Integrated (INT) lineament dataset. The workflow for the integration is as follows: all lineaments are brought together in the same map view (Figure 2A) and subparallel lineaments within the immediate proximity of each other are integrated into a single lineament where the LiDAR DEM lineaments were used as the guiding feature of the interpretation as the DEM was of significantly higher resolution than the

geophysical rasters (Figure 2B). The total amount of lineaments before integration were 3 806, but after integration the final amount was 3 476 lineaments, and 159 of these were found in all datasets (Figure 2).

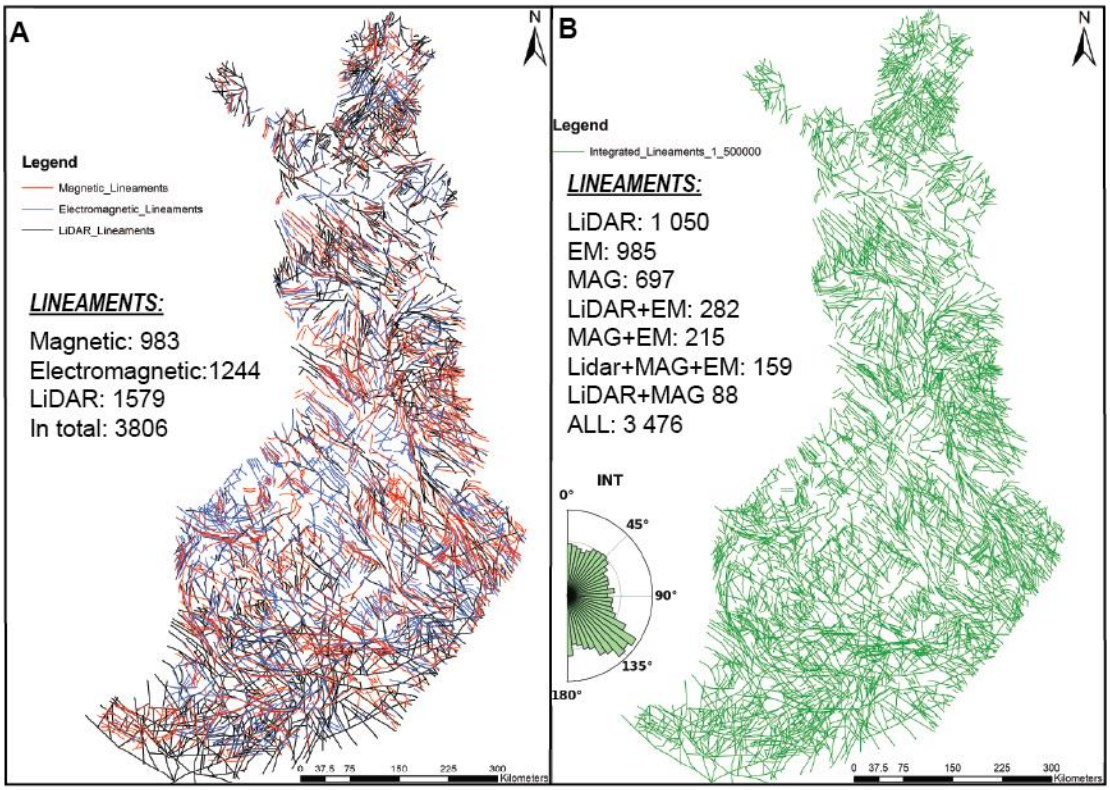

Figure 2. The lineaments in 1:500 000 scale. A) All interpreted lineaments, magnetic in red, electromagnetic in blue and LiDAR in black. B) All integrated lineaments. The rose plot shows the orientation of the lineaments.

The orientation of the lineaments shows NE-SW and E-W sets, but the most prominent NW-SE trending set, is probably partly enhanced due to the scouring effect from glacial ice-movement during the last ice ages when the whole country was covered in a thick ice-sheet (Figure 1, 2).

4. Conclusions

However, a few words of caution about the usage of the datasets are good to keep in mind: The lineament interpretation is performed in the fixed scale 1:500 000, thus the resulting accuracy is what can be expected for the scale of observation and the exact location of the lineaments might not in higher scales match the topographic features precisely. Another key point to keep in mind is that these topographical and geophysical lineaments are only representing linear features on the Earth's surface and near-surface, respectively, and thus a geological verification is needed before the geological significance of the lineaments can be defined.

While keeping these uncertainties in mind the lineaments can be used as an initial complementary tool to locate and map several geological features e.g., brittle deformation zones, ductile shear zones, dykes, lithological contacts and glacial features. Thus, these interpretations can be further utilized in several aspects in the geological research such as

regional geological mapping, groundwater research, underground construction and in geothermal projects.

References:

Hobbs, W.H., 1911. Repeating patterns in the relief and in the structure of land. GSA Bulletin 22, 123–176. https://doi.org/10.1130/GSAB-22-123

Hobbs, W.H., 1904. Lineaments of the Atlantic Border region. GSA Bulletin 15, 483–506. https://doi.org/10.1130/GSAB-15-483

Palmu, J.-P., Ojala, A.E., Ruskeeniemi, T., Sutinen, R., Mattila, J., 2015. LiDAR DEM detection and classification of postglacial faults and seismically-induced landforms in Finland: a paleoseismic database. GFF 137, 344–352.

Mineralogical and geochemical characteristics of the red 'Rektor Porphyry' associated with the Per Geijer AIO ore, Northern Sweden

S. Géhin[1], A.J. Miles[1]

LKAB, Prospektering Fält
[1]Kiirunavaaravägen 1, FK9, 981 33 Kiruna, Sweden
E-mail: exf.prospektering.falt@lkab.com

The 'Rektor Porphyry' (RP) has historically been associated with Apatite Iron-Oxide (AIO) ores of the Per Geijer (PG) deposits in the Norrbotten region of Sweden. Twenty-six rock samples were collected from both drillholes and field outcrops from the PG prospect to investigate if the 'RP' rock-type is used appropriately and to determine its relationship to mineralisation. Macro- and microscopical investigations show extensive silica and sericite alteration of the side-rock surrounding the AIO ores, in particular the replacement of primary feldspar phenocrysts. However, the intense red colouration is due to hematitic inclusions hosted within later quartz crystals and grains within the hanging wall (Matojärvi) and footwall (Luossavaara) formations of the PG ores. These findings suggest that the Rektor Porphyry reflects an alteration type whereby a Fe-rich oxidised fluid has penetrated the adjacent side-rock lithologies and therefore should be disregarded as a separate lithological unit. The red alteration itself, however, does increase in intensity towards the Fe-ore, and therefore could be used as an exploration indicator to be considered in future drilling programs.

Keywords: alteration, AIO, petrology, microscopy, hematite, Kiruna

1. Introduction

Apatite Iron-Oxide (AIO) ores of Norrbotten, Sweden, are an important source of iron for Europe's steel industry. The world-class deposit of Kiirunavaara, informally known as the Kiruna mine, contains more than 2,000 Mt of high-grade (60% Fe) Fe-ore and is the type-locality for AIO (Au-Cu poor) deposits. Despite the Kiruna mine being active for >100 years, the genesis of Kiruna-type deposits remains controversial. The hypotheses include a magmatic origin, considered to be a lava or intrusion (e.g., Troll et al., 2019), with a possible hydrothermal component (e.g., Simon et al., 2018). However, the variation in AIO deposits observed world-wide suggests it is likely that there may be multiple fluids operating together to explain the wide spectrum of ore textures, host rock relations and alterations (Williams et al., 2005).

The Per Geijer (PG) ores are a group of iron deposits 2–5 km north of the Kiirunavaara orebody and are collectively known as Nukutus, Henry, Rektorn and Haukivaara at surface, and PG Deep at depth. The ores are stratigraphically higher than the Kiirunavaara Group, however, their genesis and timing relations remain unknown. The stratiform-stratabound Fe-ores of PG are located at the upper contact of the Luossavaara Formation and are commonly hosted within the Matojärvi Formation (Fig. 1). Compared to the magnetite-dominated ore at Kiirunavaara, the PG ores contain a higher proportion of hematite relative to magnetite, and a higher phosphorus content (3–5%) with an average iron content of 30–40%. Apatite is commonly associated with calcite and quartz (Martinsson, 2015). The lithological units within the Matojärvi Formation are often described as variably but intensely altered, in comparison to the Luossavaara footwall (Martinsson, 2015).

Initially characterised in 1950 by Geijer, the Rektor Porphyry (RP) has continued to be used throughout literature and generally refers to a felsic tuff or lava unit belonging to the lower part of the Matojärvi Formation. It forms the hanging wall to the Rektorn magnetite ore and extends northeast towards the other PG iron deposits. It is red-brick in colour with sub-euhedral

feldspar phenocrysts that vary from millimetre to >centimetre in size, and localised spherulites occur within the matrix of quartz aggregates (Geijer, 1950). Common sub-centimetric bands of magnetite-hematite parallel to schistosity are accompanied by calcite and sericite, as well as rare apatite, fluorite, and zircon. The rock is generally considered as a silicic volcanic rock, recrystallised, and strongly altered by silica and K-feldspar (Geijer, 1910; Geijer, 1950; Frietsch, 1978). This study aims to re-evaluate the definition of the 'Rektor Porphyry' and the nature of the red alteration.

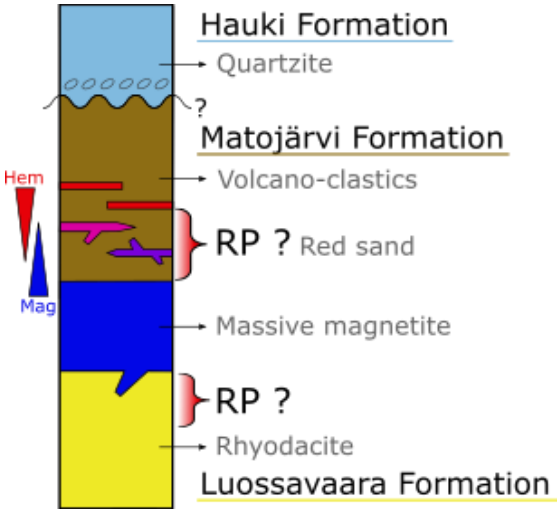

Figure 1: Basic lithological log of the Per Geijer lithologies based on this study. The location of the RP has been inferred from Geijer (1950).

2. Materials and methods

To gain an overview of red-altered rocks in the Per Geijer deposit, five diamond drillholes from the PG 2020 exploration campaign were chosen for investigation. These drillholes were logged for lithology, alteration, and minerals in conjunction with field excursions to identify surface outcrops within the PG area to provide geological context. These samples were representative of the characteristic Rektor Porphyry described in literature. Rock samples were sent to ALS and MSA laboratories for geochemical assaying (lithium borate fusion XRF and ICP) and were systematically taken from below ± above ± inside the Fe-ore. A total of 23 drillcore and 3 field samples were sent for thirty-micron-thick polished thin sections. Mineral relationships were observed using an optical polarised microscope with insight from the geochemical data.

3. Results

Rocks from both the Matojärvi and Luossavaara Formations are red-brick in colour (Figure 2a and 2b). Abundant hematite inclusions indicate the source for the red-brick colour (Figure 2c). Inclusions occur throughout the entire rock, except the late recrystallised Qtz, Ap and Cal. The altered Fsp contains the most inclusions and alters to silica and sericite. Samples from the Matojärvi Formation often show primary Qtz. The Qtz grains are deformed and commonly have a growth rim with very few hematite inclusions (Figure 2d). The textural observation from thin section indicates the rocks either side of the Fe-mineralisation (i.e., the hanging wall and footwall), are different lithologies but are altered similarly.

Major element analysis (presented in Géhin, 2021) shows a negative correlation between Fe and Si, K, Na, Al and Zr, suggesting that when the rock is iron-rich, rock-forming minerals are relatively lower in concentrations, as a result of the Fe-ore. Within the red-brick altered rocks, both Si, K, Na, Al and Zr correlate. Na and Zr tend to be higher in the footwall, whereas K is relatively higher in the hanging wall.

Throughout the 5 drillholes, all samples that display extensive red alteration were plotted using immobile element ratios. The rocks logged as footwall and hanging wall do not cluster separately, which suggests that the red alteration does not occur preferentially in one lithology. Furthermore, samples identified in thin section that are intensely affected by silicification lie on the outer edge of the spread of data. The distortion of the ratios is due to the replacement of most rock-forming minerals for silica.

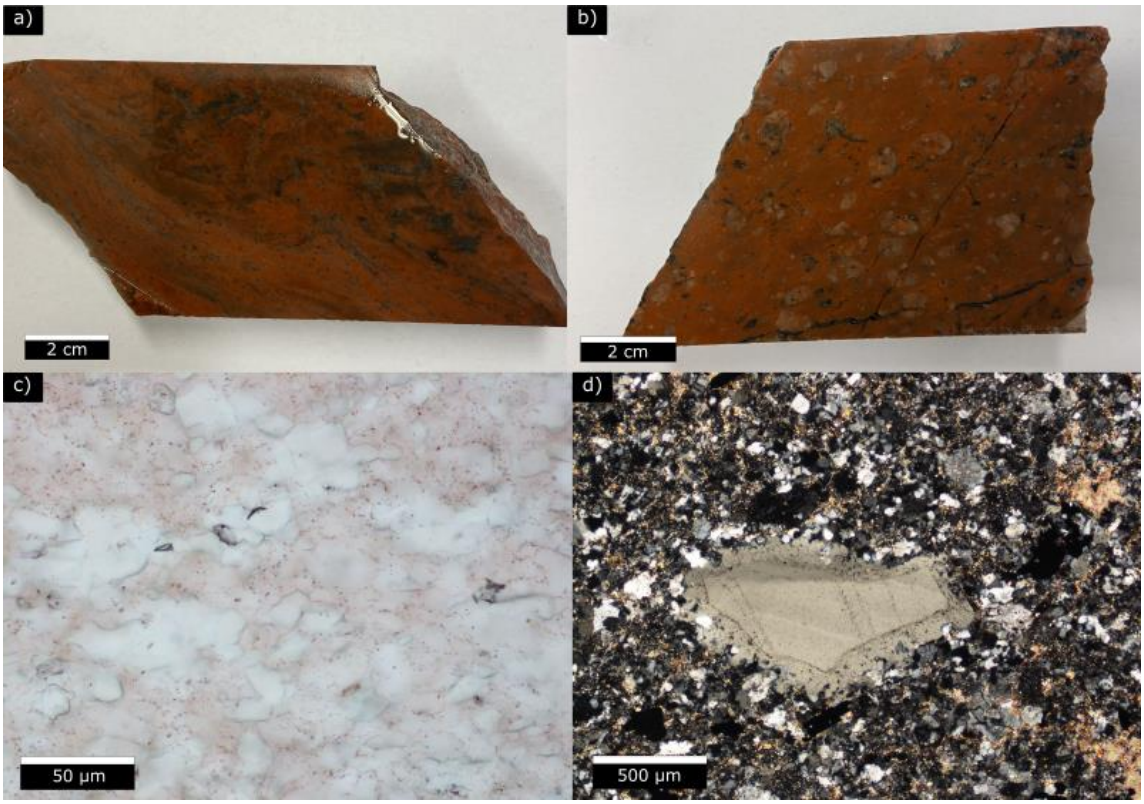

Figure 2. Macro and microscopic photos of red altered rocks. (a) Red altered sedimentary rock from the Matojärvi formation showing disruption of laminations. (b) Red altered porphyrytic rhyodacite from the Luossavaara Formation. (c) Close up picture of the red hematitic inclusions within the sand (PPL). (d) Recrystallised Qtz grain with irregular contact rim and red inclusions from an altered Matojärvi sedimentary rock.

4. Conclusion

The results indicate that the red-coloured rock that occurs above and below the massive Fe-ore is a result of hematite inclusions within late-stage silica irrespective of lithology. In the hanging wall (Matojärvi Formation), the alteration starts at or just before the hematite to magnetite transition. In the footwall (Luossavaara Formation), red-brick alteration decreases in intensity away from the Fe-lenses with depth. Although the alteration is the same, the host rock is

different between the hanging wall and footwall. The red altered rock in the Matojärvi Formation is a clastic/volcanoclastic sand – a material has been reworked before deposition. It is characteristically granular, fine-grained and quartz-rich. It commonly hosts significant amounts of calcite and apatite. Furthermore, the red-altered Luossavaara Formation is a porphyritic rhyodacite that does not vary locally and characteristically contains high contents of Na_2O when located below Fe-lenses, and Zr (>400 ppm). Within the Luossavaara Formation, feldspars are broken down into silica and sericite, quartz is grown and recrystallised with hematite inclusions which gives the rock a bright red colour.

This study suggests that the Rektor Porphyry should be reclassified as an alteration type. It is not a porphyritic rock, as one would assume from its name, nor is it a single lithology. The red alteration affects both the Matojärvi Formation and Luossavaara Formation as it is the same alteration that occurs as a halo around massive ore.

The results provide a new insight on the relationship between the ore and the host rock. The quartz recrystallisation would suggest that the rocks have been subjected to heat since its formation. It is most likely that the formation of the red alteration is related to the magnetite orebody since both the hematite inclusion and magnetite/hematite ore are Fe-rich. The ore body likely heated the surrounding silicic rocks during its emplacement and encouraged fluid convection as a result of hot ore coming into contact with cold side rock. The smaller hematite mineralisation in the upper portion of the Matojärvi Formation is also associated with the red-brick alteration and, therefore, can be used as a proximity factor during the exploration of the Per Geijer ores and may be applicable to other Fe-ores elsewhere in the region.

References:

Frietsch, R., 1978. On the magmatic origin of iron ores of the Kiruna type. Economic Geology, 73 (4), p. 478–85

Geijer, P., 1910. Igneous rocks and iron ores of Kiirunavaara, Luossavaara and Tuollavaara. Economic Geology, 5 (8), p. 699–718.

Geijer, P., 1950. The Rector ore body at Kiruna. Norstedt.

Martinsson, O., 2015. Genesis of the Per Geijer apatite iron ores, Kiruna area, northern Sweden. In Proceedings of the Abstract Volume, SGA Biennal Meeting, Nancy, France, p. 24–27.

Simon, A. C., Knipping, J., Reich, M., Barra, F., Deditius, A. P., Bilenker, L. and Childress, T., 2018. Kiruna-type iron oxide-apatite (IOA) and iron oxide copper-gold (IOCG) deposits form by a combination of igneous and magmatic-hydrothermal processes: Evidence from the Chilean iron belt. SEG 2018: Metals, Minerals, and Society, 22–25 September 2018, Keystone, Colorado, USA, p. 89–114.

Troll, V.R., Weis, F.A., Jonsson, E., Andersson, U.B., Majidi, S.A., Högdahl, K., Harris, C., Millet, M-A., Chinnasamy, S.S., Kooijman and Nilsson, K.P., 2019. Global Fe–O isotope correlation reveals magmatic origin of Kiruna-type apatite-iron-oxide ores. Nature Communications, 10.

Williams, P. J., Barton, M. D., Johnson, D. A., Fontboté, L., De Haller, A., Mark, G., and Marschik, R., 2005. Iron oxide copper-gold deposits. Geology, space-time distribution, and possible modes of origin. Economic Geology, p. 371–405.

Nickel remobilisation in Sika-aho, Kuhmo greenstone belt

T. Gråsten[1], E. Heilimo[1] and T. Halkoaho[2]

[1]Department of Geography and Geology, University of Turku, Turku, Finland
[2]Geological Survey of Finland, P.O. Box 1237 (Viestikatu 7), 70601 Kuopio, Finland
E-mail: tuangr@utu.fi

Archaean nickel deposits have been invariably metamorphosed and deformed, which has modified, for example, the geometry, mineralogy, metal content, and textures of the deposits. This study addresses the metallogeny of Sika-aho nickel deposit, which is interpreted to have formed by dominantly mechanical remobilisation of sulfides from a komatiitic source.

Keywords: nickel, remobilisation, komatiite, Kuhmo greenstone belt, Sika-aho

1. Introduction

Komatiite-associated Ni(-Cu-PGE) deposits are one of the many deposit types found in Archaean greenstone belts, but their exploration potential in Finland is significant (Konnunaho et al., 2015). The target of this study, the Sika-aho nickel deposit, is located in central northern part of Kuhmo Greenstone Belt, eastern Finland (Figure 1). The Sika-aho nickel deposit is mainly hosted by SiO_2-rich, chlorite±carbonate±sericite schist that is located along the western margin of a carbonate-altered and sheared komatiitic cumulate sequence (Figure 2; Heino, 1998; Luukkonen et al., 1998, 2002). The ore minerals found in Sika-aho are pentlandite, pyrrhotite, and Ni-Fe arsenides (Makkonen & Halkoaho, 2007), however most of the nickel is in pentlandite (Heino, 1998). The width of the deposit varies from 1 to 9 metres and the length along strike is approximately 80 metres at present erosion level. Estimated mineral reserves to a depth of 150 metres are 175 085 tons with a mean nickel concentration of 0.665 %, with cut-off value being 0.35 % (Heino, 1998).

This study aims to improve the understanding of the metallogeny of Sika-aho nickel deposit, and possibly other remobilised nickel deposits, by resolving the reasons and mechanisms for nickel remobilisation and deposition. Additionally, it is studied if geochemical haloes can be detected around the deposit, and if they can be utilised in exploration of similar nickel deposits. The study is conducted for a Master's thesis in cooperation between University of Turku and Geological Survey of Finland (GTK).

2. Background

Sulfides and metals can be mobilised mainly by four end-member mechanisms during metamorphism and deformation (Mukwakwami, 2012): 1) solid-state diffusive mobilisation (e.g., Lesher & Keays, 2002); 2) metamorphic sulfide anatexis (e.g., Tomkins et al., 2007); 3) metamorphic-hydrothermal mobilisation (e.g., Marshall et al., 2000); 4) mechanical mobilisation (e.g., McQueen, 1987). In this case, the deposit type and geological setting are heavily against the first two mechanisms, as solid-state diffusive mobilisation of sulfides has so far been interpreted to only have occurred in sulfide-rich metasedimentary rocks next to magmatic ores, and sulfide anatexis in pyrrhotite-pentlandite dominated system would require very high temperatures (Tomkins et al., 2007; Mukwakwami, 2012), which leaves the two latter mechanisms as the most plausible options for nickel remobilisation in Sika-aho.

During ore-forming processes, geochemical haloes that are either enriched or depleted in different elements can be formed (Haldar, 2013). Geochemical haloes have been recognised in komatiite-associated nickel deposits only relatively recently (e.g., Le Vaillant et al., 2016).

Advective infiltration of hydrothermal fluids, mechanical remobilisation of sulfides, or a mixed-state process all have the capacity to leave a detectable footprint that is significantly larger than the deposit itself and could therefore be utilised in exploration. However, to remobilise, transport, and redeposit nickel in hydrothermal processes, the composition and redox conditions of the fluid and the country rocks must be specific: for example, Le Vaillant (2014) found that arsenic played a critical role in the mobility of nickel in some Australian komatiite-associated Ni-Cu-(PGE) deposits. For Sika-aho, the remobilisation of nickel from its primary magmatic position by tectono-metamorphic processes has been regarded as the most plausible explanation (Heino, 1998; Luukkonen et al., 1998, 2002; Makkonen & Halkoaho, 2007), however the remobilisation mechanisms and the nature of the host rock are not as clear.

Figure 1. Location of Kuhmo greenstone belt and notable nickel deposits (modified after GTK open licence CC BY 4.0, including GTK's Bedrock of Finland 1:200 000 data).

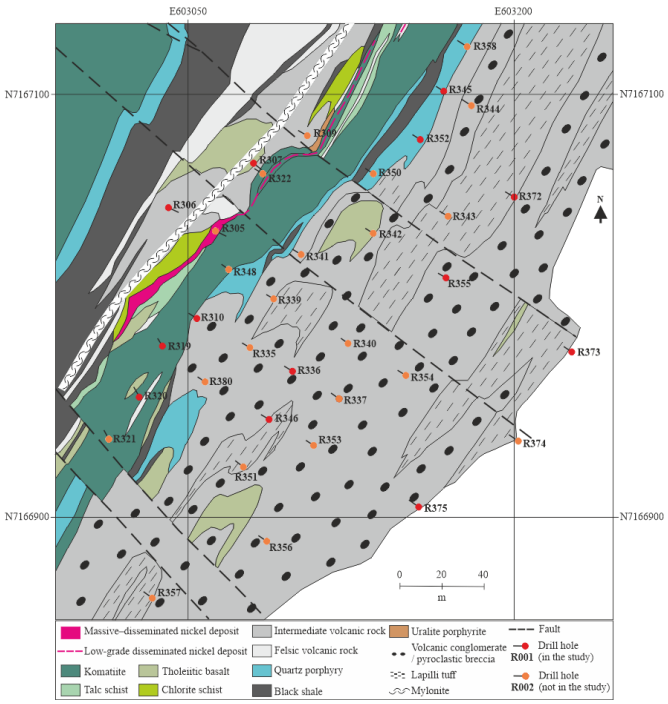

Figure 2. Bedrock map of the study area (modified after Luukkonen et al.,2002).

3. Methods and materials

Drill cores from 13 separate Sika-aho drill holes (Figure 2) were examined at GTK's national drill core archive in Loppi. A total of 89 analyses were considered for whole-rock geochemistry, which consisted of 43 new analyses, 12 analyses reported by Makkonen & Halkoaho (2007), and additional 34 analyses provided by GTK (Luukkonen et al., 2002). Furthermore, 160 aqua regia digestion analyses (detection of Ni, Co, Cu, Cr, and S) provided by GTK (Heino, 1998) were utilised in 3D-modelling. A total of 36 polished thin sections were made in Geohouse laboratory and subsequently examined with petrographic microscope. Geological and numeric 3D-modelling of the deposit and surrounding lithologies were done using Seequent's modelling software Leapfrog Geo.

4. Preliminary results and discussion

Drill core examination and petrographic study revealed the mineralogical and textural characteristics of different lithological units. Pentlandite, which hosts most of the nickel, can be found intergrown with other sulfides, as inclusions and lamellae in pyrrhotite, and as individual grains. Sulfides show flattening and elongation, as well as stretching lineations that can be observed on schistosity planes especially in the very strongly schistose mineralised rocks. In peak metamorphic temperatures reached in Kuhmo greenstone belt (500–660 °C, Tuisku, 1998), most sulfides have had very low strength compared to silicates. The textural evidence from sulfides combined with theoretical and experimental data (e.g., Marshall & Gilligan, 1987) suggest that the sulfides have undergone ductile plastic flow.

The average Ni/Cu ratios in both komatiites and mineralised rocks are very high, 79.8 and 82.0, respectively, however the Ni and Cu contents do not necessarily correlate well in the mineralised rocks. Luukkonen et al. (1998) stated that the nickel in sulfide fraction (Nisf) is high, varying between 7.2 and 30.12 wt.%. Heino (1998) reports that the average Ni/Cu ratio is 60.44 and average Nisf is 15.61 wt.% in the mineralised rocks.

In many cases where nickel has been mobilised by hydrothermal fluids, Pd, Pt, and other PGEs have also been mobilised by the same fluids (e.g., Keays & Jowitt, 2013; Le Vaillant et al., 2015), however in vastly different abundances causing decoupling between them (Pd is the most mobile element, then Pt, and lastly the IPGEs). The Pt/Pd ratio in the mineralised rocks and the komatiites is uniform and no enrichment of Pd can be detected in the mineralised rocks. The Pd/Ir ratio in the mineralised zone is quite constant, with average value of 15.2. Based on available literature on PGE solubility, these results indicate that hydrothermal processes have not caused any, or only minor remobilisation of PGE. However, this alone does not rule out the possibility that nickel could not have been remobilised by hydrothermal processes (see e.g., Capistrant et al., 2015).

Spatially, the Sika-aho nickel deposit is along the margin of a komatiitic cumulate unit for its whole length (Figure 3) and close to the Tammasuo shear zone, which is a major nearly N-S trending shear zone in the middle of the Kuhmo greenstone belt. The textural and geochemical features of Sika-aho nickel deposit together with regional geology and deformation history indicate that the remobilisation mechanism has been dominantly mechanical rather than chemical, and that the source of nickel has been komatiitic.

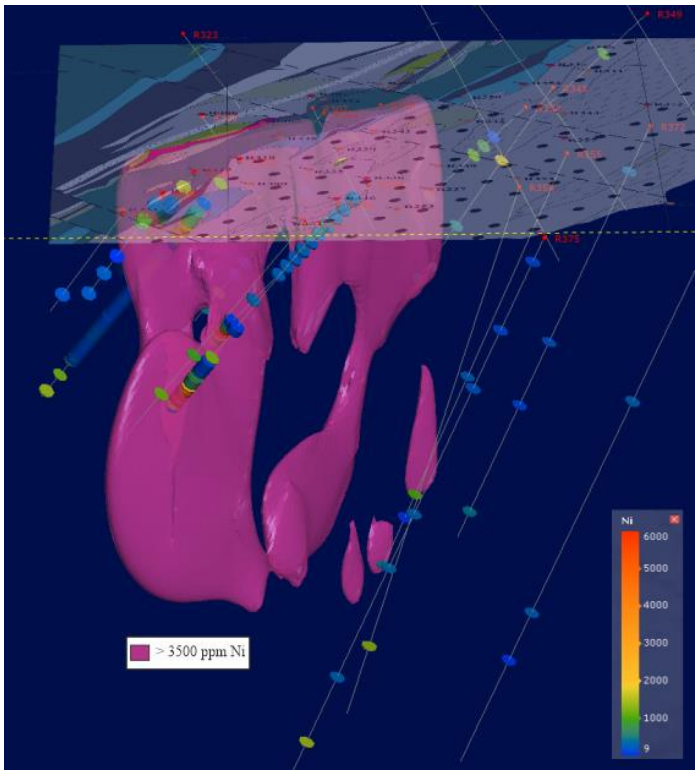

Figure 3. Snapshot of Leapfrog Geo numeric 3D-model showing the nickel deposit (cut-off value 3500 ppm), drill holes with Ni contents from geochemical analyses, and partly transparent bedrock map. Looking towards north, plunge is 20 degrees.

5. Conclusions and ongoing studies

The preliminary results from drill core examination, petrography, geochemistry, and 3D-modelling suggest that Sika-aho nickel deposit has been formed by dominantly mechanical remobilisation of nickel from a komatiitic source. Geochemical haloes have not been detected thus far. There are still some aspects in the metallogeny of Sika-aho nickel deposit that are currently being studied for the thesis. Some of the open questions include atypically high Zn and Cr contents of the deposit relative to other Archean nickel deposits (Makkonen & Halkoaho, 2007), as well as the degree and extent of remobilisation. Naturally, a more detailed study of the presented preliminary results will be conducted, as well.

References:

Capistrant, P.L., Hitzman, M.W., Wood, D., Kelly, N.M., Williams, G., et al., Zimba, M., Kuiper, Y., Jack, D., Stein, H. 2015. Geology of the Enterprise Hydrothermal Nickel Deposit, Economic Geology, 110, 9–38.

Haldar, S.K., 2013. Mineral Exploration: Principles and Applications. Elsevier, 372 pp.

Heino, T., 1998. Hyrynsalmi, Puistola 1 (kaivosrekisteri No 5657/1) ja Paatola 1 (kaivosrekisteri No 5619/1) nikkeliesiintymän mineraalivarantoarvio. Geological Survey of Finland, Archive report, M19/4421/-98/1/10, 33 pp. (in Finnish)

Keays, R.R., Jowitt, S.M., 2013. The Avebury Ni deposit, Tasmania: A case study of an unconventional nickel deposit. Ore Geology Reviews, 52 (January), 4–17.

Konnunaho, J., Halkoaho, T., Hanski, E., & Törmänen, T., 2015. Komatiite-hosted Ni-Cu-PGE Deposits in Finland. In: Maier, W.D., Lahtinen, R., O'Brien, H., 2015 (Eds.), Mineral Deposits of Finland, 93–131.

Lesher, C.M., Keays, R.R., 2002. Komatiite-associated Ni-Cu-PGE Deposits: Geology, Mineralogy, Geochemistry, and Genesis. Canadian Institute of Mining, Metallurgy and Petroleum, 54, 579–618.

Luukkonen, E., Heino, T., Niskanen, M., Tenhola, M., 1998. Tutkimustyöselostus Hyrynsalmen kunnassa valtausalueilla Kaivolampi 1-2 (Kaivosrekisteri No 6143/3 ja 6143/2), Puistola 1-2 (Kaivosrekisteri No 5657/1 ja 6143/1), Paatola 1-2 (Kaivosrekisteri No 5619/1 ja 5619/2), Geological Survey of Finland, Archive report, M06/4421/-98/1/10, 30 pp. (in Finnish)

Luukkonen, E., Halkoaho, T., Hartikainen, A., Heino, T., Niskanen, M., Pietikäinen, K., Tenhola, M., 2002. The activities of the Archean Terrains in Eastern Finland Project (12201 and 210 5000) in Suomussalmi, Hyrynsalmi, Kuhmo, Nurmes, Rautavaara, Valtimo, Lieksa, Ilomantsi, Kiihtelysvaara, Eno, Kontiolahti, Tohmajärvi and Tuupovaara areas during years 1992 – 2001. Geological Survey of Finland, report, M19/4513/2002/1, 286 pp.

Makkonen, H.V., Halkoaho, T., 2007. Whole rock analytical data (XRF, REE, PGE) for several Svecofennian (1.9 Ga) and Archaean (2.8 Ga) nickel deposits in eastern Finland. Geological Survey of Finland, report M19/3241/2007/32, 53 pp.

Marshall, B., Gilligan, L.B., 1987. An introduction to remobilization: Information from ore-body geometry and experimental considerations. Ore Geology Reviews, 2 (1–3), 87–131.

Marshall, B., Vokes, F., Larocque, A., 2000. Regional metamorphic remobilization: upgrading and formation of ore deposits. Rev. Econ. Geol., 11 (1), 19–38.

McQueen, K.G., 1987. Deformation and remobilization in some Western Australian nickel ores. Ore Geology Reviews, 2 (1–3), 269–286.

Mukwakwami, J., 2012. Structural control of Ni-Cu-PGE ores and mobilization of metals at the Garson mine, Sudbury. PhD Thesis, Laurentian University Sudbury, Ontario, 246 pp.

Tomkins, A.G., Pattison, D.R.M., Frost, B.R., 2007. On the initiation of metamorphic sulfide anatexis. Journal of Petrology, 48 (3), 511–535.

Tuisku, P., 1998. Geothermobarometry in the Archaean Kuhmo-Suomussalmi greenstone belt, Eastern Finland (Abstract). Geological Survey of Finland, Special Paper, 4, 171–172.

Le Vaillant, M., 2014. Hydrothermal Remobilisation of Base Metals and Platinum Group Elements Around Komatiite-Hosted Nickel-Sulphide Deposits: Applications To Exploration Methods. PhD Thesis, The University of Western Australia, 642 pp.

Le Vaillant, M., Barnes, S.J., Fiorentini, M.L., Miller, J., McCuaig, T.C., Mucilli, P., 2015. A hydrothermal Ni-As-PGE geochemical halo around the Miitel komatiite-hosted nickel sulfide deposit, Yilgarn craton, Western Australia. Economic Geology, 110 (2), 505–530.

Le Vaillant, M., Fiorentini, M.L., Barnes, S.J., 2016. Review of lithogeochemical exploration tools for komatiite-hosted Ni-Cu-(PGE) deposits. Journal of Geochemical Exploration, 168, 1–19.

National and international RI collaboration on Solid Earth Science

P. Haapanala[1], A. Korja[1] and FIN-EPOS community

[1]Institute of Seismology, P.O. Box 68, FIN-00014 University of Helsinki
E-mail: paivi.haapanala@helsinki.fi

The European Plate Observing System (EPOS) is a multidisciplinary research infrastructure that facilitates long-term integration of data, services and facilities for solid Earth science in Europe. Finland's participation in EPOS is coordinated by FIN-EPOS consortium that is a joint community of universities and research institutes with tasks of maintaining geophysical observatories and laboratories. Finland has also active role in EPOS related Nordic capacity building and knowledge exchange. International collaboration supports the availability, recognition, and FAIRness of EPOS data. In this abstract we shortly introduce the European Solid Earth Science research infrastructure EPOS and national and Nordic collaboration related to it.

Keywords: research infrastructure, solid earth science, EPOS, FIN-EPOS, Nordic EPOS

1. European Plate Observing System EPOS

European Plate Observing System, EPOS (epos-eu.org), is a multidisciplinary, distributed *research infrastructure* (RI). It is one of the ESFRI (European Strategy Forum on Research Infrastructures) landmark RIs (Cocco et al., 2022; Cocco and Montone, 2022). The legal entity of EPOS, EPOS ERIC (European Research Infrastructure Consortium), is based in Italy and is currently joined by sixteen countries: Austria, Belgium, Denmark, France, Greece, Iceland, Italy, the Netherlands, Norway, Poland, Portugal, Romania, Slovenia, Sweden and the United Kingdom, and Switzerland and Germany are participating as observer (Atakan et al., 2022). Furthermore, many other European countries, including Finland, are involved in EPOS by providing data, data products, software, and/or services to be integrated by 10 thematic subdisciplines of solid Earth science (Figure 1). National governments, funding agencies and institutes are responsible for the funding and operation of national instrumentation and data management in each participating country. Finland is planning to join EPOS ERIC.

The overarching goal of EPOS is to establish a comprehensive multidisciplinary research platform and principal source of geoscientific data, metadata and tools of Solid Earth science in Europe. The EPOS framework can be defined as a truly international, federated framework encompassing the data and service provision integrated within the **T**hematic **C**ores **S**ervices (TCS) and made interoperable with the central hub of the Integrated Core Services (ICS-C), the novel e-infrastructure for promoting FAIR (**F**indable, **A**ccessible, **I**nteroperable, and **R**eusable) data management. The community-specific TCS are listed in Figure 1. TCSs provide open data to EPOS multi-disciplinary open data portal for Solid Earth science datasets https://www.epos-eu.org/dataportal. EPOS also promotes transnational access to laboratories and observatories.

In our oral presentation, we will show EPOS outreach videos. Some of them are also available via EPOS YouTube channel: https://www.epos-eu.org/communication/outreach-materials?category_id[]=6.

2. FIN-EPOS

FIN-EPOS research infrastructure connects European level EPOS and national consortium in Finland. FIN-EPOS consortium is a joint RI community of universities and research institutes:

University of Helsinki (UH), University of Oulu (UOULU), Aalto University (Aalto), National Land Survey (NLS, FGI), Finnish Meteorological Institute (FMI), Geological Survey of Fin-

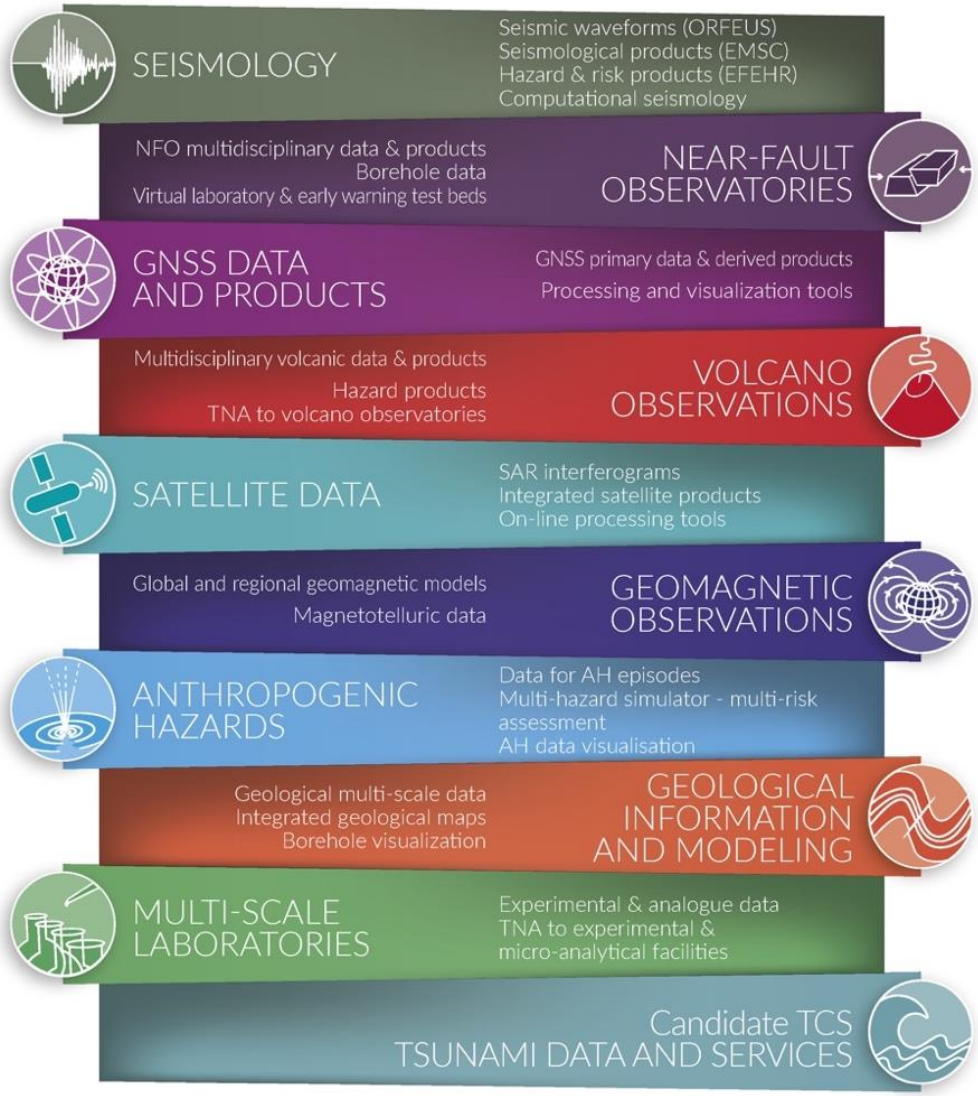

Figure 1. Listing of subdiscipline specific Thematic Core Services (TCS) currently integrated in EPOS (Figure ©EPOS ERIC).

land (GTK), VTT Technical Research Center for Finland Ltd (VTT), and CSC- IT Centre for Science Ltd (CSC). The consortium´s main goals are to promote Finland´s membership in EPOS-ERIC and to influence national research infrastructure policy and especially to secure a place on the **FI**nnish **R**easearch **I**nfrastructure (FIRI) roadmap also in the future. FIN-EPOS is on the current national FIRI roadmap 2021–2024.

FIN-EPOS consortium members own and operate national research infrastructures including geophysical and geodetic observatories, and laboratories. These RIs consist of physical measurement instrumentation and stations as well as associated data centers, services and personnel. The permanent national seismic, geodetic and magnetic observatory networks are distributed around Finland, whereas the geophysical, geodynamic and petrophysical

laboratories are located in Helsinki, Espoo, Kuopio, Rovaniemi, Oulu and Pyhäsalmi (Calliolab). Partners own their data and deliver or are preparing to deliver data via national nodes, international data centres or global scientific programs to EPOS TCSs serving EPOS data portal. FIN-EPOS activities are financed by consortium members that in turn are financed by five ministries: Ministries of Education and Culture, Agriculture and Forestry, Employment and the Economy, Transport and Communications, and Foreign Affairs.

FIN-EPOS has a coordination office at the Institute of Seismology, University of Helsinki. The partners have formed FIN-EPOS council that monitors Finnish participation in initiatives related to EPOS and outlines a long-term goals for national solid Earth sciences RI plan. During the past few years, FIN-EPOS has been upgrading the Finnish National Seismological Network (FNSN), and the geodetic and magnetic networks and laboratories. Currently, FIN-EPOS is enhancing collaboration in measurements on co-located sites. Sharing station infrastructure and deploying several independent measurement instruments on a single site enables not only new studies on the interdependencies of seismic, geomagnetic and geodetic processes but also usage as reference stations, ground truth stations for mobile instruments and airborne measurements. The so-called *"geophysical superstations"* hosting co-located geophysical instruments, will be constructed around already existing geophysical observatories and stations**.** Some of the geophysical superstations may also be collocated at research and biological stations belonging to other environmental ESFRI RIs (ICOS, ACTRIS, AnaEE, LTER, EUREF, EISCAT, GGOS) and they might a network of joint geophysical and environmental superstations.

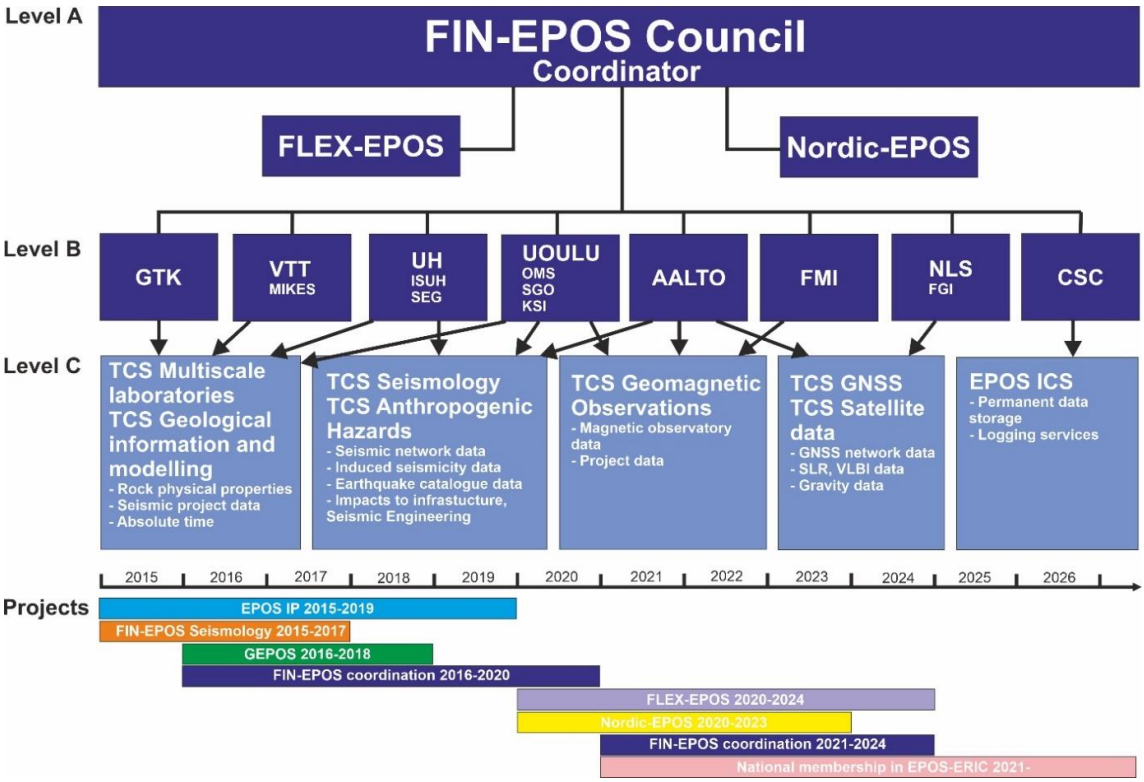

Figure 2. Organization and FIRI funding of FIN-EPOS.

5. Nordic EPOS

EPOS related cooperation is especially important in bringing forward Nordic common research interests in georesources and in the Nordic natural phenomena such as postglacial uplift, geomagnetic storms, and seismic hazard in low seismicity intraplate areas. University of Helsinki is leading a NordForsk funded Nordic EPOS consortium *Nordic EPOS- A FAIR Nordic EPOS data HUB*. Nordic EPOS support Nordic collaboration by organizing workshops, trainings and events on EPOS data usage, FAIR data principles, and on harmonizing data management. The activities are aimed for students, researchers, and technical staff working in Nordic countries in the field of Solid Earth Sciences. Our poster presentation will introduce FIN-EPOS and Nordic EPOS collaboration.

6. More information

To find more information about EPOS in general and national EPOS activities and data, visit the FIN-EPOS website helsinki.fi/en/infrastructures/fin-epos. Trough website one can get access to online databases of the Finnish geophysical and geodetic observatories and laboratories: Earthquake bulletins, FIRE data, Paleomagia, geological and geophysical data products via Hakku (GTK), Sodankylä Geophycical Observatory data (SGO/UOULU), data from magnetometer stations via IMAGE (International Monitor for Auroral Geomagnetic Effects). There are also links to EPOS related databases in Norden (helsinki.fi/en/infrastructures/nordic-epos/databases) and of course link to access the EPOS data portal (epos-eu.org/dataportal).

More information on the Nordic EPOS collaboration, activities and links to Nordic EPOS related data are available on the Nordic EPOS website (www2.helsinki.fi/en/infrastructures/nordic-epos).

Acknowledgements

The national FIN-EPOS coordination and participation in EPOS and FLEX-EPOS -project have received FIRI funding from the Academy of Finland for 2021–2024 by funding decisions 328984 and 328776, 328778-328782, 328784, 328786. Nordic EPOS – A FAIR Nordic EPOS Data Hub -project receives financial support from the NordForsk Research Infrastructure Hubs 2020–2022 call, decision number 97318.

References:

Atakan, K, Cocco, M., Orlecka-Sikora, B., Pijnenburg, R., Michalek, J., Rønnevik, C., Olszewska, D., Górka-Kostrubiec, B., Drury, M.R., 2022. National EPOS initiatives and participation to the EPOS integration plan. Annals of Geophysics, 65, 2, DM211. doi.org/10.4401/ag-8758

Cocco, M., Montone, P., 2022. EPOS a Research Infrastructure in solid Earth: open science and innovation. Annals of Geophysics, 65, 2. doi.org/10.4401/ag-8835

Cocco, M., Freda, C., Atakan, K., Bailo, D., Contell, K.S., Lange, O., Michalek, J., 2022. The EPOS Research Infrastructure: a federated approach to integrate solid Earth science data and services. Annals of Geophysics, 65, 2, DM208. doi.org/10.4401/ag-8756

SEEMS DEEP – combining seismic and electromagnetic methods for deep bedrock imaging

S. Heinonen[1], J. Kamm[1], M. Malinowski[1] and the SEEMS DEEP Working Group[2]

[1]Geological Survey of Finland, PO.Box 96 (Vuorimiehentie 5), FI-02151 Espoo, Finland
[2] SEEMS DEEP Working Group: Mathieu Darnet (BRGM), Marek Wojdyla (Geopartner Geofizyka), Antti Kivinen (GRM Services), Catherine Truffert (IRIS Instruments), Andrzej Górszczyk (Institute of Geophysics, Polish Academy of Science), Thomas Kalscheuer (Uppsala University) and Yuriy Koltun (Laakso Mineral Oy)
E-mail: suvi.heinonen@gtk.fi

SEEMS DEEP is an ERA-MIN funded project aiming to develop novel workflow integrating seismic and electromagnetic (EM) methods for deep bedrock imaging and mineral exploration. Project will acquire multimethod geophysical data in the Koillismaa Layered Ingneous Complex in Finland. Field data acquisition and data processing are conducted jointly, and most importantly, complementary data sets will be utilized in developing joint processing, inversion and interpretation capabilities in order to achieve robust 3D models of subsurface geology down to several kilometers depth.

Keywords: deep exploration, seismic reflection, electromagnetic, electric, mafic intrusion, Fennoscandia, Koillismaa

1. Introduction

Global demand for metals and other minerals is increasing due to transition towards carbo-neutral transportation and energy. Especially minerals from the EU critical mineral list, such as cobalt, wolfram, magnesium, lithium and titanium are quickly needed (European Commission, Study on the EU's list of Critical Raw Materials (2020)). Simultaneously, it is well understood that easy to find ore deposits with clear geophysical signature have already been discovered and in the future, more subtle geophysical anomalies need to be investigated, and novel deep penetrating technologies developed to facilitate society to meet the upcoming challenges. SEEMS DEEP (SEismic and ElectroMagnetic methodS for DEEP mineral exploration) is an ERA-MIN funded project (2022-2025) coordinated by Geological Survey of Finland (GTK) that aims to develop novel methodologies for imaging crystalline bedrock and deep mineral exploration. Specifically, the SEEMS DEEP project will develop seismic and electromagnetic (EM) methods in a joint manner to acquire multimethod data sets utilized for common earth modelling (CEM).

2. Workflow

SEEMS DEEP project consist of five work packages also defining the project workflow in general level (Figure 1). Project is started with a geomodelling and petrophysical analysis of the existing data (Heinonen et al., 2022). Resulting starting model is utilized in survey design and instrumentation, with aim to acquire data with optimal receiver and source point location given the interpretation of subsurface geology. Survey design also includes synthetic simulations supporting the right selection of instrument parametrization and deployment configuration for optimal target illumination.

SEEMS DEEP data acquisition will be conducted in the autumn 2023 based on the plans made regarding survey design and instrumentation. The data acquisition will include 2D and 3D seismic surveys, 3D audiomagnetotellurics (AMT) measurements, ERT-IP data acquisition, radiomagnetotelluric (RMT) and controlled source EM measurements (CSEM). For seismic

surveys, both Vibroseis and explosives are planned to be used as source and also both 1C and 3C nodal geophones will be utilized. While 2D seismic surveys provide a regional view to the geology down to 5 km depth, 3D seismic survey is targeted to more detailed imaging of orientation and location of the subsurface geological interfaces. Similarly, ERT-IP and RMT surveys aim to reveal near surface structures while AMT gives insight to the regional conductivity anomalies within subsurface.

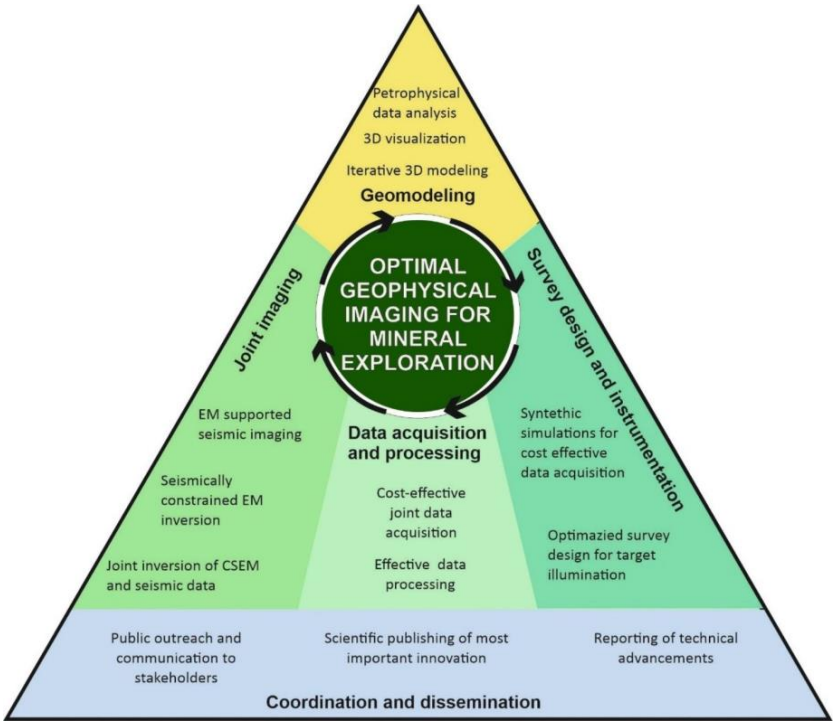

Figure 1. SEEMS DEEP work packages and general workflow illustrated.

Data acquisition is naturally followed with data processing during which SEEMS DEEP aims to use seismic data to aid EM data processing and vice versa. For example, results of seismic full waveform inversion are utilized in inversion of EM data. On the other hand, near surface models produced with ERT measurements are utilized for seismic refraction modelling for static correction. Additionally, advanced imaging and joint inversion methodologies will be developed. After successful data acquisition, processing and joint imaging, the project workflow returns to the geological modelling and initial geological model will be modified based on the newly acquired SEEMS DEEP data.

3. Test area

The Koillismaa Layered Igneous Complex (KLIC) is located in north-east part of Finland. GTK has drilled a 1.7 km long drill hole to the area based on the strong gravity anomaly (Karinen et al., 2021). The gravity anomaly is approximately 50 km long zone that is connecting the distant parts of the outcropped KLIC in Koillismaa and Näränkävaara (Figure 2). The drill core from the Koillismaa hole revealed that geological source of the intrusion indeed are 2.45 Ga mafic-ultramafic igneous rocks. These rocks are not only denser but also more conductive than their surrounding granitic rocks (Nousiainen et al., *this volume*) which enables their imaging using

seismic and electromagnetic methods. KLIC type mafic-ultramafic rocks are also well known of their high potential to host several commodities (Karinen et al., 2010), including Cobalt and Titanium from EU most critical material listing and also Nickel, Copper, Platinum Group Elements, Chromium, Vanadium and Iron.

The drilling of the Koillismaa 1.7 km long hole was preceded with sparse seismic reflection and AMT surveys that confirm the KLIC geologies being detectable for these methods, as illustrated in the Figure 2. The reflectivity along the seismic reflection profile acquired with sparse receiver and source spacing suggested the top part of the intrustion at ~1.3 km depth and bottom at 3.3 km, making intrusion approximately 2 km thick (Gislason et al., 2018). Comparison of the seismic reflectivity and lithological contacts in the drill hole show that prominent reflectors originate from the contact between mafic pyroxenite and country rocks approximately 1.5 km depth in the drill hole. Similar depths can be interpreted for the conductor from the AMT data. More high resolution seismic and EM studies conducted within SEEMS DEEP will shed light to the detailed structure of the Koillismaa intrusion.

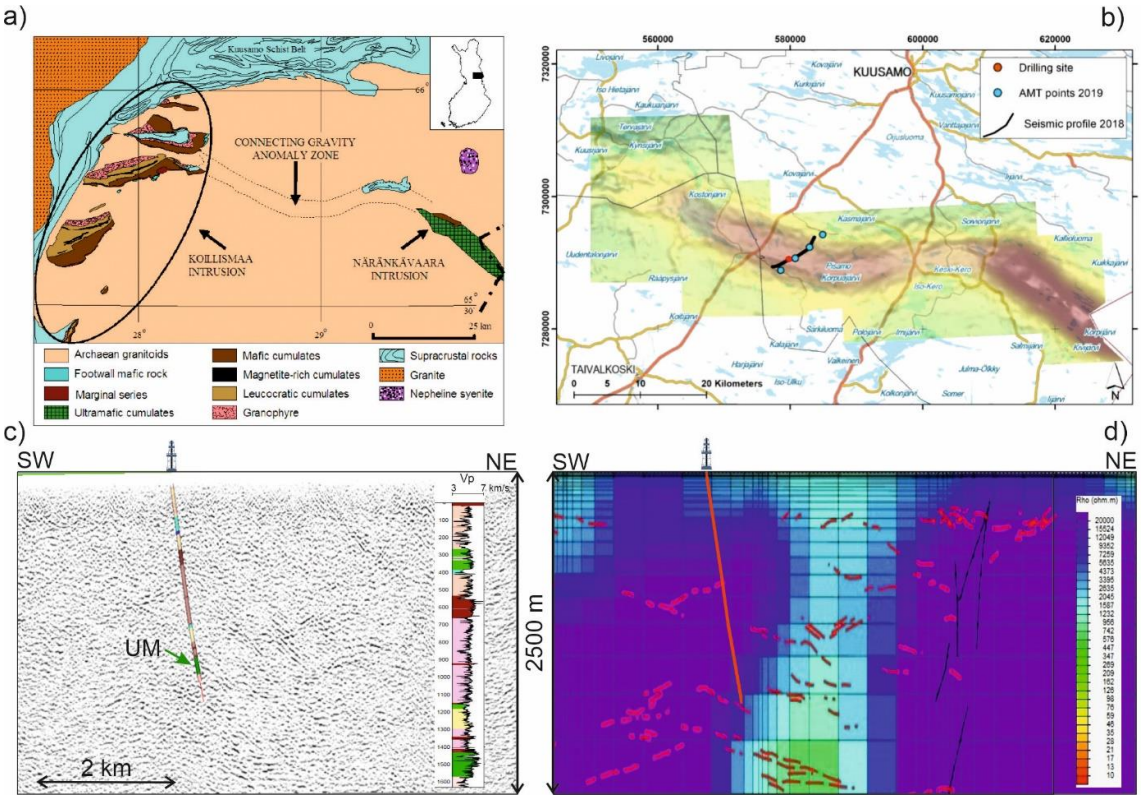

Figure 2. SEEMS DEEP will conduct geophysical measurements in the Koillismaa Layered Igneous Complex, Finland. Surface geology (a) does not explain the prominent gravity anomaly observed in the region (b) but drilling and preliminary seismic studies (c) suggest anomaly is caused by mafic and ultramafic igneous rocks at approximately 1.5 km depth. The sparse AMT profile also shows increase of conductivities at same depths.

7. Conclusions

Multimethod geophysical measurements planned in the SEEMS DEEP project aim to image Koillismaa layered igneous complex in both regional and target scale. Seismic and EM

measurements will complement each other enabling novel method development. Project field work will be conducted in 2023 after rigorous planning and survey design including also synthetic simulations for acquisition parameter and configuration optimization.

Acknowledgements
SEEMS DEEP project is funded through ERA-MIN2 program and in Finland through Business Finland (project number 640/31/2022).

References:

European Commission, Study on the EU's list of Critical Raw Materials (2020). https://rmis.jrc.ec.europa.eu/uploads/CRM_2020_Report_Final.pdf

Gislason, G., Heinonen, S., Salmirinne, H., Konnunaho, J., Karinen, T., 2019. KOSE -Koillismaa Seismic Exploration survey: Acquisition, processing and interpretation. GTK Open File Work Report 101/2018, 33 pages.

Heinonen, S., Nousiainen, M., Karinen, T., Häkkinen, T., 2022. Are Seismic P-Wave Velocities Capable of Revealing The Deep-Seated Prospective Intrusion? EAGE Conference Proceedings, NSG2022 4th Conference on Geophysics for Mineral Exploration and Mining, Sep 2022, 1–5.

Karinen, T.,2010. The Koillismaa Intrusion, northeastern Finland - evidence for PGE reef forming processes in the layered series. Geological Survey of Finland, Bulletin, 404, 176.

Karinen, T., Heinonen, S., Konnunaho, J., Salmirinne, H., Lahti, I., Salo, A.: Koillismaa Deep Hole – solving the mystery of a geophysical anomaly. in Kukkonen, I., Veikkolainen, T., Heinonen, S., Karell, F., Kozlovskaya, E., Luttinen, A., Nikkilä, K., Nykänen, V., Poutanen, M., Skyttä, P., Tanskanen, E., Tiira, T. (Eds): Lithosphere 2021 – Eleventh Symposium on the Structure, Composition and Evolution of the Lithosphere in Finland. Programme and Extended Abstracts, Virtual meeting, January 19-20, 2021. Institute of Seismology, University of Helsinki, Report S-71.

Nousiainen, M., Heinonen, S., Karinen, T., 2022. Petrophysics of the Koillismaa drill hole. *(this volume)*

Agile Exploration and Geo-modelling for European Critical Raw Materials – Introduction to the AGEMERA project

M. Holma[1,2,3,4], J. Korteniemi[2,3], G. Casini[5], E. Saura[5],
F. Šumanovac[6], J. Kapuralić[6] and F. Tornos[7]

[1]Kerttu Saalasti Institute, University of Oulu, Finland, [2]Muon Solutions Oy, Finland,
[3]Arctic Planetary Science Institute, Finland, [4]International Virtual Muography Institute, Global,
[5]Lithica SCCL, Spain, [6]Faculty of Mining, Geology and Petroleum Engineering, University of Zagreb, Croatia,
[7]Instituto de Geociencias, El Consejo Superior de Investigaciones Científicas (CSIC), Spain
E-mail: marko.holma@oulu.fi

The supply of European critical raw materials (CRMs) does not currently meet the European demand. This gap is predicted to increase, making Europe even more dependent on outside suppliers. AGEMERA is a project to help tackle this strategic problem by studying CRM sites in Finland, Poland, Spain, the Balkans, and Zambia. We conduct geological studies, develop and deploy novel mineral exploration techniques, use conventional geophysical methods, and apply machine-learning algorithms to process the acquired data. Special attention will be paid to transcrustal-scale geological domain boundaries, which may have acted as major controlling structures during mineralisation. AGEMERA will also enhance public awareness of our need for CRMs.

Keywords: critical raw materials, exploration, geochemistry, geochronology, structural geology, geophysics, passive seismics, drone geophysics, muography, data cubes

1. The need for critical raw materials in the EU

The worldwide demand for critical raw materials (CRMs) is rapidly increasing due to the transition to greener tech and energy production and a more digitalised world. For the EU to become more resilient and develop strategic autonomy, it is essential to increase Europe's domestic CRM production. Europe has a long tradition in mining and extracting base metals (e.g., Cu, Zn and Pb), but less so to source CRMs (e.g., Li, Co, Nb, W, V, and REEs). Previously, CRMs were not considered very valuable. Their demand was low as only a few applications needed CRMs, and investing in or studying them was not profitable. However, Europe has significant CRM potential locked in many ore districts. Other main bottlenecks in European mineral exploration and mining are the various and lengthy national permitting procedures and the low levels of public acceptance due to both real and perceived hazards.

It is paramount that raw material supply bottlenecks are corrected to achieve strategic autonomy for the supply chains of European industries. This is especially important for CRMs, which have an essential role in transitioning to a low-carbon and digital economy. In many cases, the same raw materials are required by multiple technologies and sectors critical for the clean energy transition (e.g., Li-ion batteries, electric vehicles, fuel cells, solar panels, and wind generators) or the overall technological upgrades (e.g., consumer electronics, drones, robots, 3D printing, digital technologies). Therefore, many competing interests need CRMs, further underlying the need for the EU to produce more CRMs domestically.

AGEMERA is a 3-year R&D project to tackle some critical CRM sourcing problems. It focuses on challenges related to the exploration, characterisation, and exploitation of CRMs in Bosnia-Herzegovina, Bulgaria, Finland, Poland, Spain, and Zambia. AGEMERA combines the resources, expertise, innovation power, and novel technologies of the 20 consortium partners (Table 1), who believe that knowledge and intelligence on CRM potential and market impact

are preconditions for informed decision-making at the country, company, and also citizen level. These will, in turn, unlock various European CRM resources for future use.

AGEMERA has a budget of 7.5 million euros funded by Horizon Europe. The 2022–2025 project is coordinated by the Kerttu Saalasti Institute of the University of Oulu in Finland. The AGEMERA activities (work packages or WPs) most relevant to geosciences and the mining industry are geology (WP1), geophysical data acquisition (WP3), and data fusion (WP4). The three are intricately linked, although, in this paper, we mainly focus on WP1.

Table 1. Partners of the AGEMERA project and their main geoscientific activities.

Organisation	Country	Type	Activities[1)]
University of Oulu	Finland	Academia	GL, DF
University of Lapland	Finland	Academia	
University of Zagreb, Faculty of Mining, Geol. & PE	Croatia	Academia	GL, GPDA, DF
University of Zambia IWRM Centre	Zambia	Academia	GL, GPDA, DF
Tallinn University of Technology	Estonia	Academia	GL, DF
Geological Institute, Bulgarian Acad. of Sciences	Bulgaria	Academia	GL, GPDA
CSIC	Spain	Research	GL, GPDA, DF
Technische Universität Bergakademie Freiberg	Germany	Academia	GL
KGHM Cuprum Research & Development Centre	Poland	Research	GL, GPDA, DF
Lithica SCCL	Spain	SME	GL, GPDA, DF
Radai	Finland	SME	GPDA, DF
Muon Solutions	Finland	SME	GPDA, DF
OPT/NET	Netherlands	SME	GPDA, DF
Geonardo Environmental Solutions	Hungary	SME	
Latitude 66 Cobalt	Finland	Industry	GL, GPDA, DF
Bauxite Mines Jajce	Bosnia-Herzegovina	Industry	GL, GPDA, DF
Bauxite Mines Posušje	Bosnia-Herzegovina	Industry	GL, GPDA, DF
MATSA	Spain	Industry	GL, GPDA, DF
Assarel Medet	Bulgaria	Industry	GL, GPDA, DF
KGHM Polska Miedź	Poland	Industry	GL, GPDA, DF

[1)] Geosciences-related work in AGEMERA: GL = geology (WP1), GPDA = geophysical data acquisition (WP3), DF = data fusion (WP4).

2. Objectives of the AGEMERA project

AGEMERA's goals are to (1) increase geologic understanding of ore districts and improve the genetic models of their known CRM deposits, and (2) enhance public awareness of the crucial role CRMs have in the green transition and the EU's strategic autonomy and resilience.

Data layers will be analysed and interpreted to better understand geological structures, lithologies, hydrothermal alteration systematics, and other footprints of mineral systems. The emphasis will be not only on assisting present miners in maintaining mining longer but also on guiding future projects in finding new ore deposit systems.

3. Research methods

The project will develop and test three novel but proven mineral exploration methods and technologies. Each of them is innovative and non-invasive. These techniques are:

1. Passive seismic methods (e.g., Ugalde et al., 2013) for shallow subsurface characterisation (CSIC & Lithica SCCL);
2. Multi-sensing drone with magnetic, radiometric and EM sensing (e.g., Heincke et al., 2019) for subsurface characterisation down to 300–500 m depth (Radai Oy); and
3. Muon-based density characterisation of rocks (i.e., cosmic-ray muography; e.g. Holma et al., 2022) down to 1 000 m depth (Muon Solutions Oy).

Drone surveys are active and rapid methods capable of covering vast areas relatively quickly, whereas muography and seismic techniques are passive and slow methods capable of covering large volumes with increasing accuracy over time (see the comparison in Figure 1).

In addition, some study sites will be surveyed with more conventional near-surface geophysical methods. Geological studies will include structural geological mapping, rock and soil sampling, and mineralogical studies (e.g., in-situ mineral chemistry and geochronology). The laboratory methods available to the project include microscopy, XRD, XRF, Cold-CL imaging, SEM, EPMA, LA-ICP-MS, and fluid inclusion studies.

Data analysis and fusion tasks include developing machine-learning algorithms to process the vast amount of acquired geoscientific data. The software MOVE is used to produce 3D models of the selected CRM deposits. Results are visualised using hyper-data cubes. Additional satellite-based data will be acquired when appropriate for the data fusion.

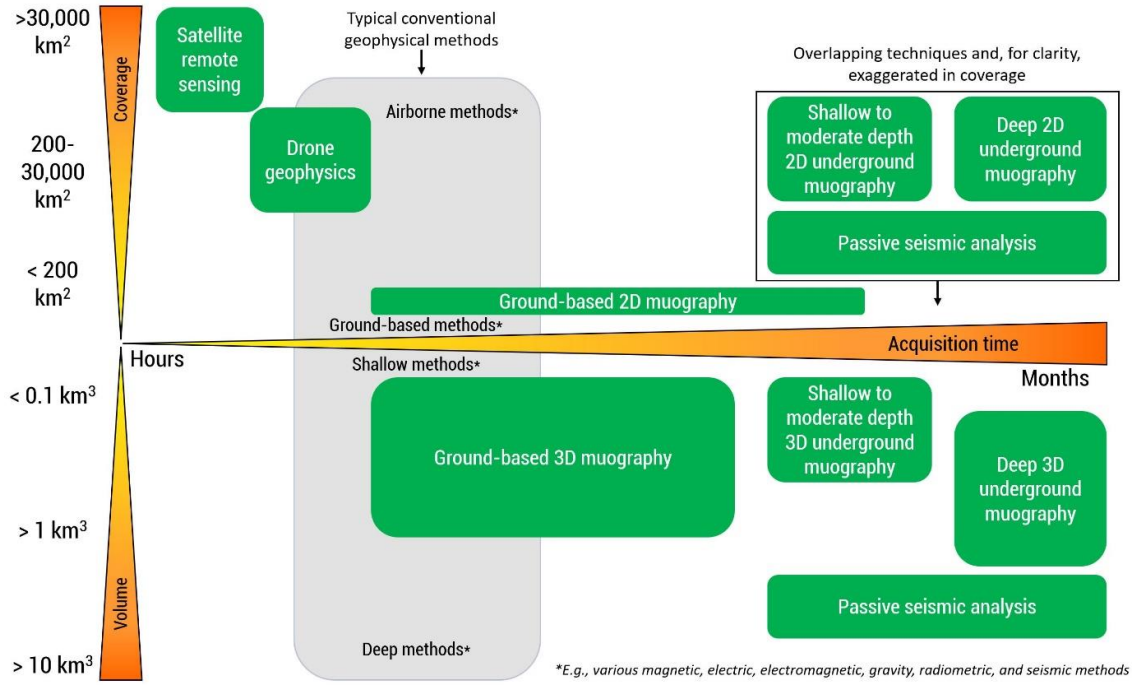

Figure 1. The geophysical technologies used in the AGEMERA project, given as a plot of survey coverage (upper y-axis) and volume (lower y-axis) vs the acquisition time (x-axis). All methods are non-invasive and hence have a minimum environmental impact.

4. Target sites

The AGEMERA consortium will conduct mineral exploration targeting, sampling, modelling, and geophysical field trialling in active mining/exploration sites in Europe and Zambia (Table 2). The targets represent ten mineral system types: orogenic Au, karst bauxite, volcanic-hosted massive sulphide, greisen, porphyry Cu, epithermal, skarn, stratabound Cu-Ag, Fe-oxide Cu-Au, and sediment-hosted stratiform Cu. The deposits to be studied are located in the Peräpohja Schist Belt (Finland), the Iberian Pyrite Belt (Spain), the Kupferschiefer district (Poland), the Panagyurishte & Rossen districts (Bulgaria), the Jajce & Posušje areas (Bosnia-Herzegovina) and the Zambian Copperbelt (Zambia). The Zinnwald Li-greisen deposit (Erzgebirge, Germany) is a backup site for alternative and complementary studies.

5. Thematic connections to lithosphere-scale processes

Crustal structures will be reviewed down to the upper mantle. Special attention will be paid to the known and suspected transcrustal-scale geological domain boundaries, such as terrane sutures, thrust zones, oroclinal bends, basin-controlling master faults, etc. These boundaries may have acted as major controlling structures during mineralisation (e.g., as fluid and/or magma pathways or as controlling factors for local subsidence, uplift, or basin inversion). These studies are based on new field data, updated conceptual orogenic and mineral system models, literature reviews, and various seismic techniques (e.g., ambient noise interferometry and Rayleigh wave ellipticity). The combination and joint inversion of different data sets are expected to provide relevant information in understanding the structural mechanisms that control the CRM mineral systems.

Table 2. List of target sites and the related mineral systems of the AGEMERA project. REE = rare earth elements, PGMs = platinum group metals.

Location	Mineral system	CRMs	Total area, minimum (km²)	Survey area, minimum (km²)
Finland	Orogenic gold with atypical metal association	Cobalt	2 950	1 500
Bosnia-Herzegovina	Karst bauxite	Bauxite, REE	343 + 620	343 + 620
Spain	Volcanic-hosted massive sulphide (VMS)	Cobalt, PGMs	3 500	800
Germany	Greisen (post-magmatic metasomatic alteration of late stage, geochemically specialised granites)	Lithium	52	0 (50)
Bulgaria	Porphyry copper systems (incl. epithermal gold and skarn deposits), iron-oxide copper-gold (IOCG)	PGMs, niobium, tantalum, lithium, REE	17	5 + 5
Poland	Strata-bound type copper and silver deposit	Cobalt, vanadium, molybdenum,	416	154
Zambia	Sediment-hosted stratiform copper (SSC)	Cobalt	32 328 + 125 826	1 200

7. Conclusions

AGEMERA is a three-year EU-funded project aimed at finding and utilising CRM deposits. The project will study ten different mineral system types in Europe and Africa. This will be done with conventional geological, geochemical and geophysical methods and the help of novel and non-invasive geophysical survey methods. The AGEMERA partners look forward to networking and collaborating with other projects which thematically adjoin our project.

Acknowledgements

This project has received funding from the European Union's Horizon Europe research and innovation programme under grant agreement N° 101058178.

References:

Heincke, B., Jackisch, R. ,Saartenoja, A., Salmirinne, H., Rapp, S., Zimmermann, R., Pirttijärvi, M. et al., 2019. Developing multi-sensor drones for geological mapping and mineral exploration: setup and first results from the MULSEDRO project. GEUS Bulletin, 43, e2019430302. doi:10.34194/GEUSB-201943-03-02.

Holma, M., Zhang, Z.-X., Kuusiniemi, P., Loo, K.,Enqvist, T., 2022. Future Prospects of Muography for Geological Research and Geotechnical and Mining Engineering. Geophysical Monograph Series, 270, 199-219. doi:10.1002/9781119722748.ch15.

Ugalde, A., Villaseñor, A., Gaite, B., Casquero, S., Martí, D., Calahorrano, A., Marzán, I., Carbonell, R., Pérez Estaún, A., 2013. Passive Seismic Monitoring of an Experimental CO2 Geological Storage Site in Hontomín (Northern Spain). Seismological Research Letters, 84 (1), 75–84. doi:10.1785/0220110137.

Lithogeochemical approach to constrain Ni-Cu-PGE fertility of Paleoproterozoic ultramafic rocks in Northern Fennoscandia

H. Höytiä[1,2], P. Peltonen[1], P. Lamberg[2] and T. Halkoaho[3]

[1] Department of Geosciences and Geography, P.O. Box 64, FI-00014 University of Helsinki, Finland
[2] Anglo American plc (AA Sakatti Mining Oy), Tuohiaavantie 2, FI-99600 Sodankylä, Finland
[3] Geological Survey of Finland, P.O. Box 1237, FI-70211 Kuopio, Finland
E-mail: henri.hoytia@helsinki.fi

In this study we present parameter-based discrimination method to constrain Ni-Cu-platinum-group elements (PGE) mineralized environments in the Paleoproterozoic greenstone belt continuum of Central Lapland (CLGB), Pulju (PGB) and Karasjok (KGB). Lithogeochemical data, as obtained from whole-rock analysis, together with knowledge of mineralized and plausibly barren environments in the study areas help to distinguish, which units are more fertile, and thus have higher potential to host economic Ni-Cu-PGE -deposits. Using lithogeochemical constraints, chemical signatures linked to ore-forming processes, e.g., magma primitivity and sulfide segregation, can be evaluated, and by fertility analysis those can be transferred into simple numerical form, which allows exploration ranking of the studied targets.

Keywords: lithogeochemistry, nickel, copper, PGE, platinum-group elements, greenstone belt, Central Lapland, Pulju, Karasjok

1. Introduction

Magmatic Ni-Cu-platinum-group element (PGE) sulfide ores comprise a major portion of the known global Ni (Mudd and Jowitt 2014) and PGE (Mudd et al. 2018) resources, as well as important portion of Cu (Mudd and Jowitt, 2018) and Co (Mudd et al., 2013) resources. Ni-Cu-PGE sulfide deposits form within long-lived magmatic plumbing systems, where mantle derived mafic-ultramafic magmas migrate to the lithosphere and interact with country rocks during their ascent and emplacement (e.g., Barnes et al., 2016). Mafic-ultramafic melts are naturally enriched in Ni, Cu, Co, and PGE, but often lack sulfur to reach sulfur saturation and formation of an immiscible sulfide phase. Addition of sulfur, e.g., by assimilation of sulfur-bearing country rocks and/or by syn- to post-magmatic fluids into mafic-ultramafic magmatic systems can lead to exsolution of immiscible sulfide melt that effectively collects metals and significantly enhances sulfide accumulation (e.g., Robertson et al., 2015). Metal collection to the sulfide phase is augmented by dynamic interaction between large volumes metal-transporting silicate magma and immiscible sulfide melt, and sulfide accumulation boosted by, e.g., turbulent flow, convection and/or diffusional processes facilitated by a fluid phase that would concentrate the sporadic sulfide globules to form anomalously sulfide-rich rock units (e.g., Barnes et al. 2016, Iacono-Marziano et al., 2022). The Paleoproterozoic greenstone belts of northern Finland and Norway host several mafic-ultramafic units that yield ages coeval with the extensional stage at cratonic margin roughly at 2.1-1.86 Ga (e.g., Peltonen et al., 2014 and references therein). This extensional period, namely the final break-up of the supercontinent Kenorland at ca. 2.06-2.05 Ga, is important in terms of Ni-Cu-PGE as it includes the formation of the Kevitsa and Sakatti deposits, and Lomalampi and Puijärvi mineralizations in CLGB, the Hotinvaara deposit as well as several smaller mineralizations in PGB, and Gállojávri and Porsvann mineralizations in KGB (Figure 1).

2. Sample collection and fertility analysis

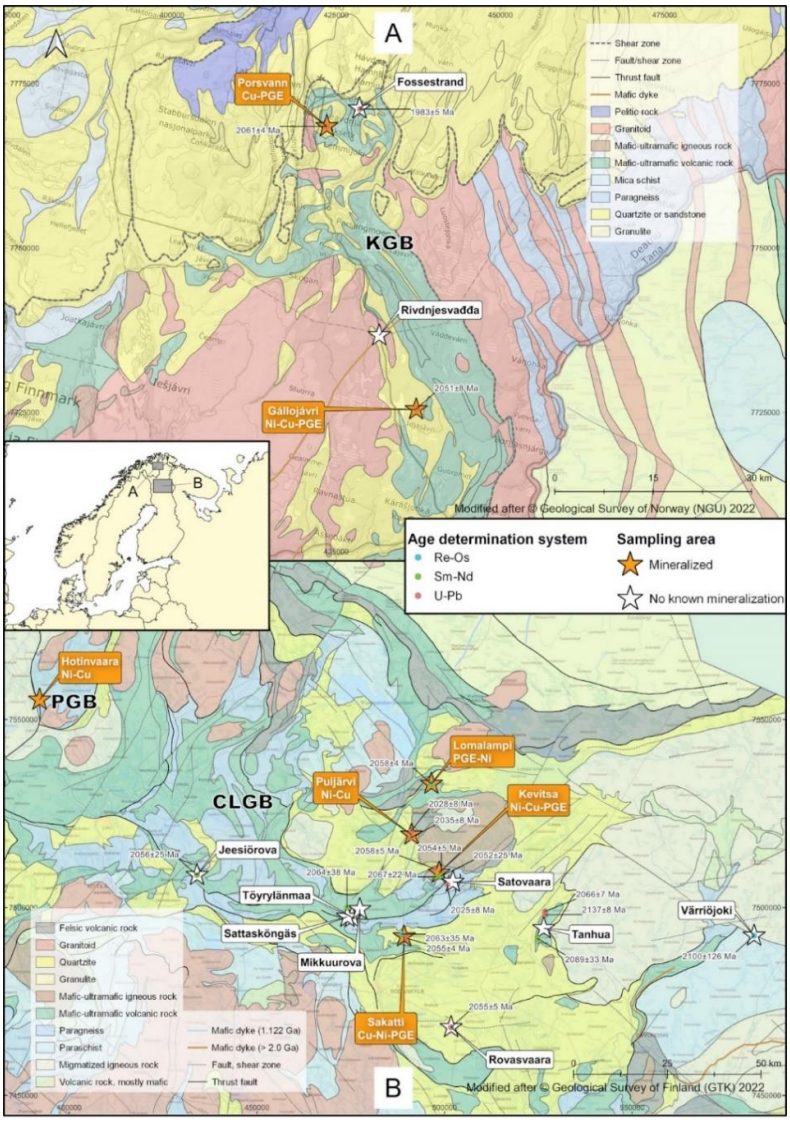

Figure 1. Simplified and unified geological maps modified after Geological Surveys of Finland (GTK 2022) and Norway (NGU, 2022) open access bedrock map databases. Study areas in the Central Lapland (CLGB), Pulju (PGB) and Karasjok (KGB) greenstone belts are shown with star symbols, if mineralized main commodities indicated. Also, relevant ages and determination systems are shown. References for the age determinations are shown in Table 1.

Fertility analysis provides a practical and measurable quantitative tool to support qualitative tools used for lithogeochemical Ni-Cu-PGE exploration. The tool is used with whole-rock analysis data and does not demand any other specific analysis method. Our approach uses the population analysis method developed by Lamberg (2005), where the processes attributed to Ni-Cu-PGE ore formation are turned into measurable parameters. Within each parameter, statistically non-representative samples are rejected by Tukey's fences method (interquartile range for outliers). By fulfilling parameters, the studied sample population is given an overall discrimination number, which allows numerical ranking in terms of Ni-Cu-PGE fertility. To test

the suitability of this fertility analysis to the Paleoproterozoic greenstone belts in northern Finland and Norway, we have gathered whole-rock major element and trace element data, including Pt, Pd and Au that represent known mineralized (fertile) units and units that share a similar age, lithology and regional stratigraphy but lack a known mineralization (Table 1).

3. Results

Bedrock mapping and data acquisition of the chosen units was conducted during 2021-2022. Most of the known Ni-Cu-PGE mineralization are hosted by pyroxenitic units albeit massive type mineralizations only occur in peridotitic units. Mineralization related to gabbroic rocks is only known in the Sakatti deposit. First results of the fertility analysis and its implications to Ni-Cu-PGE prospectivity within the studied units will be shown and discussed in the meeting.

Table 1. Sampling localities, relevant age determinations, state of known mineralization and their main lithogeochemical phase as represented by whole-rock analysis data. KGB komatiites include Fossestrand and Rivdnjesvađđa areas, CLGB komatiites include Jeesiörova, Mikkuurova, Sattasköngäs and Töyrylänmaa areas shown in Figure 1.

Area	Age, reference	Ni-Cu-PGE mineralization	Main phase
Gállojávri	2051 ± 4 Ma, Orvik et al. (2022)	disseminated	pyroxenitic
Kevitsa	2058 ± 4 Ma, Mutanen and Huhma (2001)	disseminated	pyroxenitic
Lomalampi	2058 ± 93 Ma, Moilanen et al. (2019)	disseminated	peridotitic
Porsvann	2061 ± 4 Ma, Hansen et al. (2022)	disseminated	pyroxenitic
Puijärvi	2035 ± 8 Ma, Huhma et al. (2018)	disseminated	pyroxenitic
Pulju (Hotinvaara)	Correlation to KGB & CLGB, Papunen (1998)	massive, disseminated, and remobilized	peridotitic
KGB komatiites	1983 ± 5 Ma, Hansen et al. (2022)	no known mineralization	peridotitic
Rovasvaara	2055 ± 5 Ma, Rastas et al. (2001)	no known mineralization	gabbroic
Sakatti	2063 ± 35 – 2055 ± 4 Ma, Moilanen et al. (2021), Anglo American unpublished data	massive, disseminated and stringer	peridotitic
Satovaara	2025 ± 8 Ma, Huhma et al. (2018)	no known mineralization	pyroxenitic
CLGB komatiites	2064 ± 38 - 2056 ± 25 Ma , Hanski et al. (2001), Huhma et al. (2018)	no known mineralization	peridotitic
Tanhua	2134 ± 10 - 2066 ± 7, Räsänen and Huhma (2001), Huhma et al. 2018	no known mineralization	gabbroic/ peridotitic
Värriöjoki	2100 ± 126 Ma, Heller (2020)	no known mineralization	peridotitic

References:

Barnes, S.J., Cruden, A.R., Arndt, N., Saumur, B.M., 2016. The mineral system approach applied to magmatic Ni–Cu–PGE sulphide deposits. Ore Geol.Rev., 76, 296–316. https://doi.org/10.1016/j.oregeorev.2015.06.012

GTK, 2022. WFS map server, bedrock database 1:5m. Used on 14th of October 2022. https://gtkdata.gtk.fi/arcgis/rest/services/Rajapinnat/GTK_Maapera_WFS/MapServer/WFSServer?

Hansen, H., Slagstad, T., Bergh, S.G., 2022. Geochronology of the northern part of the Karasjok Greenstone Belt records ~500 million years of plume induced magmatism and rifting. Conference presentation at the 35th Nordic Geological Winter Meeting: Reykjavik, Iceland, 26 pages.

Hanski, E., Huhma, H., Rastas, P., Kamenetsky, V.S., 2001. The Palaeoproterozoic Komatiite-PicriteAssociation of Finnish Lapland. Jour. Petr., 42, 855–876, https://doi.org/10.1093/petrology/42.5.855

Heller, A.T., 2020. Petrology, geochemistry, geochronology, and Ni-Cu-PGE potential of the Värriöjoki Ultramafic Complex. M.Sc. thesis, Oulu Mining School, 80 pages.

Huhma, H., Hanski, E., Kontinen, A., Vuollo, J., Lahaye, Y., 2018. Sm–Nd and U–Pb isotope geochemistry ofthe Palaeoproterozoic mafic magmatism in eastern and northern Finland. Geological Survey of Finland Bulletin, 405, 150 pages.

Iacono-Marziano, G., le Vaillant, M., Godel, B.M., Barnes, S.J., Arbaret, L., 2022. The critical role of magma degassing in sulphide melt mobility and metal enrichment. Nat.Com. 13. https://doi.org/10.1038/s41467-022-30107-y

Lamberg, P., 2005. From genetic concepts to practice – lithogeochemical identification of Ni-Cu mineralised intrusions and localisation of the ore. GTK Bulletin, 402, 264 pages.

Moilanen, M., Hanski, E., Konnunaho, J., Yang, S.H., Törmänen, T., Li, C., Zhou, L.M., 2019. Re-Os isotope geochemistry of komatiite-hosted Ni-Cu-PGE deposits in Finland. Ore Geol.Rev., 105, 102–122. https://doi.org/10.1016/j.oregeorev.2018.12.007

Moilanen, M., Hanski, E., Yang, S.H., 2021. Re-Os isotope geochemistry of the Palaeoproterozoic Sakatti Cu-Ni-PGE sulphide deposit in northern Finland. Ore Geol.Rev., 132, 104044. https://doi.org/10.1016/j.oregeorev.2021.104044

Mudd, G.M., Jowitt, S.M., 2014. A Detailed Assessment of Global Nickel Resource Trends and Endowments. Economic Geology, 109, 1813–1841. https://doi-org.libproxy.helsinki.fi/10.2113/econgeo.109.7.1813

Mudd, G.M., Jowitt, S.M., 2018. Growing global copper resources, reserves and production: Discovery is not the only control on supply. Economic Geology 113, 1235–1267. https://doi.org/10.5382/econgeo.2018.4590

Mudd, G.M., Jowitt, S.M., Werner, T.T., 2018. Global platinum group element resources, reserves and mining – A critical assessment. Sci.Tot.Env., 622-623, 614-625. https://doi.org/10.1016/j.scitotenv.2017.11.350

Mudd, G.M., Weng, Z., Jowitt, S.M., Turnbull, I.D., Graedel, T.E., 2013. Quantifying the recoverable resources of by-product metals: the case of cobalt. Ore Geol.Rev., 55, 87–98. https://doi.org/10.1016/j.oregeorev.2013.04.010

Mutanen, T., Huhma, H., 2001. U-Pb geochronology of the Koitelainen, Akanvaara and Keivitsa layered intrusions and related rocks. In: Vaasjoki, M., 2001 (ed.). Radiometric age determinations from Finnish Lapland and their bearing on the timing of Precambrian volcano-sedimentary sequences. Geological Survey of Finland, Special paper, 33, 229-247.

NGU, 2022. Open access Bedrock N1350 (1:1.350.000). Downloaded on 13th of October 2022. https://geo.ngu.no/download/order?dataset=606&lang=eng

Orvik, A.A., Slagstad, T., Sørensen, B.E., Millar, I., Hansen, H., 2022. Evolution of the Gállojávri ultramafic intrusion from U-Pb zircon ages and Rb-Sr, Sm-Nd and Lu-Hf isotope systematics. Precambrian Res., 379, 106813. https://doi.org/10.1016/j.precamres.2022.106813

Papunen, H., 1998. Geology and Ultramafic Rocks of the Paleoproterozoic Pulju Greenstone Belt, Western Lapland. Integrated Technologies for mineral exploration pilot project for nickel ore deposits. Turku University, Dep.Geol. Tech.Rep., 55, 55 pages.

Peltonen, P., Santaguida, F., Beresford, S., Huhma, H. 2014. U-Pb zircon and Sm-Nd isotopic constraints for the timing and origin of magma Ni-Cu-PGE deposits in Northern Fennoscandia. Poster at SEG 2014 Conference: Keystone, Colorado, USA, 1 page.

Rastas, P., Huhma, H., Hanski, E., Lehtonen, M.I., Härkönen, I., Kortelainen, V., Mänttäri, I., Paakkola, J., 2001. U-Pb isotopic studies on the Kittilä greenstone area, central Lapland, Finland. In: Vaasjoki, M., 2001 (ed.). Radiometric age determinations from Finnish Lapland and their bearing on the timing of Precambrian volcano-sedimentary sequences. Geological Survey of Finland, Special paper, 33, 95–143.

Robertson, J., Ripley, E.M., Barnes, S.J., Li, C., 2015. Sulfur liberation from country rocks and incorporation in mafic magmas. Economic Geology 110, 1111–1123. https://doi.org/10.2113/econgeo.110.4.1111

Räsänen, J., Huhma, H., 2001. U-Pb datings in the Sodankylä schist area, central Finnish Lapland. In: Vaasjoki, M., 2001 (ed.). Radiometric age determinations from Finnish Lapland and their bearing on the timing of Precambrian volcano-sedimentary sequences. Geological Survey of Finland, Special paper 33, 143-153.

Determining the age and metamorphic evolution of the Pyhäsalmi region, Central Finland: relationship between metamorphism, ore genesis and evolution

S.R. Islam[1], E. Heilimo[1] and K. Cutts[2]

[1] Department of Geography and Geology, University of Turku, FI-20500, Turku, Finland
[2] Geological Survey of Finland, P.O. Box 96, FI-02151 Espoo, Finland
Email: rakibul.islam@utu.fi

The influences of pressure and temperature on the formation of metamorphic rocks were first presented by Finnish geologist Pentti Eskola in 1915. Since this time, metamorphic petrology has advanced with new techniques allowing us to tie regional structures, ages and metamorphic/ore mineral assemblages together to make interpretations about the tectonic setting of metamorphism and ore genesis. This study aims to constrain the metamorphic conditions for ore potential Pyhäsalmi region. Additionally, we will study the remobilization of the ore minerals and microstructures which relate porphyroblasts and ore mineral growth. The study will provide new approach in the study of Pyhäsalmi area and Raahe-Ladoga zone.

Keywords: metamorphism, mineral paragenesis, remobilization, porphyroblast, microstructures, Pyhäsalmi

1. Introduction

The Pyhäsalmi region is characterized by volcanic massive sulfide (VMS) type ore deposits, litho-stratigraphically located in altered sericite-cordierite-anthophyllite rock, belonging to a bimodal volcanite series with pelitic interlayers. Genetically the Pyhäsalmi region is part of a proposed primitive Paleoproterozoic (1.93-1.92 Ga) island arc (Mäki, 1986; Gaál and Gorbatschev 1987; Ekdahl, 1993; Lahtinen, 1994; Kousa et al., 1994; Roberts et al., 2004; Eilu et al., 2013; Laine et al., 2015). The Pyhäsalmi Cu-Zn ore deposit is located on the northern edge of the Svecofennian continental crust in the ore-potential Raahe-Ladoga zone (Laine et al., 2015). The size of the mined ore exceeds 75.7 Mt. and the average composition of the ore is 0.9 wt % Cu, 1.9 wt % Zn, 0.4 g/t Au, and 14.1 g/t Ag (Mäki et al. 2015).

Previous geological studies of the Pyhäsalmi region have focused mainly on the regional geology, the geological evolution of the region, 3D modelling and the seismic characteristics of mineralized sites (Helovuori, 1979; Roberts et al., 2004; Heinonen et al., 2012; Laitala, 2015; Laine et al., 2015). However, studies constraining the metamorphic influence on the ore deposit have been limited. Especially, studies of the effects of metamorphism on the ore minerals that would let us interpret the pressure and temperature of the ore genesis and temporal evolution. Moreover, uncovering the metamorphic history of the pelitic rocks will not only provide information about the metamorphic processes and tectonic setting, but will also yield new information about the ore potential of the region.

The composition of metamorphic index minerals (i.e cordierite, sillimanite, garnet, biotite, staurolite and anthophyllite) found in equilibrium around the Pyhäsalmi ore deposit will allow us to determine the peak P-T conditions. Combining the P-T conditions with in-situ age determinations will help to model the P-T-t paths for the region. Monazite, titanite and garnet

in stable metamorphic mineral assemblages can be used for U-Pb dating to date the P-T conditions.

2. Approach

To construct the P-T-t paths, identifying suitable equilibrium mineral assemblages such as sillimanite + cordierite + garnet using a petrographic study is our first priority. This will additionally allow us to identify minerals that are suitable for U-Pb dating such as zircon, titanite, garnet and apatite. We want to also identify the relationship of these chronometers with the rest of the mineral assemblage in order to tie ages with the metamorphic evolution of the samples. Furthermore, our approach also includes textural studies of the metamorphosed rocks of the region to connect the crystal growth with deformational structures. The observed crystal growth textures, mineral compositions, and nucleation relationships will provide useful information in the study of remobilization of ore minerals. Several modern day in-situ methods such as Electron Probe Micro Analysis (EPMA) including area compositional analysis, X-ray microtomography (micro-CT) and laser ablation-inductively coupled plasma mass spectrometer (LA-ICP-MS) geochronology will be executed to gather the necessary data.

3. Significance of the study

The study generates new metamorphic information from an economically significant area and combines previous knowledge about the metamorphism of the Pyhäsalmi area. We aim to understand the metamorphic P-T-t path and the formation of related ore minerals. Combining the research results with the metamorphic map of Finland (Hölttä & Heilimo, 2017) would strengthen the national scientific knowledge about metamorphism. Understanding the retrograde metamorphism of the region would provide new exploration ideas for remobilized ore deposits in Pyhäsalmi and other ore potential regions.

4. Preliminary results

At the moment our preliminary results are limited to the identification of metamorphic mineral assemblages from petrographic thin section. The metamorphic mineralogy of the studied supracrustal rock is quartz, biotite, cordierite, anthophyllite (prismatic and occasionally also hornblende), muscovite, plagioclase, K-feldspar, albite, chlorite, garnet, sillimanite (fibrolite) and opaque minerals as the major minerals. Whereas zircon, titanite (± rutile), apatite, allanite and monazite are present as accessory minerals.

Overall, subhedral to euhedral quartz and cordierite grains exhibit granoblastic texture. The prismatic anthophyllite and fibrolitic sillimanite represent a nematoblastic texture occasionally. Parallel orientation of the platy and elongated mica grains imparts schistosity. Alternate layering of biotite, chlorite and anthophyllite with quartz, plagioclase and cordierite gives the impression of gneissosity partly related to partial melting.

Chloritization of biotite, as well as saussuritization and epidotization of plagioclase are very common features likely related to retrograde hydrothermal alteration. A conspicuous reaction rim of biotite, cordierite, sillimanite and a symplectic intergrowth of quartz and K-feldspar around a σ-type garnet porphyroblast shows evidence of retrograde metamorphism where a low-pressure mineral, cordierite produces a rim around high pressure mineral, garnet (Figure 1). The alignment of mica and quartz inclusions within the garnet implies syn-kinematic

metamorphic mineral growth. Folding and shearing of elongated micas around porphyroblast and kink banding of biotite that overlaps the orientation of the S_1 foliation represented by parallelly oriented platy elongated biotite and muscovite provide information of D_2 stage deformation of S_1 foliation.

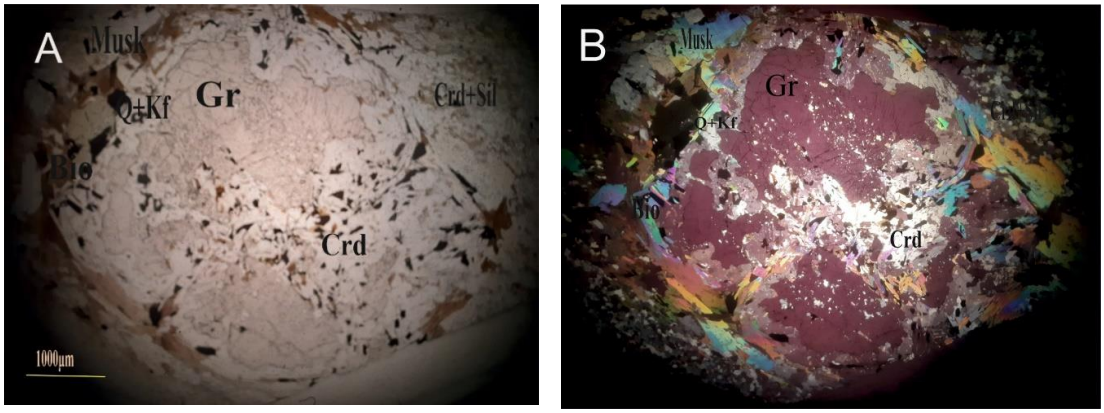

Figure 1. Photomicrograph of thin section from the sample PYS-144 1326.15; A) under plane polarized light, and B) under cross-polarized light. A porphyroblast of garnet in contact with cordierite, sillimanite and symplectic intergrowth of quartz and K-feldspar. The low-pressure mineral, cordierite rim around high pressure mineral garnet indicates retrograde metamorphism. Cordierite, sillimanite, quartz, K-feldspar, biotite, muscovite forming a reaction rim around the retrograde garnet. Abbreviations: Bio – biotite, Crd – cordierite, Gr – garnet, Kf – K-feldspar, Musk – muscovite, Q - quartz, and Sil – sillimanite.

5. References:

Eilu, P., Bergman, T., Bjerkgård, T., Feoktistov, V., et al., 2013. Metallic Mineral Deposit Map of the Fennoscandian Shield 1:2,000,000. Revised edition (comp.). Geological Survey of Finland, Geological Survey of Norway, Geological Survey of Sweden, the Federal Agency of Use of Mineral Resources of the Ministry of Natural Resources of the Russian Federation.

Ekdahl, E., 1993. Early Proterozoic Karelian and Svecofennian formations and the evolution of the Raahe-Ladoga Ore Zone, based on the Pielavesi area, central Finland. Geological Survey of Finland, Bulletin, 373, 137 p.

Eskola, P., 1915. Om sambandet mellan kemisk och mineralogisk sammansättning hos Orijärvitraktens metamorfa bergarter. Bulletin de la Commission géologique de Finlande, 44, 1-145 p. (in Swedish)

Gaál, G., Gorbatschev, R., 1987. An outline of the Precambrian evolution of the Baltic Shield. Precambrian Research, 35, 15–52.

Helovuori, O., 1979. Geology of the Pyhäsalmi ore deposit, Finland. Economic Geology, 74, 1084-1101.

Heinonen, S., Imaña, M., Snyder, D.P., Kukkonen, I.T., Heikkinen, P.J. 2011. Seismic reflection profiling of the Pyhäsalmi VHMS-deposit: A complementary approach to the deep base metal exploration in Finland. Geophysics, 77, WC15-WC23.

Hölttä P.S., Heilimo, E., 2017. Metamorphic map of Finland. Geological Survey of Finland. Special paper 60, 41-76 p.

Kousa, J., Marttila, E., Vaasjoki, M., 1994. Petrology, geochemistry and dating of Paleoproterozoic metavolcanics rocks in the Pyhäjärvi area, central Finland. In: Geochemistry of Proterozoic supracrustal rocks in Finland. IGCP Project 179 Stratigraphic methods as applied to the Proterozoic record and IGCP Project 217 Proterozoic geochemistry, Geological Survey of Finland. Special Paper, 19, 7-27.

Lahtinen, R., 1994. Crustal evolution of the Svecofennian and Karelian domains during 2.1–1.79 Ga, with special emphasis on the geochemistry and origin of 1.93–1.91 Ga gneissic tonalites and associated supracrustal rocks in the Rautalampi area, central Finland. Geological Survey of Finland, Bulletin, 378, 128 p.

Laine, E., Luukas, J., Mäki, T., Kousa, J., Ruotsalainen, A., Suppala, I., Imana, M., Heinonen, S., Häkkinen, T. 2015. The Vihanti-Pyhäsalmi Area. In: Weihed, P. (Ed.) 3D, 4D and Predictive Modelling of Major Mineral Belts in Europe. Cham: Springer International Publishing.123-144.

Laitala, J., 2015. Minerology and geochemistry of the pyrrhotite horizon in the Pyhäsalmi district, Central Finland. University of Turku, 86 p. (Unpublished)

Mäki, T., 1986. The Lithogeochemistry of the Pyhäsalmi Zn-Cu-Pyrite Deposit, Finland. In: Prospecting in areas of glaciated terrain symposium, Sept. 1–2, Kuopio. Finland. Institute of Mining and Metallurgy, London, .69–82.

Mäki, T., Imaña, M., Kousa, J., Luukas, J. 2015. Chapter 7 - The Vihanti-Pyhäsalmi VMS Belt In: Maier, W.D., Lahtinen, R., O'Brien, H. (Eds.) Mineral Deposits of Finland. Elsevier, 507-530.

Roberts, M.D., Oliver, N.H.S., Lahtinen, R. ,2004. Geology, lithogeochemistry and paleotectonic setting of the host sequence to the Kangasjärvi Zn-Cu deposit, central Finland: Implications for volcanogenic massive sulphide exploration in the Vihanti-Pyhäsalmi district. Bulletin of Geological Society of Finland 76, 31-62 p.

Petrographic and micro-XRF studies of Co-Cu mineralized Tanhua mafic intrusion

P. Jänkävaara[1], J. Konnunaho[2] and E. Heilimo[1]

[1]Department of Geography and Geology, University of Turku
[2]Geological Survey of Finland, P.O. Box 77, FI-96101 Rovaniemi, Finland
E-mail: patrik.s.jankavaara@utu.fi

This study presents petrographic descriptions and lithological variety of the Tanhua mafic intrusion within the Paleoproterozoic Central Lapland Greenstone Belt (CLGB). Additionally, new geochemical data have been obtained by micro-XRF studies. The aim of this study is increase understanding about the petrology and internal geology of the Tanhua intrusion. Based on Geological Survey of Finland (GTK) studies, elevated concentrations of cobalt and copper have been identified the intrusion's mineralized rocks. Based on benchtop micro-XRF studies, we propose the substitution of Fe^{2+} with Co^{2+} within pyrite crystal lattice.

Keywords: Tanhua, Pelkosenniemi, Central Lapland greenstone belt, petrography, mafic intrusion, gabbro, cobalt

1. Introduction

The Tanhua mafic intrusion locates in the municipality of Savukoski, northern Finland ca. 45 km NE from Sodankylä. It is a metamorphosed and partly hydrothermally modified mafic intrusion, which has strong positive magnetic characteristics (Korvuo, 1977). The age of the intrusion is estimated to be ca. 2.11-2.15 based on U-Pd and Pb-Pb analyses (Huhma et al., 2018). The Tanhua mafic intrusion surrounded by supracrustal metasedimentary and metavolcanic rocks of CLGB such. The intrusion's major present silicate minerals are hornblende and plagioclase, as well as minor amounts of sulfide minerals such as pyrite, chalcopyrite, and pyrrhotite locate as sparse disseminations and thin veins. Magnetic portions of the intrusions host oxide (magnetite) dissemination and semimassive portions. Whole-rock geochemical analyses indicate that mineralized part of the Tanhua gabbro contains high Co, up to 3000 ppm and Cu 1.4 wt% (Konnuaho et al., 2022).

The Tanhua area has been studied by Rautaruukki Oy as a part of an exploration project (Mattila, 1973; Korvuo, 1977). In 1977 Rautaruukki Oy drilled four drillholes, two intersected northern part (i.e., Kylälampi area) and two southern part of the intrusion (i.e., Kannusvaara area). The Tanhua intrusion remained relatively unstudied, and its economical V-Ti-Fe potential was estimated to be poor, and further studies were cancelled (Korvuo, 1977). However, these historical studies showed that the intrusion hosts mineral potential for Co and Cu (Konnunaho et al., 2022).

The main objective of this study is to make petrographic descriptions for different rock types of Tanhua intrusion. Additionally, the study aims to identify cobalt beraing minerals in Tanhua intrusion. In terms of methodology, we have used petrography and benchtop micro-X-ray fluorescence (XRF) instrument.

2. Studies in 2019-2022 by GTK

In 2019-2020 Geological Survey of Finland (GTK) started more extensive investigations in Tanhua mafic intrusion for its Co-Cu potential. GTK conducted two drilling campaign between 2019 and 2020 with total 14 drillhole. The drill core loggings evidenced intrusive rocks from mafic to felsic in composition with variable textures. Distribution of magnetic minerals is

uneven, magnetite bearing rocks have similar attributes like non-magnetic rocks of the intrusion.

Major part of the intrusion shows significant albitization and biotitization. In parts of the intrusion that show the strongest biotitization, biotite has formed large biotite crystals (mottled gabbro or biotite gabbro). These large biotite crystals are found generally together with albitization. Additionally, the mottled gabbro areas are lack of magnetite. Inside of the intrusion, chilled margins have been observed at places, likely indicating internal magmatic pulses. In mineralized rock, moderate amount of pyrite, chalcopyrite and pyrrhotite locate as disseminaton, veinlets and veins typically with magnetite but minor amount of sulphides can be found as weak disseminations without magnetite throughout the intrusion (Konnunaho et al., 2022).

3. Petrography

The petrographic study was made for better understanding of the geology and the mineralogy of Tanhua intrusion. The main focus of this study was to determine the existing minerals in the intrusion, define different rock types present in the intrusion, and investigate found microtextures.

The Tanhua mafic intrusion contains mainly silicate minerals such as hornblende, plagioclase, quartz, biotite and moderate amounts of magnetite. Accessory minerals of the Tanhua mafic intrusion are scapolite, pyrite, chalcopyrite, ilmenite, titanite, zircon, apatite, chlorite, sericite and colourless clinoamphibole. The most abundant minerals of the intrusion are hornblende and plagioclase and the major difference between different rock types of the intrusion can be observed in the abundance of these two minerals. The studied samples can be divided to four different groups based on the estimated amounts of hornblende in the thin section. We propose the following division for the intrusion rock types: tonalites, diorites, and gabbros (Figure 1A and B). Peridotites occurs also in drill cores, which possibly do not belong to the Tanhua mafic intrusion.

In general, the studied samples are strongly metamorphosed, and as the result minerals has been recrystallized. In majority of the thin sections the texture is granoblastic. Some samples are oriented, and the grade of orientation varies from strong to non-existent. Exsolution texture of quartz in hornblende is common in gabbroic samples, indicating that pyroxene has altered to hornblende leaving additional silica as quartz inclusions (Figure 1A). In some samples, plagioclase is altered to albite (Figure 1B), sericite, or scapolite.

The most voluminous rock type of the intrusion is gabbro (Figure 1A). It consists of about 40-60% of hornblende, about 30-40% of plagioclase, 5-10% of quartz, and 0-10% of biotite, 0-10% magnetite as modal amounts and accessory minerals. Occasionally, gabbro can be found with mottled texture due to biotitization. The mottled textures are strongly oriented and formed several aggregated biotite grains that are likely results of alteration from hornblende or pyroxene (Figure 2).

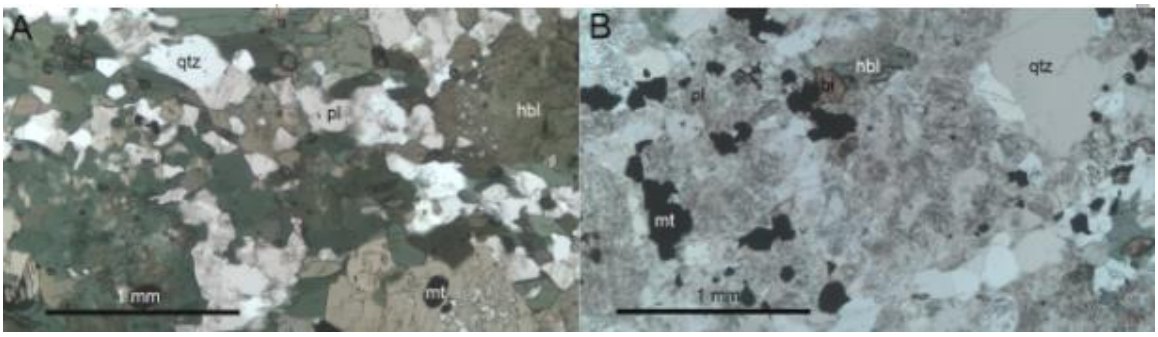

Figure 1. A. Microphotograph of the metamorphosed Tanhua gabbro, sample U5212020R16 41.40m. PPL, 5x. B. Microphotograph of the altered Tanhua tonalite, sample U5212019R7 120.70. PPL 5x. Abbreviations: qtz − quartz, pl − plagioclase, hbl − hornblende, bi − biotite, mt − magnetite.

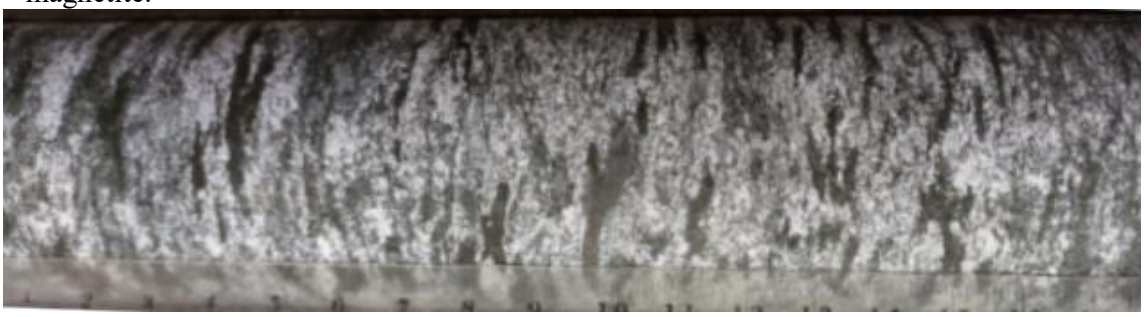

Figure 2. Photograph of Tanhua drillcore of biotitized gabbroic rock referred as mottled gabbro (Konnunaho et al. 2022).

4. Benchtop micro-XRF results

The Bruker M4 TORNADO benchtop micro-XRF instrument was used to determine the placement of cobalt. The benchtop XRF-analyses were made from four samples at University of Turku. Two of the studied samples represented gabbro and two represented tonalite. As result, the tonalite samples did not show significant amounts of Co. The gabbro samples evidenced elevated Co content on top of the pyrite grain (Figure 3). As Co^{2+} ion has similar properties (radius and charge) than Fe^{2+} ion, the Co^{2+} substitutes Fe^{2+} in pyrite's crystal structure.

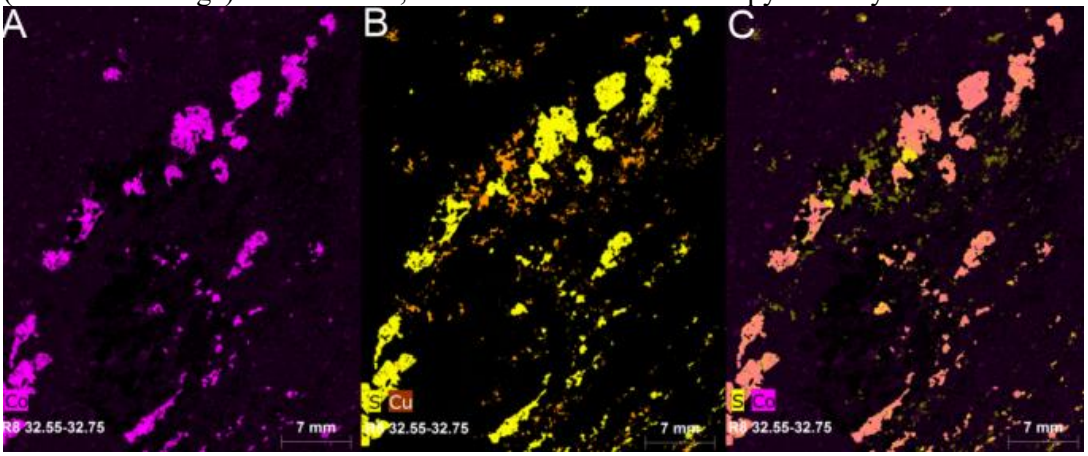

Figure 3. Benchtop micro-XRF-maps from drillhole U5212019R8, depth 32.55-32.75. The figures highlight elevated contents A) cobalt, B), sulphur and copper, C) sulphur and cobalt. Areas which are enriched in sulphur and cobalt represent disseminated pyrite minerals.

5. Conclusions

Based on drill core logging, petrographic descriptions, and benchtop micro-XRF results, we propose the following for the Tanhua mafic intrusion.

- The changes in grain size and existing chilled margins reported by Konnunaho et al. (2022) might indicate different internal pulses of differentiated magma.
- The magmatic pyroxene has altered to hornblende and quartz (±biotite). Albite, sericite, and possible scapolite are alteration products of plagioclase.
- Some parts of the intrusion have biotitized and formed mottled gabbro with accumulated biotite grains.
- Cobalt locates in the pyrite crystal lattice as a result of a substitution of Fe^{2+} to Co^{2+}.

References:

Huhma, H., Hanski, E., Kontinen, A., Vuollo, J., Mänttäri, I., Lahaye, Y., 2018. Sm-Nd and U-Pd isotope geochemistry of the Paleoproterozoic mafic magmatism in eastern and northern Finland. Geological Survey of Finland, Bulletin, 405, 150 p

Konnuaho J., Karinen T., Autio, U., Telkkälä, P., 2022. Mineral potential studies on Tanhua gabbro. Geological Survey of Finland, work report 66/2021, 15 p.

Korvuo, E., 1977. Kylälammen ja Kannusjängän magneettisten anomalioden tunnustelukairaus 1976. Rautaruukki Oy exploration report 050/3732/EK/77, 5 p. + 9 appendixes. (in Finnish)

Mattila, H., 1974 Karelidit Savukosken Tanhuan alueella, Keski-Lapissa. Thesis, Departure of Geology, University of Oulu. 89 p. (Unpublished M.Sc. In Finnish)

Intraorogenic mafic magmatism in Nagu, SW Finland

A. E. Johnson[1] and O. Eklund[1]

[1]Åbo Akademi University, Faculty of Science and Engineering, Geology and Mineralogy, Geohouse, Akademigatan 1, 20500 Åbo, Finland.
E-mail: anna.johnson@abo.fi

The Kaiplot gabbro in Nagu, SW Finland, is emplaced in several pulses with varying geochemical fingerprints. The most MORB-resembling samples concentrate towards an extensional back-arc basin environment in geotectonic diagrams. Fluids and crustal contamination have affected the samples in various amounts. The intraorogenic magmatism in the archipelago area is bimodal and probably more widespread than previously thought.

Keywords: intraorogenic magmatism, gabbro, tholeiitic, MORB, back-arc basin, SW Finland

1. Introduction

The Svecofennian orogeny in southern Finland is traditionally divided into two compressional stages, the 1.88-1.87 Ga (synorogenic) stage and the 1.84-1.82 Ga (lateorogenic) stage. The timespan between these, the intraorogenic stage 1.87-1.84 Ga, is thought to include an extensional event that has not yet been clearly identified. Lately, an increasing amount of bimodal intraorogenic magmatism has been identified in the Southern Finland Subprovince (SFS) especially in the Late Svecofennian Granite and Migmatite zone (LSGM, Ehlers et al., 1993), continuing into both Sweden and Russia. In this presentation one such mafic occurrence from the southwestern archipelago of Finland is presented.

2. Intraorogenic MORB-related magma in Nagu

The Kaiplot gabbro is situated in Nagu in the southwestern archipelago of Finland (Figure 1). The outcrops occur as dike intrusions as well as massive plutonic bodies and have been emplaced in at least two separate pulses. U-Pb dating (TIMS, zircon) gave an age of 1865±2 Ma, which falls in the intraorogenic time span.

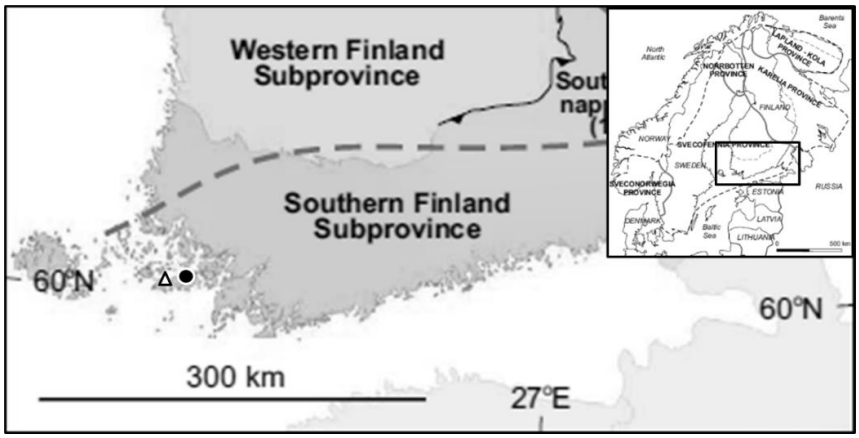

Figure 1. Map of southern Finland (after Nironen, 2017). The Kaiplot area in Nagu is marked by a circle, the location for the Korpo study (Väisänen et al., 2012) by a triangle.

The Kaiplot gabbro has SiO_2 contents ranging from 48.22–56.25 wt%, the majority falls in the 49-52 wt% range. Total alkalis (Na_2O+K_2O) are 2.46–4.58 wt%. In the TAS diagram by Middlemost (1994), most of the samples fall in the gabbro field. The Al_2O_3 content ranges from 13.35–20.27 wt%, MgO 2.46–9.66 wt%, total Fe (Fe_2O_3T) is 7.78–14.13 wt% while the TiO_2 variation is 0.846–3.176 wt%. Mg# range from 62.75 to 37.05.

To be able to compare basalts and gabbros geochemically and investigate their geotectonic origin, according to Pearce (1996), the data should be screened to exclude samples that can be cumulates or highly differentiated/contaminated. After the screening, only samples that fall in the ranges 5<MgO<12 wt%, Al_2O_3<18 wt%, Ni<200 ppm and Cr<600 ppm are used in geotectonic discrimination diagrams, but the screening is useful also to visualize for instance processes during the differentiation/contamination. Black dots pass the basalt screening; grey triangles and squares fail the screening with one or more criteria, the darker grey squares are the U-Pb dated samples (Figures 2-4).

The high Mg# values of the Kaiplot gabbro indicate that the initial magma was in a close chemical equilibrium with the mantle, but during transport and emplacement both differentiation and assimilation of crustal material have taken place. The Zr/Y ratio shows little variation over different Mg# for the dataset (Figure 2A), which implies that all samples have a similar magma source. The overall low Zr/Y values imply a mantle source beneath a thin lithosphere. The samples outside the screening criteria could originate from an earlier pulse from beneath a somewhat thicker lithosphere during initial rifting. Crustal contamination has affected the samples in varying extent as the Rb/Y ratios are more variable for different Mg# values (Figure 2B).

In the spider plot normalized to MORB (Figure 3A), the Kaiplot gabbro has geochemical characteristics transitional between arc basalts and MORB. This is expected of a back-arc basalt with components from both a subduction-modified mantle and spreading-centre basalts produced by a high degree of partial melting of depleted mantle. The samples that pass the

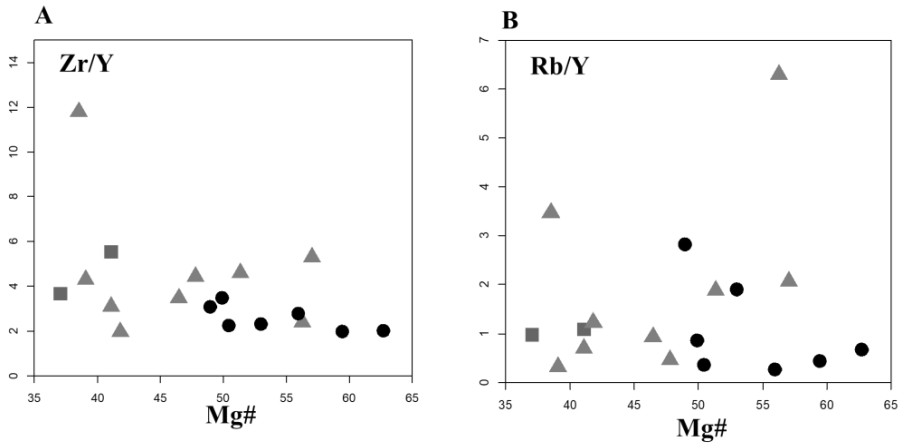

Figure 2. Geochemical variation diagrams. A) Mg# - Zr/Y. The variation in the Zr/Y ratio is fairly stable for different Mg#. B) Mg# - Rb/Y. Variation in the Rb/Y ratio for the same Mg# imply crustal contamination.

(●) pass the basalt screening

(▲) outside the basalt spectrum on one/more criteria

(■) U-Pb dating, outside the basalt spectrum on one/more criteria.

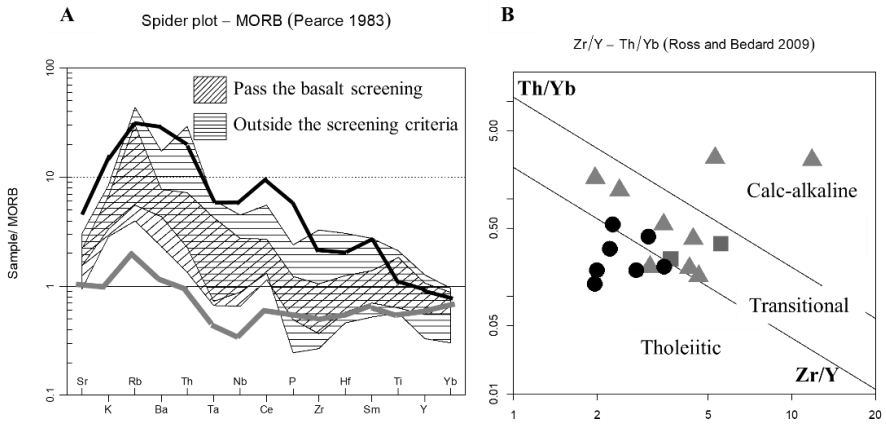

Figure 3. Symbols as in Figure 2. A) MORB-normalized trace element spider diagram (Pearce, 1983). Black curve = volcanic arc from Föglö, Åland (Hellsten, 2009). Grey curve = back-arc basin basalt from Lau basin (Keller et al., 2008). B) Magma series by trace elements (Ross & Bédard, 2009).

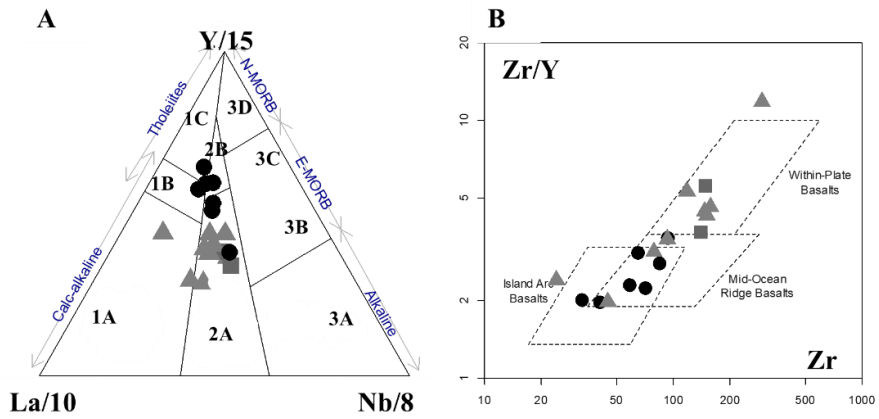

Figure 4. Geotectonic diagrams, symbols as in Figure 2. A) La/10-Y/15-Nb/8 diagram for basalts (Cabanis & Lecolle, 1989). The Kaiplot gabbro samples trend from 2A (continental basalts) towards 2B (back-arc basin basalts). Volcanic arc basalts: 1A calc-alkaline, 1B overlap, 1C volcanic arc tholeiites. Continental basalts: 2A continental, 2B back-arc basin. Oceanic basalts: 3A alkaline (intercont. rifts), 3B&C E-MORB, 3D N-MORB. B) Zr-Zr/Y diagram for basalts (Pearce & Norry, 1979). The screened samples concentrate in the field for MORB.

basalt screening plot in the tholeiitic magma series, while the samples outside the screening criteria trend towards a more calc-alkaline magma series due to a higher degree of crustal and fluid involvement (Figure 3B).

The tectonic environment for emplacement of the Kaiplot gabbro (Figure 4) varies from continental arc and within-plate towards back-arc basin and MORB, i.e. from a thicker lithosphere towards a thinner lithosphere. The samples that pass the basalt screening concentrate towards and around the fields for back-arc basin (Figure 4A) and mid-ocean-ridge basalts (Figure 4B). The samples that don't pass the screening are trending towards within-plate environments and volcanic arc basalts.

3. Coeval felsic magmatism in the area

The contacts between the Kaiplot gabbro and the surrounding rocks are mostly eroded and hidden under vegetation but mingling structures between the gabbroic magma and a felsic magma is seen at some places. This is manifested as net-veining and incomplete mixing between two magmas with different physical properties. Further west, in Korpo (Figure 1), Väisänen et al. (2012) have described bimodal magmatism of intraorogenic ages (diorite 1852±4 Ma, granite 1849±8 Ma).

4. Discussion and future work

The intraorogenic Kaiplot gabbro is tholeiitic and has MORB affinities. During emplacement of the gabbro, the heat transfer has led to melting of the surrounding crust, which is manifested as bimodal mingling. Since this is seen not only in the Kaiplot area but in other places in the region, one can only assume that the intraorogenic mafic magmatism is more voluminous and widely spread than what is previously known.

Is the high heat flow in the LSGM zone a consequence of an initiated but interrupted back-arc spreading in an extensional regime during tectonic switching (Collins, 2002)? Or maybe an orogenic collapse with convective removal of the lithospheric mantle? Are we dealing with post-collisional slab break-off, or intracratonic rifting due to a mantle plume?

Future research will shed light on the extent of the intraorogenic magmatism and give answers about the tectonic regime in southern Finland and south-central Sweden during this time.

References:

Cabanis, B., Lecolle, M., 1989. Le diagramme La/10-Y/15-Nb/8: un outil pour la discrimination des series volcaniques et la mise en evidence des processus de melange et/ou de contamination crustale. C.R. Acad. Sci. Ser. II, 309, 2023-2029.

Collins, W.J., 2002. Hot orogens, tectonic switching, and creation of continental crust. Geology 30, 535–538.

Ehlers, C., Lindroos, A., Selonen, O., 1993. The late Svecofennian granite-migmatite zone of southern Finland – a belt of transpressive deformation and granite emplacement. Precambrian Research 64, 295–309.

Hellsten, M., 2009. Föglön yleinen geologia sekä magmakivien petrogenesis. Pro gradu tutkielma. Turun yliopisto, Geologian laitos. 66 p.

Keller, N.S., Arculus, R.J., Hermann, J., Richards, S., 2008. Submarine back-arc lava with arc signature: Fonualei Spreading Center, northeast Lau Basin, Tonga. Journal of geophysical research, VOL. 113, B08S07, doi: https://doi.org/10.1029/2007JB005451

Middlemost, E.A.K., 1994. Naming materials in the magma/igneous rock system. Earth-Science Reviews, Volume 37, Issues 3–4, p 215-224. https://doi.org/10.1016/0012-8252(94)90029-9

Nironen, M., 2017. Bedrock of Finland at the scale 1:1000000 – Major stratigraphic units, metamorphism and tectonic evolution. Geological Survey of Finland, Special Paper 60, pp 41-76.

Pearce, J.A., 1983. Role of the sub-continental lithosphere in magma genesis at active continental margins. In: Hawkesworth C.J. and Norry M.J. (eds.), Cont. basalts and mantle xenoliths. Shiva, Nantwich, pp 230-249.

Pearce, J.A., 1996. A User's Guide to Basalt Discrimination Diagrams. In Wyman, D.A., (ed.), Trace Element Geochemistry of Volcanic Rocks: Applications for Massive Sulphide Exploration. Geological Association of Canada, Short Course Notes, v. 12, p. 79–113.

Pearce, J.A., Norry, M.J., 1979. Petrogenetic implications of Ti, Zr, Y and Nb variations on volcanic rocks. Contrib. Mineral. Petrol., 69, 33-47.

Ross, P.-S., Bédard, J.H., 2009. Magmatic affinity of modern and ancient subalkaline volcanic rocks determined from trace-element discriminant diagrams. Canadian Journal of Earth Sciences, Vol. 46, Nr 11. https://doi.org/10.1139/E09-054

Väisänen, M., Eklund, O., Lahaye, Y., O'Brien, H., Fröjdö, S., Högdahl, K., Lammi, M., 2012a. Intra-orogenic Svecofennian magmatism in SW Finland constrained by LA-MC-ICPMS zircon dating and geochemistry. GFF 134 (2), 99–114. https://doi.org/10.1080/11035897.2012.680606

SEISMIC RISK – Mitigation of induced seismic risk in urban environment

N. Junno[1], L. Fülöp[2], K. Oinonen[1], P. Mäntyniemi[1], A. Korja[1] and SEISMIC RISK working group

1Institute of Seismology, Department of Geosciences and Geography, P.O. Box 68, FIN-00014 University of Helsinki
[2]VTT Technical Research Centre of Finland Ltd.
E-mail: niina.junno@helsinki.fi

SEISMIC RISK – mitigation of induced seismic risk in urban environment – project studies how to evaluate, mitigate, communicate, and govern induced seismic risk associated with deep geothermal energy production. The research consortium consists of the University of Helsinki, VTT Technical Research Center of Finland and Geological Survey of Finland.

Keywords: induced seismicity, seismic risk, geothermal energy

1. General

Deep geothermal energy has a huge potential as environmentally friendly carbon-free district heat source in urban centers. Currently, there are several geothermal (pilot) projects ongoing and in planning in Finland. A drawback is that geothermal systems can induce small-magnitude earthquakes that pose a risk to critical sensitive infrastructure (such as hospitals, data centers and underground construction). The multidisciplinary SEISMIC RISK – Mitigation of induced seismic risk in urban environments – project is studying how to evaluate, mitigate, communicate and govern induced seismic risk associated with deep geothermal energy in Finland. The project is studying

- What kind of threat is the induced seismicity associated with deep geothermal district heating plants to the urban centers?
- How could the risks be assessed and monitored?
- What kind of information decision makers need?

SEISMIC RISK project aims to promote seismic risk-related discussion between different stakeholders, and therefore, it organizes annual Open seminars on research topics and results and produces popular, open access materials about geothermal energy and the related seismic risk.

2. Objectives and outcomes

The project is divided into nine work packages, each dealing with a specific task contributing to the overall aim of SEISMIC RISK project. The objectives of the work packages are to

1. Prepare the best possible seismic hazard map for the national needs. This is a prerequisite for an analysis of seismic risk. Natural seismicity is addressed at this point.
2. Develop a general scheme for separating the seismic hazard related to induced seismicity and natural seismicity
3. Construct a 3D tomography image of the subsurface structures of the target region
4. Prepare a 3D geological model of the target region
5. Collect data to assess the vulnerabilities of the building stock
6. Investigate the factors that control disturbing earthquake-related sound patterns during stimulations
7. Manage the various datasets created during the project

8. Highlight the gaps in governing geothermal energy processes and how this phenomenon should be governed to foster sustainable and societally acceptable development.
9. Disseminate the research outcomes and produce general outreach material. The largest possible impact of the project is ensured by focusing on presenting the results in a way that they can be understood by all possible end users as well as providing open access results for scientific purposes.

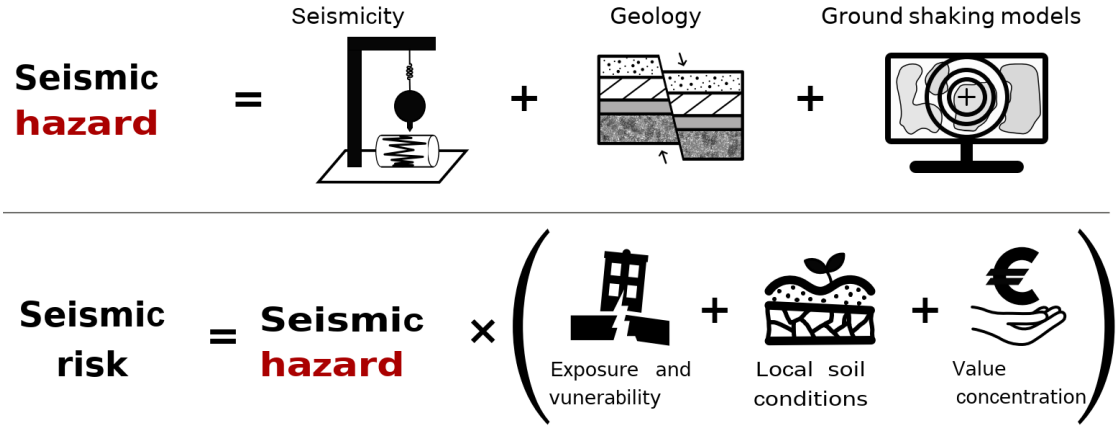

Figure 1. General outreach material produced by the project. Seismic hazard represents the best possible estimate of the level of seismicity in a given target region. The level of seismic hazard cannot be altered by human activities. A probabilistic seismic risk analysis is a product of seismic hazard and the fragility of the environment. This fragility can include different factors such as exposure, vulnerability, soil conditions, and sometimes cost is added (adapted from Crowley et al., 2021, and Danciu et al., 2021).

Acknowledgements
SEISMIC RISK project is funded through the Academy of Finland's call for new research projects on crisis preparedness and security of supply for 2020-2023 (decision numbers 337913, 338075, 339670).

References

Crowley H., Dabbeek J., Despotaki V., Rodrigues D., Martins L., Silva V., Romão X., Pereira N., Weatherill G., Danciu L. 2021. European Seismic Risk Model (ESRM20), EFEHR Technical Report 002, V1.0.1, 84 pp, https://doi.org/10.7414/EUC-EFEHR-TR002-ESRM20

Danciu L., Nandan S., Reyes C., Basili R., Weatherill G., Beauval C., Rovida A., Vilanova S., Sesetyan K., Bard P-Y., Cotton F., Wiemer S., Giardini D. 2021. The 2020 update of the European Seismic Hazard Model: Model Overview. EFEHR Technical Report 001, v1.0.0, https://doi.org/10.12686/a15

Studying the crust and its mineral systems with deep electromagnetic induction [INVITED]

J. Kamm[1]

[1]Geological Survey of Finland, Vuorimiehentie 5, 02151 Espoo
E-mail: jochen.kamm(at)gtk.fi

Recently, the new paradigm of studying mineral systems by mapping large-scale structures from the lower to the upper crust, thereby identifying and following potential source, migration and accumulation zones for metallic minerals, has shown great promise. With the advent of novel data acquisition and modelling technologies, 3D magnetotelluric surveys consisting of hundreds of measurement locations are now tractable, and being applied to various Fennoscandian mineral systems.

Keywords: Electromagnetics, Magnetotellurics, Mineral systems

Over the past decades, the Fennoscandian lithosphere has been studied extensively using electromagnetic induction methods. Many of the earlier experiments aimed at mapping the large-scale features in the crust and even the upper mantle (Jones 1980, Korja et al. 2000, Lahti et al. 2002, Smirnov et al. 2006). Over the years the focus shifted to studies of individual tectonic provinces (Korja et al. 1989, Vaittinen et al. 2012, Autio et al., 2020). At the same time, shallower audio-magnetotellurics is frequently used in higher-resolution studies for mineral exploration (e.g., Lahti et al., 2019).

In a relatively recent study, deep geophysical images of the World-class Olympic Dam deposit have revealed strong electromagnetic signatures associated with key components of the mineral system at large, particularly a deep-seated conductor was found that is conjectured to be a source region for metallic fluids, as well as three several conductive channels, interpreted as fluid conduits, each leading to a major ore deposit at the surface (Heinson et al., 2018). Further results from other areas in Australia (Jiang et al., 2019) and from Canada (Roots et al. 2022) have refined the concept delineating some of the mineral system components in Precambrian terranes.

The conductivity structure correlates strongly with important indicative features of the mineral system, e.g. carbon (graphite sheets are often tectonic interfaces), sulphides and alteration (related to metal endowment processes), conductive fluids / fracture systems (tectonically weak areas), and in active regions, also molten rock. However, these studies also have emphasized that it is useful to combine several mutually supporting data types (e.g. magnetotellurics, reflection seismics, gravity) because electrical conductivity alone is in many cases not a good proxy for differentiating rock types.

In various recent activities with a relatively young group of scientists, the Geological Survey of Finland and its collaborators attempt the application of the electromagnetics-supported mineral systems approach to areas in Fennoscandia: For example in the larger Pyhäsalmi area (studied in the D-Rex project), which is characterised by both deep and shallow reaching conductors (interpreted as black shales), their geometry can be better understood in 3D yielding clearer conclusions about the tectonic movements. Additional subvertical conductors close to surface expressions of known VMS mineral deposits have been observed. In the Kuusamo shist belt (studied in the BatCircle2.0 project) remnants of a postulated failed rift, genetically connected to the Co-Au mineralization, are sought at depth, and although the area is generally highly resistive, the existence of a deep conductor at relevant depth levels is deemed likely from the data.

While this type of research is carried out with the economic and societal well-being of future generations in mind, it serves the equally important goal of providing new high-resolution information particularly about the mid- to upper crust.

Acknowledgements
Contributions to this work come from the D-Rex Working Group: Pankaj Mishra, Cedric Patzer, Uula Autio, Jarkko Jokinen, Jouni Luukas and Jani Jäsberg (Geological Survey of Finland); Maxim Yu. Smirnov, Thorkild M. Rasmussen, Tobias Bauer and Oskar Rydman (Luleå University of Technology); Graham Hill, Svetlana Kovachikova, Jorge Puente, Nazia Hassan and Nooshin Najafipour (Institute of Geophysics Czech Academy of Sciences); Jan Vozar, Jozef Madzin, Lenka Ondrasova and Peter Vajda (Earth Science Institute Slovak Academy of Sciences); Tobias Hermansson and Kirsi McGimpsey (Boliden Minerals AB); Katri Vaittinen (Boliden Kevitsa Mining OY); Niklas Juhojuntti and Harald Van Den Berg (LKAB); Sofie Gradmann and Jomar Gellein (Geological Survey of Norway) and Janne Kaukolinna. Further contributions from the BatCircle2.0/1.2.1/KuSb Working Group: Hanna Leväniemi, Uula Autio, Jarkko Jokinen, Tero Niiranen, Johanna Salminen, Maarit Nousiainen, Noora Thurman (Geological Survey of Finland). Further contributors: Jirigalatu (Luleå University of Technology) and Kenneth Muhumuza. The author wishes to acknowledge CSC – IT Center for Science, Finland, for computational resources and Business Finland for providing research funding both through national and through European research infrastructure (ERA-MIN2).

References:

Autio, U.A., Smirnov, M.Y., Smirnova, M., Bauer, T.E., Korja, T., 2020. Magnetotelluric array in the central Finnish Lapland II: 3-D inversion and tectonic implications. Tectonophysics, 794, p.228574.

Heinson, G., Didana, Y., Soeffky, P., Thiel, S., Wise, T., 2018. The crustal geophysical signature of a world-class magmatic mineral system. Scientific reports, 8 (1), pp.1-6.

Jiang, W., Korsch, R.J., Doublier, M.P., Duan, J., Costelloe, R., 2019. Mapping deep electrical conductivity structure in the mount isa region, northern australia: implications for mineral prospectivity. Journal of Geophysical Research: Solid Earth, 124 (11), pp.10655-10671.

Jones A. G., 1980. Geomagnetic induction studies in Scandinavia—I. Determination of the inductive response function from the magnetometer array data. Journal of Geophysics, 48 (1), 181-194.

Korja, T., Hjelt, S.E., Kaikkonen, P., Koivukoski, K., Rasmussen, T.M., Roberts, R.G., 1989. The geoelectric model of the POLAR profile, Northern Finland. Tectonophysics, 162(1-2), 113-133.

Korja, T., the BEAR Working Group, 2000. The structure of the crust and upper mantle in Fennoscandia as imaged by electromagnetic waves. Pp. 25-34, In L. Pesonen, A. Korja and S.-E. Hjelt (Eds.), Lithosphere 2000. Program and extended abstracts, Institute of Seismology, University of Helsinki, Helsinki, Finland, Report S-41, 179 pp.

Lahti, I., Korja, T., Pedersen, L. B., BEAR Working Group, 2002. Lithospheric conductivity along GGT/SVEKA Transect: implications from the 2-D inversion of magnetotelluric data. Lithosphere, 75-78.

Lahti, I., Kontinen, A., Nykänen, V., 2019. AMT survey in the Outokumpu ore Belt, Eastern Finland. Exploration Geophysics, 50 (4), pp.351-363.

Roots, E.A., Hill, G.J., Frieman, B.M., Wannamaker, P.E., Maris, V., Calvert, A.J., Craven, J.A., Smith, R.S., Snyder, D.B., 2022. Magmatic, hydrothermal and ore element transfer processes of the southeastern Archean Superior Province implied from electrical resistivity structure. Gondwana Research, 105, pp.84-95.

Smirnov, M., Korja, T., Pedersen, L.B., 2006. Deep lithosphere structure isa target for electromagnetic arrays. Electromagnetic Mini Array (EMMA) project in Fennoscandia. Bull. Geol. Soc. Finland, Special Issue 1, p. 150.

Vaittinen, KKorja, .,T. Kaikkonen, P. Lahti, I. Smirnov, Yu. M. 2012. High-resolution magnetotelluric studies of the Archaean-Proterozoic border zone in the Fennoscandian Shield, Finland, Geophysical Journal International, Volume 188 (3), Pp. 908–924, https://doi.org/10.1111/j.1365-246X.2011.05300.x.

Arclogite formation beneath the Svecofennian orogen

J. Kara[1], M. Väisänen[1], J.S. Heinonen[2] and H. O'Brien[3]

[1]Department of Geography and Geology, University of Turku, Finland
[2]Department of Geosciences and Geography, University of Helsinki, Finland
[3]Geological Survey of Finland, Espoo, Finland
E-mail: jkmkar@utu.fi

Arclogites, i.e., lower crustal garnet-pyroxenite cumulates, are recently identified igneous rocks, which are suggested to play an important role in controlling magma differentiation and crust formation in modern continental arcs. Until now, arclogite-related magmatism has only been described from the Phanerozoic Era. Recent findings, however, suggest arclogite formation during the Svecofennian orogeny.

Keywords: arclogite, continental crust, upper mantle, Svecofennian orogen

1. Introduction

The recently identified arclogites are igneous high-pressure garnet pyroxenite rocks (Lee and Andersson, 2015), which are suggested to play a major role in the magma generation in modern continental arcs, hence contributing to the formation of continental crust (Figure 1; Lee et al., 2006; Tang et al., 2019; Ducea et al., 2021) and potentially provide the "missing link" between the composition of continental crust and parental magma. Arclogites are found in the roots of the thickest arcs, and they represent the residue (cumulates and/or restites) of the fractionation/partial melting processes that produce the prominent intermediate-felsic magmas of arcs in subduction-related systems (Ducea et al., 2021). After the growth stage, during production of intermediate-felsic magmas, arclogite partially founder into upper mantle within 5–30 Myr cycles due to their higher relative density (Lee and Andersson, 2015).

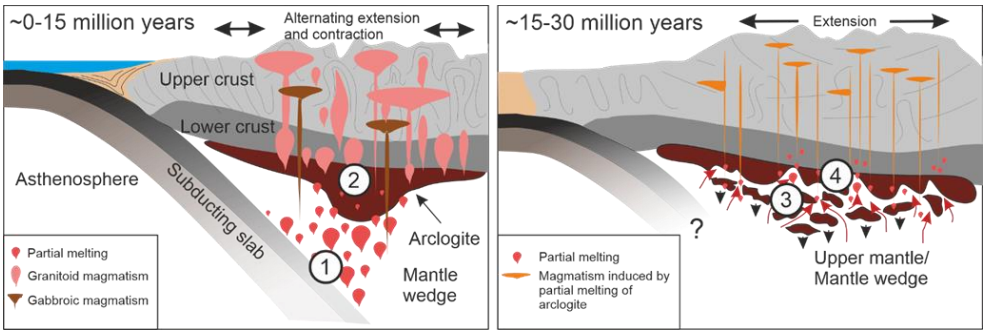

Figure 1. Schematic diagram of the growth (0-15 Myr) and foundering (15-30 Myr) of the arclogite in a continental arc system. 1. water-induced partial melting of the mantle wedge (=production of the parental melts); 2. growth of arclogite layer as a complementary for the intermediate-felsic magmatism; 3. (partial) foundering of the dense arclogite into the upper mantle; 4. heat-induced partial melting of the arclogite due to ascending hot upper mantle material.

The speciality of arclogites relates to their potential role in solving the two major paradoxes of the continental crust: i) continental crust is dominantly intermediate-felsic (~dacitic) although the parent magmas formed by partial melting of the mantle are mafic (~basaltic; e.g., Ducea et al., 2021), and ii) the continental crust shows extremely low Nb/Ta ratios and low Nb concentrations ("missing Nb paradox") compared to chondritic meteorites

(Rudnick et al., 2000, Tang et al., 2019), which are considered as building blocks of the continental crust and whole silicate Earth.

2. Arclogites and the Svecofennian orogen

The late discovery of the arclogites relates to their poor preservation potential (Lee and Andersson, 2015), and to date only few xenoliths of arclogites have been found globally in modern arcs such as Sierra Nevada, Colombia and Kohistan (e.g., Ducea et al., 2021). So far, xenoliths of arclogites have not been identified from older orogenies. However, indirect evidence based on melt modelling, isotope and geochemical compositions indicate that the rare 1.86 Ga enriched mafic magmas of the Paleoproterozoic Svecofennian orogen in southern Finland (Figure 2) originated by partial melting of arclogites during their foundering Kara et al. (2020). Further, Kara et al. (2020) also suggested that mafic lower crustal xenoliths found in kimberlite pipes in eastern Finland (Hölttä et al., 2000) are pieces of arclogite. These findings suggest that arclogites have an essential but previously unrecognized role in the formation of thick Precambrian orogens.

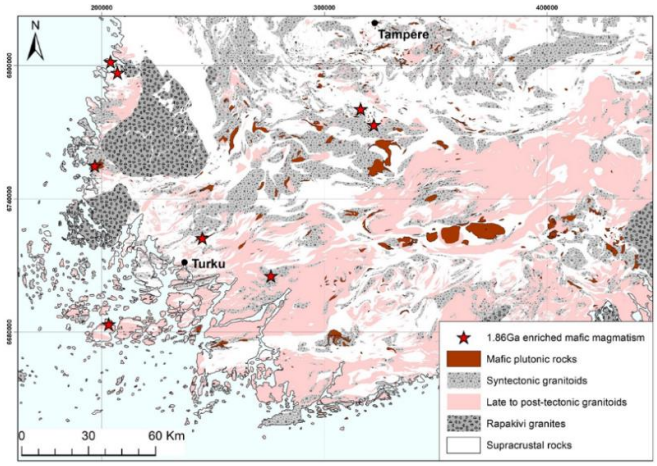

Figure 2. Simplified geological map of southern Finland with 1.86 Ga enriched mafic rocks indicated by red stars.

References:

Ducea, M., Chapman, A., Bowman, E., Triantafyllou, A., 2021. Arclogites and their role in continental evolution; part 1: Background, locations, petrography, geochemistry, chronology and thermobarometry. Earth-Science Reviews, 214, 103375.

Hölttä, P., Huhma, H., Mänttäri, I., Peltonen, P., Juhanoja, J., 2000. Petrology and geochemistry of mafic granulite xenoliths from the Lahtojoki kimberlite pipe, eastern Finland. Lithos, 51, 109-133.

Kara J., Väisänen M., Heinonen J., Lahaye Y., O'Brien H., Huhma H., 2020. Tracing arclogites in the Palaeoproterozoic Era – a shift from 1.88 Ga calc-alkaline to 1.86 Ga high-Nb and adakite-like magmatism in central Fennoscandia. Lithos, 372, 105663.

Lee, C.T.A., Cheng, X., Horodyskyj, U., 2006. The development and refinement of continental arcs by primary basaltic magmatism, garnet pyroxenite accumulation, basaltic recharge and delamination: insights from the Sierra Nevada, California. Contribution to Mineralogy and Petrology, 151, 222–242.

Lee, C.T.A., Anderson, D.L., 2015. Continental crust formation at arcs, the arclogite "delamination" cycle, and one origin for fertilemelting anomalies in the mantle. Science Bulletin, 60, 1141–1156.

Rudnick, R. L., Barth, M., Horn, I., McDonough, W. F., 2000. Rutile-bearing refractory eclogites: missing link between continents and depleted mantle. Science, 287, 278-281.

Tang, M., Jiang, H., Erdman, M., Costin, G., Chen, K., Lee, C.T.A., 2019. Nb/Ta systematics in arc magma differentiation and the role of arclogites in continent formation. Nature Communications, 10, 1-8.

Zircon U-Pb age of the Haveri basalt and felsic dyke

J. Kara[1], M. Väisänen[1] and H. O'Brien[2]

[1]Department of Geography and Geology, University of Turku, Finland
[2]Geological Survey of Finland, Espoo, Finland
E-mail: jkmkar@utu.fi

In this contribution we present the first U-Pb zircon ages of the E-MORB type Haveri basalt and crosscutting felsic dyke located in the Tampere belt, SW Finland. The basalt and the felsic dyke yielded $^{207}Pb/^{206}Pb$ ages of ~1.90 Ga and ~1.89 Ga, respectively, interpreted as crystallisation ages. The basalt also contains older 1.98 Ga grains while the felsic dyke contains older 1.92 Ga, 1.94 Ga, 1.98 Ga and 2.0 Ga grains. The age dating of E-MORB type basalts can be used to identify the extensional stages in accretionary orogens.

Keywords: Svecofennian orogen, Haveri formation, age determination, zircon U-Pb

1. Introduction

The Haveri formation located in the northern part of the Tampere belt in SW Finland (Fig. 1) is characterised by E-MORB type basalts, which differ from the surrounding volcanic arc type rocks by showing no subduction signature. The Haveri basalts are considered to have formed in a marginal basin prior to the volcanic arc (Kähkönen & Nironen, 1994) but back-arc setting (Strauss, 2003) or an initial stage island arc environment (Mäkelä, 1980) have also been suggested. However, poorly defined age, in addition to the fact that rocks predating Haveri have not been found, make these interpretations unclear. Here, we present zircon U-Pb dating on the basalt and crosscutting felsic dyke from Haveri.

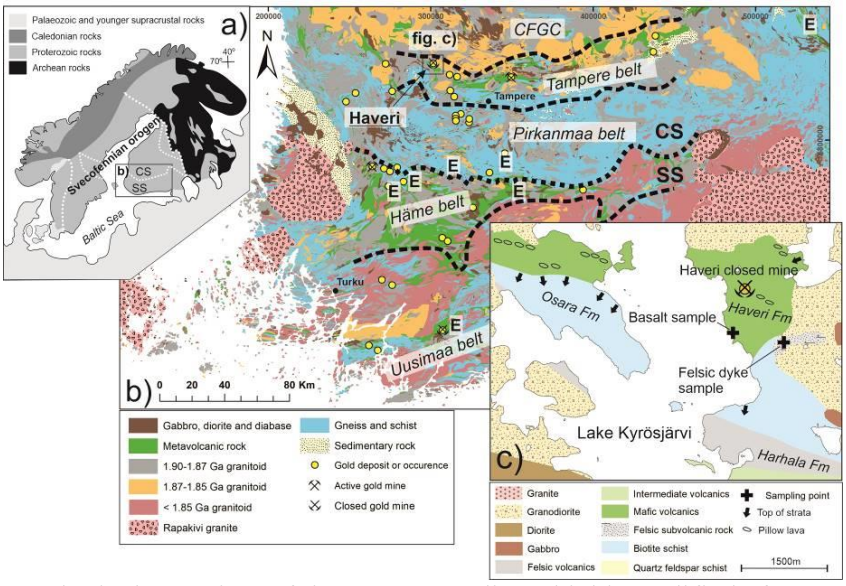

Figure 1. a) Geological overview of the Fennoscandian Shield, modified after Koistinen et al. (2001). CS = Central Svecofennia, SS = Southern Svecofennia. b) Lithological map of southern Finland, modified after Bedrock of Finland – DigiKP. The study area is indicated by a black rectangle. CFGC = Central Finland Granitoid Complex, E = E-MORBs. c) Lithological map of the Haveri region. Modified after Bedrock of Finland – DigiKP and Kähkönen & Nironen (1994).

2. Geological setting

The Paleoproterozoic Svecofennian Orogen formed approximately between 1.95 and 1.75 Ga ago (e.g., Lahtinen et al., 2005). In Finland, it consists of three main arc complexes: the Savo belt, Central Svecofennia and Southern Svecofennia (Figure 1a).

The medium metamorphic-grade Tampere belt (Figure 1b) in the southern part of the Central Svecofennian is characterised by volcanic rocks and associated sediments formed in a mature volcanic arc or continental margin environment ~1.90–1.88 Ga ago (Kähkönen, 2005).

The Haveri formation is located in northern edge of the Tampere belt (Fig. 1c) and consists of mafic metalavas with E-MORB affinities (Strauss, 2003). Kähkönen (2005) considered that Haveri is the lowermost unit in the Tampere belt formed in submarine conditions in an extension-related setting based on the tholeiitic pillow lavas and depositional structures in sedimentary rocks.

3. Results and discussion

Two samples were collected for the dating: a basalt and a crosscutting felsic dyke (Fig. 1c). Both sampling sites were selected using a study by Kähkönen & Nironen (1994). The zircon U-Pb age determinations were performed using a Nu Plasma AttoM single collector ICPMS in the Finnish Geosciences Research Laboratory (SGL) at the Geological Survey of Finland.

Eleven zircons were recovered from the basalt sample. Seven analyses yielded $^{207}Pb/^{206}Pb$ and upper intercept ages of ~1.90 Ga, interpreted as the age of crystallisation. An older population of 1.98 Ga was also found. Abundant zircons were recovered from the felsic dyke and 36 analyses yielded a crystallisation age of ~1.89 Ga. Several older populations were found: 1.92 Ga, 1.94 Ga, 1.98 Ga and 2.0 Ga groups.

Extensional episodes and related MORB/E-MORB-type magmatism in subduction-related volcanic arcs are common (Xia & Li, 2019). The age dating of E-MORB type basalts can be used to identify the extensional stages in accretionary orogens and, furthermore, in modelling the evolution of the Svecofennian orogeny.

References:

Bedrock of Finland – DigiKP. Digital map database [electronic resource]. Espoo: Geological Survey of Finland [referred 1.7.2022] Version 2.1.

Kähkönen, Y., 2005. Svecofennian supracrustal rocks. In: Lehtinen, M., Nurmi, P.A., Rämö, O.T., (Eds.), Precambrian Geology of Finland – Key to the Evolution of the Fennoscandian Shield, Elsevier Science B.V., Amsterdam, 43–406.

Kähkönen, Y., Nironen, M., 1994. Supracrustal rocks around the Paleoproterozoic Haveri Au-Cu deposit, southern Finland: evolution from a spreading center to a volcanic arc environment. Geological Survey of Finland, Special Paper 19, 141-159.

Koistinen, T., Stephens, M.B., Bogatchev, V., Nordgulen, Ø.,Wennerström, M., Korhonen, J., 2001. Geological map of the Fennoscandian Shield, scale 1:2000 000. Geological Surveys of Finland, Norway and Sweden and the North-West Department of Natural Resources of Russia.

Lahtinen, R., Korja, A., Nironen, M., 2005. Paleoproterozoic tectonic evolution. In: Lehtinen, M., Nurmi, P.A., Rämö, O.T. (Eds.), Precambrian Geology of Finland – Key to the Evolution of the Fennoscandian Shield. Elsevier Science B.V., Amsterdam, 481–532.

Mäkelä, K., 1980. Geochemistry and origin of Haveri and Kiipu, Proterozoic strata-bound volcanogenic gold-copper and zinc mineralizations from southwestern Finland. Geological Survey of Finland, Bulletin, 310, 79 p.

Strauss, T.A.L., 2003. The geology of the Proterozoic Haveri Au-Cu deposit, southern Finland. PhD thesis, Rhodes University, 306 p.

Xia, L., Li, X., 2019. Basalt geochemistry as a diagnostic indicator of tectonic setting. Gondwana Research, 65, 43-67.

Structural evolution of the Archaean Siilinjärvi carbonatite complex

T. Kauti[1], P. Skyttä[1] and E. Heilimo[1]

[1]Department of Geography and Geology, FI-20014 University of Turku, Finland
E-mail: tuomas.kauti@utu.fi

This paper presents the structural evolution of the Siilinjärvi carbonatite complex from the initial ultramafic magma intrusion through mafic dyke emplacement to structural overprint and present-day state. Our interpretation is based on diverse datasets which were used to produce sub-models of different resolution, and subsequent cross-validation of these sub-models to gain a coherent understanding of the observed structures. The recognized succession of emplacement of carbonatite magma and successive mafic dykes, followed by localized structural overprint may be attributed to an initial stage of Archaean rifting, which shifted to transpressional and eventually to thrust tectonic regime during Svecofennian rework.

Keywords: structural geology, Archaean, rifting, 3D modelling, mafic dykes, carbonatite

1. Introduction

The Archean 2.61 Ga Siilinjärvi carbonatite-glimmerite complex in Finland (Kouvo, 1984 unpublished report; O'Brien et al., 2015) is a steeply-dipping, lenticular body of carbonatite–glimmerite rocks enclosed within Archean gneisses (Puustinen, 1971; O'Brien et al., 2015). The complex is cut by several generations of mafic dykes (Puustinen, 1971; Mattsson et al., 2019) commonly attributed to the Paleoproterozoic rifting events (Vuollo and Huhma, 2005).

However, no earlier detailed structural evidence is publically available to i) understand the primary intrusive setting of the complex, ii) understand the relationships of the mafic dykes, and iii) the structural overprint at various stages in the evolution of the complex. As such both the mechanism of the primary emplacement of the ultramafic magma, and the overall structural geometry of the deposit, with particular reference to the mafic dyke network, have been poorly known.

In this study we provide a comprehensive structural model of the Siilinjärvi suite, addressing its structural development, including the emplacement of the carbonatite magmas and related dykes, several generations of post-carbonatite mafic dykes, and the subsequent structural overprint. Moreover, our work highlights the need for integrated 3D-modelling using diverse datasets in constructing geologically valid 3D-models within complexly deformed Precambrian settings.

2. Data and methods

Our data consist of production hole (76,955 pcs) and diamond drill hole (256 utilized) data, delimited to the main open pit area and its immediate surroundings. Furthermore, we made structural field observations from 243 localities, and complemented the data by using 3D-photogrammetric model and high-resolution gigapixel images (Järvinen et al. 2018) of the southern wall of the main pit to define structural details and cross-cutting relationships of the complex. We constructed a 3D mafic dyke model based on production drillings, and used the diamond drill hole data to perform a structural analysis of mafic dykes and to delineate the major ~N-S striking deformation zones in 3D. Open pit mapping data was compiled into host-rock model, mafic dyke model and into a model of structural overprint of localised deformation. These submodels were then integrated into one unified model, addressing the occurrence of the

mafic dykes, their geometries, orientation sets and relative ages based on cross-cutting relationships.

3. Structural evolution

Our findings can be summarized in the following conceptual model of the structural evolution of the complex (Figure 1): The carbonatite-glimmerite magma intrusion was followed by development of a penetrative moderately SW dipping foliation, indicating a shift in paleostress conditions (rifting-compression). This was followed by carbonatite remobilization within an extensional regime, a point in time which likely also marks the onset of major shear zones. Progressive mafic dyking probably started at Archaean times (Mattson et al. 2019), was associated with shearing along carbonatite-glimmerite margins, and continued under transpressional conditions during the Paleoproterozoic (likely at 2.45-1.98 Ga; Vuollo and Huhma, 2005). The present state of the complex was reached at ca. 1.86 Ga (Lukkarinen, 2008), associated with composite dioritic-tonalitic intrusions and minor structural overprint.

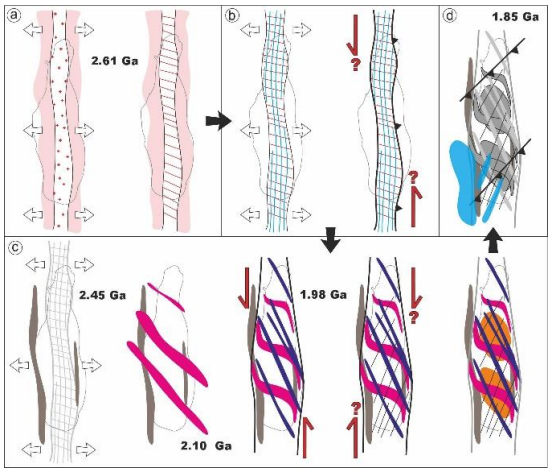

Figure 1. Conseptual evolution model of the complex. a) Initial magma intrusion and formation of the pinkish fenitized halo, uniform foliation into glimmerite phase. b) Carbonatite remobilization and tectonized margins develop. c) Progressive mafic dyke emplacement. Note the time constraints are only indicative, different colours represent one temporal mafic dyke group. d) Late tonalite-diorite intrusions and structural overprint as minor reverse faulting.

Acknowledgements

We thank Yara Suomi Oy of fruitful collaboration. This study was carried out in the Smart Exploration project, which has received funding from the European Union's Horizon 2020 research and innovation programme under grant agreement no. 775971.

References:

Järvinen, J., Piippo, S.V., Silvennoinen, S.E.E., Kultti, S.K. and Koivisto, E.A.-L., 2018. New digital learning materials for teaching in geosciences. LITHOSPHERE 2018: 10th Symposium on Structure, Composition and Evolution of the Lithosphere, Programme and Extended Abstracts.

Lukkarinen, H., 2008. Pre-Quaternary rocks of the Siilinjärvi and Kuopio map-sheet areas. Geological map of Finland 1:100 000. Explanation to the maps of Pre-Quaternary rocks, Sheets 3331 and 3242. Espoo.

Mattsson, H.B., Högdahl, K., Carlsson, M., Malehmir, A., 2019. The role of mafic dykes in the petrogenesis of the Archean Siilinjärvi carbonatite complex, east-central Finland. LITHOS 342–343, 468–479.

O'Brien, H., Heilimo, E., Heino, P., 2015. The Archean Siilinjärvi Carbonatite Complex. Mineral Deposits of Finland. Elsevier Inc., 327–343.

Puustinen, K., 1971. Geology of the Siilinjärvi carbonatite complex, eastern Finland. Geological Survey of Finland, Bulletin - Bulletin de La Commission Géologique de Finlande, 249, 43.

Vuollo, J., Huhma, H., 2005. Paleoproterozoic mafic dikes in NE Finland. In: Lehtinen, M., Nurmi, P.A., Rämö, O.T. (Eds.), Precambrian Geology of Finland - Key to the Evolution of the Fennoscandian Shield. Elsevier, Amsterdam, 195–236.

Basement tectonics along the margins of the Jormua-Outokumpu suture zone

J. Kohonen[1], J. Jäsberg[1], J. Laitala[1] and J. Luukas[1]
[1]Geological Survey of Finland
E-mail: jarmo.kohonen@gtk.fi

We describe structural features along the Jormua-Outokumpu suture zone and present examples of basement-cover relationships. Finally, we discuss the nature of the suture and the alternative structural evolution models of the region.

Keywords: Archean basement, structural domain, deformation, thrust, strain partitioning, Karelia, Finland

1. Introduction

Jormua–Outokumpu Suture (J–OS) refers to the boundary of two tectonic provinces (Karelia province and Iisalmi-Pudasjärvi subprovince; see Kohonen et al., 2021). The boundary between the two Archean crustal blocks resulted in a collisional (Svecofennian) closure of a proto-oceanic rift basin (e.g. Lahtinen et al., 2015). Jormua-Outokumpu suture zone is the spatial approximation of the collision zone and links together the Outokumpu-Rääkkylä and Kainuu belts.

The proto-oceanic basin developed ca. 1.97 – 1.93 Ga ago as a response to an extreme crustal extension manifested by the sheeted dyke complexes and the exhumation of the lithospheric mantle. The central part of the basin was floored by Archean sub-continental mantle (e.g. Peltonen, 2005) and the developing remnant-ocean basin was filled by orogenic 'Upper Kalevian' sediments ca. 1.95 – 1.91 Ga ago (e.g. Kontinen, 1987; Kohonen, 1995). The suture zone is characterized by ophiolitic serpentinite lenses, tightly infolded outliers of Paleoproterozoic cover and excessive shortening localized to the previous rift zone.

2. Thin-skinned or thick-skinned foreland deformation?

The western Iisalmi-Pudasjärvi subprovince consists of three informal tectonostratigraphic units (Iisalmi and Rautavaara thrust blocks, Kuopio thrust stack; see Luukas & Kohonen, 2021) and shows increasing basement ductility towards the SSW.

We have divided the eastern side of the suture zone (the W-margin of the Karelia province) to structural domains representing variable amounts of shortening and different structural styles. In North Karelia, the basement-involved thin-skinned structures and cover allochthons are modified by folding resulting in basement-cored anticlines. The cross-section across the Polvela anticline shows gradual steepening and tightening of the basement-involving structures towards the east. Major amount of the basement deformation is partitioned to high-strain zones of variable width.

In Kainuu belt, all the cover rocks are buttressed tightly against the bounding Archean blocks, and both the primary rock-unit relationships and the thrust-related structures are mostly beyond recognition. The southernmost tip of the Kainuu belt exposes the deep levels of the synclinal structure where the central part and the both margins of proto-oceanic basin can still be identified. The location of the suture zone is here marked by the ultramafic bodies (e.g. Alanen serpentinite) and associated Upper Kalevian greywackes, representing the depositional basement and turbiditic fill in the central part of the remnant-ocean basin, respectively.

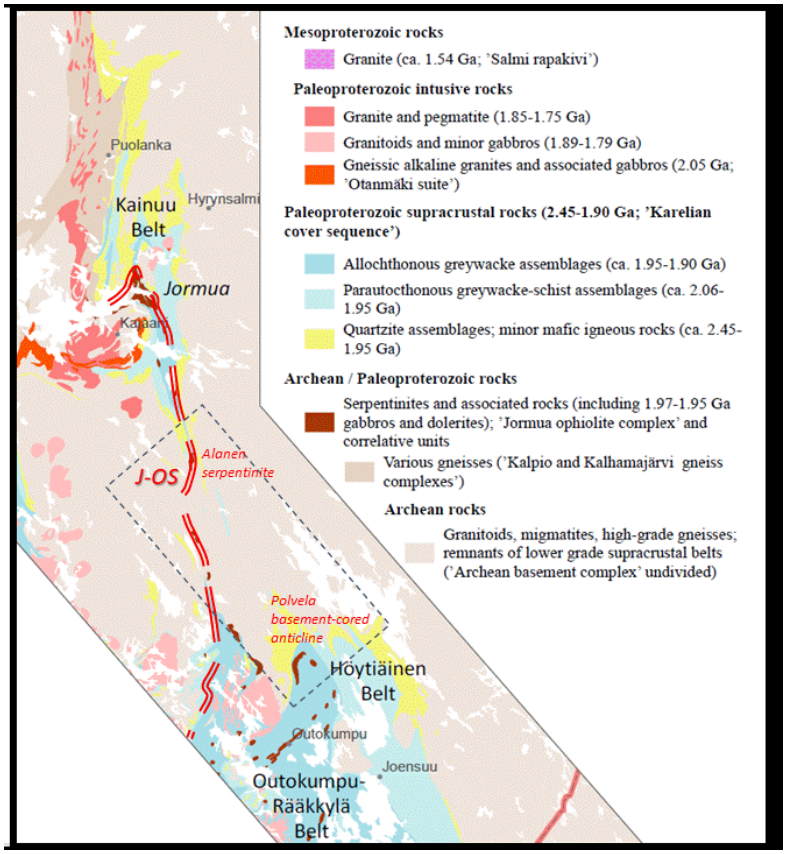

Figure 1. General geological map of the Kainuu, Outokumpu-Rääkkylä and Höytiäinen belts (simplified from Koistinen et al., 2001). The approximate location of the Jormua-Outokumpu suture zone (J-OS) and the extent of the current study area (dotted line) are indicated.

References:

Kohonen, J., 1995. From continental rifting to collisional crustal shortening - Paleoproterozoic Kaleva metasediments of the Höytiäinen area in North Karelia, Finland. Geol. Surv. Finland Bull. 380. 79 p.

Kohonen, J., Lahtinen, R., Luukas, J., Nironen, M. 2021. Classification of regional-scale tectonic map units in Finland. In: Kohonen, J., Tarvainen, T., (eds) Developments in map data management and geological unit nomenclature in Finland. Geological Survey of Finland, Bulletin, 412. Available at: https://doi.org/10.30440/bt412.2

Kontinen, A., 1987. An early Proterozoic ophiolite the Jormua mafic-ultramafic complex, northeastern Finland. Precambrian Res., 35, 313-341.

Lahtinen, R., Huhma, H., Lahaye, Y., Kousa, J., Luukas, J., 2015. Archean-Proterozoic collision boundary in central Fennoscandia: revisited. Precambrian Research 261, 127–165.

Luukas, J., Kohonen, J., 2021. Major thrusts and thrust-bounded geological units in Finland: definitions and descriptions. In: Kohonen, J., Tarvainen, T., (eds) Developments in map data management and geological unit nomenclature in Finland. Geological Survey of Finland, Bulletin, 412. Available at: https://doi.org/10.30440/bt412.2

Peltonen, P., 2005. Ophiolites. In: Lehtinen, M., Nurmi, P., Rämö, T., (eds) The Precambrian Bedrock of Finland – Key to the Evolution of the Fennoscandian Shield. Elsevier Science B.V., 237–278.

Lieksa-4: a P-rich iron meteorite from Lieksa

L. Kotomaa[1], M. Väisänen[1], E. Mäkilä[2], H. O'Brien[3] and P. Kokko[4]

[1]1Department of Geography and Geology, University of Turku, Finland
[2]Department of Physics and Astronomy, University of Turku, Finland
[3]Geological Survey of Finland, Espoo, Finland
[4]87900, Kajaani, Finland
E-mail: lehkot@utu.fi

Lieksa-4 is an iron meteorite find from Löpönvaara, Lieksa. The meteorite consists of approximately 84 wt% Fe, 11 wt% Ni, and 4 wt% P. Trace elements Ga, Ge, Au, and Ir occur in low abundances. The sample consists mainly of rounded kamacite granules in a schreibersite-matrix. Troilite occurs in the matrix in low abundances. Moreover, Neumann deformation lines were detected. The optical, mineralogical, and geochemical features indicate that Lieksa-4 is an anomalous iron meteorite.

Keywords: iron meteorite, anomalous iron meteorite, LA-SC-ICPMS, FE-SEM, XRD

1. Introduction

A total of 14 meteorites have been found in Finland so far (Kuva et al., 2017). Two of these have been investigated in more detail, the Haverö ureilite (e.g., Neuvonen et al., 1972) and the Bjurböle chondrite (Maksimova et al., 2021). The latest meteorite find in Finland is the Lieksa iron meteorite (Kuva et al., 2017). Both the Lieksa meteorite and Lieksa-4 were discovered from the same area together with 3 other suspected meteorites (Moilanen, 2018). Lieksa-4 was found by Pekka Kokko, and the sample was suspected of being a meteorite. However, the preliminary investigation revealed that Lieksa-4 consisted of unusually high amounts of P, so the object was tentatively considered man-made, and the studies were brought to a halt. The suspected meteorite was then sent to Geohouse in Turku, Finland for further study.

Lieksa-4 is about 3.5 cm in diameter, and its total mass at the time of discovery was 163.7 g (Moilanen, 2018). The polished surface of the endcut is highly reflective which makes it appear light in colour, and it consists of several fractures along the surface plane (Figure 1). The texture consists of round, ≤ 0.5 mm granules in a much finer grain-size matrix. A few larger, ~ 3 mm granules occur on the polished endcut. The meteorite has no visible fusion crust, and nothing is known about its fall. The outer layers of the meteorite show significant signs of weathering (class C), suggesting that it has been on the ground for an extended period.

The aim of this research is to determine the mineralogy, geochemistry, and texture of Lieksa-4, and to attempt to classify it based on these data.

2. Methods

Several research methods were utilized to reveal the nature of Lieksa-4. A corner of the meteorite was cut off and the endcut was polished. The cut off piece was divided into four parts. Part of it was pulverised and separated into two different fractions: metallic hard granules, and soft matrix. The two pulverised fractions were analysed by X-ray diffraction (XRD) at the University of Turku. In addition, an epoxy-mounted polished section, and a steel plate-mounted unpolished section were made. The pieces were investigated under the optical microscope and analysed with scanning micro-X-ray fluorescence (μ-XRF) and field emission scanning electron microscope equipped with an energy dispersive X-ray spectrometer (SEM-EDS) at the

University of Turku, and with laser ablation inductively coupled plasma mass spectrometry (LA-SC-ICPMS) at the Geological Survey of Finland, Espoo.

Figure 1. The endcut of Lieksa-4 showing its reflective material and the internal structure. The meteorite consists of small (≤ 0.5 mm), round granules with a few larger (~ 3.0 mm) granules present as well. The outer layer is covered in a thick (~ 1 mm) layer of rust, suggesting that Lieksa-4 has been on the ground for an extended period.

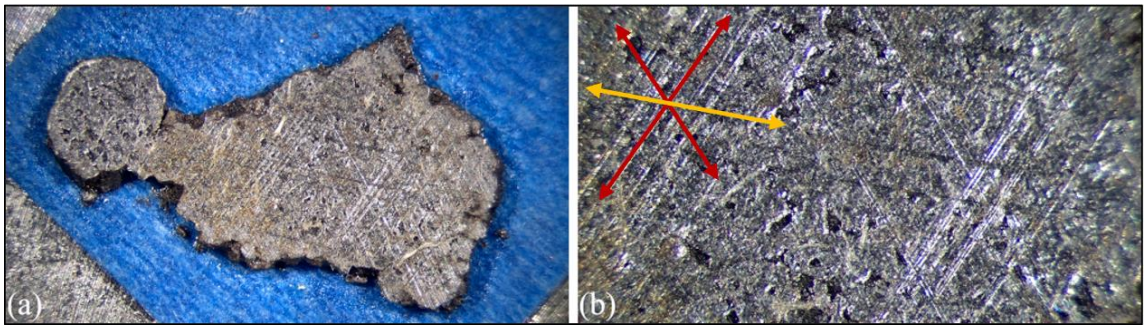

Figure 2. The unpolished section of Lieksa-4, showing the Neumann deformation lines. (a) 0.63x and (b) 2.5x magnifications. The lines seen here occur in at least 3 different directions, with two main directions (highlighted with red arrows in b) that form 110° and 70° angles relative to each other. A third set of lines (highlighted with a yellow arrow in b) occur in 60° and 50° angles relative to the main set of lines.

3. Results

The microscopic study revealed several crosscutting lines, most obvious on the unpolished section (Figure 2). They are similar to the Neumann deformation lines observed in several iron meteorites (e.g., Buchwald 1975).

The XRD analyses of the round granules show X-ray diffraction pattern corresponding to kamacite (α-(Fe, Ni)), while the matrix consists of schreibersite ($(Fe,Ni)_3P$) and minor amounts of troilite (FeS).

The SEM-EDS analyses suggest that kamacite constitutes roughly 70 wt% of the meteorite, schreibersite 20 wt%, and troilite ≤ 1 wt%. In addition, various types of kamacite exsolution can be seen in schreibersite throughout the sample (Fig. 3).
The LA-SC-ICPMS analysis was carried out successfully only on the kamacite granules, since the schreibersite grains were far too small for a 50 µm spot size needed to get adequate LOD on the critical elements Ir and Ge. Trace amounts of several elements common to iron meteorites were detected in both the SEM-EDS and LA-SC-ICPMS analyses (Table 1).

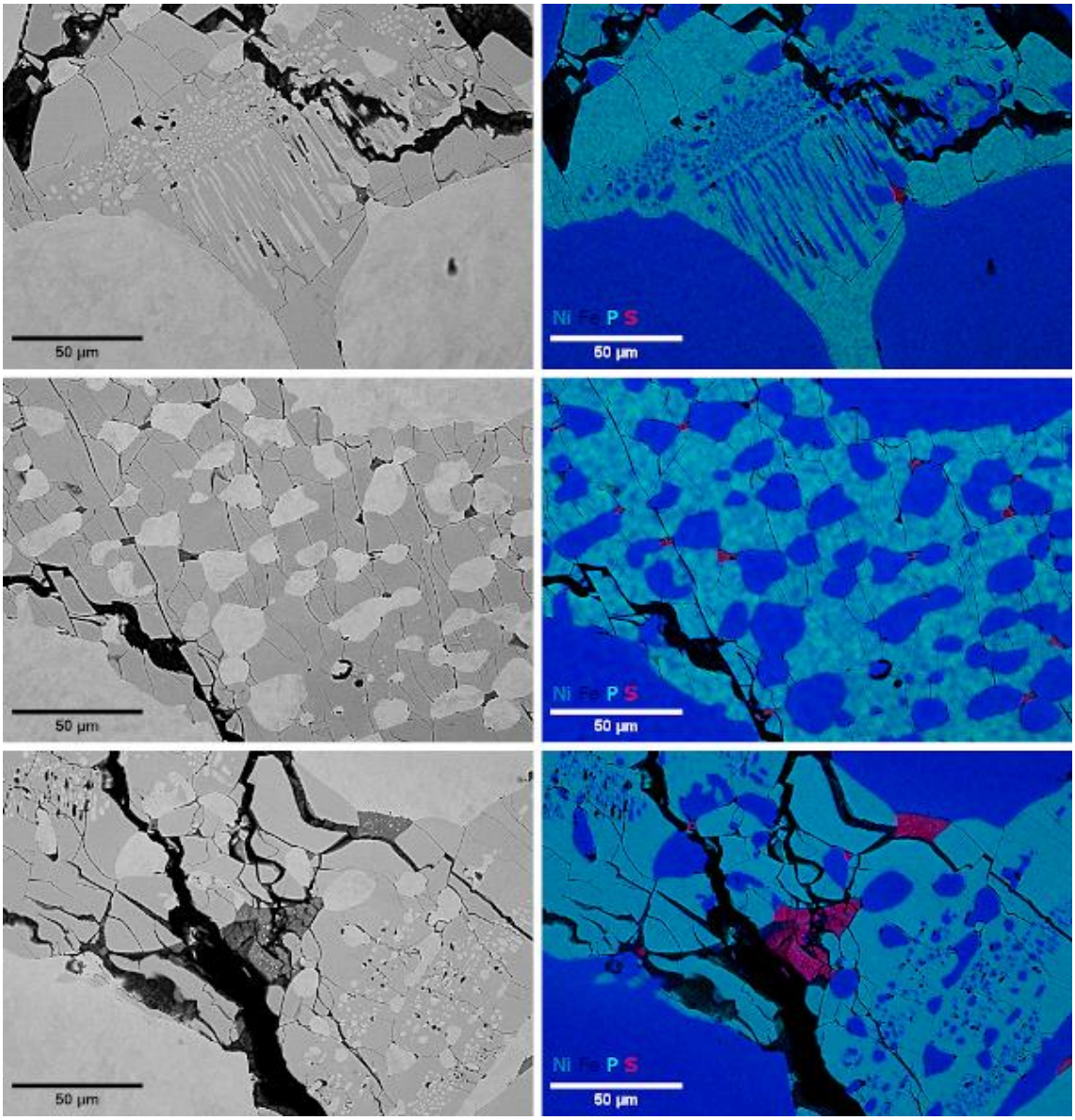

Figure 3. Backscattered electron micrographs and elemental maps showing the details of the kamacite exsolution. Dark blue areas represent kamacite, light blue schreibersite. Magenta areas correspond to troilite. The exsolution occurs in different textures and greatly varying sizes from sub-micron size globules to elongated, several tens of microns long patches. Troilite occurs always angular in the schreibersite-matrix, and it contains often sub-micron size inclusions of an unidentified material.

Table 1. The results of Lieksa-4 composition using LA-SC-ICPMS and SEM-EDS methods. The results are rounded upwards. All results in ppm, except for Fe, Ni, P, Co, and S which are in wt%.

Method	Fe	Ni	P	Co	S	Ir	Ga	Ge	Au	V	Cr
LA-ICP-MS*	85	10		< 1		2	11	5	< 1	< 1	300
FE-SEM	83	11	4	< 1	< 1						400

*Results obtained solely from the kamacite phase.

4. Discussion

Optical study of Lieksa-4 shows Neumann lines on the sample. These are believed to represent shock-induced, severe structural deformation of the kamacite lamellae (e.g., Buchwald, 1975). The XRD analysis shows that the sample consists of kamacite and schreibersite, with minor amounts of troilite. The FE-SEM analysis shows that the kamacite phase occurs in two different forms: (1) round, ≤ 0.5 mm granules; and (2) small, several tens of microns to sub-micron wide and tens of micros long lamellae in the matrix. LA-SC-ICPMS analysis of the kamacite granules detected minor amounts of Au, Ga, Ge, and Ir. Overall, the meteorite consists of approximately 84 wt% Fe, 11 wt% Ni, 4 wt% P and > 1 ppm S. These results clearly suggest that Lieksa-4 is an iron meteorite.

The compositional and textural features of the Lieksa-4 meteorite suggest the following solidification scenario: 1) nucleation and rapid growth of the round macroscopic kamacite granules from a P-rich parent melt; 2) exsolving of phosphate liquids from the residual liquid; 3) crystallisation of the schreibersite matrix and exsolution of the microscopic kamacite; 5) final crystallisation of troilite from the residual iron sulphide. The crystallisation of the schreibersite phase likely took place at lower temperatures compared to the kamacite phase. The kamacite within the schreibersite-matrix then formed as a result of exsolution phenomena.

Based on its chemical and structural features, Lieksa-4 does not fit into any of the existing iron meteorite classes. Thus, the meteorite should be classified as an anomalous iron meteorite for now (Kotomaa, 2022).

References:

Buchwald, V. F., 1975. Handbook of Iron Meteorites. University of California Press, 1418 p.

Kotomaa, L., 2022. Classification of iron meteorites and description of mineralogy, geochemistry, and texture of the Lieksa-4 meteorite. Master's thesis, University of Turku.

Kuva, J., Kinnunen, K. A., Pakkanen, L., Lukkari, S., Vuoriainen, S., 2017. Tomographic investigation of a complete iron meteorite. Geological Survey of Finland (GTK).

Maksimova, A. A., Petrova, E. V., Chukin, A. V., Nogueira, B. A., Fausto, R., Szabó, Á., Dankházi, Z., Felner, I., Gritsevich, M., Kohout, T., Kuzmann E., Homonnay, Z., Oshtrakh, M. I., 2021. Bjurböle L/LL4 ordinary chondrite properties studied by Raman spectroscopy, X-ray diffraction, magnetization measurements and Mössbauer spectroscopy. Spectrochimica Acta Part A: Molecular and Biomolecular Spectroscopy, 248, 119196.

Moilanen, J., 2018. Meteoriitit. Website, http://www.somerikko.net/meteoriitit/lieksa.html, accessed 15 August 2022. (In Finnish)

Neuvonen, K.J., Ohlson, B., Papunen, H., Häkli, T.A., Ramdohr, P., 1972. The Haverö ureilite. Meteoritics, 7.4, 514–531.

Evolution, structure and fluids of lithosphere in Finland [INVITED]

I.T. Kukkonen[1]
[1]University of Helsinki
E-mail: ilmo.kukkonen@helsinki.fi

The evolution, structure and fluids of the lithosphere in Finland are briefly reviewed. I discuss the lithosphere evolution and structure, lithological composition of the crust, nature of Moho in the anomalously thick crust area, geothermics of the lithosphere, saline fluids in the crust and late thermochronological evolution.

Keywords: lithosphere, crust, upper mantle, saline fluids, gas, AFT, Fennoscandia, Finland

1. Lithosphere and crust: Thickness and composition

The lithosphere in Finland, in the central part of the Fennoscandian Shield, is 200 - 250 km thick (Kukkonen et al., 2003, Sandoval et al., 2003, Plomerova and Babuška, 2010) and the crustal thickness attains 46 – 63 km (Grad et al., 2009, Figure 1). In southern and central Finland, the crustal thickness is on the average 54 km and most of the extra thickness in comparison to average continental crust (42 km) is due to a high-velocity (V_P 7.4 km/s) lower crust at depths deeper than 40 km (Heikkinen and Luosto, 2000). The layer has been interpreted either as a mafic underplate (Korja et al., 1993) or a layer of mafic granulites and partly eclogitized mafic rocks (Kukkonen et al., 2008). The wide-angle velocity models indicate that P-wave velocity does not only increase step-wise at boundaries of major crustal layers, but there is also gradual increase of velocity within the layers (Heikkinen and Luosto, 2000). The lithological composition of the crust was solved by fitting the *in situ* velocities with representative rock type velocities measured in laboratory. Results imply that the crust becomes more mafic with increasing depth (Kuusisto et al., 2006). In the area of the anomalously thick crust in central and southern Finland there is no density contrast between the lower crust and upper mantle due to delamination of high-density eclogitic crust after the thermal peak of the Svecofennian metamorphism (in central Finland about 1860–1850 Ma). The present density of the remaining layer is about 3290 kg/m^3. Although the crust is very thick there is no corresponding negative Bouguer gravity anomaly (Kukkonen et al., 2008).

2. Evolution of the lithosphere

The driving force for thermal evolution of the lithosphere in the Svecofennian orogeny 1.9 – 1.8 Ga was provided by collisions of plates. It resulted in collisional thickening of crust and conductive heating of the lithosphere by normal concentrations of radioactive elements of the U-Th-K decay series, partial melting of mid-lower crust and emplacement of extensive granitoid intrusions and migmatites in southern and central Finland (Kukkonen et al., 2008, Kukkonen and Lauri, 2009). The conductive heating of the thickened crust continued after the orogeny and contributed to formation of the rapakivi granite intrusions about 250 Ma later.

The shield area in Finland is characterized by deep roots of the Precambrian orogenies outcropping on the present erosion level. About 15-20 km of rock has been removed as indicated by the metamorphic pressures of rocks (Kukkonen and Lauri, 2009). Nevertheless, the crust is still very thick. Geothermal heat flow and temperature are low (Kukkonen et al., 2003).

An important result is that the Fennoscandian lithosphere thickened already in the Archaean and Proterozoic as evidenced by the Re-Os isotope data of mantle xenoliths (Peltonen and Brugmann, 2006). While partial melting of the subcrustal mantle produced the crustal rocks

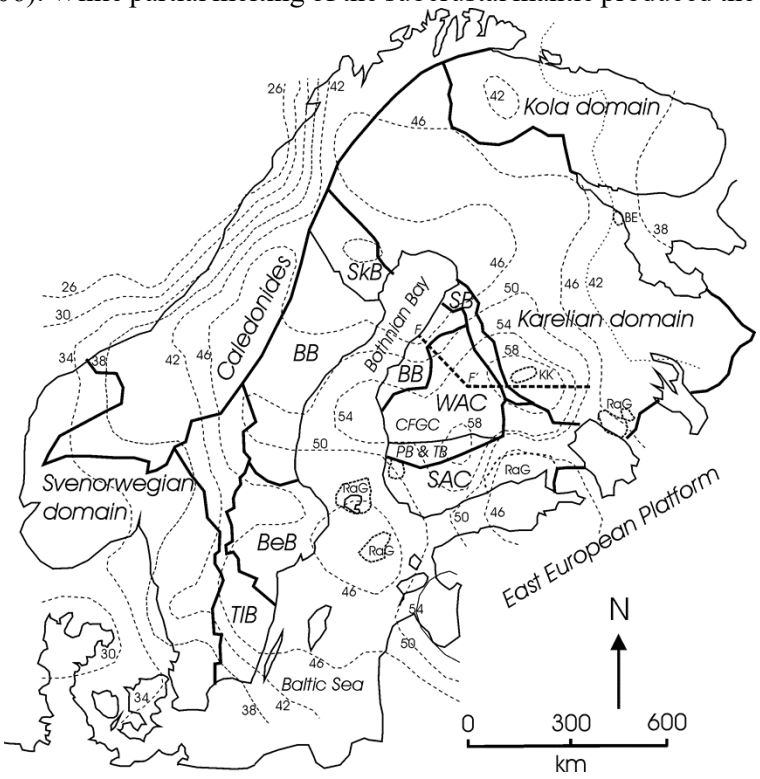

Figure 1. The main geological domains and crustal thickness in Fennoscandia. Based on Koistinen et al. (2001) and Lahtinen et al. (2005)

it also left behind layers of depleted mantle rocks which made the lithosphere buoyant. It has helped to preserve the lithosphere thick through times.

3. Fluids and microbial life in the bedrock

The fractured upper crust is characterized by groundwater increasing in salinity (Ca-Mg-Na-Cl solutions) with depth and hosting microbial life forms (Nurmi et al., 1988, Kietäväinen et al., 2013, 2014, Itävaara et al., 2011, Purkamo et al., 2016, Nuppunen-Puputti et al., 2020). Best data is available from the Outokumpu 2.5 km deep research drill hole (Kukkonen, 2011). There the saline fluids are gas-bearing and contain typically N_2, CH_4, He, Ar and H_2, and sometimes more complicated hydrocarbon compounds. He-isotopes suggest residence times of fluids of 10 – 50 Ma (Kietäväinen et al., 2014, 2017). The fluids were originally meteoric fluids recharged in the Eocene-Miocene but evolved thereafter in water-rock interaction. Fluid salinity is attributed to slow downward migration of water and hydration of feldspars and other rock-forming minerals on fracture surfaces resulting in salinities of up to 100 g/l in the uppermost 2 - 3 km and saturated brines at deeper levels (Bucher and Stober, 2000; Kietäväinen et al., 2014).

4. Evolution of the lithosphere in post-orogenic time

The shield was not similar to the present shield at the end of orogenies and magmatism in the Mesoproterozoic. Murrell and Andriessen (2004) studied apatite fission track (AFT) thermochronology in Finland and reported two phases of Late-Proterozoic cooling, a Late-Silurian re-heating, and a Cenozoic cooling. According to most recent results by Green et al. (2021) the Fennoscandian area has experienced up to 13 periods of cooling each representing kilometre-scale exhumation during the Neoproterozoic and Phanerozoic according to AFT thermochronology. Their results define a history involving repeated episodes of regional burial and exhumation. Key post-Caledonian episodes began in the intervals 311–307 Ma (late Carboniferous), 245–244 Ma (Middle Triassic), 170–167 Ma (Middle Jurassic), 102–92 Ma (mid-Cretaceous) and 23–21 Ma (early Miocene). Therefore, the late evolution of the lithosphere was not a peaceful denudation from the orogenic times as is sometimes suggested (Hall et al., 2021) but instead shows several periods of activity induced by plate tectonic and/or mantle processes in the surrounding areas (Green et al., 2021). With more data it may be possible to correlate the fluid residence times and periods of sedimentation with the AFT data.

A high research potential is provided by combining AFT results and deep biosphere studies. As the partial annealing zone of apatite fission tracks is 60 – 120°C, and the upper temperature limit of life is 122°C (Kashefi and Lovley, 2003), it is possible to constrain the habitability of bedrock through time with AFT results (Drake and Reiners, 2021). Episodes of burial and heating above 122°C would sterilize the bedrock. However, conclusions should not be drawn straightforward as the inverse modelling of AFT data includes ambiguities. The presence subsurface microbial life at depths previously heated above 122°C implies life is able to effectively inhabit again the sterilized depth ranges.

References:

Bucher, K., Stober I., 2000. The composition of groundwater in the continental crystalline crust. In: Stober, I. and Bucher, K. (Eds.), Hydrogeology of crystalline rocks, Kluwer, Dordrecht, pp. 141-176.

Drake, H., Reiners, P.W., 2021. Thermochronologic perspectives on the deep-time evolution of the deep biosphere. PNAS 2021 Vol. 118 No. 45 e2109609118. https://doi.org/10.1073/pnas.2109609118

Grad, M., Tiira, T., ESC Working Group, 2009. The Moho depth map of the European Plate. Geophys. J. Int., 176, 279–292. doi: 10.1111/j.1365-246X.2008.03919.x

Green, P.F., Japsen, P., Bonow, J.M., Chalmers, J.A., Duddy, I.R., Kukkonen, I.T., 2022. The post-Caledonian thermo-tectonic evolution of Fennoscandia. Gondwana Research, https://doi.org/10.1016/j.gr.2022.03.007

Heikkinen, P., Luosto, U., 2000. Review of some features of the seismic velocity models in Finland. In: L.J. Pesonen, A. Korja and S.-E. Hjelt, (eds.). Lithosphere 2000—A Symposium on the Structure, Composition and Evolution of the Lithosphere in Finland. Espoo, Finland, Oct. 4–5, 2000. Institute of Seismology, University of Helsinki, Report S-41, 35–41.

Itävaara, M., Nyyssönen, M, Bomberg, M., Kapanen, A., Nousiainen, A., Ahonen, L., Hultman,J., Paulin, L., Auvinen, P., Kukkonen, I.T., 2011. Microbiological sampling and analysis of the Outokumpu Deep Drill Hole biosphere in 2007-2009. In: I.T. Kukkonen (ed.), Outokumpu Deep Drilling Project 2003-2010, Geological Survey of Finland, Special Paper, 51, 199-206.

Hall, A.M., Putkinen, N., Hietala, S., Lindsberg, E., Holma, M., 2021. Ultra-slow cratonic denudation in Finland since 1.5 Ga indicated by tiered unconformities and impact structures. Prec. Res., 352, 106000. https://doi.org/10.1016/j.precamres.2020.106000.

Kashefi, K., Lovley, D. R., 2003. Extending the upper temperature limit for life. Science, 301, 934.

Kietäväinen, R., Ahonen, L., Kukkonen, I.T., Hendriksson, N., Nyyssönen, M., Itävaara, M., 2013. Characterisation and isotopic evolution of saline waters of the Outokumpu Deep Drill Hole, Finland – Implications for water origin and deep terrestrial biosphere. Applied Geochemistry, 32, 37-51. https://doi.org/10.1016 j.apgeochem.22012.10.013

Kietäväinen, R., Ahonen, L., Kukkonen, I.T., Niedermann S., Wiersberg, T., 2014. Noble gas residence times of saline waters within crystalline bedrock, Outokumpu Deep Drill Hole, Finland. Geochimica et Cosmochimica Acta, 145, 159-174.

Kietäväinen, R., Ahonen, L., Niinikoski, P., Nykänen, H., Kukkonen, I.T., 2017. Abiotic and biotic controls on methane formation down to 2.5 km depth within the Precambrian Fennoscandian Shield. Geochimica Cosmochimica Acta, 202, 124-145.

Koistinen, T., Stephens, M. B., Bogatchev, V., Nordgulen, Ø. Wennerström, M., Korhonen, J., 2001. Geological map of the Fennoscandian Shield, scale 1:2 000 000: Geological Surveys of Finland, Norway and Sweden and the North-West Department of Natural Resources of Russia.

Korja, A., Korja, T., Luosto, U., Heikkinen, P., 1993. Seismic and geoelectric evidence for collisional and extensional events in the Fennoscandian Shield—implications for Precambrian crustal evolution. Tectonophysics, 219, 129–152.

Kukkonen, I.T., Lauri, L.S., 2009. Modelling the thermal evolution of a collisional Precambrian orogen: high heat production migmatitic granites of southern Finland. Precambrian Research, 168 (3-4), 233-246.

Kukkonen, I.T., Kinnunen, K., Peltonen, P., 2003. Mantle xenoliths and thick lithosphere in the Fennoscandian Shield. Phys. Chem. Earth, 28, 349-360.

Kukkonen, I.T, Kuusisto, M., Lehtonen, M., Peltonen, P., 2008. Delamination of eclogitized lower crust: Control on the crust–mantle boundary in the central Fennoscandian shield. Tectonophysics, 457, 111–127.

Kuusisto, M., Kukkonen, I.T., Heikkinen, P., Pesonen, L.J., 2006. Lithological interpretation of crustal composition in the Fennoscandian Shield with seismic velocity data. Tectonophysics, 420 (1-2), 283-299.

Lahtinen, R., Korja A., Nironen, M., 2005. Paleoproterozoic tectonic evolution, in Lehtinen, M., Nurmi, P.A. and Rämö, O.T., (Eds.), Precambrian Geology of Finland – Key to the Evolution of the Fennoscandian Shield: Amsterdam, Elsevier, p. 481-532.

Murrell, G.R., Andriessen, P.A.M., 2004. Unravelling a long-term multi-event thermal record in the cratonic interior of southern Finland through apatite fission track thermochronology. Physics and Chemistry of the Earth, 29, 695–706.

Nuppunen-Puputti, M., Kietäväinen, R., Purkamo, L., Rajala, P., Itävaara, M., Kukkonen, I., Bomberg, M., 2020. Rock surface fungi in deep continental biosphere—Exploration of microbial community formation with subsurface in situ biofilm trap. Microorganisms 2021, 9, 64. https://doi.org/10.3390/microorganisms9010064.

Nurmi, P., Kukkonen, I., Lahermo, P., 1988. Geochemistry and origin of saline ground-waters in the Fennoscandian Shield. Applied Geochemistry, 3, pp. 185-203.

Peltonen, P., Brügmann, G., 2006. Origin of layered continental mantle (Karelian craton, Finland): Geochemical and Re–Os isotope constraints. Lithos 89, 405–423.

Plomerová, J., Babuška, V., 2010. Long memory of mantle lithosphere fabric — European LAB constrained from seismic anisotropy. Lithos 120, 131–143.

Purkamo, L., Bomberg, M., Kietäväinen, R., Salavirta, H., Nyyssönen, M., Nuppunen-Puputti, M., Ahonen, L., Kukkonen, I., Itävaara, M., 2016. Microbial co-occurrence patterns in deep Precambrian bedrock fracture fluids. Biogeosciences, 13, 3091-3108.

Sandoval, S., Kissling, E., Ansorge, J., the SVEKALAPKO Seismic Tomography Working Group, 2004. High-resolution body wave tomography beneath the SVEKALAPKO array – II. Anomalous upper mantle structure beneath the central Baltic Shield. Geophys. J. Int., 157, 200–214.

Finnish Seismic Instrument Pool

I. Kukkonen[1], G. Hillers[1], P. Haapanala[1] and the FLEX-EPOS team

[1]Department of Geosciences and Geography, P.O. Box 64, FIN-00014 University of Helsinki
E-mail: ilmo.kukkonen@helsinki.fi

University of Helsinki, University of Oulu, Geological Survey of Finland, National Land Survey of the Finnish Geospatial Research Institute, Aalto University, VTT Technical Research Center of Finland, and University of Turku are constructing an extensive state-of-the-art pool of seismic instruments for basic and applied studies. In 2024 when the infrastructure will be complete there will be 1200 portable short-period stations and 44 long-period stations available for projects. The pool facilitates detailed multi-instrument deployments with very high numbers of stations.

Keywords: Seismic instrument pool, seismology, FIRI, EPOS, research infrastructure

1. FLEX-EPOS

The *Flexible instrument network for enhanced geophysical observations and multi-disciplinary research* (FLEX-EPOS) is an on-going Academy of Finland funded research infrastructure project. It's a subproject of the national FIN-EPOS research infrastructure that is the Finnish connection to the European Plate Observing System EPOS (https://www.epos-eu.org) (see Korja et al., this volume).

The objective of FLEX-EPOS is to create a national research infrastructure of geophysical instruments and multi-disciplinary geophysical superstations to be further utilized in separately funded research projects aiming at solving fundamental scientific questions in seismology, geomagnetism and geodesy.

The FLEX-EPOS consortium includes Finnish universities and research organizations: University of Helsinki (UH), University of Oulu (UOULU), Geological Survey of Finland (GTK), National Land Survey, Finnish Geospatial Research Institute (FGI), Aalto University (Aalto), VTT Technical Research Center of Finland (VTT), and University of Turku (UTU).

2. Seismic Instrument Pool

Within the FLEX-EPOS project, a Seismic Instrument Pool (SIP) is created, maintained, and operated in a national co-operation with four universities (UH, UOULU, UTU, and Aalto) and three research institutions (GTK, VTT, FGI). The SIP provides seismic instruments for seismological (both controlled source and earthquake seismology) experiments of the FLEX-EPOS consortium parties (Table 1). The greatly expanded observational capability of SIP will contribute to science by providing massive new seismic datasets, observations and results, and strengthen and extend the role of Finland in EPOS.

SIP coordinator (UH) coordinates the 5-year build-up and operation of the pool in collaboration and under the guidance of the instrument owners and the FLEX-EPOS Steering Group. Principles of operation have been agreed for practical purposes to aid the application procedures and operations of the SIP.

5. Instruments

The FLEX-EPOS Seismic Instrument Pool instruments have been available for use via application process since fall 2021. Next bi-annual application round opens in November 2022 and closes in January 2023. Only projects including at least one FLEX-EPOS partner

organization are accepted and the main applicant (project Principal investigator) needs to be from that organization. Current instrumentation (Table 1) and instrument availability are given in the FLEX-EPOS Wiki pages.

Table 1. Instruments of the Finnish Seismic instrument pool.

SIP Instruments	**number**
Large-N 3-component nodes • Geospace Seismic Recorder with Battery (GSB) • Geophones 3C Land Cartesian • Adapters, line viewers, portable data transfer modules, time stamp recorders, etc • GSX3-LTE (pending)	**~1200** **(**Currently 764)
Broadband seismometers • Broadband Guralp 3ESPC seismometers (BB) • Minimus 24-bit, 4-chan digitizer, cables, GNSS antenna, etc	**50**

Figure 1. a) First testing of the short period large-N 3-component nodes on the Kumpula campus in 2021, b) Large-N nodes installed in racks for data download and battery recharging. Photos: P. Haapanala.

5. More information

More information on FLEX-EPOS and details e.g. on SIP instrumentation, application process, Principles of Operation, fees and liabilities etc are available at the FLEX-EPOS wiki pages: https://wiki.helsinki.fi/display/FLEX/Flex-epos+Home.

Website of the Finnish national node of EPOS, FIN-EPOS provides more insight into Finnish EPOS activities: https://www2.helsinki.fi/en/infrastructures/fin-epos.

Reflection seismic profiling in the Kevitsa Ni-Cu-PGE mining area for mineral exploration

V. Laakso[1], S. Heinonen[1], E. Koskela[1] and M. Malinowski[1]

[1]Geological Survey of Finland, Espoo
E-mail: viveka.laakso@gtk.fi

We present a preliminary interpretation of the 2D reflection seismic profile acquired at the Kevitsa Ni-Cu-PGE deposit, Sodankylä March 2022. Aim of the survey was to map the possible subsurface continuation of the ore hosting mafic intrusion south of the active mine in area mostly covered by swamps. The profile was about 10 km long with 10 m receiver and 20 m source spacing. The survey utilized wireless receivers and explosives as source. The acquired profile crosscuts two earlier seismic profiles acquired in Kevitsa enabling integration of the newly acquired data to the existing 3D models. Additionally, drill hole data accompanied with sonic logging enable correlation between reflectivity and lithologies as well as provide constrain for velocity models needed for migration and depth conversion of the data.

Keywords: Reflection seismic, Kevitsa, Mineral exploration, 3D modelling

1. Introduction

In March 2022, Geological Survey of Finland (GTK) together with subcontractor Geopartner Geofizyka acquired a 2D reflection seismic profile in the Kevitsa Ni-Cu-PGE mining and exploration area in Sodankylä for Boliden Kevitsa Mining Oy. Aim of the survey was to gain more information on the geological formations south of the Kevitsa mine. The acquired profile crosscuts two earlier seismic profiles acquired in Kevitsa (Kukkonen et al., 2008, Koivisto et al. 2012). This enables direct comparison of the data acquired in 2007 and 2022 in the location where profiles cross, as well as it helps to extend the existing 3D models south of the currently active mine.

The Kevitsa Ni-Cu-PGE deposit is a disseminated magmatic type mineralization within an ultramafic intrusion in the Lapland Greenstone Belt. The ore body has an irregular shape due to the disseminated style of the mineralization. Earlier petrophysical studies (Koivisto et al. 2012, Junno et al. 2020) have shown that ore-hosting mafic lithologies are reflective in contact with country rock, encouraging the use of seismic reflection method in the area.

2. Data acquisition

The acquired 2D reflection seismic line was about 10 km long with 10-meter receiver and 20-meter source spacing (Figure 1). Due to the line crossing multiple wet swamps not accessible during the summer, the survey was conducted during winter. Snow was kept packed along the profile to facilitate the drilling of holes for explosives and actual deployment of the receivers. The geophones were deployed by placing them to holes dug to the snow and then covering the geophones with snow. This was done to enable better coupling with the ground and to decrease the noise caused by wind. The Wireless Seismic RT2 system was used for the data acquisition. The total number of wireless receivers deployed was 974. Each receiver station consists of vertical-component 10-Hz GSOne high-sensitivity geophone, data logger unit and antenna that is utilized to send the data from each receiver to the computer in the operator van during the data acquisition. Explosions were used as the source (240 g charge) and for these 2-meter-deep holes were drilled beforehand the acquisition.

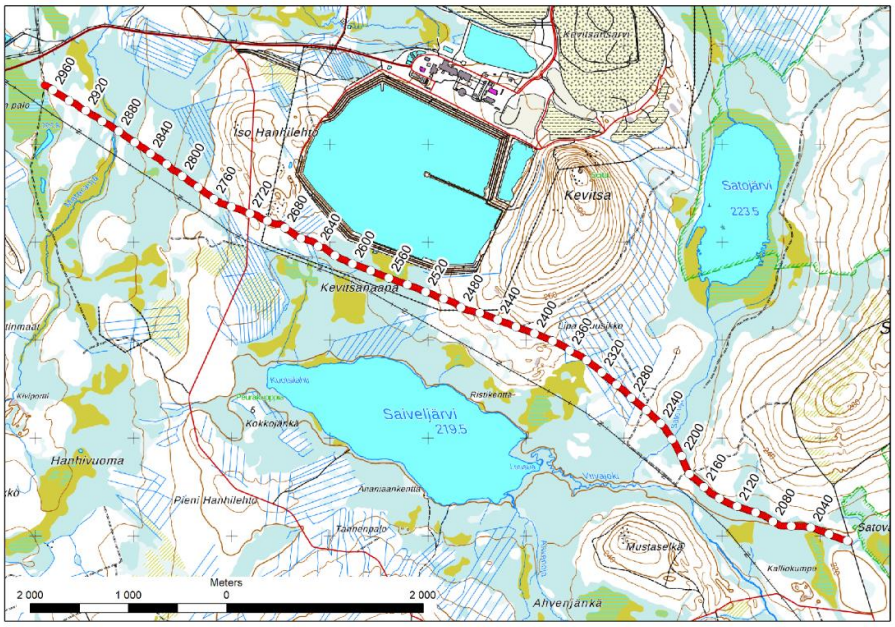

Figure 1. Location of the seismic reflection profile acquired in Kevitsa. Every 20th receiver location marked with white circles.

3. Data processing

Quality of the acquired data is overall good but varies depending on the near surface condition. It was expected that in the swampy areas the seismic signal is weaker compared to the areas with moraine soils, due to the peatland efficiently damping the seismic waves and the energy produced by explosions. In moraine areas, the energy of the explosions has been efficiently propagating over offset of 5000 m and first breaks are clear. In the swampy areas, the explosions have mostly caused low frequency noise trapped in the wet peat leading the waves to propagate insufficiently through the bedrock. Seismic signals contaminated by low frequency noise can be seen on all the geophones deployed on the wet swamp areas. Another major noise source is ongoing pumping in the tailing pond area next to the survey line. The pumping has created repeated high energy features to the data.

Processing of the seismic data acquired in Kevitsa followed a standard hard rock seismic data processing flow. First the geometry of the 2D line was defined and the first breaks were picked. First break picking was followed by calculation of refraction static corrections, that are required to compensate for time delays caused to the seismic signal by variation in near surface condition (topography, overburden thickness and type). The signal-to-noise ratio of the reflected arrivals was improved by bandpass filtering, deconvolution and amplitude corrections. These pre-processing steps were followed by velocity analysis in which optimal stacking velocity for reflections is defined. Results of velocity analysis are implemented in Normal Move-Out corrections (NMO) before stacking the data from each theoretical reflection point to form a seismic section. Finally, data has been migrated using Stolt algorithm and two-way travel time has been converted to depth. The processing parameters were selected to be comparable to those used by Koivisto et al. (2012) to facilitate later comparison between different seismic data sets.

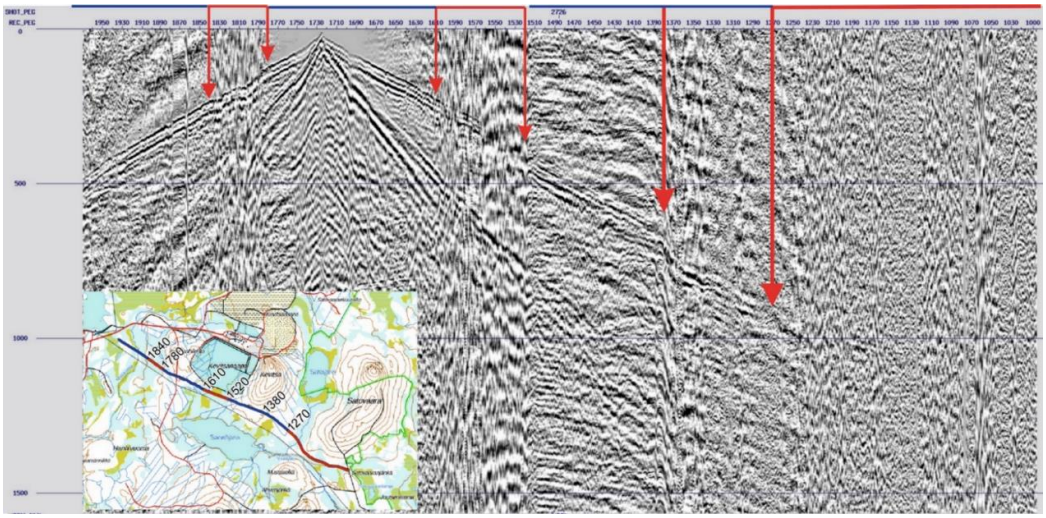

Figure 2. Raw example shot gather from the seismic data acquired in Kevitsa. Automatic gain control has been applied for plotting purposes. Noisy receivers are marked with red and can be seen to correlate with swamp areas.

4. Discussion

In the processing phase the effects of the noise was aimed to be minimised. Nevertheless, a good solution to suppress the noise caused by the pumping in the tailings pond was not found, due to the noise being present in all frequencies. This noise caused by pumping is strong among several of the receiver points and repeats at regular interval within a shot gather. However, these do not repeat at exactly same millisecond in different shot gathers and the pumping noise is not stacking coherently. Anyhow it is a factor deteriorating the data quality and the quality could be further improved by suppressing this noise. In addition, the quality of the final section could be improved by implementing iterative process of residual static corrections and improvement of NMO-velocity functions and to utilize advanced migration algorithms.

Figure 3 shows a 3D view of the seismic data acquired in 2022, geological map and data acquired within the HIRE project (Kukkonen et al., 2008) and processed by Koivisto et al. (2012). The current results from 2022 survey show good correlation with the HIRE profiles, and reflections likely arising from the base of the intrusion are clearly imaged in both data.

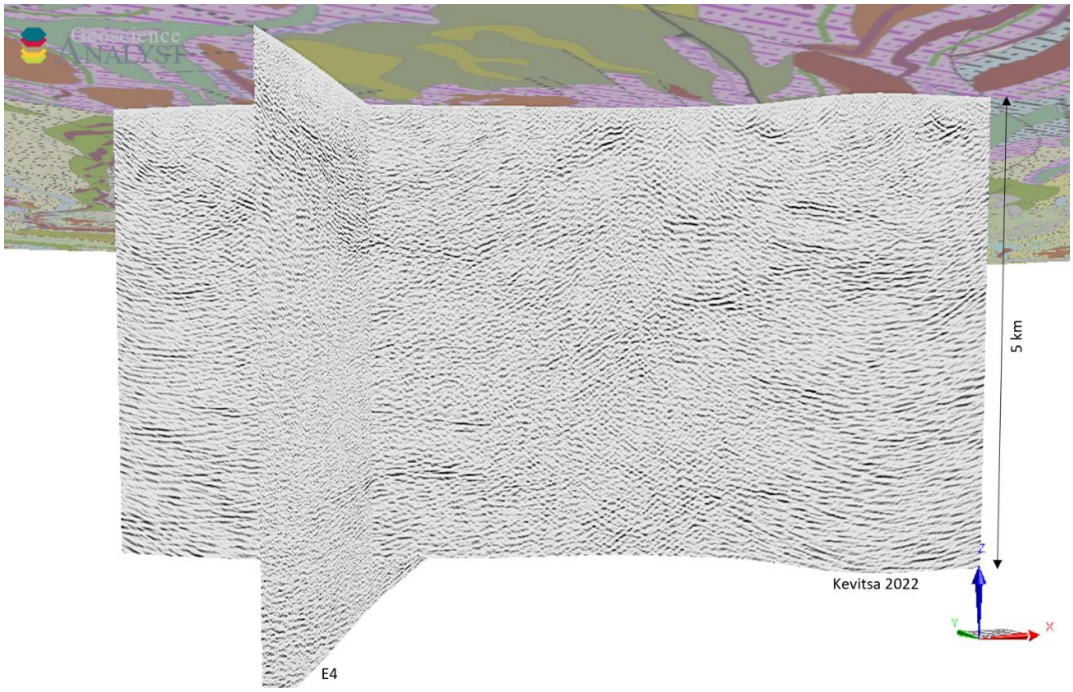

Figure 3. A 3D view of the seismic line acquired in 2022 together with HIRE line E4 processed by Koivisto et al. (2012) looking towards north-east. Surface geology from © Geological Survey of Finland (Bedrock of Finland 1:200 000).

5. Conclusions

The seismic reflection section obtained from the Kevitsa 2022 survey contains abundant reflectivity marking abrupt changes of subsurface physical properties. Reflectors at the north-west end of the profile are projected to the surface and can thus be correlated to geological observations. The reflections seen in the profile show correlation with the earlier profiles by Koivisto et al. (2012) crosscutting the section. Timing the acquisition during the wintertime enabled surveying on wet swamps which on the summertime would be hard or impossible to access. The work will be continued by improving the velocity model by using sonic data and with a 3D modelling utilizing the known surface geology, drillhole information and the previous seismic profiles.

Acknowledgements

Thank you, Boliden Kevitsa, for the data and for the opportunity to present it.

References:

Junno, N., Koivisto, E., Kukkonen, I., Malehmir, A., Wijns, C., Montonen, M., 2020. Data mining of petrophysical and lithogeochemical borehole data to elucidate the origin of seismic reflectivity within the Kevitsa Ni–Cu–PGE bearing intrusion, northern Finland. Geophysical Prospecting, 68, 82–102.

Koivisto, E., Malehmir, A., Heikkinen, P., Heinonen, S., Kukkonen, I., 2012. 2D reflection seismic investigations at the Kevitsa Ni-Cu-PGE deposit, northern Finland, GEOPHYSICS, VOL. 77, NO. 5, WC149–WC162.

Kukkonen, I., Lahti, I, Heikkinen, P., 2008. HIRE Seismic Reflection Survey in the Kevitsa Ni-PGE deposit, North Finland. GTK working report, Q23/2008/59

Sm-Nd and Lu-Hf isotopes in the Svecofennian rocks of southernmost Finland

N. Lindén[1], A. Saukko[1], M. Kurhila[2] and O. Eklund[1]

[1]Geology and Mineralogy, Åbo Akademi University
[2]Geological Survey of Finland, Espoo
E-mail: nicolas.linden@abo.fi

The granite-rich area surrounded by metaigneous and metasedimentary migmatites around the Hanko peninsula has an unclear history regarding its magmatic origin. The area hosts several compositionally different early Svecofennian and late Svecofennian granitoids. It is unclear how much mantle input the igneous rocks in the area received and how the magmas behaved during this tectonically active period. By using the two isotope systems of Sm-Nd and Lu-Hf, this study aims to provide further clues about the origins and evolution of the magmas in the area.

Keywords: Svecofennian orogeny, granite, migmatite, neodymium, hafnium

1. Introduction

The arc complex of Southern Finland hosts synorogenic granitoids. The accretionary orogen produced both volcanic rocks and their plutonic counterparts (e.g., Väisänen & Mänttäri, 2002), of which related granitoids have been U-Pb dated to 1.89-1.87 Ga (e.g., Vaasjoki, 1996, Väisänen & Mänttäri, 2002). Another collisional event at 1.84-1.79 Ga heavily metamorphized and partially melted the rocks formed in the earlier event (e.g., Kurhila et al., 2010). This later collisional event produced most of the granite and migmatite that are today characteristic of the bedrock of southernmost Finland around Hanko and Ekenäs. The aim of the study is to investigate the magmatic source by using both Lu/Hf and Sm/Nd analysis, concentrating on the Hanko-Ekenäs area. Earlier studies, conducted within a larger area in southern Finland by Kurhila et al. (2005), have shown initial εNd values between -0.3 and -1.1 with a negative southbound trend.

2. Materials and analytical methods

Samples for this study have been taken in the Hanko archipelago, and on the mainland between Hanko and Ekenäs. The sampled early Svecofennian rock types are amphibolite (n=1), leucosomes from amphibolitic metatexite (n=2), megacryst-bearing supracrustal metatexites (n=2), granitic metatexites (n=4), and an even-grained granodiorite (n=1). The late Svecofennian samples are red (n=2) and grey (n=2) leucogranites, and a leucocratic dike (n=1). For more detailed rock type description, see Saukko et al. (this volume).

Lu/Hf analysis was performed on six samples consisting of 10 previously hand-picked zircon fractions. These were mounted on epoxy and SEM-BSE imaged with a JEOL IT-100 InTouchScope Scanning Electron Microscope at Top Analytica Oy Ab to study the internal structures of the zircons and to locate suitable spots on which beam analysis was performed.

Sm/Nd analysis was performed on 11 finely ground whole-rock samples at The Finnish Geosciences Research Laboratory at the Geological Survey of Finland (GTK) in Espoo, using conventional cation exchange chromatography for LREE separation and Multi-Collector Inductively Coupled Plasma Mass Spectrometer for measuring.

Previously obtained U/Pb ages were used to calculate epsilon values. The Sm/Nd samples were dated by secondary ion mass spectrometer (SIMS), and sample ages were used to calculate

the epsilon values. Of the six Lu/Hf samples, two were dated by laser ablation inductively coupled mass spectrometry (LA-ICP-MS) (Bredenberg, E., 2019), and four by SIMS (Saukko et al., 2022). Where possible, the Lu/Hf analyses were performed on top of the age dating analysis spots and the corresponding spot ages were used for calculating the epsilon value. For analyses without corresponding spot ages, the sample ages were used.

3. Results and discussion

Both the early and late Svecofennian collisional events are visible in the data as crystallization peaks (Figure 1 and 2). εHf results produced averaged spreads from -1.2 to -2.1, while εNd results ranged from 2.8 to -1.4.

The isotope data suggest there was no Archean component to the earlier Svecofennian (1.89-1.87 Ga) magma. Rather, a mildly depleted mantle source seems to have mixed with partially melted crust as part of the earlier collisional event. The lack of an Archean component in Svecofennian materials has previously been noted by Kara et al. (2018). The εHf values (Figure 1) vary within each sample but compared to each other show approximately the same internal variation. This can be understood as a sign of heterogeneity within the earlier (1.89-1.87 Ga) magma. The lower values most likely represent reworked Paleoproterozoic crust, while the higher values point to mantle sources contributing to the magma.

The late Svecofennian samples are most likely recycled early Svecofennian rocks that were subjected to high-grade metamorphism. This is supported by the lower εNd values around 1.84-1.81 Ga, suggesting the lack of mantle material at that time. The later samples probably inherited zircons from the rocks that melted during the later collisional event. The >20 Ma active period during the later event may also have presented a possibility for the magma to cool down and homogenize. The narrower εHf and εNd spreads in the later crystallization peak may be a sign that the magma was indeed more homogenized during that time.

The results do not seem to follow the southbound negative εNd trend previously discussed by Kurhila et. al. (2005). More negative εNd values point to longer crustal residence times. The data suggests a maximum crustal residence time has been found within the study area, at least compared to the rest of southern Finland.

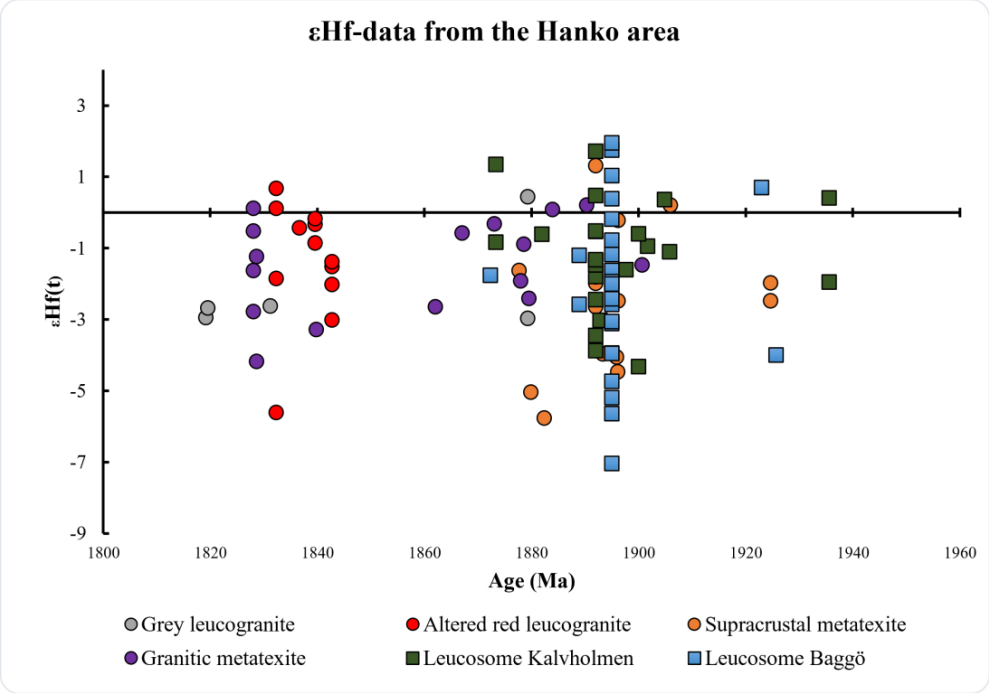

Figure 1. εHf vs. age (Ma) of the analyzed zircons from the Hanko area granites and migmatites. Kalvholmen and Baggö age determinations were made by LA-ICPMS, other samples with SIMS.

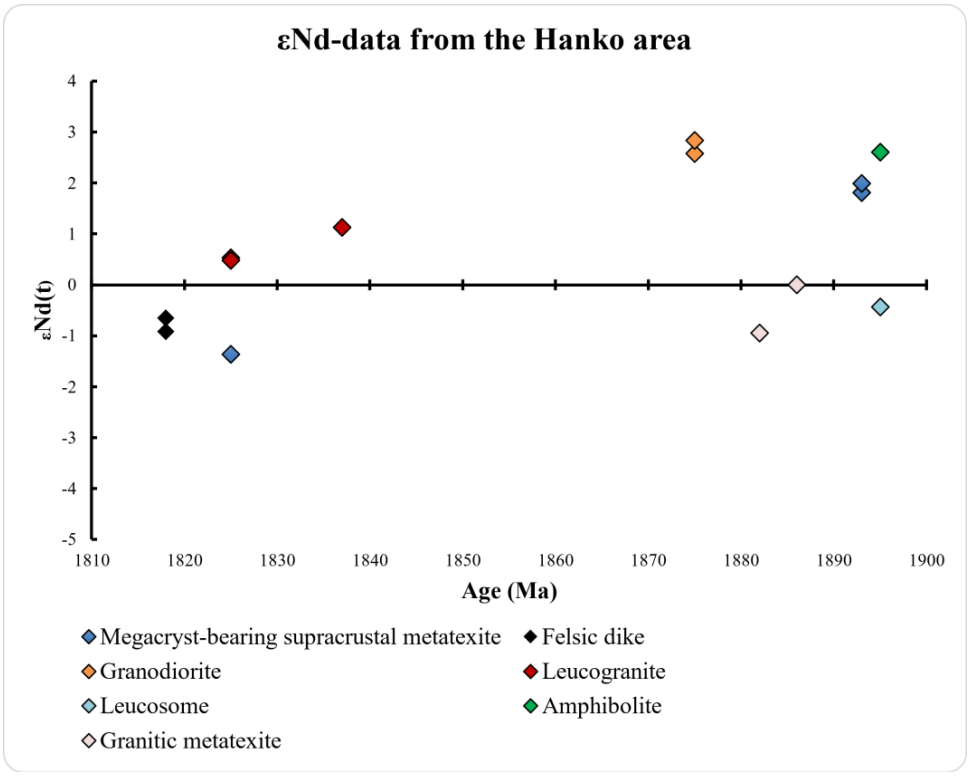

Figure 2. εNd vs. age (Ma) of the analyzed samples from the Hanko area granites and migmatites.

4. Conclusions

Mantle input to the magmas during the two Svecofennian collisional events varied. During the early collisional event (1.89-1.87 Ga) there seems to have been a mantle component, evidenced by larger proportions of radiogenic Hf and Nd. However, during the late Svecofennian event (1.84-1.81 Ga) the data suggests recycling of earlier Svecofennian material without mantle input. This is consistent with models suggesting a mildly depleted mantle source under Fennoscandia during the early collisional event. The later collisional event may also have facilitated a plausible homogenization of the magmas.

References:

Bredenberg, E., 2019. Tonalit migmatit i Södra Finland – åldersbestämning och petrografisk analys. Master's thesis, Åbo Akademi University. 48 p. (in Swedish)

Huhma, H., 1986. Sm-Nd, U-Pb and Pb-Pb isotopic evidence for the origin of the Early Proterozoic Svecokarelian crust in Finland. Geological Survey of Finland, Bulletin, 337, 48 p.

Kara, J., Väisänen, M., Johansson, Å., Lahaye, Y., O'Brien, H., Eklund, O., 2018. 1.90-1.88Ga arc magmatism of central Fennoscandia: geochemistry, U-Pb geochronology, Sm-Nd and Lu-Hf isotope systematics of plutonic-volcanic rocks from southern Finland. Geologica Acta. 16. 1-23. https://doi.org/10.1344/GeologicaActa2018.16.1.1

Kurhila, M.,Vaasjoki, M., Mänttäri, I., Rämö, T.,Nironen, M., 2005. U-Pb ages and Nd isotope characteristics of the lateorogenic, migmatizing microcline granites in southwestern Finland. Bulletin of the Geological Society of Finland, 105–128

Kurhila, M., Andersen, T., Rämö, T. 2010. Diverse sources of crustal granitic magma: Lu–Hf isotope data on zircon in three Paleoproterozoic leucogranites of southern Finland. Lithos, 115, 1–4, 263-27. https://doi.org/10.1016/j.lithos.2009.12.009

Saukko, A., Nikkilä, K., Fröjdö, S., Eklund, O., Väisänen, M., 2022. Magmas, metasomatism, and melting – the Svecofennian orogeny in southernmost Finland. This abstract volume.

Vaasjoki, M., 1996. Explanation to the geochronological map of southern Finland: The development of continental crust with special refence to the svecofennian orogeny. Geological Survey of Finland Report of Investigation 135, 30 p.

Väisänen, M., Mänttäri, I., 2002. 1.90-1.88 Ga arc and back-arc basin in the Orijärvi area, SW Finland. Bulletin of the Geological Society of Finland 74, 185-214.

Integrated modelling of bedrock surface and bedrock deformation zones for induced seismic risk assessments – improved constraints for thickness of sedimentary cover

T. Lindqvist[1,2], E. Ruuska[1], E. Kosonen[2], N. Hornborg[2], P. Skyttä[1] and N. Putkinen[3]

[1] Department of Geography and Geology, FI-20014 University of Turku, Finland
[2] Geological Survey of Finland, P.O. Box 96, FI-02151 Espoo, Finland
[3] Geological Survey of Finland, P.O. Box 97, FI-67101 Kokkola, Finland
E-mail: teemu.lindqvist@gtk.fi

Seismic waves become amplified when propagating from the crystalline bedrock to the overlying sediments due to the change in the mechanical properties of the ground. Also, the increasing thickness of sediments increases the amplification of seismic waves. In this study, we show that integrated modelling of the bedrock deformation zones and the bedrock surface morphology results in improved constraints for the modelling of thickness of the sedimentary cover.

Keywords: seismic risk, deformation zone, bedrock, digital elevation model, superficial deposit, structural geology

1. Introduction

Deep geothermal operations increase the risk of induced earthquakes due to the induced stress changes which may cause reactivation of existing deformation zones within the bedrock (e.g. Berre et al., 2020; Buijze et al., 2019). Deformation zones are mechanically weaker than the surrounding bedrock and susceptible for glacial erosion processes resulting in linear depressions at the bedrock surface, and thus linear depositional basins for glaciogenic sediments (Krabbendam & Bradwell, 2014; Saresma et al., 2021; Skyttä et al., 2015). The seismic waves (earthquakes) become amplified when they propagate from stiff crystalline bedrock to the overlying soft sediments, and the amplification increases as the thickness of the sedimentary deposits increase. In this study, we show that characterisation of bedrock deformation zones can be integrated with modelling of bedrock surface topography, and the resulted sub-models can be further used as improved constraints for thickness analysis of the sedimentary cover, and eventually, gain improved understanding of areas with increased seismic hazard. Our study focuses on an area in southern Finland characterised by partially exposed crystalline bedrock where no comprehensive bedrock surface model is available, nor the thickness variations of the cover sediments have been systematically studied. Existing methods for creating integrated geological models of the bedrock surface and the sedimentary cover do not adequately consider the effect of bedrock deformation zones on the erosion surface of the bedrock.

We used 2D geological and geophysical datasets for conducting a 2D-interpretation of the network of bedrock deformation zones (location, orientation, topology). We extracted bedrock surface elevation points from multiple sources to generate digital elevation models of the bedrock surface (bedrock-DEMs). We further extracted elevation points representing the top of the load-bearing sediment horizon (till) and used them in analysis of the thickness of till deposits both within and outside of the bedrock deformation zones. Finally, we improved the bedrock-DEMs through structurally controlled interpolation (Ordinary Kriging) and new constraints about the erosional signatures of the erosion zones and the associated spatial variation in the till thicknesses.

This study focuses on the area around the 6.1 km deep enhanced geothermal system (EGS) test site owned by St1 Deep Heat Oy in Espoo, southern Finland, where hydraulic stimulations of the reservoir in 2018 and 2020 produced tens of thousands of microearthquakes (Kukkonen et al., 2021; Kwiatek et al., 2019; Leonhardt et al., 2021). The Precambrian bedrock of the area is complexly deformed including multiple ductile and brittle phases of deformation and overlain by glacial deposits of Quaternary age.

2. Data and methods

We interpreted ductile structures using overlay analysis of a 1:200 000 lithologic map (Geological Survey of Finland, GTK), foliation data (n=1867; City of Helsinki, City of Espoo, GTK) and aeromagnetic map (GTK) to understand their control over the brittle deformation zones (e.g. Stephens et al., 2015). For the deformation zones, we interpreted discontinuities from the lithologic map, the aeromagnetic map and additionally from a LiDAR dataset (National Land Survey, NLS).

We generated the bedrock-DEMs by utilising bedrock surface points extracted from the LiDAR data, geotechnical ground investigations (City of Espoo, City of Helsinki, GTK) and acoustic-seismic surveys (GTK). The outcrop areas identified from the LiDAR data (n=151 925), and those geotechnical ground investigations that include confirmation of the bedrock surface (n=28 828) were classified as *confirmed bedrock elevation points*. We used the other geotechnical ground investigations (n=69 913), which have terminated against the load-bearing stratum, as the points representing the top of till deposits. Furthermore, we subtracted one metre from the top of till points and classified them as *interpreted bedrock surface points*. The points from acoustic-seismic surveys from marine areas (n=11 313) were also classified as interpreted bedrock surface points.

From these elevation point clouds, we generated a bedrock-DEM using Delaunay Triangulation and further used it to estimate the till thickness on top of the bedrock within the deformation zones and outside of their influence. To further improve the bedrock-DEM, we used Ordinary Kriging (OK-DEM) for optimising the interpolation method to emphasise the linear depressions. Finally, we utilised the recognized faults as abrupt breaks and used 'tear existing horizon' tool in MOVE™ to compile the final structurally constrained bedrock-DEM (after Ruuska et al., submitted).

3. Preliminary results

The 2D form line analysis shows that the study area is characterised by folding dominated by sub-vertical axial surfaces striking E-W. The interlimb angles of the folds vary from isoclinal to open. The 2D form lines show major deformation zones with E-W, WNW-ESE, and NE-SW strikes, which correlate well with the linear depressions identified from the bedrock-DEMs. Analysis of elevation difference between the confirmed and interpreted bedrock surface points illustrate that till thickness can be 10-15 m within the deformation zones while outside of their influence the thickness typically varies between 1 and 3 m (Figure 1.)

4. Concluding remarks

- Till deposits can be an order of magnitude thicker within deformation zones than outside
- of their influence
- Interpolation method substantially affects the resulting bedrock-DEM which can be further improved with deformation zone constraints (abrupt) breaks applied on the 3D surface.
- The structurally constrained bedrock-DEM gives more realistic constraints for modelling the thickness of sedimentary cover than using a DEM generated with basic triangulation.

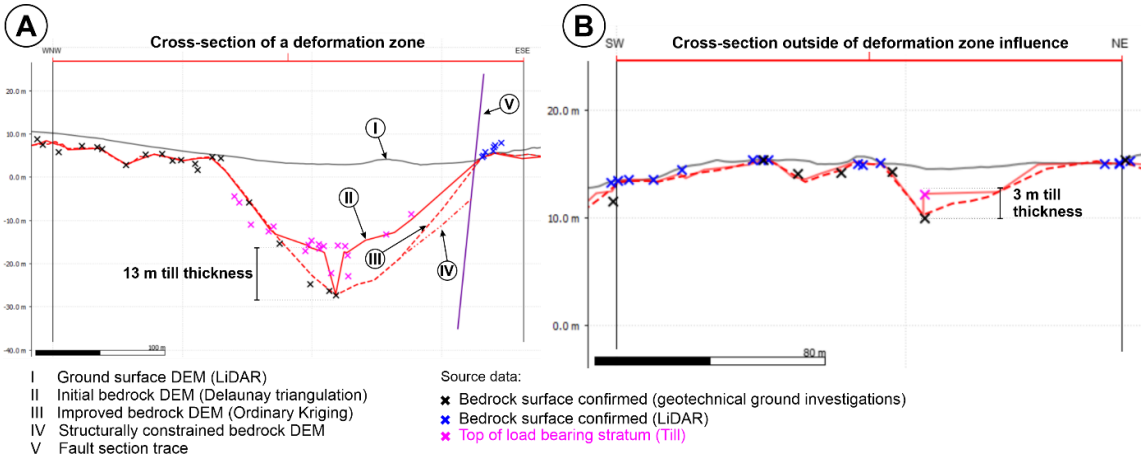

Figure 1. Till thickness analysis from cross-sections. A) Cross-section of a deformation zone showing till thickness of 13 m (elevation difference between the confirmed bedrock surface points and the top of load bearing stratum (till)). B) Cross-section from outside of deformation zone influence shows till thickness of 3 m.

References:

Berre, I., Stefansson, I., Keilegavlen, E., 2020. Fault slip in hydraulic stimulation of geothermal reservoirs: Governing mechanisms and process-structure interaction. The Leading Edge, 39 (12), 893–900. https://doi.org/10.1190/tle39120893.1.

Buijze, L., van Bijsterveldt, L., Cremer, H., Paap, B., Veldkamp, H., Wassing, B. B. T., van Wees, J.-D., van Yperen, G. C. N., ter Heege, J. H., & Jaarsma, B., 2019. Review of induced seismicity in geothermal systems worldwide and implications for geothermal systems in the Netherlands. Netherlands Journal of Geosciences, 98. https://doi.org/10.1017/njg.2019.6.

Krabbendam, M., & Bradwell, T., 2014. Quaternary evolution of glaciated gneiss terrains: pre-glacial weathering vs. glacial erosion. Quaternary Science Reviews, 95, 20–42. https://doi.org/10.1016/j.quascirev.2014.03.013.

Kukkonen, I., Pentti, M., Heikkinen, P., 2021. St1 Deep Heat Project: Hydraulic stimulation at 5 – 6 km depth in crystalline rock. In Kukkonen, I., Veikkolainen, T., Heinonen, S., Karell, F., Kozlovskaya, E., Luttinen, A., Nikkilä, K., Nykänen, V., Poutanen, M., Skyttä P., Tanskanen, E., Tiira, T., 2021 (Eds.). Lithosphere 2021– Eleventh Symposium on the Structure, Composition and Evolution of the Lithosphere in Finland. Program and Extended Abstracts, January 19-20, 2021. Institute of Seismology, University of Helsinki, Report S-71, 69-72 pages (pdf).

Kwiatek, G., Saarno, T., Ader, T., Bluemle, F., Bohnhoff, M., Chendorain, M., Dresen, G., Heikkinen, P., Kukkonen, I., Leary, P., Leonhardt, M., Malin, P., Martínez-Garzón, P., Passmore, K., Passmore, P., Valenzuela, S., Wollin, C., 2019. Controlling fluid-induced seismicity during a 6.1-km-deep geothermal stimulation in Finland. Science Advances, 5 (5). https://doi.org/10.1126/sciadv.aav7224

Leonhardt, M., Kwiatek, G., Martínez-Garzón, P., Bohnhoff, M., Saarno, T., Heikkinen, P., Dresen, G., 2021. Seismicity during and after stimulation of a 6.1 km deep enhanced geothermal system in Helsinki, Finland. Solid Earth, 12 (3), 581–594. https://doi.org/10.5194/se-12-581-2021

Ruuska, E., Skyttä, P., Putkinen, N., Valjus, T. submitted. Contribution of bedrock structures to the bedrock surface topography and groundwater flow systems within deep glaciofluvial aquifers.

Saresma, M., Kosonen, E., Ojala, A. E. K., Kaskela, A., Korkiala-Tanttu, L., 2021. Characterization of sedimentary depositional environments for land use and urban planning in Espoo, Finland. Bulletin of the Geological Society of Finland, 93 (1), 31–51. https://doi.org/10.17741/bgsf/93.1.003

Skyttä, P., Kinnunen, J., Palmu, J.-P., Korkka-Niemi, K., 2015. Bedrock structures controlling the spatial occurrence and geometry of 1.8Ga younger glacifluvial deposits — Example from First Salpausselkä, southern Finland. Global and Planetary Change, 135, 66–82. https://doi.org/10.1016/j.gloplacha.2015.10.007

Stephens, M. B., Follin, S., Petersson, J., Isaksson, H., Juhlin, C., Simeonov, A., 2015. Review of the deterministic modelling of deformation zones and fracture domains at the site proposed for a spent nuclear fuel repository, Sweden, and consequences of structural anisotropy. Tectonophysics, 653, 68–94. https://doi.org/10.1016/j.tecto.2015.03.027

The Black Shale Database of Finland: Precambrian metasedimentary rocks rich in graphite and sulphides

K. Loukola-Ruskeeniemi[1], E. Hyvönen[2], J. Lerssi[3], H. Arkimaa[1], M.-L. Airo[1], J. Vanne[3], S. Vuoriainen[1], R. Turunen[3], J. Eskelinen[3]

[1]Geological Survey of Finland, P.O. Box 96, FI-02151 Espoo, Finland
[2]Geological Survey of Finland, P.O. Box 77, FI-96101 Rovaniemi, Finland
[3]Geological Survey of Finland, P.O. Box 1237, FI-70211 Kuopio, Finland
E-mail: kirsti.loukola-ruskeeniemi@gtk.fi

Graphite- and sulphide-rich bedrock can be distinguished in low-altitude airborne geophysics with a combination of magnetic and electromagnetic anomalies. The procedure is valuable especially in areas where bedrock is rarely exposed. The digitizing of black shale polylines was carried out using aeromagnetic total intensity data, AEM ratio of the real to imaginary component and apparent resistivity data, geological outcrop and drill core observations and exploration reports, and geophysical field measurement data. Geochemical and petrophysical data of samples selected from drill cores were correlated with the airborne geophysical data. There was a linear correlation between the magnetic susceptibility and the content of monoclinic pyrrhotite. The Black Shale Database is used in geological and geophysical studies, exploration and bedrock mapping. Since black shales may cause acid rock drainage if exposed to weathering during anthropogenic activities, the Database is used also by environmental authorities. The Black Shale Database will be published in 2023, together with a guide, at https://hakku.gtk.fi/fi/locations/search.

Keywords: graphite, sulphides, geophysical measurements, exploration, acid rock drainage, Finland

1. Introduction

Geological Survey of Finland has carried out mapping of black shales for a couple of decades. The first version of the Black Shale Map was published in 2000 (Arkimaa et al., 2000) although during that time the low-altitude aerogeophysical programme was not completed yet for the whole of Finland. We started the present phase of the black shale mapping project in 2008 (Hyvönen et al., 2013). Black shale mapping has been a 'third priority' project for all of us. For several years we didn't have any opportunity to continue the work.

The mapping was based mainly on airborne geophysics because only some 3% of the bedrock is outcropped in Finland. Airborne geophysical surveys reveal coupled magnetic and electrically conductive patterns. Electrical conductivity is related to the graphite and sulphide contents, producing continuous and bending electromagnetic anomaly patterns. The magnetic anomalies in the black shale units, if present, result from ferrimagnetic monoclinic pyrrhotite (Airo and Loukola-Ruskeeniemi, 2004).

We correlated the airborne magnetic and electromagnetic survey with petrophysical and chemical data. During the present project, we collated the geological reports for the exploration drill cores searching for 'grafiittiliuske', graphite schist, 'grafiitti-kiisuliuske', graphite-sulphide schist, 'mustaliuske', black schist, which refers to a metamorphosed black shale. In the Precambrian of Finland, the metamorphic grade varies from greenschist to granulite facies, and amphibolite facies is most common (Hölttä and Heilimo, 2017).

We selected rock samples from over 60 prospects and mines and over a hundred deep drill cores. In addition to the Proterozoic study sites, we studied drill cores from some Archaean prospects where graphite was reported. The same piece of drill core was first measured for petrophysical properties and then analysed for major and trace elements by XRF and ICP-MS.

Total C, carbonate C and S contents were determined with LECO analysers. Polished thin sections were prepared for mineralogical studies.

The Proterozoic of Finland and NW Russia include formations deposited during an extraordinary period in the history of the Earth, from 2.1 to 1.9 Ga, with widespread and thick (> 20 m) black shale units and high average concentrations of organic carbon (*e.g.*, Loukola-Ruskeeniemi, 1999). Folding has still increased the thickness of the organic-rich formation in the black-shale-hosted Talvivaara Ni–Zn–Cu–Co deposit at Sotkamo, where maximum thickness of the package containing several black shale units can reach 800 m in places (Loukola-Ruskeeniemi and Lahtinen, 2013; Kontinen and Hanski, 2015).

2. The black shale polylines

We carried out the interpretation and digitizing of the black shale polylines using previous geological, geochemical and geophysical studies as well as the chemical characteristics and petrophysical properties of the drill core samples. In addition, we used geophysical field measurement data if available. The petrophysical properties of some 700 graphite-rich samples listed in the Petrophysical Database of Finland were studied and compared with our data.

We compiled shaded relief and derivative maps with the aeromagnetic total intensity data and used the AEM ratio of the real to the imaginary component (Re/Im) and apparent resistivity data. Geologists and geophysicists specialized in different regions in Finland were interviewed during the digitizing of the black shale polylines.

We classified black shales into two main categories, namely 1) verified black shale units with observations in drill cores or in outcrop and 2) interpreted black shale units with comparable geophysical properties to the verified black shales.

3. Exploration and bedrock mapping

Black shales host sulphide deposits such as the Talvivaara Ni–Zn–Cu–Co (Loukola-Ruskeeniemi and Lahtinen, 2013; Kontinen and Hanski, 2015). In addition, the Proterozoic black shales of Finland contain graphite because of the medium to high-grade regional metamorphism. Over 30 small graphite mines have operated in Finland in the past (Puustinen, 2003). Some of the graphite deposits and occurrences represent metamorphosed black shales like those of the Raisjoki prospect at Evijärvi (Kuusela et al., 2020).

Moreover, black shales occur in the vicinity of many types of sulphide deposits and occurrences. For example, two black shale units occur in the Vihanti Lampinsaari Zn–Cu mine (Loukola-Ruskeeniemi et al., 1997) and a hanging-wall black shale caused challenges in the mining operations at the Hammaslahti Cu–Zn mine (Loukola-Ruskeeniemi et al., 1991, 1993). The chemical and petrophysical characteristics of black shales can in some cases be used as a pathfinder for sulphide deposits in exploration (*e.g.*, Loukola-Ruskeeniemi, 1992, 1999). For example, black shales in a komatiite-hosted Ni–Cu–PGE occurrence in Central Lapland showed increased Na and Si values compared with black shales studied in other parts of Finland due to intense multiphase alteration (Loukola-Ruskeeniemi et al., 2022b).

The relationships of black shales with other types of sulphide deposits include (Loukola-Ruskeeniemi, 1992):

1) Deposition on seafloor under anoxic conditions which favour preservation of both organic matter and S-rich compounds. S-rich fluids of sufficient density migrate to seafloor depressions.
2) After deposition, black shale sediment forms a local reducing environment and may capture ore-forming fluids.

3) During diagenesis beneath the seafloor, a black shale layer may enhance fluid circulation underneath and direct fluids into certain fractures.

The Black Shale Database shows the distribution of bedrock with elevated electrical conductivity and indications of abundant graphite and/or sulphides. The magnetic anomalies, if present in the black shale units, suggest the occurrence of ferrimagnetic monoclinic pyrrhotite. In the Database, it is further presented if an 'Interpreted black shale' has been outlined based on an electromagnetic or both on electromagnetic and magnetic anomaly. 'Verified black shale' may represent ancient seafloor mud rich in organic matter and sulphur and deposited in anoxic or euxinic conditions.

4. Regional planning and environmental permit procedures

Sulphide-rich black shales may cause acid rock drainage even under natural conditions (Gustavsson et al., 2012; Loukola-Ruskeeniemi et al., 1998, 2003; Parviainen and Loukola-Ruskeeniemi, 2019). The distribution of Ni–Mn -rich black shales is reflected in elevated Ni–Mn concentrations of the hair samples of local residents as well as in elevated Ni–Mn in private well waters at Sotkamo (Kousa et al., 2021) pointing out the need for risk assessment and subsequently, risk management actions in areas hosting S-rich black shales.

Environmental authorities and consulting companies use the Black Shale Database to locate sulphur-rich bedrock and soil which increases the risk for acid rock drainage during anthropogenic activities. However, we would like to point out that scale limitations given by airborne geophysics in many cases request more detailed geological, geophysical and geochemical studies. The black shale polylines are drawn with a 'thicker ink' compared with the actual width of the black shale unit in many locations due to the 1 : 200 000 scale of the Database. Moreover, all black shales don't contain a lot of sulphur and heavy metals. If the thickness of the black shale unit is < 3 m, it contains < 3% S and bedrock and soil are not exposed to weathering, the black shale may not provide an environmental risk (Loukola-Ruskeeniemi et al., 2022a).

References:

Airo, M.-L., Loukola-Ruskeeniemi, K., 2004. Characterization of sulfide deposits by airborne magnetic and gamma-ray responses in eastern Finland. Ore Geology Reviews, 24, 67–84.

Arkimaa, H., Hyvönen, E., Lerssi, J., Loukola-Ruskeeniemi, K., Vanne, J. 2000: Proterozoic black shale formations and aeromagnetic anomalies in Finland. Database and map 1:1 000 000. Geological Survey of Finland, Special Maps 45. ISBN: 951-690-762-8

Gustavsson, N., Loukola-Ruskeeniemi, K., Tenhola, M., 2012. Evaluation of geochemical background levels around sulfide mines – A new statistical procedure with beanplots. Applied Geochemistry 27, 240–249.

Hyvönen, E., Airo, M.-L., Arkimaa, H., Lerssi, J., Loukola-Ruskeeniemi, K., Vanne, J., Vuoriainen, S., 2013. Airborne geophysical, petrophysical and geochemical characteristics of Palaeoproterozoic black shale units in Finland: applications for exploration and environmental studies. Geological Survey of Finland, Report of Investigation 198, 2013 Current Research − GTK Mineral Potential Workshop, Rauhalahti/Kuopio, May 2012. pp. 58–60.

Hölttä, P. and Heilimo, E., 2017. Metamorphic map of Finland. In: Nironen, M. (ed.) Bedrock of Finland at the scale 1:1 000 000 – Major stratigraphic units, metamorphism and tectonic evolution. Geological Survey of Finland, Special Paper, 60, 77–128.

Kontinen, A., Hanski, E., 2015. The Talvivaara Black Shale-Hosted Ni-Zn-Cu-Co Deposit in Eastern Finland. In: Maier, W., Lahtinen, R., O´Brien, H. (Eds.). Mineral Deposits of Finland, Elsevier, pp. 557–612.

Kousa, A., Loukola-Ruskeeniemi, K., Hatakka, T., Kantola, M. 2021: High manganese and nickel concentrations in human hair and well water and low calcium concentration in blood serum in a pristine area with sulphide-rich bedrock. Environmental Geochemistry and Health, 44, pages 3799–3819. https://doi.org/10.1007/s10653-021-01131-6

Kuusela, J., Nygård, H., Leväniemi, H., Al-Ani, T., 2020. The investigations of the Raisjoki metavolcanic rocks in Evijärvi, Western Finland. Geological Survey of Finland. GTK Open File Work Report, 57/2020. 11 p. Available at: https://tupa.gtk.fi/raportti/arkisto/57_2020.pdf

Loukola Ruskeeniemi, K. 1992. Geochemistry of Proterozoic metamorphosed black shales in eastern Finland, with implications for exploration and environmental studies. Geological Survey of Finland, Special Publication, 9, 97 p.

Loukola-Ruskeeniemi, K. 1999. Origin of black shales and the serpentinite-associated Cu-Zn-Co ores at Outokumpu in Finland. Economic Geology, 94, 1007–1028. http://dx.doi.org/10.2113/gsecongeo.94.7.1007

Loukola Ruskeeniemi, K., Gaál, G., Karppanen, T., 1991. Geochemistry, structure and genesis of the Hammaslahti copper mine explorational tools for a sediment hosted massive sulphide deposit. In: Autio, S. (Ed.) Geological Survey of Finland, Current Research 1989–1990. Geological Survey of Finland, Special Paper, 12, 101–106.

Loukola Ruskeeniemi, K., Gaál, G., Karppanen, T., 1993. Geochemical and structural characteristics of a sediment hosted copper deposit at Hammaslahti, Finland: comparison with Besshi type massive sulphide deposits. In: Maurice, Y. T. (ed.) Proceedings of the Eighth Quadrennial IAGOD Symposium, Ottawa, Canada, August 12–18, 1990. Stuttgart: E. Schweizerbart'sche Verlagsbuchhandlung, pp. 551–569.

Loukola-Ruskeeniemi, K., Hyvönen, E., Lerssi, J., Arkimaa, H., Auri, J., 2022a. Maankäytön vaikutus pintavesien laatuun mustaliuskealueilla. Ympäristö ja Terveys, 4_2022, 64–69. (In Finnish)

Loukola-Ruskeeniemi, K., Hyvönen, E., Airo, M.-L., Lerssi, J., Arkimaa, H., 2022b. Country-wide exploration for graphite- and sulphide-rich black shales with airborne geophysics and petrophysical and geochemical studies. Journal of Geochemical Exploration (revised version submitted 10.10.2022)

Loukola-Ruskeeniemi, K., Lahtinen, H., 2013. Multiphase evolution in the Talvivaara Ni-Cu-Zn-Co deposit, Finland. Ore Geology Reviews, 52, 85–99. https://doi.org/10.1016/j.oregeorev.2012.10.006

Loukola Ruskeeniemi, K., Kuronen, U., Arkimaa, H., 1997. Geochemical comparison of metamorphosed black shales associated with the Vihanti zinc deposit and prospects in western Finland. In: Autio, S. (ed.) Geological Survey of Finland, Current Research 1995-1996. Geological Survey of Finland, Special Paper, 23, 5–13.

Loukola-Ruskeeniemi, K., Uutela, A., Tenhola, M., Paukola, T., 1998. Environmental impact of metalliferous black shales at Talvivaara in Finland, with indication of lake acidification 9000 years ago. J. Geochem. Explor., 64, 395–407.

Loukola-Ruskeeniemi, K., Kantola, M., Seppänen, K., Henttonen, P., Kallio, E., Kurki, P., Savolainen, H., 2003. Mercury-bearing black shales and human Hg intake in eastern Finland: impact and mechanisms. Environmental Geology, 43, 283–297.

Parviainen, A. and Loukola-Ruskeeniemi, K., 2019. Environmental impact of mineralised black shales. Earth-Science Reviews, 192, 65–90. https://doi.org/10.1016/j.earscirev.2019.01.017

Puustinen, K., 2003. Suomen kaivosteollisuus ja mineraalisten raaka-aineiden tuotanto vuosina 1530-2001, historiallinen katsaus erityisesti tuotantolukujen valossa Geological Survey of Finland Archive Report, M101/2003/3. Available at: https://tupa.gtk.fi/raportti/arkisto/m10_1_2003_3.pdf (in Finnish)

Åland seismic network

T. Luhta[1] and J. Hällsten[1]

[1]Institute of Seismology, University of Helsinki
E-mail: tuija.luhta@helsinki.fi

In August 2022 the Institute of Seismology, University of Helsinki installed a temporary seismic network of three broad-band stations and nine geophone stations on Åland, Finland. The network was motivated by four earthquakes that occurred during the summer 2021 having characteristics of seismicity encountered in the Wyborg rapakivi batholith in southeastern Finland. Åland is the second largest rapakivi occurrence in Finland. The aims of the network are better detection and analysis capability of seismic events happening on or near Åland. Data from the network will also be used for structural studies of the area.

Keywords: intra-plate seismicity, seismic monitoring, rapakivi seismicity

1. Introduction

In summer 2021 four earthquakes were detected on Åland. Locations of the epicenters can be seen in Figure 1. The first event occurred on July 18th with a local magnitude M_L 1.7. It was followed by two smaller events in July 19th and 28th with M_L 1.2 and 0.56, respectively. The largest event, M_L 1.8, occurred on August 7th. The earthquakes were all shallow, happening in the uppermost 1-3 kilometres of the crust. The smallest event was not detected by the Finnish National Seismic Network (FNSN), but by the Swedish National Seismic Network (SNSN), thus it was located with a different set of stations and appears to be from a slightly different location. After more detailed analyses all the events will probably be re-located closer to each other, i.e. to the same fault or fault system.

Åland is the second largest rapakivi occurrence in Finland (Figure 2). Its larger counterpart, the Wyborg rapakivi batholith, in southeastern Finland hosts characteristic seismicity with shallow earthquake sequences (e.g. Luhta et al, 2022). The 2021 earthquakes on Åland can be interpreted to have the same kind of seismicity, which makes it compelling to cover also Åland in the on-going rapakivi seismicity studies.

2. Network and data

The Åland network can be seen in the Figure 1. Three on-line broad-band stations were installed to complement the existing permanent network in the area. Previously there has only been one SNSN station, AAL, on Åland. The closest stations of the FNSN are in Tvärminne and Raumo. Data of the on-line stations is sent near real-time to the data servers of the Institute of Seismology, and can be used in the daily seismic monitoring of the area.

In addition to broad-band stations, nine geophone stations were installed covering some known fault structures. Geophone stations are off-line, and the data will be retrieved in the summer 2023 to be used later in detecting very small seismic events, re-analysing larger seismic events recorded during the project, as well as in other structural studies

3. Objectives

A dense seismic research network was installed on Åland for better detection capability of the area, which has had a higher detection threshold than mainland Finland. The earthquakes in summer 2021 implicated that Åland rapakivi batholith may also host characteristic rapakivi seismicity. More data is needed to confirm this. If seismicity observed in the Wyborg rapakivi batholith appears to be a characteristic of rapakivi batholiths in general, this will give new

insights to the mechanisms triggering these seismic events. Data of the network can also be used for mapping seismically active faults in the area and producing seismic velocity models, revealing subsurface properties and structures of the bedrock on Åland.

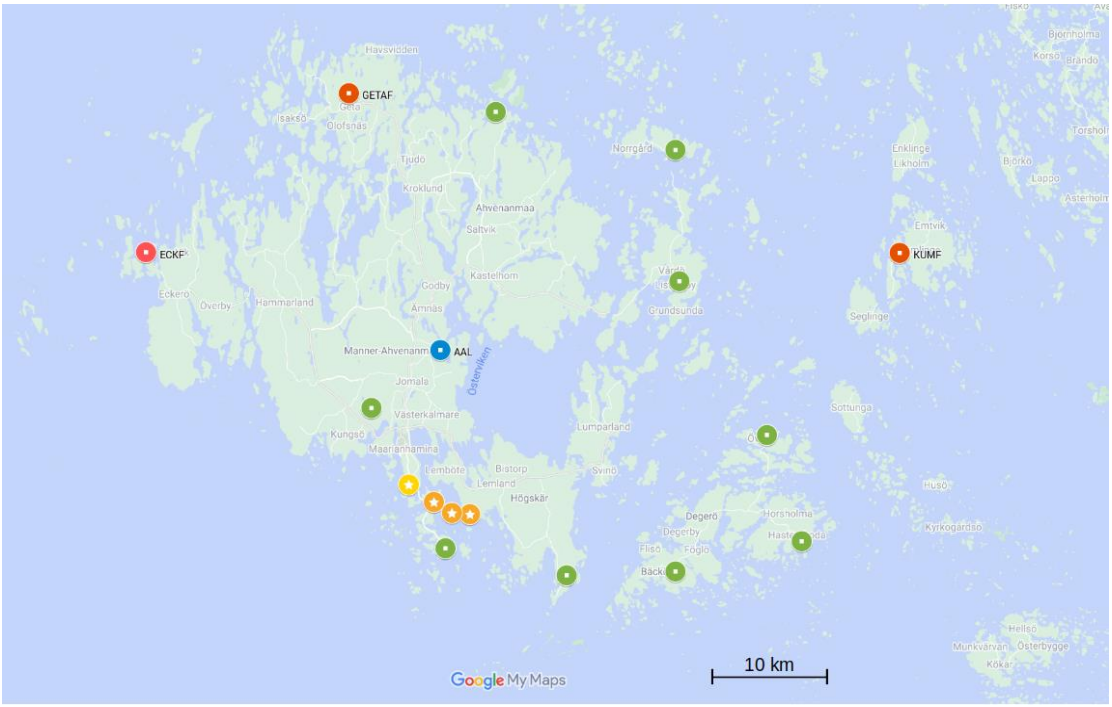

Figure 1. Earthquakes detected on Åland in summer 2021. Yellow star: detected only by SNSN, orange star: detected by both FNSN and SNSN. Åland seismic network. Red circles: broad-band stations, green circles: geophone stations, blue circle: SNSN permanent station.

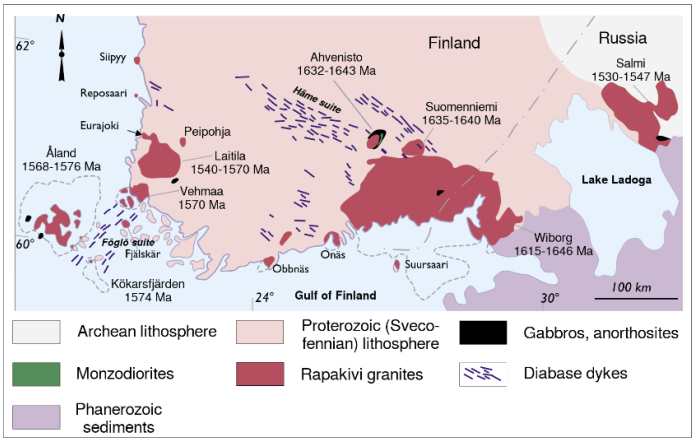

Figure 2. Rapakivi occurrences in Finland. Modified from: Lehtinen, M., Nurmi, P., & Rämö, T. (1998). Suomen Kallioperä, 3000 Vuosimiljoonaa. Suomen Geologinen Seura, Jyväskylä.

Acknowledgements:
The project is supported by the Nordenskiöld-samfundet.

References:

Luhta, T., Komminaho, K., and Mäntyniemi, P., 2022. Seismisyyttä Viipurin rapakivialueella. In: Veikkolainen et al, 2022 (Eds.). XXX Geofysiikan päivät. Programme and Extended Abstracts, Helsinki, Finland, May 18-19, 2022. 73 pages.

New reliable ~1885 Ma paleomagnetic pole from Svecofennian gabbro intrusions, central Finland

T. Luoto[1, 2], J. Salminen[1, 2], S. Mertanen[2], S.-Å. Elming[3] and L. J. Pesonen[4]

[1]Department of Geosciences and Geography, University of Helsinki, Finland
[2]Geological Survey of Finland, Espoo, Finland
[3]Department of Civil, Environmental and Natural Resources engineering, Luleå University of Technology
[4]Department of Physics, University of Helsinki

E-mail: toni.luoto@helsinki.fi; toni.luoto@gtk.fi

In this work we provide a new reliable ca. 1885 Ma paleomagnetic pole for Fennoscandia obtained from Svecofennian gabbro intrusions in central Finland. This new pole fills the gap in the Paleoproterozoic high-quality paleomagnetic record of Fennoscandia, and verifies the location of Fennoscandia at shallow to moderate latitudes at 1885–1790 Ma.

Keywords: Fennoscandia, paleomagnetism, Paleoproterozoic, Svecofennian gabbros

1. Introduction

As high-quality paleomagnetic poles allow the determination of the ancient latitudes and azimuthal orientations recorded in rock formations, they have a key role in paleogeographic reconstructions. Typically, these high-quality poles are derived from mafic intrusions, which often are amenable for precise dating, and can reliably record the directions of the ancient geomagnetic fields. During the period from the break-up of the Paleoproterozoic supercratons to the onset of the formation of the Mesoproterozoic supercontinent Nuna, global paleomagnetic record shows large oscillating back-and-forth movements for several cratons. This oscillation is particularly well observed in the 2020–1870 Ma Coronation loops of the Slave craton, with data derived not only from mafic intrusions but also from the high-resolution sedimentary rock record of the Coronation, Great Slave and Kilohigok basins (Mitchell et al., 2010; Gong and Evans, 2022).

Suggested explanations for these oscillations include inertial interchange true polar wander events, in which the whole solid body of the planet shifts relative to its spin axis; basin-scale or local-scale rotations; unstable geomagnetic field; or any combination of these (Gong and Evans, 2022). However, the global Paleoproterozoic paleomagnetic record is sparse (Evans et al., 2021), and high-resolution data is available only for relatively short time interval from the Slave craton. Filling the gaps in the paleomagnetic record is therefore crucial, to better understand the mechanisms behind the oscillations.

The amalgamation of Nuna was associated with the global 2100–1800 Ma orogenies. In Fennoscandia, several gabbro intrusions with radiometric ages of ca. 1885 Ma, 1860 Ma, 1800 Ma and 1780 Ma, were formed during the Svecofennian orogeny. Paleomagnetism of these gabbros have been previously studied (see review of poles in Salminen et al., 2021), but only 1786 Ma pole from Hoting gabbro, was evaluated as a high-quality pole in the previous Nordic Paleomagnetic Workshop (July 31st – August 6th, 2022 in Kringlerdalen, Nannestad, Norway). In this work, we committed a paleomagnetic study on Svecofennian gabbro intrusions in central Finland. Some of these ca. 1885 Ma gabbros have been previously studied by Pesonen and Stigzelius (1972), but their sampling scheme at the time was to take only one sample from each gabbro intrusion, which is insufficient to meet the present-day requirements for statistics. In addition, three outcrops of Kiuruvesi gabbrodiorite were previously sampled by Neuvonen et

al. (1981). We aimed to complement these old studies to provide a new reliable paleomagnetic pole satisfying the present-day statistical requirements, to fill the gaps in the Paleoproterozoic high-quality paleomagnetic record of Fennoscandia.

2. Sampling

For this work, two gabbro units were sampled in the Ylivieska area, which belongs to the accretionary arc complex of central and western Finland. Sampling included six outcrops of well-dated 1883±8 Ma (Patchett and Kouvo, 1986) Ylivieska gabbro and eight outcrops of a smaller undated gabbro unit. In addition, five outcrops of the 1886±5 Ma (Marttila, 1981) Kiuruvesi gabbrodiorite were sampled. Kiuruvesi gabbrodiorite is located in central Finland on the Raahe-Ladoga tectonic zone separating the Svecofennian domain from the Archean Karelian Province (Marttila, 1981).

3. Results and discussion

Data obtained in this study from the Kiuruvesi gabbrodiorite and two separate gabbro units in Ylivieska area were combined with the data from previous studies on the same rock units (Pesonen and Stigzelius, 1972; Neuvonen et al., 1981) to provide statistically sufficient data to meet the present-day standards. This new reliable ~1885 Ma paleomagnetic pole has a well-determined rock age (1886±5, Marttila, 1981; 1883±8 Ma, Patchett and Kouvo, 1986), but lacks the paleomagnetic field tests to prove the primary nature of magnetization. However, typical cooling rates of similar gabbro intrusions and comparison of the new pole to the high-quality paleomagnetic poles of Fennoscandia indicate that the magnetization ages of the studied gabbro intrusions are likely close to their crystallization ages. The new pole overlaps the cluster of ca. 1870–1790 Ma poles of Fennoscandia, supporting relatively stable position for Fennoscandia at ca. 35–20 °N at 1885–1790 Ma, indicated also by occurrences of evaporites, lateritic paleosols and stromatolite-like structures in Finland and Sweden.

References:

Evans, D.A.D., Pesonen, L.J., Eglington, B.M., Elming, S.-Å., Gong, Z., Li, Z.-X., McCausland, P.J., Meert, J.G., Mertanen, S., Pisarevsky, S.A., Pivarunas, A.F., Salminen, J., Swanson-Hysell, N.L., Torsvik, T.H., Trindade, R.I.F., Veikkolainen, T., Zhang, S., 2021. An expanding list of reliable paleomagnetic poles for Precambrian tectonic reconstructions. In: Pesonen, L. J., Salminen, J., Elming, S.-Å., Evans, D.A.D., Veikkolainen, T., (Eds.) Ancient Supercontinents and the Paleogeography of the Earth. San Diego: Elsevier. pp. 605-640.

Gong, Z., Evans, D.A.D., 2022. Paleomagnetic survey of the Goulburn Supergroup, Kilohigok Basin, Nunavut, Canada: Toward an understanding of the Orosirian apparent polar wander path of the Slave craton. Precambrian Res., 369, 106516.

Marttila, E., 1981. Kiuruveden kartta-alueen kallioperä. Summary: Pre-Quaternary rocks of the Kiuruvesi map-sheet area. Suomen geologinen kartta 1:100 000, Kallioperäkartan selitykset, 3323 Kiuruvesi.

Mitchell, R. N., Hoffman, P. F., Evans, D. A. D., 2010. Coronation loop resurrected: Oscillatory apparent polar wander of Orosirian (2.05–1.8 Ga) paleomagnetic poles from Slave craton. Precambrian Res., 179, 121-134.

Neuvonen, K. J., Korsman, K., Kouvo, O., Paavola, J., 1981. Paleomagnetism and age relations of the rocks in the Main Sulphide Ore Belt in central Finland. Bull. Geol. Soc. Finland, 53, 109-133.

Patchett, J., Kouvo, O., 1986. Origin of continental crust of 1.9-1.7 Ga age: Nd isotopes and U-Pb zircon ages in the Svecokarelian terrain of South Finland. Contrib. Mineral. Petrol., 92, 1-12.

Pesonen, L. J., Stigzelius, E., 1972. On petrophysical and paleomagnetic investigations of the gabbros of the Pohjanmaa region, Middle-West, Finland. Geol. Surv. Finland Bull., 260, 1-27.

Salminen, J., Lehtonen, E., Mertanen, S., Pesonen, L.J., Elming, S.-Å., Luoto, T., 2021. The Precambrian drift history and paleogeography of Baltica. In Pesonen, L. J., Salminen, J., Evans, D. A. D., Elming, S.-Å., Veikkolainen, T. (Eds.). Ancient Supercontinents and the Paleogeography of the Earth. San Diego: Elsevier. pp. 155-205.

Proximal hydrothermal alteration assemblages in the Kiruna deposit – a preliminary petrographic study.

P. Lupoli[1], L. Lobo[1], O. Katai[1], R. Prata[1], C. Santana[1], L. Gerlach[1], C. Benedicto[1], S. Johansson[1], M.-L. Friedländer[1], M. Martins[1] and P. Biedzio[1]

[1]Luossavaara-Kiirunavaara AB, Near Mine Exploration, FK9, 981 86 Kiruna, Sweden
E-mail: philip.lupoli@lkab.com

Based on microscopic investigation of thin sections from drill core samples, this study brings new insights regarding the hydrothermal alteration assemblages that occur in the giant Kiruna IOA deposit in the Norrbotten region, northern Sweden.

Keywords: Kiruna deposit, hydrothermal alteration, petrography

1. Introduction

The Kiruna deposit, located in the Norrbotten region of northern Sweden, is characterised as a world-class iron oxide-apatite (IOA) deposit that has been mined for over 120 years by Luossavaara-Kiirunavaara Aktiebolag (LKAB), and is one of the main sources of iron ore in Europe. The Kiruna deposit consists of a steeply dipping massive magnetite body with >2.5Bt, grading at 55-65 wt% Fe and 0.05 to 5 wt% P. The NNE striking mineralisation occurs as a tabular body with a length of 5km and thickness of >100m, hosted by Paleoproterozoic (ca. 1880 Ma) alkali altered metavolcanic rocks, comprising andesite-trachyandesites of the Hopukka formation (footwall) and rhyolite-rhyodacites of the Luossavaara formation (hanging wall). The emplacement of the ore body has been suggested to have occurred around 1874 ± 7 Ma and 1877 ± 4 Ma (Westhues et al., 2017; Andersson et al., 2021).

The genesis of Kiruna-type IOA deposits in Norrbotten is a controversial topic. Authors suggest magmatic-hydrothermal (e.g., Westhues et al., 2017), magmatic (e.g., Troll et al., 2019), hydrothermal (e.g., Hitzman et al., 1992), or sedimentary-exhalative origins (e.g., Parák, 1975). Very few studies have focused on defining the hydrothermal alterations in the area. This study has built on the work of Paolillo & Giapis (2021) who established a preliminary alteration characterisation for the orebody based on macroscopic descriptions of mineral assemblages in drill core samples. The addition of microscopic descriptions is crucial for a greater understanding of the spatial and temporal relationships between mineral phases and their associated alteration assemblages proximal to the mineralisation.

3. Methodology

25 thin sections were selected from representative drill core samples from the Kiruna mine based on the preliminary alteration characterisation by Paolillo & Giapis (2021). Microscopy descriptions were performed using a Nikon Eclipse LV100N POL microscope at the LKAB headquarters in Kiruna. NIS-Elements software was used to capture PPL, XPL, and reflected light images. Additional XRF and ICP-MS whole rock geochemical data and core logging observations were used to support the interpretation.

4. Results Hanging wall: In the proximal part of the rhyolite-rhyodacite hanging wall rocks, two main zones are distinguished: (I) Close to the mineralisation, a dominant Ca-rich alteration assemblage consisting of actinolite, titanite and occasionally epidote is common (Figure 1B).

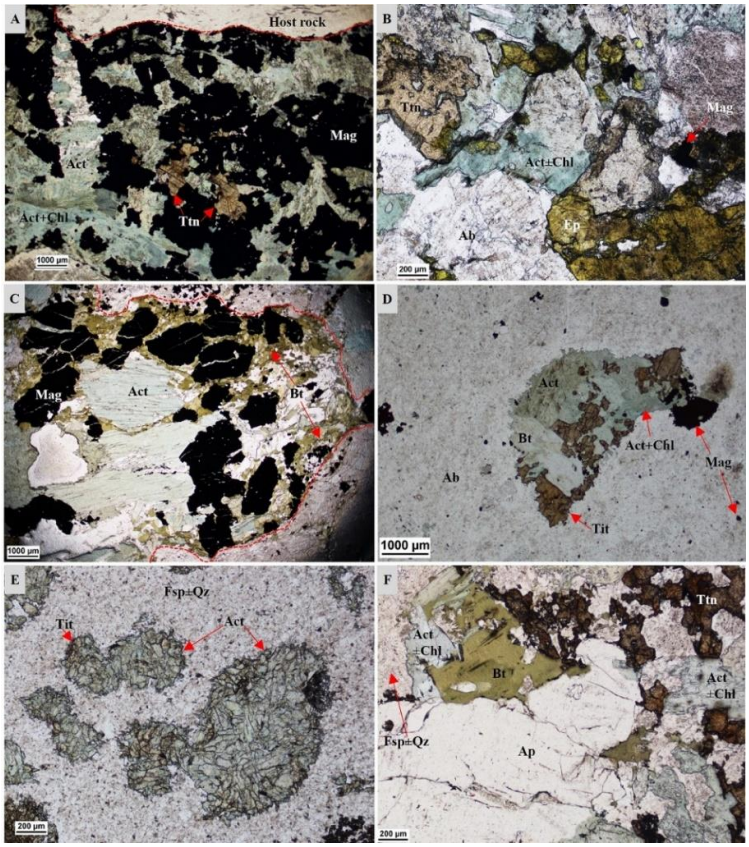

Figure 3. A. BXK20107-193m: Actinolite, magnetite and titanite vein, part of the Ca-Fe alteration of the hanging wall rocks. Some of the actinolite crystals are overprinted by chlorite. B. BXK20009-275m: Calcic alteration of the hanging wall rocks represented by aggregates of titanite, epidote and actinolite filling spaces between the feldspar phenocrysts. Magnetite is present as disseminations. Actinolite is partially altered to chlorite. C. BXK20083-845m: Ca-Fe-(K) assemblage of the hanging wall in a vein including coarse-grained actinolite and magnetite ± interstitial fine-grained secondary anhedral to subhedral biotite. Possible reactivation of vein. Vein surrounded by a very-fine grained albite + quartz groundmass. D. BXK20108-1266m: Amygdaloidal Ca-Fe-(K)-rich assemblage in the footwall including subhedral coarse-grained actinolite and titanite ± anhedral fine-grained magnetite + coarse-grained euhedral biotite. Biotite appears to be secondary, overprinting the Ca-Fe assemblage. Amygdale surrounded by a very fine-grained feldspar ± quartz groundmass with very-fine grained magnetite dissemination. E. BXK20079-1314m: Amygdaloidal Ca-rich assemblage of the footwall including very-fine to medium grained subhedral to anhedral actinolite ± anhedral titanite. Amygdales surrounded by a very fine-grained feldspar ± quartz groundmass. F. BXK20091-336m: Ca-(K) vein from the footwall consisting of actinolite, titanite, apatite and biotite crosscutting the very fine-grained feldspar ± quartz groundmass. Red line in Fig 1A,C represents sinuous boundary between vein and side rock. Mineral abbreviations: actinolite = Act; albite = Ab; apatite = Ap; biotite = Bt; chlorite = Chl; epidote = Ep; feldspar = Fsp; magnetite = Mag; quartz = Qz; titanite = Ttn.

(II) In an outer zone, but still in the proximal region, magnetite crystallises together with actinolite and titanite (Figure 1A, C). A pervasive Na-rich alteration is present both in the

proximal and distal zones, albitising the very fine-grained groundmass of the rocks with varying intensities. Additionally, albite also occurs as halos around veins or as part of the veins and aggregates (Figure 1B).

Footwall: In the andesitic-trachyandesitic rocks the alteration types occur mostly in veins, as dissemination throughout the groundmass and as an amygdale infill. Overall, two alteration types are predominant in the footwall rocks. The first consists of actinolite ± titanite ± epidote. The second type involves magnetite – actinolite ± titanite. In this assemblage the magnetite occurs in varying concentration and can also form halos around veins or completely filling amygdales. Both alteration types can in some cases be accompanied by a halo of fine-grained albite around veins or amygdales.

Both hanging wall and footwall rocks display a dissemination of fine-grained magnetite associated with veins, aggregates, and in the groundmass. Biotite occurs in these rock units as either a replacement of actinolite (Figure 1F), or interstitially around minerals in vein assemblages (Figure 1C). Chlorite occurs predominantly as a replacement of biotite and/or actinolite (Figure 1A,B,D). In some samples, chloritisation seems to be limited to actinolite, whereas the biotite is generally unaffected (Figure 1D,F). From drill core observations the occurrence of biotite and chlorite is commonly associated with faults. Regarding the crystallisation of apatite, it is observed that it occurs not only as part of the Ca-rich assemblage (Figure 1F), but also as monomineralic veinlets.

5. Discussion

Preliminary microscopic observations show several distinct alteration assemblages, previously described macroscopically by Paolillo & Giapis (2021). The earliest alteration style appears to be of a pervasive sodic type, which has been also observed in other IOA/IOCG deposits (Corriveau et al., 2016; Barton, 2014). The main product of the sodic alteration in the Kiruna deposit is sodium-bearing feldspar, most likely albite, which occurs as very fine-grained crystals in the groundmass. Intensification of albitisation proximal to the mineralisation gives the rock a whitish colour. Despite this, the whole rock geochemistry from the selected drillholes, shows a homogeneous Na concentration throughout the side rocks (~4-9% Na_2O), with a slight increase in the footwall rocks compared to the hanging wall.

Adjacent to the sodic halo, at least three Ca-rich alteration assemblages can be distinguished. These are Ca ± Na, characterised by actinolite ± titanite ± epidote ± albite; Ca-Fe ± Na, containing actinolite – magnetite ± titanite ± albite; Ca ± Fe comprising anhydrite ± epidote ± garnet ± hematite ± actinolite; and a later Ca alteration consisting of monomineralic actinolite veins, which has been seen crosscutting all the other assemblages in the drill core. In the Ca ± Na and Ca-Fe ± Na assemblages the Na component can occur as fine-grained albite forming a halo around veins and amygdales filled by actinolite ± titanite ± magnetite. Geochemical data show that Ca has a higher variation in concentration (<1-10 wt% CaO), with the highest values closer to the mineralisation, suggesting that these Ca alteration assemblages might be related to the mineralisation. Currently, there is only macroscopic evidence of temporal relationship between the three Ca-rich alteration types based on vein-vein interactions in the drill core. Further studies in microscale on this matter are ongoing.

K-rich, moderate to high temperature alteration type, proximal to the mineralisation in IOCG/IOA deposits, has been described previously (Barton, 2014; Corriveau et al., 2016). In this variety, K-feldspar and/or biotite are typically associated with magnetite. Other minerals such as chlorite, titanite, actinolite, or epidote can also occur. In Kiruna, the dominant K phase is biotite, which is typically replacing actinolite or related to a later vein reactivation (Figure 1C,F), suggesting a later potassic event in relation to the calcic assemblage. Additionally, some

early biotite has been found in association with distal K-Fe alteration (biotite + magnetite) as described by Paolillo & Giapis (2021). In Figure 1A,B,D,F there is evidence of chloritisation, which can be the result of a retrograde alteration process, while in Figure 1D,F it is limited to the actinolite, suggesting that the biotite was formed later. These observations may indicate that at least two potassic (biotitic) events have occurred: (i) overprinting actinolite, potentially taking place after a chloritisation event; and (ii) in veins with magnetite (K-Fe). In the second case, biotite could be forming with the magnetite or reopening earlier Fe-rich veins. Further investigation is necessary to understand these events and their interactions with the Ca alteration types (e.g., is there a K-Ca alteration event or is biotite only formed as a replacement?).

The apatite occurs primarily in veins, both in association with other calcic minerals, and on its own, which has been also observed macroscopically. It is important to highlight that apatite was found in samples close to the mineralisation, which based on chemistry is enriched in phosphorus. The occurrence of apatite together with actinolite, titanite and occasionally magnetite might suggest that apatite is part of the Ca-Fe ± Na and Ca ± Na assemblages, which is in agreement with observations at other IOA deposits (Corriveau et al., 2016).

6. Conclusion

This study provides a closer look at the proximal alteration assemblages Ca-Fe ± Na, Ca ± Fe and Ca ± Na. Sodic alteration is predominantly pervasive and seems to be the earliest ingress of fluids. Veins and amygdales are typically composed of actinolite, magnetite, titanite, and epidote, with minor apatite and occasionally albite halos. These halos are more commonly found in the footwall rocks (55-60 wt% SiO_2), which are intermediate in composition compared to the felsic hanging wall rocks (65-70 wt% SiO_2). In relation to the proximal assemblages, biotite and chlorite occur mostly as replacement of actinolite. Additionally, the results have shown the potential occurrence of multi episodic, Ca-rich (with crosscutting relationship between several actinolite generations observed macroscopically) and K-rich fluid influxes in the system. Further studies in the transition between Ca-rich and K-rich alteration assemblages are needed to better understand the overprinting relationship between these hydrothermal events.

References:

Andersson, J.B., Bauer, T.E., Martinsson, O., 2021. Structural Evolution of the Central Kiruna Area, Northern Norrbotten, Sweden: Implications on the Geologic Setting Generating Iron Oxide-Apatite and Epigenetic Iron and Copper Sulfides. Economic Geology, 116 (8), pp. 1981-2009.

Barton, M.D., 2014. Iron oxide(-Cu-Au-REE-P-Ag-U-Co) systems. In: Treatise on Geochemistry. 2nd edition, Elsevier, v. 11, pp. 515-541

Corriveau, L., Montreuil, J.-F., Potter, E.G., 2016. Alteration Facies Linkages Among Iron Oxide Copper-Gold, Iron Oxide-Apatite, and Affiliated Deposits in the Great Bear Magmatic Zone, Northwest Territories, Canada. Economic Geology, 111 (8), pp. 2045-2072.

Hitzman, M.W., Oreskes, N., Einaudi, M.T., 1992. Geological characteristics and tectonic setting of Proterozoic iron-oxide (Cu-U-Au-REE) deposits: Precambrian Research, v. 58, pp. 241-287.

Paolillo, L., Giapis, C., 2021. A preliminary assessment of hydrothermal alterations in the giant Kiruna IOA deposit, Kiruna, Sweden. In: Lithosphere 2021 - Eleventh symposium on structure, composition and evolution of the lithosphere. Programme and Extended Abstracts, January 19-20, 2021 pp. 107-110.

Parák, T., 1975. Kiruna iron ores are not “intrusive magmatic ores of the Kiruna type”: Economic Geology and the Bulletin of the Society of Economic Geologists, v. 70, pp. 1242–1258.

Troll, V.R., Weis, F.A., Jonsson, E., Andersson, U.B., Majidi, S.A., Högdahl, K., Harris, C., Millet, M.A., Chinnasamy, S.S., Kooijman, E., Nilsson, K.P., 2019. Global Fe–O isotope correlation reveals magmatic origin of Kiruna-type apatite-iron-oxide ores. Nature Communications, 10 (1), pp.1-12.

Westhues, A., Hanchar, J. M., LeMessurier, M. J., Whitehouse, M. J., 2017. Evidence for hydrothermal alteration and source regions for the Kiruna iron oxide–apatite ore (northern Sweden) from zircon Hf and O isotopes. Geology, 45 (6), pp. 571-574.

Distributed acoustic sensing walkaway vertical seismic profiling in Koillismaa deep drillhole

M. Malinowski[1], B. Brodic[1], I. Martinkauppi[2], E. Koskela[1] and V. Laakso[1]

[1]Geological Survey of Finland, Espoo
[2]Geological Survey of Finland, Kokkola
E-mail: michal.malinowski@gtk.fi

In this article we present some initial results of a multi-offset vertical seismic profiling performed using fibre-optic distributed acoustic sensing (DAS) in the Koillismaa deep drillhole.

Keywords: vertical seismic profile, distributed acoustic sensing, Koillismaa

1. Introduction

Distributed acoustic sensing (DAS) is a relatively new tool in several geophysical applications (see recent overview by Li et al., 2022 and Willis, 2022). It allows recording of seismic signals along tens of kilometers along the fiber optic cables based on the principle of light backscattering. Most of the DAS applications so far focused on downhole measurements, especially vertical seismic profiles (VSP). DAS VSP measurements were already performed in hardrock / mining environment including fiber optic cables freely hanging in a water-filled drillhole (Riedel at al., 2018) or cemented in the boreholes (Bellefleur et al., 2020), indicating feasibility of DAS acquisition in such conditions. Here we report some initial results of the pilot multi-offset (walkaway) DAS VSP measurements carried out at the Koillismaa deep drillhole.

2. Data acquisition

Koillismaa deep borehole was drilled in Kuusamo area as a part of the Geological Survey of Finland project devoted to studying the Koillismaa Layered Intrusion Complex (Karinen, 2010). The borehole reached maximum depth of 1700 m, but due to numerous fracture zones was open for wireline logging down to ca. 1045 m depth. The 76-mm diameter borehole is deviated, with a mean inclination of 15 degrees, cased to ca. 240 m depth and water filled.

VSP measurements were performed in the beginning of September 2022. We used fiber optic cable manufactured by Solifos (BRUsens DTS) armoured with stainless steel loose tube. The cable hosts 2 multi-mode and 2 single-mode optical fibers. The cable was deployed using a dummy and reached maximum depth of ca. 1140 m. After some testing, it was concluded that a cable under tension is providing a better signal-to-noise ratio. For the actual DAS measurements, we used an ASN OptoDAS interrogator provided by NORSAR. During the acquisition we tested different gauge lengths (GL) (5, 10, 15 m) with different energy sources (Vibroseis and dynamite) and finally used 10 m GL for the dynamite shots and 15 m GL for Vibroseis. DAS channel spacing was set to 1 m. For dynamite shot points a small charge (240 g) at 2 m depth was used. Vibroseis acquisition was made with Failling Y-2400 Vibrator mounted on Mark IV buggy (provided by Geopartner Geofizyka). We used 20-s long sweeps from 20 to 160 Hz (+1dB per octave), repeated 6 times at given shotpoint. The shotpoints were distributed along available forest paths (with 50 m spacing) providing surface offsets up to 2.5 km from the borehole. During the acquisition, we noted that the maximum distance at which we observe seismic signal was ca. 1.5 km. In the end, we recorded about 90 sources with clear seismic energy (Figure1).

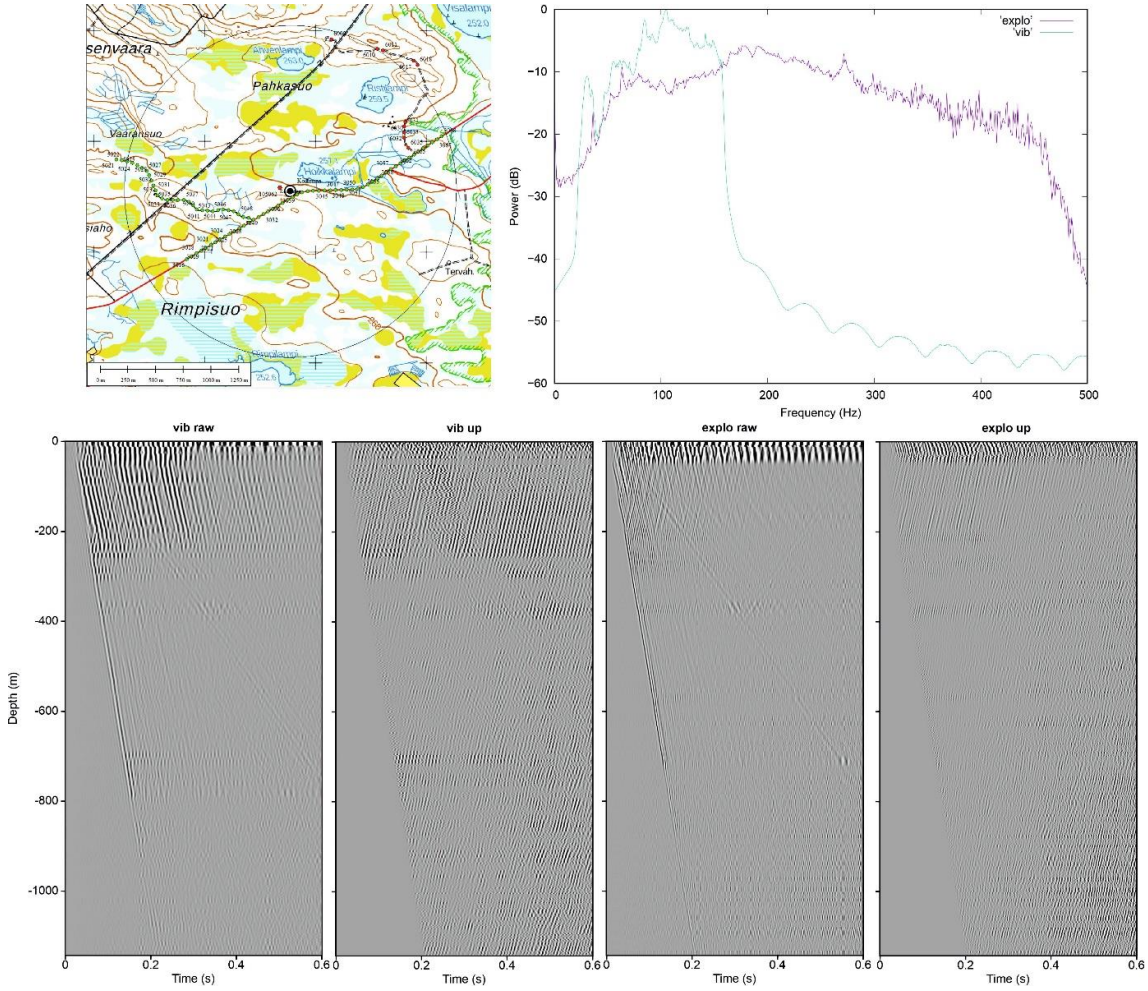

Figure 1. Acquisition layout for the VSP measurements at the Koillismaa borehole. Amplitude power spectra of the zero-offset Vibroseis ('vib') and dynamite records ('explo'). Raw and processed DAS shot gathers recorded in the Koillismaa borehole from zero-offset Vibroseis and dynamite sources. Upgoing wavefield ('up') was separated by median filtering, followed by bandpass filtering of 82-86-200-250 Hz.

3. Initial results

Figure 1 compares zero-offset VSP records from a Vibroseis (single sweep) and a dynamite source. The data in the display were converted from strain rate to velocity by integration along the channels and scaled. Frequency spectra indicate a very broadband response for the dynamite shot, while the Vibroseis record is limited to the selected sweep bandwidth but shows higher amplitudes signal then dynamite. We can follow the downgoing P-wave energy down to maximum cable depth (1142 m), however the pulse gets strongly attenuated beyond ca. 800 m depth. We observe also the downgoing S-wave energy, as well as the tube waves inside the cased part of the borehole. Deeper parts are also masked by optical noise of the DAS system. The upgoing part of the wavefield (obtained by median filtering), contains some distinct reflected arrivals along the cable length. Figure 2 shows a comparison of logging based acoustic impedance plot with the two-way-time shifted upgoing wavefield from the same dynamite shot

as in Figure 1. We can note the correlation of the reflections marked R1-R4 with the distinct lithology and rock property change: R1 at a major fault/fracture zone at

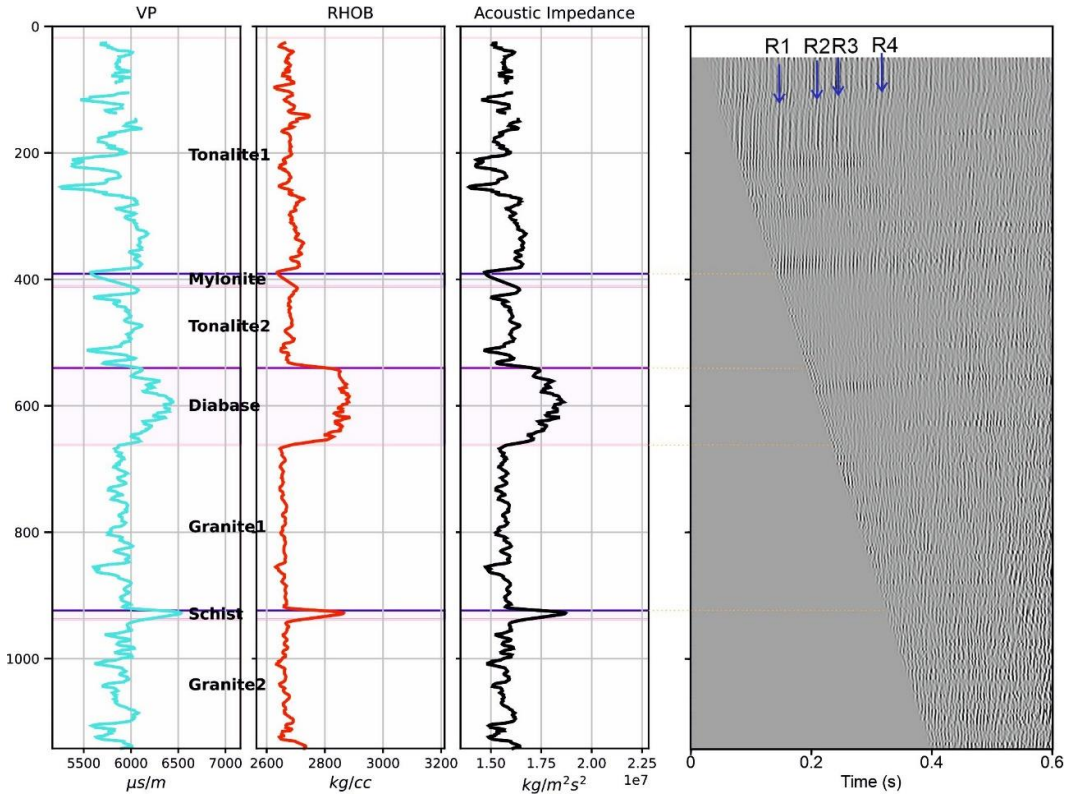

Figure 2. P-wave velocities and densities from the laboratory measurements on the core samples (Heinonen et al., 2022) and processed zero-offset VSP section from a dynamite shotpoint (shifted to a two-way time).

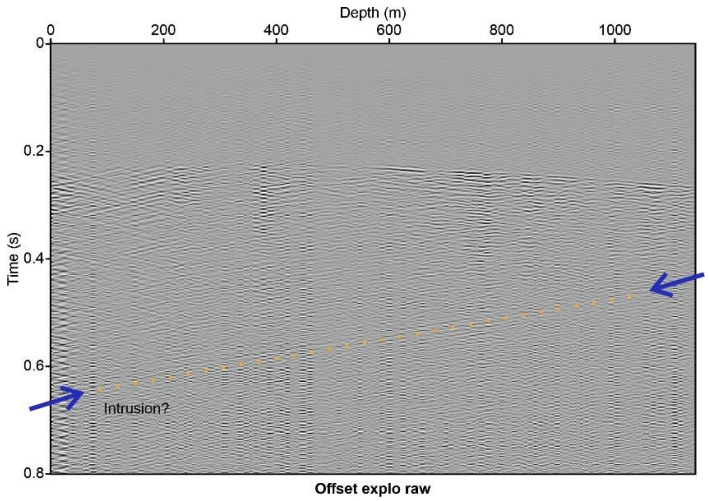

Figure 3. Raw VSP record from an offset (1.2 km distance from the collar) dynamite shotpoint. There is a clear deeper reflector (projected depth is ca. 1600 m, which corresponds to a granodiorite – peridotite contact).

400 m (mylonite), R2 and R3 at the top and bottom of a diabase dyke (550-650 m), R4 at schist (altered diabase) at ca. 900 m. Deeper reflectors, beyond the extend of the cable (especially from the mafic intrusion, i.e. beyond 1400 m) are harder to be identified. However, some offset shot points contain deeper reflectors (see example in Figure 3).

3. Conclusions

A pilot multi-offset VSP survey was performed in the Koillismaa borehole using the DAS technology. The initial processing results suggest the ability to image reflectors originating at the impedance contrasts along the maximum cable depth (1142 m). Reflectors from below (from the mafic intrusion) are more difficult to be identified in the raw records. Maximum distance at which the seismic energy propagated to the borehole was ca. 1.5 km. It was also clear that despite the strongly reduced frequency bandwidth (20-160 Hz), the Vibroseis source provided much cleaner records than the small explosive charges. On the other hand, the dynamite shots yield a very broadband frequency response.

Acknowledgements

Special thanks to A. Wuestefeld and S. Stokkan (NORSAR) for providing us with the DAS interrogator and technical assistance during data acquisition. Thanks to Geopartner Geofizyka for the efficient source operations. Open-source software packages (*welly*, *wellpathpy*, *lasio* as well as *Seismic Unix*) are also acknowledged.

References:

Bellefleur, G., Schetselaar, E., Wade, D., White, D., Enkin, R., Schmitt, D.R., 2020. Vertical seismic profiling using distributed acoustic sensing with scatter-enhanced fibre-optic cable at the Cu–Au New Afton porphyry deposit, British Columbia, Canada. Geophysical Prospecting, 68, 313-333.

Heinonen, S., Nousiainen, M., Karinen, T. and Häkkinen, T., 2022, Are Seismic P-Wave Velocities Capable of Revealing The Deep-Seated Prospective Intrusion? In NSG2022 4th Conference on Geophysics for Mineral Exploration and Mining, pp. 1-5.

Karinen, T.,2010. The Koillismaa Intrusion, northeastern Finland - evidence for PGE reef forming processes in the layered series. Geological Survey of Finland, Bulletin, 404, 176 p.

Li, Y., Karrenbach, M., Ajo-Franklin, J., (Eds.) 2022. Distributed acoustic sensing in geophysics: Methods and applications. John Wiley & Sons.

Riedel, M., Cosma, C., Enescu, N., Koivisto, E., Komminaho, K., Vaittinen, K., Malinowski, M., 2018. Underground vertical seismic profiling with conventional and fiber-optic systems for exploration in the Kylylahti Polymetallic Mine, Eastern Finland. Minerals, 8, 538 p.

Willis, M.E., 2022. Distributed Acoustic Sensing for Seismic Measurements–What Geophysicists and Engineers Need to Know. Society of Exploration Geophysicists.

Exploring East European Craton crust in Poland using state-of-the-art deep reflection seismic profiling [INVITED]

M. Malinowski[1,2], S. Mazur[3] and M. Mężyk[4]

[1]Geological Survey of Finland, Espoo
[2]Institute of Geophysics PAS, Warsaw
[3]Institute of Geological Sciences PAS, Krakow
[4]formerly at Institute of Geophysics PAS, Warsaw
E-mail: michal.malinowski@gtk.fi

In this article we summarize some key findings of the PolandSPAN™ regional seismic survey based on the recent reprocessing work focused on crustal-scale imaging.

Keywords: East European Craton, Fennoscandia, Sarmatia, deep reflection seismics, crustal structure

1. Introduction

The beginning of the second decade of the 21st century has revolutionized the study of the deep structure of the Earth's crust in Poland. Intensification of shale gas exploration indirectly contributed to the acquisition of the first regional deep reflection seismic profiles in Poland including ION Geophysical PolandSPAN™ project. It comprises a net of 10 regional seismic profiles with a total length of about 2,200 km. Although these profiles were mainly aimed at the regional characterization of the lower Palaeozoic shale basins developed along the margin of the East European Craton (EEC), the measured data enable imaging of the whole crust through the application of the extended correlation method and recent reprocessing efforts. After the FIRE project (Kukkonen and Lahtinen, 2006), PolandSPAN™ is probably the second largest onshore deep reflection seismic program targeting Fennoscandian-affinity crust. The notable difference between the two, beside the acquisition parameters, is that the EEC crust in Poland is concealed under a thick Phanerozoic platform cover and is penetrated by sparse, deep research wells. In this paper, we summarize recent findings from the reprocessed crustal-scale sections of the PolandSPAN™ project.

2. Geological background

According to Bogdanova et al. (1996), the EEC was formed as a result of Paleoproterozic successive amalgamation of three crustal segments i.e., Fennoscandia, Sarmatia and Volgo-Uralia. Each of the segments is characterised by differences in crustal structure, lithology, and age of crust-forming processes spanning from the Archaean to the Paleoproterozoic. The crystalline basement of the EEC in Poland belongs to the SW Fennoscandia and the adjacent NW Sarmatia (Figure 1). The junction between these two amalgamated segments begins in Poland (Figure 1), where the marginal part of the EEC is bounded to the SW by the TTZ, a tectonic zone separating thinner crust underlying the West European Palaeozoic Platform from the thick crust of the EEC (e.g., Guterch and Grad, 2006).

3. Seismic data

The PolandSPAN™ project employed state-of-the-art acquisition parameters that were primarily optimized to provide a continuous image of the lower Palaeozoic shale basins. Table

1 compares PolandSPAN™ acquisition parameters with FIRE (Kukkonen and Lahtinen, 2006) and Metal Earth (Naghizadeh et al., 2019) seismic programs. ION Geophysical original time and depth imaging were focused on the sedimentary cover. The nominal record length of 12 s enabled imaging down to the lower crust on average. Mężyk et al. (2019, 2021) reprocessed the whole survey using extended correlation method, obtaining a record length of ~20 s. Processing followed typical steps used in deep reflection seismics with a lot of emphasis on signal coherency enhancement. Mężyk and Malinowski (2021) and Mężyk et al. (2021) introduced a novel approach of automatic classification of crustal reflectivity patterns based on seismic attributes and unsupervised clustering. The replacement of amplitudes in the seismic section with the supercluster's membership number allows to highlight the crustal-scale reflection distributions and aids seismic interpretation.

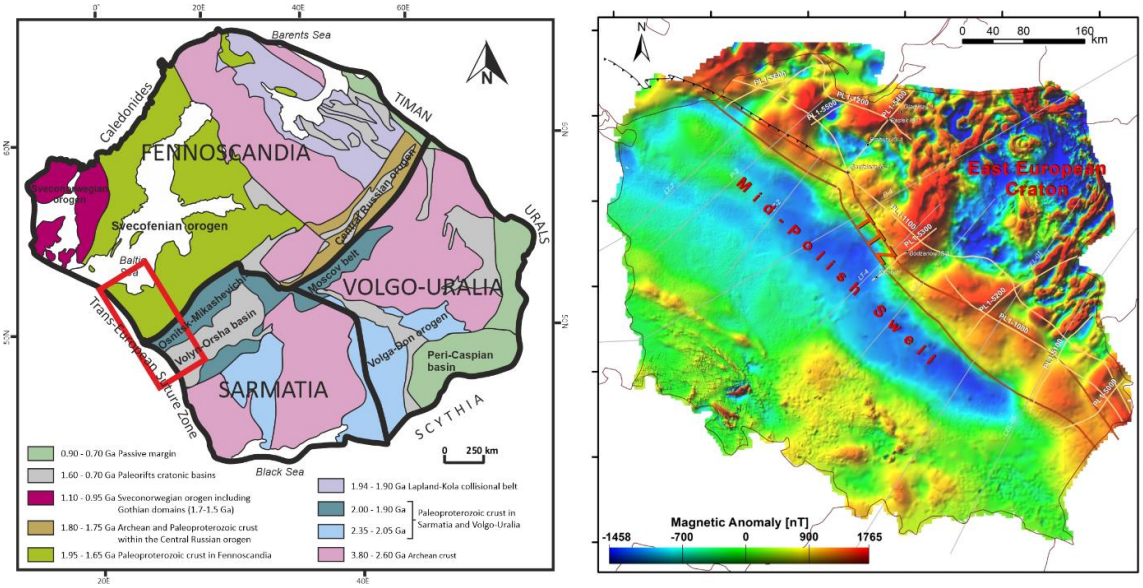

Figure 1. Precambrian units the EEC (left). The red rectangle shows the study area. Modified from Mezyk et al. (2021). Location of PolandSPAN™ survey (yellow lines) on the background of the reduced-to-pole magnetic anomaly map (compiled by S. Mazur) (right).

4. Interpretation highlights

Mężyk et al. (2019) presented interpretation of PolandSPAN™ data from northern Poland. We found reflectivity patterns that we primarily associate with Paleoproterozoic crustal formation during the Svekofennian orogeny and that are similar to those observed along the BABEL and FIRE profiles in the Baltic Sea and onshore Finland, respectively (Korja and Heikkinen, 2005; Torvela et al., 2013). We suggest that a seismic-scale S–C′ fabric of the Paleoproterozoic crust (Figure 2) was shaped by mid- to lower-crustal flow in a convergent setting during the Svekofennian orogeny. Crustal fabric observed in the vicinity of the Mesoproterozoic AMCG suites in NE Poland supports their emplacement due to the delamination of the thickened Svecofennian lithosphere and resulting asthenospheric ascent, partial melting of the lithospheric mantle, and ponding of gabbroic melt at the crust–mantle interface. Mężyk et al. (2021) focused on the central and southern segment of the EEC in Poland – at the junction between Fennoscandia and Sarmatia. Following the model of Bogdanova et al. (2015), we propose that the Paleoproterozoic collision between Sarmatia and Fennoscandia led to the formation of a cryptic and diffuse crustal suture represented by a c. 150 km wide deformation zone.

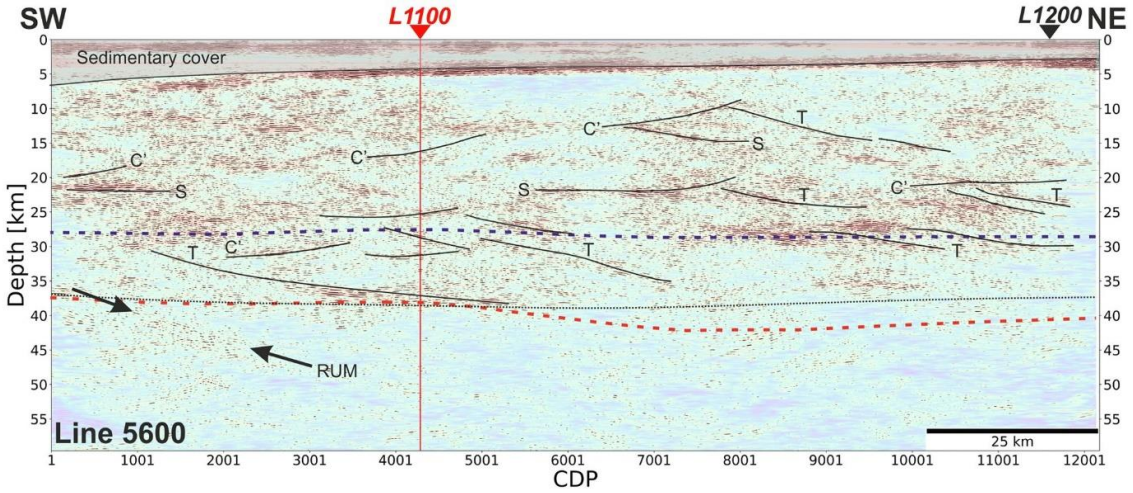

Figure 2. Final migrated depth-converted sections along PolandSPAN™ profile 5600. S – subhorizontal structural layering (Svekofennian orogenic fabric); T – ductile thrust shear zones; C′ – extensional shear zones. After Mężyk et al. (2019).

Table 1. Comparison of PolandSPAN™ acquisition parameters with FIRE and MetalEarth regional seismic programmes.

	PolandSPAN™	**FIRE**	**MetalEarth R1**
Vibroseis unit	INOVA AHV-IV, 32 t	Geosvip, 15.4 t	INOVA AHV-IV, 32 t
Number of Vibrators	4	5	4
Sweep parameters	2-150 Hz, 16 s	12-80 Hz, 30 s	2-96 Hz, 28 s
Number of sweeps / VP	2	8	4
Source interval	25 m	100 m	50 m
Receiver interval	25 m	50 m	25 m
Nominal active channels	960	362	1200
Maximum offset	12 000 m	9 000 m	15 000 m
Nominal fold	480	90	300
Number of geophone per channel	12	12	1
Geophone frequency	10 Hz	10 Hz	5 Hz
Recoding system	Wireless, Geospace GSR	Cabled, I/O System II	Wireless, Geospace GSR

5. Conclusions

High-end acquisition parameters of the PolandSPAN™ survey coupled with the dedicated reprocessing workflow allowed to image the whole crust in the marginal zone of the EEC in Poland. Until recently, this area was covered only by the wide-angle reflection and refraction profiles, which depicted a relatively simple crustal structure with a typical three-layer cratonic crust. PolandSPAN™ data revealed a wealth of different reflectivity patterns, which were attributed e.g., to the Svekofennian orogeny or collisional suture between Sarmatia and Fennoscandia.

6. Acknowledgements

This study was funded by the Polish National Science Centre grant no UMO-2015/19/B/ST10/01612.We are indebted to ION Geophysical for permission to use and show PolandSPAN™ data.

References:

Bogdanova, S., Gorbatschev, R., Skridlaite, G., Soesoo, A., Taran, L. and Kurlovich, D., 2015. Trans-Baltic Palaeoproterozoic correlations towards the reconstruction of supercontinent Columbia/Nuna. Precambrian Research, 259, 5-33.

Bogdanova, S., Pashkevich, I.K., Gorbatschev, R. and Orlyuk, M.I., 1996. Riphean rifting and major Palaeoproterozoic crustal boundaries in the basement of the East European Craton: geology and geophysics. Tectonophysics, 268, 1-21.

Guterch, A., Grad, M., 2006. Lithospheric structure of the TESZ in Poland based on modern seismic experiments. Geological Quarterly, 50, 23-32.

Korja, A., Heikkinen, P., 2005. The accretionary Svecofennian orogen—insight from the BABEL profiles. Precambrian Research, 136, 241-268.

Kukkonen, I.T., Lahtinen, R., 2006 (Eds.). Finnish reflection experiment FIRE 2001-2005. Geological Survey of Finland, Special Papers, vol 43.

Mężyk, M., Malinowski, M., Mazur, S., 2021. Structure of a diffuse suture between Fennoscandia and Sarmatia in SE Poland based on interpretation of regional reflection seismic profiles supported by unsupervised clustering. Precambrian Research, 358, 106176.

Mężyk, M., Malinowski, M., 2021, Deep Embedded Clustering As a Seismic Attribute: A Case Study of 2D Crustal-Scale Interpretation. In 82nd EAGE Annual Conference & Exhibition, pp.1-5.

Mężyk, M., Malinowski, M., Mazur, S., 2019. Imaging the East European Craton margin in northern Poland using extended correlation processing of regional seismic reflection profiles. Solid Earth, 10, 683-696.

Naghizadeh, M., Snyder, D., Cheraghi, S., Foster, S., Cilensek, S., Floreani, E., Mackie, J., 2019. Acquisition and processing of wider bandwidth seismic data in crystalline crust: Progress with the Metal Earth project. Minerals, 9, 145.

Torvela, T., Moreau, J., Butler, R.W., Korja, A., Heikkinen, P., 2013. The mode of deformation in the orogenic mid-crust revealed by seismic attribute analysis. Geochem. Geophys, Geosys, 14, 1069-1086.

Lithological units and geological evolution of Outokumpu allochthon's western parts, update based on recent studies

P. Mikkola[1], J. Jäsberg[1], J. Luukas[1] and M. Kurhila[2]

[1]Geological Survey of Finland, P.O. Box 1237, 70211 Kuopio, Finland
[2] Geological Survey of Finland, P.O. Box 96, 02151 Espoo, Finland
E-mail: perttu.mikkola@gtk.fi

In this article we provide a summary of results from a recent research project by Geological Survey of Finland studying the lithological units and geological evolution of Outokumpu allochthon's western parts. A brief summary of the major rock units and structural interpretation is made.

Keywords: paragneiss, granitoids, granites, structural geology, thrust faults, shear zones, modelling, zircon, Archaean, Palaeoproterozoic, Outokumpu Area, Finland

1. Introduction

Our study area is located in Central Finland in an area interpreted as the western boundary of the Outokumpu allochthon, which hosts, in addition to voluminous paragneisses, the highly ore potential rocks of the Outokumpu assemblage. The area also includes the south-westernmost known exposures of Archaean crust in Finland and its southwest corner is transected by the Raahe-Ladoga suture zone. Geological Survey of Finland has recently completed a four year project in the area and this abstract and presentation aims to provide a brief summary of the key findings by Mikkola et al. (2022).

2. Archaean rocks

In addition to the southern parts of the Kuopio complex, the Archaean rocks are present in the study area as variably sized domes and thrust sheets (Figure 1). Porphyritic granodiorites interpreted as belonging to the sanukitoid suite (high Ba, K2O, Mg#, Cr, Ni) are relatively abundant within the Kuopio complex, where also small amounts of quartz diorites are present. The domes and thrust sheets are dominated by rocks belonging to the Tonalite–Trondhjemite–Granodiorite suite (TTG).

Due to significant lead loss during the Svecofennian orogeny, most of the ages obtained from Archaean samples are poorly constrained, but interpreted crystallisation ages for TTGs vary between 2.8 and 2.7 Ga, whereas sanukitoids and quartz diorites likely crystallised close to 2.7 Ga. Together the chemical and age data support the interpretation that the domes and thrust sheets are continuations of the Kuopio complex and not exotic terranes accreted during the Svecofennian orogeny.

3. Karelia supergroup

Rocks of the Karelia supergroup deposited during the prolonged rifting period on top of the the Archaean rocks are variably preserved. When preserved, the succession displays the characteristic change from conglomerates to sandier sediments and onwards to carbonate rocks followed by typically pillow-structured mafic volcanic rocks. A new addition to the stratigraphic sequence are the arkosites locally overlaying the volcanic units and grading into the more typical paragneisses, which were deposited originally as turbidites. Largest change to regional interpretations is that the autochthonous paragneisses occupy significantly smaller areas than previously thought.

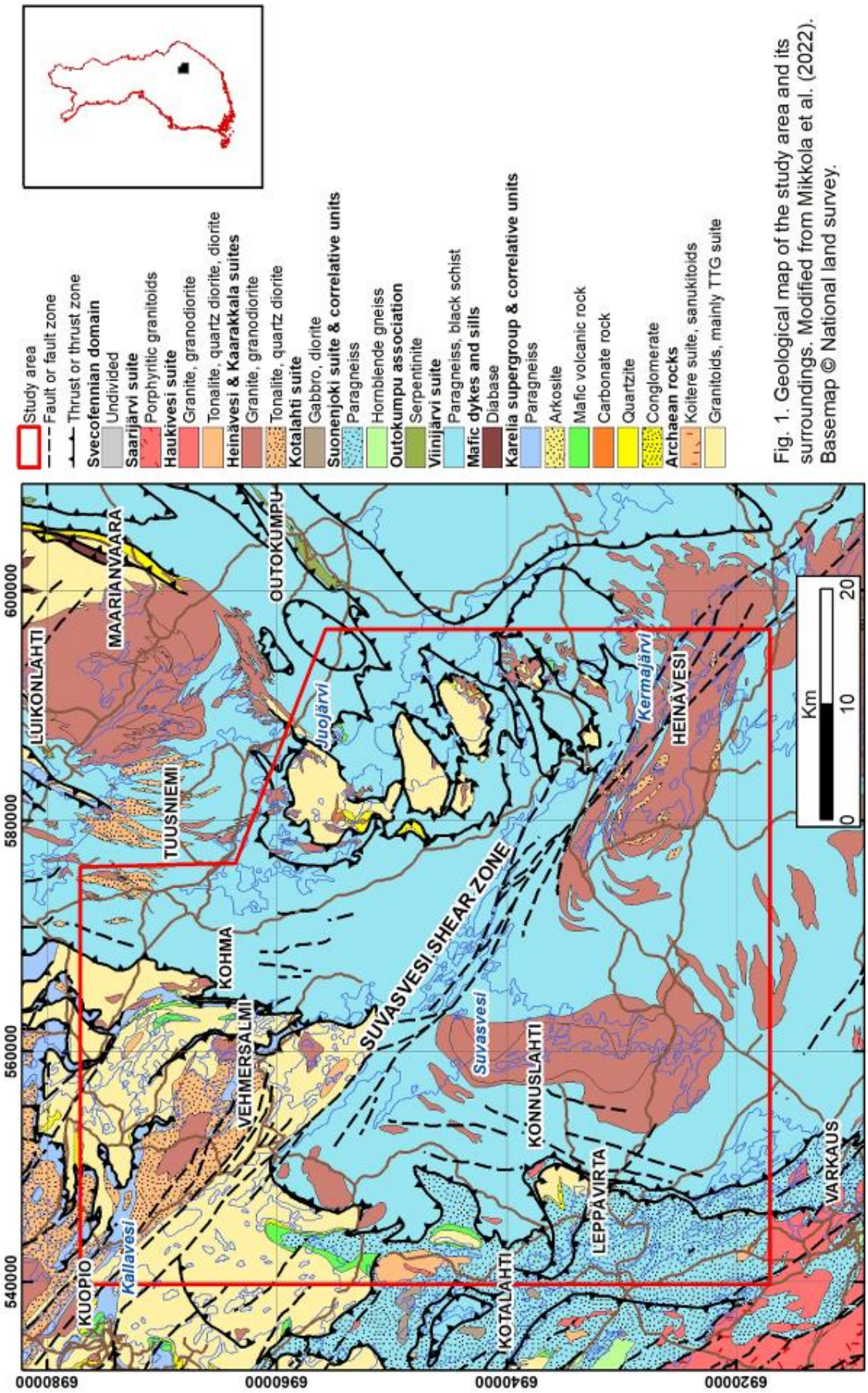

Fig. 1. Geological map of the study area and its surroundings. Modified from Mikkola et al. (2022). Basemap © National land survey.

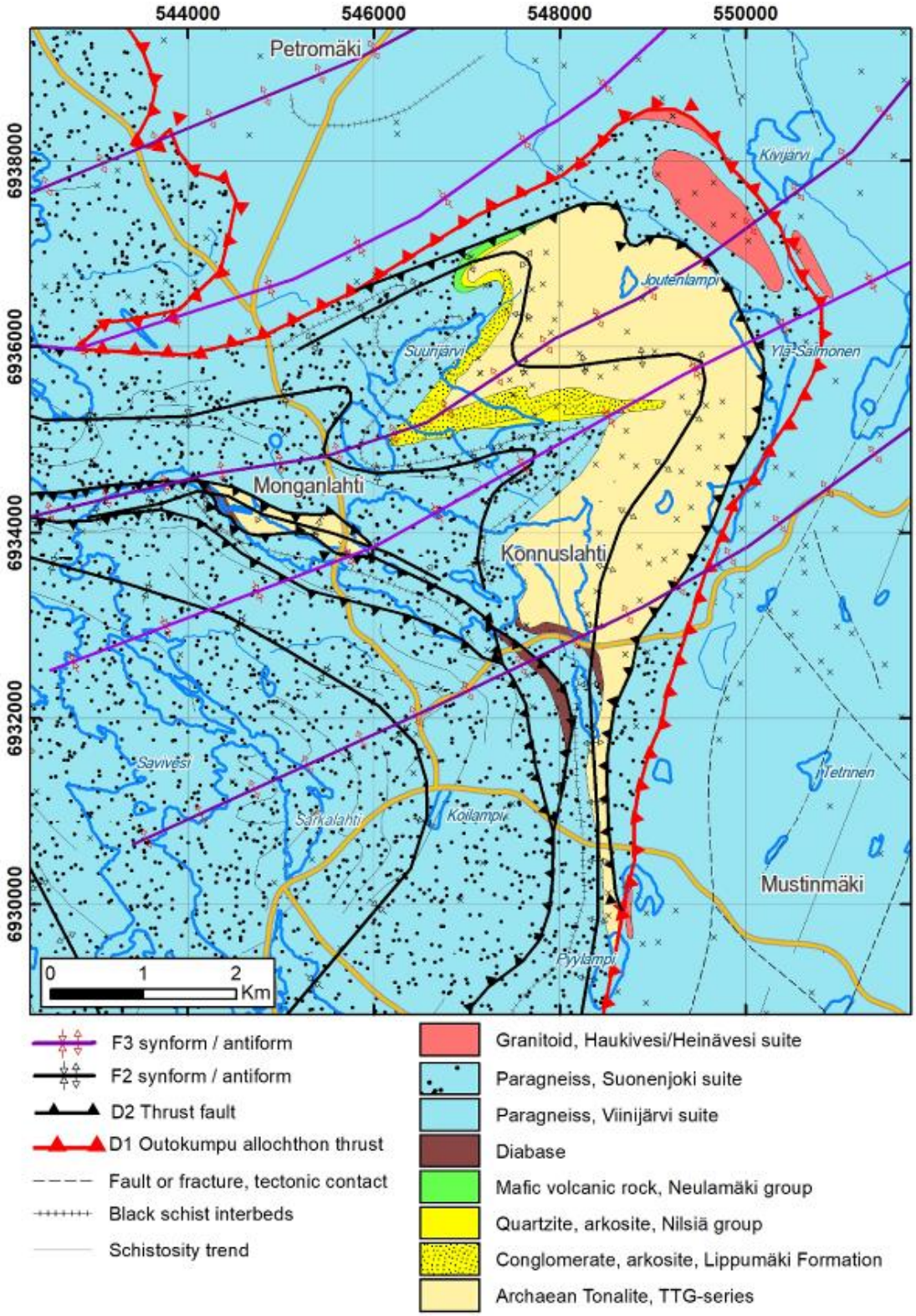

Figure 2. Bedrock map of the Konnuslahti dome and its immediate surroundings with interpreted D1, D2 and D3 structures. For location see Figure 1. Map modified from Mikkola et al. (2022). Basemap © National Land Survey.

4. Paragneisses of the Viinijärvi and Suonenjoki suites

The voluminous paragneisses in the study area represent two major allochthonous units, Viinijärvi and Suonenjoki suites. The Viinijärvi suite in the east, together with the ore potential Outokumpu assemblage forms the Outokumpu allochthon. Western part of the study area is dominated by the Suonenjoki suite.

Apart from slightly more pelitic composition of the Suonenjoki suite, the two units do not differ significantly. Both have similar detrital zircon populations, yielding maximum deposition ages of 1.92–1.91 Ga. Thus, in our opinion the current interpreted boundary between these units reflects a post-depositional structure and not differences in depositional basins or the source material of the paragneisses.

4. Outokumpu assemblage

Due to extensive exploration activity numerous small occurrences of Outokumpu assemblage rocks were known north of the Suvasvesi shear zone. South of the shear zone, only few small occurrences were known, which had not been studied in detail. The new data confirms that they are true members of the Outokumpu assemblage associated with specific structural features. This strict spatial association limits the potential for new Outokumpu-type deposits southwest of the Suvasvesi shear zone.

5. Granitoids

Granitoids with ages around 1.87 Ga have been divided into Heinävesi, Kaarakkala and Haukivesi suites based on the unit(s) they are intruding. The units however do not display significant compositional differences. They are variably voluminous in the study area, and can be found from nearly any larger outcrop as veins. Larger intrusions (e.g. Suvasvesi granite) have been formed in structurally favourable locations. Variable deformation of the veins indicate intrusion during regional D3 and after it. The more thoroughly studied Heinävesi suite is defined by its compositional characteristics, mainly felsic I-type with locally more mafic compositions, indicating some input also from the mantle (Rantanen, 2021).

5. Structural evolution

Our structural interpretation is based on four major deformation phases. The first (~1.92 Ga) was caused by collision of Archaean blocks and resulted in thin-skinned thrusting characterizing the Outokumpu allochthon. The second deformation phase (~1.91 Ga) was a response to collision of the Savo arc from west and resulted in thick skinned thrusting and folding of both, the Archaean basement and autochthonous cover rocks. The third deformation phase (~1.90–1.87 Ga) was caused by accretion of the Bergslagen microcontinent from the south and, in addition to folding (Figure 2), the major SE-NW-trending dextral shears, e.g. Suvasvesi shear zone, and their conjugates developed. The fourth deformation phase (1.84–1.80 Ga) is only observable as continued activity along the shear zones.

References:

Mikkola, P., Aatos, S., Halkoaho, T., Heinonen, S., Hietava, J., Hietala, S, Kurhila, M., Jäsberg, J., Laine, E.-L., Luukas, J., Niskanen, M., Nousiainen, M., Nygård, H., Piispanen, A., Pirinen, H., Rantanen, H., Romu, I., 2022. Geological evolution and structure along the western boundary of the Outokumpu allochthon. Geological Survey of Finland, GTK Open File Research Report, 23/2022. 117 pages, 7 appendices. Available at: https://tupa.gtk.fi/raportti/arkisto/23_2022.pdf

Rantanen, H., 2021. Mineralogy, Petrology, and Petrogenesis of the Suvasvesi Granitoid Intrusion. University of Helsinki, Department of Geosciences and Geography. Unpublished master thesis, 77 pages. Available at: https://tupa.gtk.fi/opinnayte/rantanen_hanna_gradu.pdf

Petrophysics of the Koillismaa drill hole

M. Nousiainen[1] S. Heinonen[2] and T. Karinen[3]

[1] Geological Survey of Finland, Viestikatu 7 A, PL 1237,70211 KUOPIO
[2] Geological Survey of Finland, Vuorimiehentie 5, PL 96, 02151 ESPOO
[3] Geological Survey of Finland, Lähteentie 2, PL 77, 96101 ROVANIEMI
E-mail: maarit.nousiainen@gtk.fi

In this article we introduce petrophysical data of the Koillismaa drillhole. We use the data to estimate the feasibility to use different geophysical methods, including seismic reflection and EM methods, to delineate the potentially ore-hosting mafic-ultramafic rock formations in the research area. We also compare three different methods to measure seismic p wave velocity: laboratory data, sonic logging in the drillhole and using a handheld instrument. If successful, the handheld device would be a cost-efficient method to get approximate P-wave velocities from the drill core.

Keywords: Petrophysics, Koillismaa, P-wave velocity, conductivity, mafic intrusion

1. Introduction

Petrophysical data is essential for improving geophysical surveys from the planning stage to the interpretation, but physical rock properties are still often poorly known and understood. Physical properties of the main rock types within the area of interest are important for forward modelling aiming to optimize survey design, to define realistic processing and modeling parameters and to determine model reliability in the interpretation phase. Moreover, petrophysical properties, and especially their differences between various lithological units dictate the usability of a given geophysical method in the first place.

In the Koillismaa area in Finland, we have collected and studied petrophysical data sets available from a 1.7 km long drill hole. The hole was drilled by Geological Survey of Finland (GTK) in 2020 for research purposes (Karinen et al., 2021).

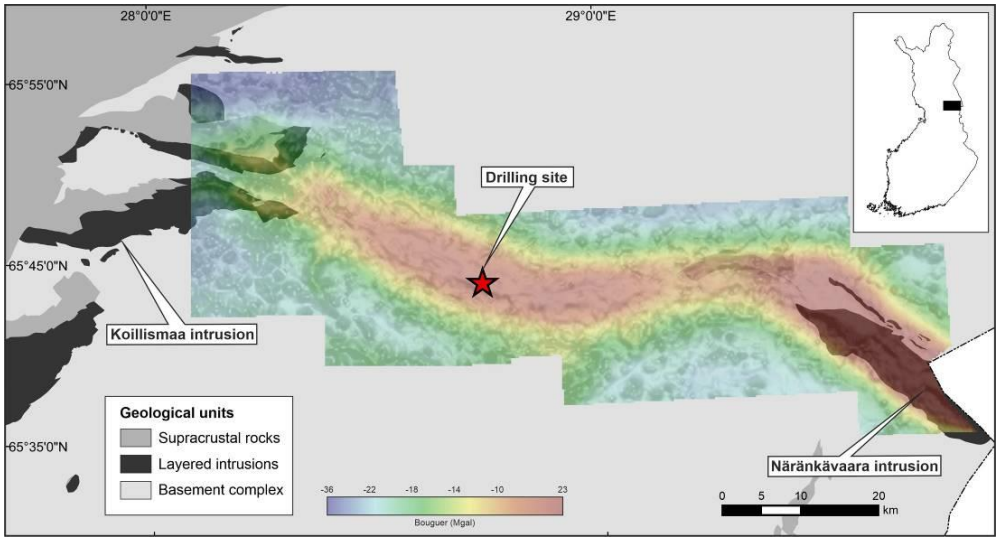

Figure 4: Location of the Koillismaa research site in Finland and a map showing the substantial gravity anomaly caused by the mafic-ultramafic layered igneous intrusion at depth.

2. Study area

The Koillismaa area (Figure 1) is considered potential for economic Ni-Cu-Co-PGE and Cr-V-Ti-Fe occurrences due to the bodies of mafic layered intrusions in the area. The intrusions comprise the Koillismaa-Näränkävaara layered igneous complex and the exposed layered intrusions are connected by a zone of high magnetic and gravimetric anomaly (Salmirinne and Iljina, 2003). Figure 1 shows that the bedrock at the surface of the diamond drilling site consists of homogenous orthogneisses and granitoids, but the gravity anomaly reveals a high-density body at depth. The drilling of a 1700 m long research hole in 2020 revealed mafic-ultramafic igneous rocks (gabbronorite, pyroxenite and peridotite), which likely are similar in their age as the exposed mafic-ultramafic layered igneous intrusions North-West and South-East from the drill site (Koillismaa and Näränkävaara intrusions, respectively).

3. Petrophysics

The samples for petrophysical studies were collected with approximately 1.5 meter intervals from the Koillismaa drill core. These selected samples were studied for their seismic P-wave velocity, density, magnetic susceptibility, remanent magnetization, inductive resistivity, and galvanic resistivity have been measured at the Geophysics Laboratory in GTK.

Figure 2 presents the p-wave velocities and densities of each rock type as a box and whisker chart. P-wave velocity and density of the samples are plotted in Figure 3 together with acoustic impedance isocurves. Salisbury et al. (1996) concluded massive sulfide ore bodies make strong seismic reflectors because of their high acoustic impedance compared to typical host rock sequence. The results from Koillismaa drill hole petrophysical measurements also support the seismic imaging of the mafic rocks hosting the possible ore formation. Especially pyroxenite shows high density and P-wave velocity values indicating that it as a lithological unit will be a strong reflector and can be used as a lead horizon when delineating the mafic intrusion. We can also see differences between the other most common rock types observed in the Koillismaa drill hole. The results confirm the usability of the seismic reflection methods in the study area.

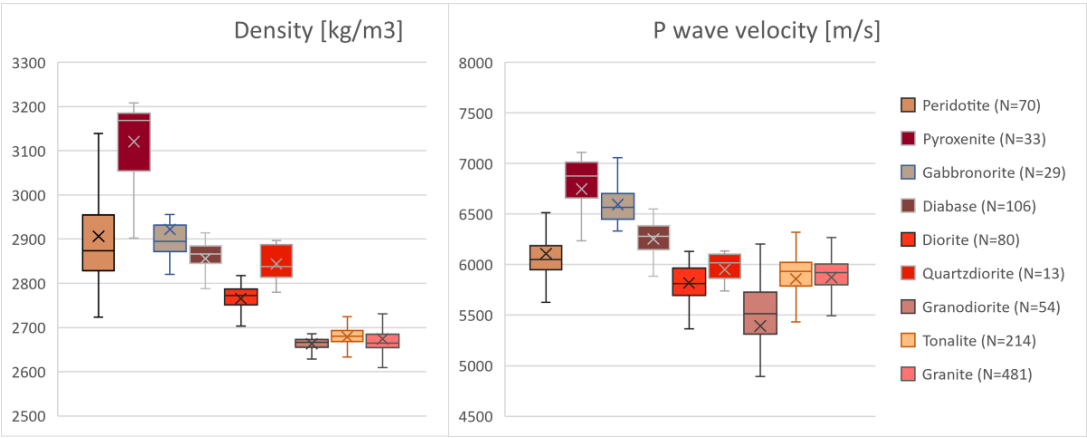

Figure 2. Comparing densities and p-wave velocities of different rock types in the drillhole. The boxes range from 1st to 3rd quartile of the data so 50 % of the data values are within the box. The whiskers extend up from the top of the box to the largest data element that is less than or equal to 1.5 times the interquartile range (IQR) and the same under the box. The interquartile range is defined as the distance between the 1st quartile and the 3rd quartile. Data points outside

the whiskers are not presented. The number of samples of each rock type is mentioned in the legend.

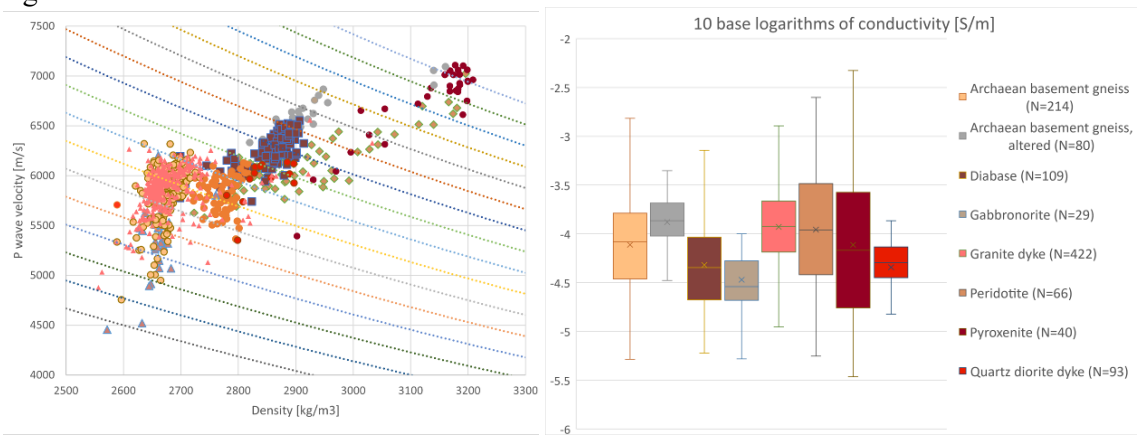

Figure 3. On the left: P-wave velocities and densities measured in the laboratory. Blue lines are isocurves corresponding to 6% difference in acoustic impedance. On the right: Conductivity of different rock types as 10-base logarithms. Refer to Figure 2 for explanation of the plot type.

In Figure 3 we display conductivities of the drill core samples. Resistivities were measured with GTK's in house built Mafrip instrument using wet electrodes. We measured the resistivity in three different frequencies: 0.1 Hz, 10 Hz and 500 Hz to be able to calculate IP values. Conductivities illustrated in Figure 3 are the inverses of the resistivity measured with the lowest frequency 0.1 Hz. Please note the lithological classification differs a bit from what is used with density and p-wave velocity data. We can see that in Koillismaa, the conductivity does not correlate with lithology as clearly as density and P-wave velocity. That is typical because for example porosity and fractures affect conductivity significantly.

4. Measuring seismic p wave velocities in three different ways

We measured seismic p-wave velocity with three different methods:

(1) laboratory measurements of the samples taken from the drill core
(2) from the drill core using ultrasonic handheld device
(3) by full waveform sonic logging in the drill hole.

The laboratory samples were taken on average on 1.5 m intervals and ultrasonic measurement on 1 m intervals while sonic logging data provides information about in situ seismic velocities with approximately 5 cm resolution.

In the drilling site, sonic logging started after casing in the depth of 200 m and finished at a major fracture zone at about the depth of 1045 m. The sonic logging was made with a four channel sonde. We selected to use p-wave velocity derived from the time difference of the first arrivals of the first two channels 20 cm apart from each other, thus results being comparable for the handheld ultrasonic device.

Inspection of median and average P-wave velocity derived for each rock type shows, that velocities measured in the laboratory are typically higher compared to the values determined with other methods. The average velocity for granite was 5910 m/s in the laboratory measurement whereas sonic logging indicated velocity of 5870 m/s. Sonic logging results are influenced by fracturing on the drill hole site while samples in the laboratory represent intact rock.

The handheld device used for P-wave velocity measurement is Surfer UK1401 which is originally planned for concrete inspection. The device requires intact core with minimum 15

cm length which is problematic where core is fractured. The device is also extremely sensitive to small fractures and cracks in the drill core as well as positioning of the tool, which is seen as low values and high variability of velocity. Each measurement point was repeated three times to achieve more reliable result. Velocities measured with ultrasonic device are approximately 85% lower than those determined with laboratory measurements.

5. Conclusions

The Koillismaa drill hole penetrates mafic-ultramafic rocks (gabbronorite, pyroxenite and peridotite) that have high density values. Based on this, the prominent gravity anomaly has been interpreted to reflect the location of a magma flow system between the two surface-exposed mafic-ultramafic intrusions in the research area. Petrophysical methods reveal that the mafic-ultramafic rocks have substantial contrast in terms of their acoustic properties in comparison to the granitic rocks above them. This contrast justifies the use of seismic methods to explore the assumed deep-seated magma flow system.

Comparison of seismic velocities derived with different methods suggest that seismic p-wave velocity is scale dependent. Handheld ultrasonic device is very sensitive for small fractures and position of the device, thus providing highly variable velocity log. In our work this device was hardly suitable for precise measurements but could be used to cost-efficiently achieve general understanding of relative velocities of different rock types. Sonic logging provides in situ velocities from the drill hole with high resolution but this method has disadvantage when drill hole is cased or inaccessible because of fracture zones blocking the hole.

Resistivities measured provide background information for planning electric and electromagnetic surveys. Compared to density and magnetic properties, resistivity is less controlled by the lithology and more by e.g. fractures and porosity.

More detailed analysis of the petrophysical properties will be performed in the SEEMS DEEP project, in which a comprehensive multicomponent seismic and electromagnetic data will be acquired in the Koillismaa region.

6. Acknowledgements

Special thanks to GTK's Koillismaa Deep Drill hole project which has acquired the data used in this research. SEEMS DEEP project is funded through ERA-MIN2 program and in Finland through Business Finland (project number 640/31/2022).

6. References

Karinen, T., Heinonen, S., Konnunaho, J., Salmirinne, H., Lahti, I., Salo, A., 2021. Koillismaa Deep Hole – solving the mystery of a geophysical anomaly. In: Kukkonen, I., Veikkolainen, T., Heinonen, S., Karell, F., Kozlovskaya, E., Luttinen, A., Nikkilä, K., Nykänen, V., Poutanen, M., Skyttä, P., Tanskanen, E., Tiira, T.:Lithosphere 2021 – Eleventh Symposium on the Structure, Composition and Evolution of the Lithosphere in Finland. Programme and Extended Abstracts, Virtual meeting, January 19-20, 2021. Institute of Seismology, University of Helsinki, Report S-71.

Salisbury, M.H., Milkereit, B., Bleeker, W., 1996. Seismic imaging of massive sulfide deposits; Part I, Rock properties. Economic Geology, 91 (5), 821–828.

Salmirinne, H. and Ilijina, M. 2003. Koillismaan kerrosintruusio-kompleksin tulokanavamuodostuman painovoimatulkinta ja alueen malmimahdollisuudet (osa 1). Geologian Tutkimuskeskus. Q 21/2003/1, 23 p. (in Finnish)

Brittle structural characterization of the Åland rapakivi

N. Ovaskainen[1], N. Nordbäck[1] and P. Skyttä[2]

[1] Geological Survey of Finland, FI-02151 ESPOO
[2] Department of Geography and Geology, FI-20014 University of Turku, Finland
E-mail: nikolas.ovaskainen@gtk.fi

This study explores the brittle structural record within the Mesoproterozoic Åland rapakivi batholith in SW Finland. Our approach included mapping of large-scale lineaments using topographic and aerogeophysical datasets and mapping of mesoscopic outcrop scale brittle structures (fractures, faults, and veins) utilising both field and photographic UAV (Unmanned Aerial Vehicle) based methods. We used UAV photogrammetric data and remotely mapped fracture datasets as a base for more detailed structural outcrop surveys including structural classifications, orientation, kinematic fault slip indicators and relative age relationships. Paleostress analysis of the kinematic dataset revealed two separate strike-slip faulting stages which predate orthogonal tensional fracture formation.

Keywords: brittle deformation, photogrammetry, structural geology, Fennoscandia, Åland

1. Introduction

During Precambrian times, multiple tectonic events occurred which caused the formation of brittle fault systems in Fennoscandia and further reactivations of these (Saintot et al., 2011; Viola et al., 2013; Mattila and Viola, 2014; Nordbäck et al., 2022). The tectonic events described include initial brittle deformation at 1.75 Ga (Marchesini et al., 2019; Prando et al., 2019), formation of faults at around 1.6 Ga, followed by reactivation of pre-existing faults between 1.3–1.2 Ga and further fault formation and reactivation during the Sveconorwegian orogeny 1.1-0.9 Ga ago (Nordbäck et al., 2022). Due to the long and complex history, involving both ductile and repeated brittle events, the brittle development of Svecofennian rocks is highly multifaceted. To complement the current understanding about the complex tectonic development, investigations within younger stratigraphical domains is needed, to unravel some of the details of later brittle events that may remain obscured by previously formed structures within older domains.

The aim of this study was to enhance the understanding of the Mesoproterozoic tectonic geological evolution within Fennoscandia, which based on previous studies include a 1.6-1.3 Ga period lacking recognised brittle events. In this regard the 1.58 Ga Åland rapakivi (Suominen, 1991), lacking Paleoproterozoic ductile and brittle anisotropies, offers possibilities to observe any potential Mesoproterozoic brittle development without precursors that typically may affect the localisation and reactivation of brittle structures within older Svecofennian rocks.

2. Methods

Our study in the Åland rapakivi batholite, included field mapping of mesoscopic faults, tensional fractures, and the interpretation of lineaments representing large scale structures. The lineament interpretation was based on both topographical (LiDAR and Bathymetry) and aerogeophysical datasets analysed in the 1:200 000 scale. For the field mapping purposes we first acquired UAV based photogrammetric datasets covering a 5 km long outcrop area in Geta, along northern shores of the Åland Islands. The photogrammetric data was processed into two-dimensional orthomosaic images which we used for digitizing fracture traces in GIS. The produced fracture maps were used as a base for our fieldwork and supplemented by field

classifications and collection of structural data, e.g. fault orientation and kinematic measurements. The acquired kinematic fault slip dataset was analysed by paleostress inversion with the Wintensor software (Marrett and Allmendinger, 1990; Angelier, 1994).

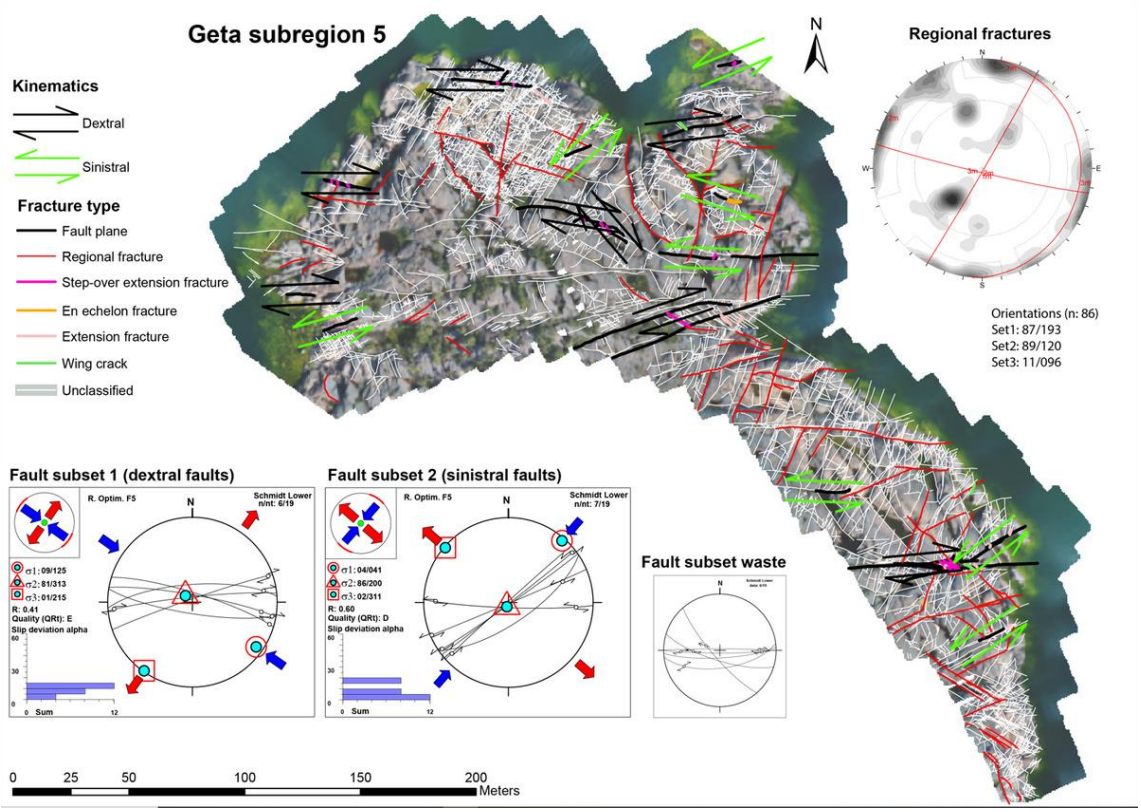

Figure 1. Example of the fracture and fault dataset from Geta, Åland Islands. Digitized fracture traces are coloured according to type (defined in the field) and visualised on top of a UAV orthomosaic image.

3. Results

A total of 328 lineaments were interpreted in 1:200 000 scale, with WNW-ESE, N-S and NE-SW trending orientations dominating. Prior to fieldwork, a total of 43 701 fracture traces were digitised from the UAV orthomosaics. On the outcrops of Geta we observed several types of fractures and faults; e.g. mesoscopic strike-slip faults characterized by shear fractures, step-over fractures, en echelon fractures, horse tail fractures and wing cracks. In addition, orthogonal tensional fractures (or regional fractures) were also documented. The field data from Geta includes structural information from a total of 160 fault planes, 115 secondary fractures associated with the faults, and 500 mapped tensional fractures unrelated to faulting. The mesoscopic fault structures are composed of E-W striking dextral and sinistral faults, but some N-S trending dextral ones also occur. Thus, within the mesoscopic scales, there is observed a deviation from the orientation of the largest lineaments (inferred brittle structures). In Geta the orientation of extension fractures is quite similar as the mapped fault structures but based on the relative age relationships observed both from the remotely mapped fracture traces and in the field, the fault structures predate the orthogonal extensional fracture system. Paleostress

inversion analysis of our datasets revealed two different stages of potential Mesoproterozoic strike-slip faulting and two stages of extension fracture formation.

4. Conclusions

Our combined methodology including UAV photogrammetry, remote GIS fracture mapping and field mapping proved to be an efficient way to survey large areas in high detail. This resulted in comprehensive datasets of faults and related fractures that could be readily used for e.g., paleostress analysis. The identified brittle events include two strike-slip faulting stages, which both preceded later formation events of the extension fracture system.

References:

Angelier, J., 1994. Fault slip analysis and palaeostress reconstruction, in: Continental Deformation. Pergamon, Oxford, United Kingdom, pp. 53–100.

Marchesini, B., Garofalo, P.S., Menegon, L., Mattila, J., Viola, G., 2019. Fluid-mediated, brittle–ductile deformation at seismogenic depth – Part 1: Fluid record and deformation history of fault veins in a nuclear waste repository (Olkiluoto Island, Finland). Solid Earth 10, 809–838. https://doi.org/10.5194/se-10-809-2019

Marrett, R., Allmendinger, R.W., 1990. Kinematic analysis of fault-slip data. Journal of Structural Geology, 12, 973–986. https://doi.org/10.1016/0191-8141(90)90093-E

Mattila, J., Viola, G., 2014. New constraints on 1.7 Gyr of brittle tectonic evolution in southwestern Finland derived from a structural study at the site of a potential nuclear waste repository (Olkiluoto Island). Journal of Structural Geology, 67, 50–74. https://doi.org/10.1016/j.jsg.2014.07.003

Nordbäck, N., Mattila, J., Zwingmann, H., Viola, G., 2022. Precambrian fault reactivation revealed by structural and K-Ar geochronological data from the spent nuclear fuel repository in Olkiluoto, southwestern Finland. Tectonophysics, 824, 229208. https://doi.org/10.1016/j.tecto.2022.229208

Prando, F., Menegon, L., Anderson, M.W., Marchesini, B., Mattila, J., Viola, G., 2019. Fluid-mediated, brittle-ductile deformation at seismogenic depth: Part II – Stress history and fluid pressure variations in a shear zone in a nuclear waste repository (Olkiluoto Island, Finland). Solid Earth Discussions, 1–41. https://doi.org/10.5194/se-2019-142

Saintot, A., Stephens, M.B., Viola, G., Nordgulen, Ø., 2011. Brittle tectonic evolution and paleostress field reconstruction in the southwestern part of the Fennoscandian Shield, Forsmark, Sweden. Tectonics 30, 1–36. https://doi.org/10.1029/2010TC002781

Suominen, V., 1991. The chronostratigraphy of southwestern Finland: with special reference to Postjotnian and Subjotnian diabases, Geological Survey of Finland bulletin. Geologian Tutkimuskeskus, Espoo.

Viola, G., Zwingmann, H., Mattila, J., Käpyaho, A., 2013. K-Ar illite age constraints on the Proterozoic formation and reactivation history of a brittle fault in Fennoscandia. Terra Nova 25, 236–244. https://doi.org/10.1111/ter.12031

A thermogeological analysis of medium-deep borehole heat exchangers in low-enthalpy crystalline rocks

K. Piipponen[1] and A. Martinkauppi[2]

[1] Geological Survey of Finland, Vuorimiehentie 5, PL 96, 02151 Espoo, Finland
[2] Geological Survey of Finland, Teknologiankatu 7, PL 97, 67101 Kokkola, Finland
E-mail: kaiu.piipponen@gtk.fi

In densely populated urban areas, deep geothermal boreholes offer an alternative over shallow geothermal systems, which demand extensive surface area for large-scale heat production. We compared the thermogeological parameters of four locations across Finland and tested two types of coaxial borehole heat exchangers to compare the variables that affect heat production in a Finnish geological setting. The borehole depths range from 600–3000 m. We used a range of collector fluid flow rates for each depth, location, and heat collector type. Our results indicate a trade-off between thermal energy production and outlet fluid temperature depending on the fluid flow rate, and that the local thermogeological factors impact heat production. In addition, the results indicate that the vacuum-insulated tubing outperforms high-density polyethylene pipe in producing warm fluids. We demonstrate that understanding the interplay of the site-specific and engineering parameters is necessary to maximize the potential of medium-deep geothermal boreholes.

Keywords: geothermal energy, low enthalpy, borehole heat exchanger, crystalline rock, COMSOL Multiphysics, space heating, Muhos Formation

1. Introduction

Heat extraction from medium-deep wells (500–3000 m) has been attracting interest as a feasible and reliable technology for district heating and large building space heating. As drilling techniques of geothermal boreholes are advancing at a rapid pace, companies are willing to invest in drilling deeper. Moreover, deep boreholes have a smaller land footprint, which is beneficial in densely built environments. As of 2022, there is one 1300 meters deep geothermal borehole in operation in Finland, and five more medium-deep systems are in the drilling phase across the country (Arola and Wiberg, 2022).

In this work, we summarize and combine data from our two studies in Finland to further compare the thermal energy yield of medium-deep geothermal boreholes in different geological regimes. We created a numerical geothermal well model with COMSOL Multiphysics® finite element method software and optimized the thermal energy yield from wells of lengths between 600–3000 meters, with two borehole thermal collector types and various collector fluid flow rates. Our resulting models clearly show the effect of local geology and heat collector type, and the trade-off between thermal energy yield and production temperature depending on increasing circulation fluid flow rate.

Currently, the growth of the medium-deep geothermal sector is limited by the challenges related to site selection and drilling costs. Our resulting models will increase the likelihood of locating and designing profitable systems, scaling up the possibilities to low-carbon solutions for the heating sector.

2. Materials and methods

The areas assessed in this study span across Finland, the southernmost studied location being Vantaa in the Capital area, the northernmost location being Rovaniemi, and two other locations are Jyväskylä in Central Finland and the Muhos formation in Northern Ostrobothnia. The

dominant rock types in Vantaa and Rovaniemi are microcline and porphyritic granite, respectively and in Jyväskylä, the rock type is granodiorite (Nironen, 2005). Formation, The Muhos formation is an exceptional sedimentary deposit in Finland where the rock type is claystone underlined by crystalline granitic bedrock (Kalla, 1960). The formation thickness varies between 50–1000 meters, and it is covered by superficial sediments with a thickness of 20–120 meters. The significant difference between the sites is the ground surface temperature that decreases towards the north. All thermogeological parameters of the sites are summarized in Table 1.

Table 1. Thermogeological parameters of study sites and their sources.

	Vantaa	**Jyväskylä**	**Muhos**		**Rovaniemi**	**Source**
Mean annual air temperature [°C]	4.51	3.38	2.40		0.89	Aalto et al. (2016)
Mean annual ground temperature [°C]	6.1	5.3	4.6		3.6	Calculated from T_{air} after Kukkonen (1986)
Rock thermal conductivity [W/(m·K)]	3.30	3.19	soil	1.70	3.30	Peltoniemi and Kukkonen (1995)
			claystone	1.86		
			granite	3.20		
Radiogenic heat prod. [μW/m^3]	2.96	1.33	1.84		2.56	Veikkolainen and Kukkonen (2019)
Geothermal heat flux [mW/m^2]	44.5	44.0	42.0		42.8	Veikkolainen and Kukkonen (2019)

We evaluated the geothermal energy potential of the Muhos Formation considering a layered subsurface model with geological scenarios determined by Martinkauppi and Piipponen (2022) as the best and least-producing scenarios. The low thermal conductivity of the claystone and soil layer creates a "blanketing effect" on the geothermal heat flux, thus increasing the local geothermal gradient. Thermal energy yield varies significantly depending on whether the geothermal well reaches the granitic bedrock underneath. Therefore, the best geological scenario for the wells of 1000 meters and less is where the claystone layer is at its thinnest, whereas for the deeper wells the thick claystone layer yields better results.

The heat collector was modelled as a coaxial open-loop system with two collector type options: a vacuum-insulated tube (VIT) with thermal conductivity of 0.02 W/(m·K) and 22 mm thickness and a high-density polyethylene (HDPE) pipe (k=0.42 W/(m·K), thickness 10 mm) as a cheaper alternative. The maximal energy yield was gained by setting the boundary condition of the borehole wall to decrease to 0 °C after 25 years of simulation. The maximum flow rates were determined for each collector based on the fluid resistance and the minima were set so that the collector annulus fluid flow remains turbulent. Fluid flow ranges are 2-10 L/s for HDPE pipes of 2-3 km and 1-5 L/s for all other collector types. The full borehole and collector parameter summary is found in Piipponen et al. (2022). The quantities of the energy yield presented are obtained purely from the ground without considering the heat pump coefficient of performance. We assume unfractured rock and purely conductive heat transfer.

3. Results and discussion

Our results indicate that thermal energy yield is the highest in the best case of Muhos formation parameters, and then thermal energy yield decreases the further north the site is (Figure 1). We observe that as the BHE depth increases from 600 to 1000 m, the thermal energy yield roughly doubled, nearly tripled from 1000 to 2000 m, and almost doubled when increasing the depth from 2000 to 3000 m. These results show that the BHE energy production can increase over 10-fold from 600 to 3000 m depth boreholes.

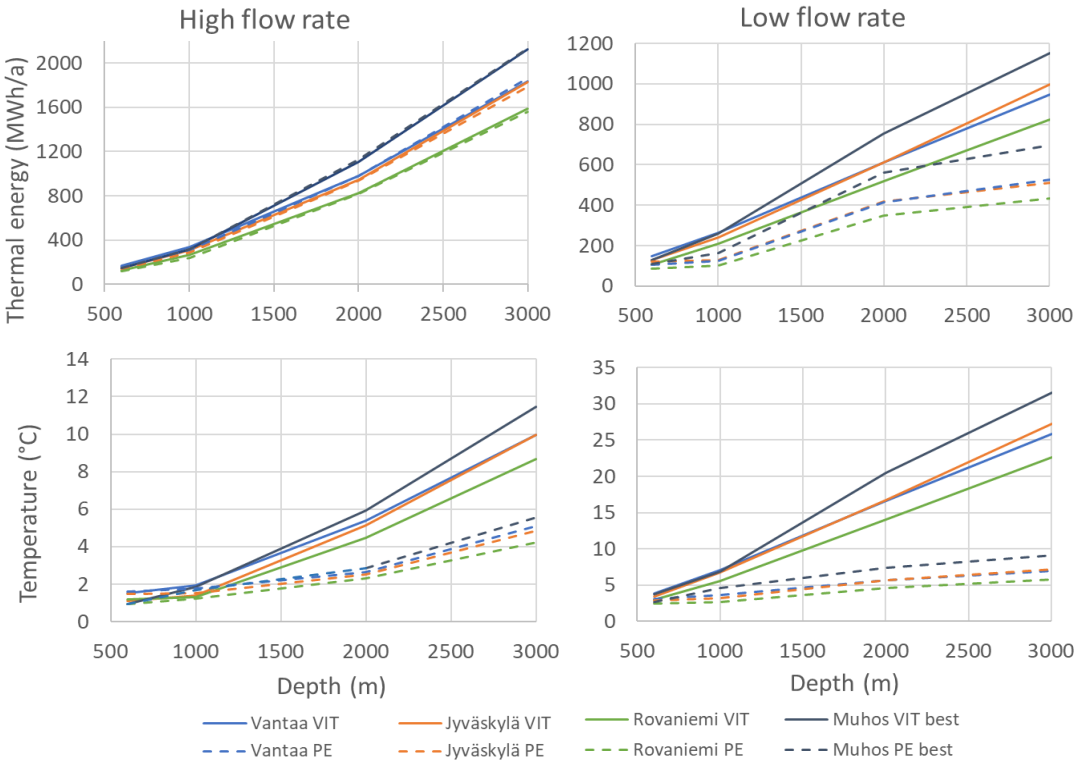

Figure 1. Comparison of thermal energy and fluid temperatures produced by constant heat extraction over 25 years, at high and low flow rates for each modelled depth, location, and two collector pipe types.

The variation in rock thermal conductivity is reflected in the subsurface temperature. Considering the constant geothermal heat flux density, the low thermal conductivity of sediments is compensated by a high geothermal gradient. Therefore, especially at deeper levels, the subsurface temperature in the Muhos area is higher than in other areas, and consequently, thermal energy yield is the highest. In purely crystalline rock settings, the highest thermal energy yield is observed in Vantaa as a result of the three factors: the highest ground surface temperature, high geothermal heat flux density, and high radiogenic heat production values due to the presence of microcline granites. In Jyväskylä, where the geothermal gradient is higher than in Vantaa, the outlet temperatures and thermal energy yield are higher with deeper wells but lower at shallower wells and especially at higher fluid flow rates. This difference is attributed to the lower thermal conductivity of the granodiorite than microcline granite and consequently less efficient heat exchange between the host rock and the fluid. For the same reason, the best geological scenarios for thermal energy yield in Muhos are different for the

600–1000 m and 2-3 km wells: heat exchange happens mainly in granite, so production of the shallower wells is higher with the thin claystone layer.

In a conclusion, we observe that the geothermal gradient and initial ground surface temperature have a significant impact on geothermal energy yield, while the thermal conductivity of the local rock type on one side increases the geothermal gradient, but on the downside, decreases heat exchange between the geothermal well and rock.

It is apparent, that the efficient insulation of VIT allows thermal energy production comparable with HDPE pipe with a larger hydraulic diameter and consequently higher fluid circulation rates. This relationship between flow rate and types of pipe material is an essential finding, considering that HDPE pipe is significantly lower in price than VIT. However, the fluid temperatures produced with HDPE pipe are relatively low at all flow rates and borehole lengths due to the thermal short-circuiting effect. We arrive at the same conclusion as Nalla et al. (2005), that either the thermal power production or the outlet temperature of the working fluid can be individually maximized. Alternatively, they can be simultaneously optimized so that reasonable temperatures for the heat pump as well as a reasonable heat production rate can be achieved.

5. Conclusions

The results of this work indicate that: (1) the deeper the borehole is, the better its thermal energy production, (2) the higher the subsurface temperature, the better the energy yield, when considering minor variations in thermogeological parameters, but (3) considering a significant geological variation, such as the thick sedimentary layer, the system becomes more complex, (4) VIT outperforms HDPE pipe in terms of outlet temperature production and reaches similar thermal energy yield with lower collector fluid circulation rates and (5) with an increasing flow rate, we obtain more thermal energy but a significantly lower outlet fluid temperature. All these variables should be taken into consideration during the design and operation phases of medium-deep geothermal systems.

References:

Aalto, J., Pirinen, P., Jylhä, K., 2016. New gridded daily climatology of Finland: Permutation-based uncertainty estimates and temporal trends in climate. J. Geophys. Res. Atmos., 121, 3807–3823.

Arola, T., Wiberg, M., 2022. Geothermal Energy Use, Country Update for Finland, In: European Geothermal Congress 2022.

Kalla, J., 1960. Muhoksen muodostuman alueella, Limingan Tupoksessa suoritettu syväkairaus. Oulujoki Osakeyhtiö, Betoni- ja geoteknillinen toimisto, Raportti M 17/Lka-60/1, 5 p. (In Finnish)

Kukkonen, I.T., 1986. The effect of past climatic changes on bedrock temperatures and temperature gradients in Finland, Geol. Surv. Finland, Nucl. Waste Dispos. Res. Espoo.

Martinkauppi, A., Piipponen, K., 2022. Geothermal energy modelling of medium-deep boreholes in a sedimentary formation with crystalline basement, in: European Geothermal Congress 2022.

Nalla, G., Shook, G.M., Mines, G.L., Bloomfield, K.K., 2005. Parametric sensitivity study of operating and design variables in wellbore heat exchangers. Geothermics, 34, 330–346.

Nironen, M., 2005. Proterozoic orogenic granitoid rocks. Precambrian Geol. Finl. – Key to Evol. Fennoscandian Shield, 14, 443–479.

Peltoniemi, S., Kukkonen, I., 1995. Kivilajien lämmönjohtavuus Suomessa: yhteenveto mittauksista 1964–1994, Geological Survey of Finland, arkistoraportit, 14. (In Finnish)

Piipponen, K., Martinkauppi, A., Korhonen, K., Vallin, S., Arola, T., Bischoff, A., Leppäharju, N., 2021. The Deeper the Better? A Thermogeological Analysis of Medium-deep Borehole Heat Exchangers in Low-enthalpy Crystalline Rocks. Geothermal Energy.

Veikkolainen, T., Kukkonen, I.T., 2019. Highly varying radiogenic heat production in Finland, Fennoscandian Shield. Tectonophysics, 750, 93–116.

KEYNOTE: Hard breakup - the rifted margin of western Fennoscandia

A. Rotevatn[1]

[1]Department of Earth Science, University of Bergen, Norway
E-mail: Atle.Rotevatn@uib.no

At the western extreme of Fennoscandia, a rifted passive margin marks the transition from the Fennoscandian Shield to the continental shelf and ocean basins of the Norwegian Sea and the North Atlantic. This passive margin developed in geologically relatively recent times (~55 Ma), when continental break-up finally occurred after a period of protracted rifting over c. 300 million years following the Ordovician to Devonian Caledonian Orogeny. But what role did the structure of the Fennoscandian Shield play in the setup of Caledonian orogenic template, and the ensuing rifting that eventually led to breakup at the current western extreme of Fennoscandia? In this keynote talk we address these issues, exploring how the ancient structure of the Fennoscandian Shield helped shape of the most spectacular rifted margins globally.

Keywords: Fennoscandia, inheritance, orogeny, Wilson cycle, margin formation

1. Introduction

The Fennoscandian shield contains some of the oldest parts of the European continent and presents us with rocks dating back as far as to Paleoproterozoic and the Archaean times. The Fennoscandian shield is also deeply imprinted and scarred from being shaped in the cauldron of plate tectonics over oceans of time, where the opening and closure of oceans, the break-up and amalgamation of continents, and the formation of mighty orogens and basins is an integral part of its history.

In present-day western Fennoscandia, the crust is dominated by the imprint of the Caledonian orogen (Figure 1), but gives way westward across the Norwegian rifted passive margin to the continental shelf and ocean basins of the Norwegian Sea and the North Atlantic. Here, we explore how the long and complex tectonic history of the Fennoscandian Shield influenced the Caledonian orogen and the ensuing rifting that eventually led to breakup at the current western extreme of Fennoscandia.

2. Orogenic history through repeated Wilson cycles

The Caledonian orogen, and the major crustal structures related to its formation and demise (large-scale extensional shear zones), are generally considered to a key structural template which strongly influenced the formation of Paleozoic and Mesozoic rift basins, and, later, wholesale continental breakup in the North Atlantic. However, structural inheritance can be traced much further back in time, to the many orogenic and extensional events of the past through repeated Wilson cycles, relating to the assembly and break-up of ancient supercontinents Rodinia and Pangea (e.g., Torsvik, 2003).

Some of the key tectonic events that have affected the Fennoscandian Shield through time, and which contributed to setting up a crustal template prior to Paleozoic to Cenozoic rifting, margin formation and breakup, include (see Schiffer et al., 2020, and references therein, for an overview): (i) the Archaean Karelian and Lapand-Kola events in northern Scandinavia, (ii) the Paleoproterozoic Svecofennian orogeny in central Scandinavia, (iii) the formation of the Trans-Scandinavia Igneous Belt in SW Sweden to NW Norway, (iv) the Mesoproterozoic Sveconorwegian accretionary orogeny, (v) post-Sveconorwegian orogenic collapse and a

period of rifting and Neoproterozoic basin development and rift basin formation (e.g. Gee et al., 2008), (vi) the Neoproterozoic Timanide Orogeny, recording the accretion of island arc complexes, terranes and microcontinents onto the northern Baltic margin (Gee and Pease, 2004), and (vii) the Caledonian Orogeny in Ordovician to Devonian times, following Iapetus closure, arc-continent collision, before the culmination of the main Scandian phase of continent-continent collision and the formation of the orogen itself (e.g. Cocks et al., 2006). Finally, (viii) in late to post-Caledonian times, extensional collapse and the formation of intra-montane continental basins in the Devonian, was associated with the formation of massive, extensional detachment that record 100s km of westward displacement of the hangingwall basins (e.g. Vetti and Fossen, 2012).

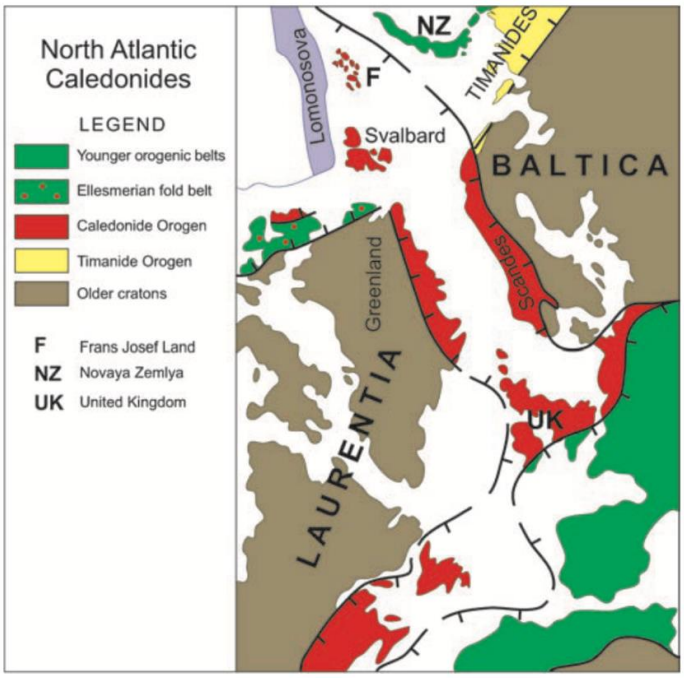

Figure 1. Outline of the North Atlantic Caledonides, its position across Fennoscandia/Baltica, and relationship between Laurentia and Baltica. From Gee at al. (2008).

3. Influence of ancient Fennoscandian crustal structure on margin formation and break-up

In the talk we explore these key questions: How has this series of successive events have made their imprint of the crustal structure of Fennoscandia? How did this imprint affect the rifted margin formation and break-up at the western margin of Fennoscandia and the North Atlantic? In addition to discussing the influence of the Caledonian structural fabric on rift basin structure, margin formation and break-up (e.g. Phillips et al., 2016; Rotevatn et al., 2018, Osagiede et al., 2020), we also discuss the influence of pre-Caledonian crustal fabric. This includes i) the effect of the perpendicular-to-margin arrangement of Precambrian terranes in eastern Fennoscandia (Figure 2), which likely affected the location of transforms as well as margin segmentation rifting and margin development in Paleozoic to Cenozoic times (e.g., Bergh et al., 2007;

Schiffer et al., 2020), ii) the effect of the post-Sveconorwegian Neoproterozoic basins, and their influence on the Caledonian orogen (e.g. Jakob et al., 2019), and iii) the effect of Timanide fabric on the structuration in the eastern and central Barents Sea on the northern margin of Fennoscandia (e.g., Gee et al. 2008; Pease 2011; Klitzke et al. 2019).

Understanding how the structure of the Fennoscandian Shield helped shape one of the most spectacular rifted margins in the world, has implications for understanding the effects of structural inheritance globally, and in particular how events of the very ancient past may bridge across billions of years through structural inheritance, to affect events occurring much, much later.

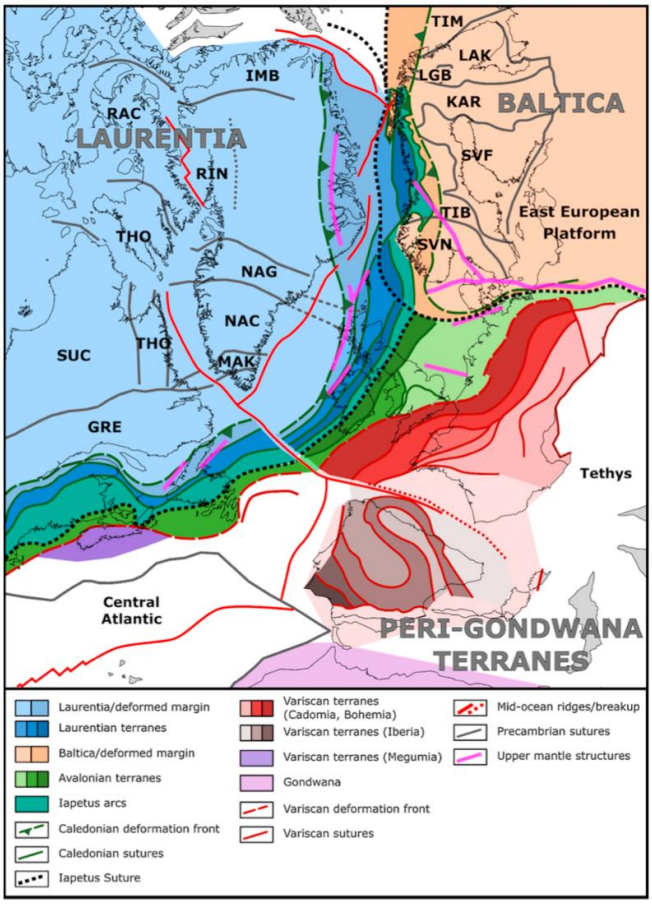

Figure 2. Terrane and structure map of the Circum-North Atlantic region at 145 Ma showing continents, terranes, suture zones and upper mantle structures; from Schiffer et al. (2020). GRE – Grenvillian Orogen, IMB – Inglefield Mobile Belt, KAR – Karelian, LGB – Lapland Granulite Belt, MAK – Makkovik-Ketilidian Orogen, NAC – North Atlantic Craton, NAG – Nagssugtoqidian Orogen, RAC – Rae Craton, RIN – Rinkian Orogen, SUC – Superior Craton, SVF – Svecofennian, SVN – Sveconorwegian Orogen, THO – Trans-Hudson Orogen, TIB – Transscandinavian Igenous Belt, TIM – Timanian Orogen.

References:

Bergh, S.G., Eig, K., Kløvjan, O.S., et al., 2007. The Lofoten-Vesterålen continental margin: a multiphase Mesozoic-Palaeogene rifted shelf as shown by offshore-onshore brittle fault-fracture analysis, Norwegian Journal of Geology, 87, 55-77.

Cocks, L. R. M., Torsvik, T. H., Gee, D. G., & Stephenson, R. A. 2006. European geography in a global context from the Vendian to the end of the Palaeozoic, Geological Society, London, Memoirs, 32, 83.

Gee, D. G., Fossen, H., Henriksen, N., & Higgins, A. K. 2008. From the early Paleozoic platforms of Baltica and Laurentia to the Caledonide Orogen of Scandinavia and Greenland, Episodes Journal of International Geoscience, 31(1), 44-51.

Gee, D. G., & Pease, V. (2004). The Neoproterozoic Timanide Orogen of eastern Baltica: introduction, Geological Society, London, Memoirs, 30, 1-3.

Jakob, J., Andersen, T. B., & Kjøll, H. J. 2019. A review and reinterpretation of the architecture of the south and south-central Scandinavian Caledonides—a magma-poor to magma-rich transition and the significance of the reactivation of rift inherited structures, Earth-Science Reviews, 192, 513-528.

Klitzke, P., Franke, D., Ehrhardt, A., et al., 2019. The Paleozoic evolution of the Olga Basin region, northern Barents Sea – a link to the Timanian Orogeny, Geochemistry, Geophysics, Geosystems. https://doi.org/10.1029/2018GC007814.

Osagiede, E.E., Rotevatn, A., Gawthorpe, R., Kristensen, T.B., Jackson, C.A.L., Marsh, N., 2020, Pre-existing intra-basement shear zones influence growth and geometry of non-colinear normal faults, western Utsira High–Heimdal Terrace, North Sea. Journal of Structural Geology 130, 103908. https://doi.org/10.1016/j.jsg.2019.103908.

Pease, V., 2011. Chapter 20 Eurasian orogens and Arctic tectonics: an overview. Geol Soc Lond Mem 35, 311–324. https://doi.org/10.1144/M35.20.

Phillips, T.B., Jackson, C.A., Bell, R.E., et al., 2016. Reactivation of intrabasement structures during rifting: A case study from offshore southern Norway, Journal of Structural Geology, 91, 54–73.

Rotevatn, A., Kristensen, T.B., Ksienzyk, A.K., et al., 2018. Structural inheritance and rapid rift-length establishment in a multiphase rift: the East Greenland rift system and its Caledonian orogenic ancestry, Tectonics 37, 1858–1875.

Schiffer, C., Doré, A., Foulger, G. et al., 2020. Structural inheritance in the North Atlantic, Earth-Science Reviews, 206, 102975.

Torsvik, T.H., 2003. The Rodinia jigsaw puzzle, Science, 300, 1379–1381.

Vetti, V. V., & Fossen, H. 2012. Origin of contrasting Devonian supradetachment basin types in the Scandinavian Caledonides, Geology, 40, 571-574.

Classification of mafic dikes in the Hanko-Inkoo archipelago

M. Rydberg[1], M. Kurhila[2] and K. Nikkilä[1]

[1]Geology and Mineralogy, Åbo Akademi University
[2]Geological Survey of Finland, P.O. Box 96, 02151 Espoo, Finland
E-mail: markus.rydberg@abo.fi

We study potential intra-orogenic dikes from Southern Finland, more precisely, the Hanko and Inkoo archipelago. Southern Finland's geological history consists of an accretionary period ending in continent-continent collision. An intra-orogenic extensional period has been proposed to have taken place roughly 1.86 Ga. The study of potential intra-orogenic dikes could give a better understanding of the setting they have formed in and thus of the extensional period.

Keywords: Intra-orogenic, dike, extensional period

1. Introduction

The Svecofennian orogenic evolution in southern Finland can be divided into the accretionary Fennian orogeny (1.92-1.87 Ga), an intra-orogenic period (1.87-1.84 Ga) and the Svecobaltic stage (1.84-1.79 Ga;Lahtinen et al., 2005). The accretionary Fennian orogeny consisted of microcontinent accretion against the Archean continent, followed by an intra-orogenic extensional period, which was then followed by the Svecobaltic continent-continent collision (Väisänen et al., 2012; Kara et al., 2020). Hermansson et al. (2008) and Stephens and Andersson (2015) have presented an alternative scenario that consists of subduction underneath an active continental margin in combination with retreating and advancing slab, which resulted in switching between contractional and extensional tectonics. Both models still agree that an extensional phase took place approximately at 1.86 Ga.

The intra-orogenic period has been studied in southern Finland recently by Kara et al. (2020), Väisänen et al. (2012) and Nevalainen et al. (2014), but is only vaguely studied in our study area (Hopgood, 1984). Potential intra-orogenic dikes in the Hanko-Inkoo archipelago have been previously mapped by Sederholm (1926). There are only a few age determinations of the mafic dikes (Väisänen et al., 2012) and no geochemical classification of them in the area. In this study we characterize the mafic dikes by using petrographic analyses and age determinations.

2. Materials

The study area, located in the Hanko-Inkoo archipelago, consists of migmatized volcano-sedimentary rocks, which the mafic dikes cross-cut sharply. Some of the mafic dikes have been deformed (folded or boudinaged), and they may cross-cut each other. In some places granitic dikes (c. 1.83 Ga, Saukko et al., this volume;) cross-cut the mafic dikes. The composition of the dikes varies. A total of 14 observations were made, 9 samples were collected, all of them were petrographically studied and 3 of them were dated.

3. Analytical methods

Zircons for age determination were separated using a crusher, pulverizer, panning, hand magnet, heavy liquid, magnetic separator and by hand picking. The zircons were placed on an epoxy disc that was ground down to expose the interior of the zircon grains. The disc was then polished. Zircons were then imaged with a Phenom XL SEM, at Åbo Akademi. The final stage

of the age determination was done with laser ablation and a mass spectrometer, referred together as laser ablation-single collector-inductively coupled plasma mass spectrometry, or LA-SC-ICPMS, at the Geological Survey of Finland (GTK), in Espoo.

4. Results and discussion

All the dikes have a fairly sharp contact with the surrounding host rock and often show a chilled margin within the dike. The dikes can be divided into two groups, based on their mineralogical composition: group 1) is dominated by amphiboles and group 2) is dominated by plagioclase. Group 1) shows a mafic mineralogical composition, with abundance in biotite and plagioclase, in addition to amphibole. Quartz is often present in only minor amounts, if at all. Common accessory minerals in group 1) are apatite and opaque minerals. Titanite and epidote are also present in some samples Group 2) shows a more felsic mineralogical composition, with abundant quartz and minor amounts of biotite, in addition to plagioclase. Common accessory minerals in group 2) are titanite and apatite. Calcite and epidote can be found in a few samples.

Age determination results were achieved from three different dikes (11A-MAR-2021, 11B-MAR-2021, 12-MAR-2021). Sample 11A-MAR-2021 indicates an age of 1867.3±5.1 Ma (Figure 1), 11B-MAR-2021 has a spread of ages from ~1830 Ma to ~1950 Ma. It is thus clear that the zircons represent a heterogeneous source. Accepting only the ages of <1.90 Ga, a weighted average age of 1871±11 Ma can be calculated (Figure 2). 12-MAR-2021 also shows some scatter, but the main population has an age of 1878±9.5 Ma (Figure 3). 11A-MAR-2021 is cross-cutting the 11B-MAR-2021, and hence our U-Pb results are in line with field observations.

Both 11A-MAR-2021 and 11B-MAR-2021 fall into group 1), based on their petrography. Sample 11A-MAR-2021 has a roughly 10% lower amphibole content and a roughly 10% higher plagioclase content, when compared to sample 11B-MAR-2021. Sample 12-MAR-2021 belongs to group 2) based on its petrography.

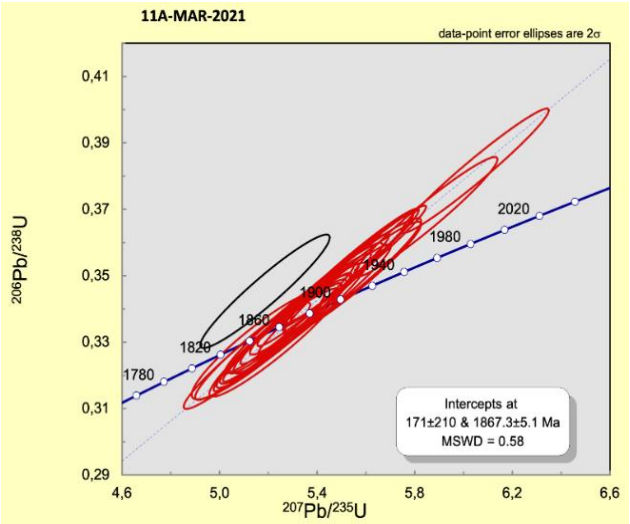

Figure 1. Concordia diagram showing the age of sample 11A-MAR-2021.

The age determination results show ages that are older than expected by the earlier literature (Kara et al., 2020; Väisänen et al., 2012). 11A-MAR-2021 is the only dated dike that clearly fits within the proposed extensional period, with an age of 1867.3±5.1. Zircon ages of both 11B-MAR-2021 and 12-MAR-2021 are more scattered and imply the presence of xenocrystic as well as igneous zircons. Their tentative ages place them closer to the main magmatic period in southern Finland at 1880-1870 Ma.

This is an ongoing project and more detailed information needs to be studied to conclude the extensional period and possible reasons for the older ages in the area, compared to other areas in southern Finland.

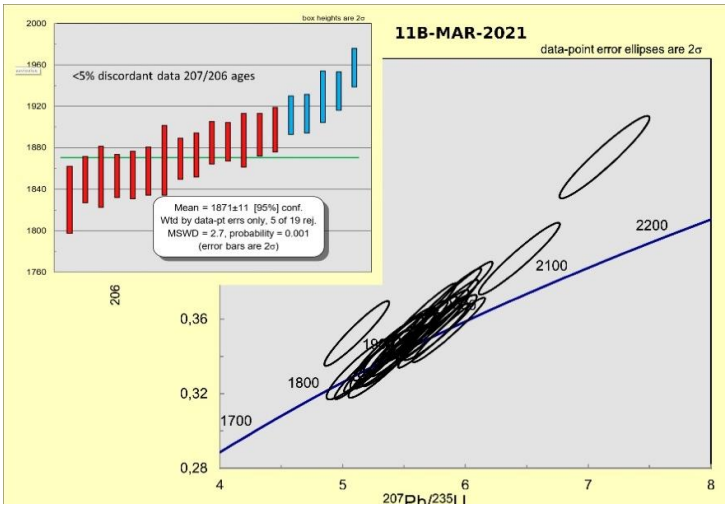

Figure 2. Concordia diagram showing the age of sample 11B-MAR-2021.

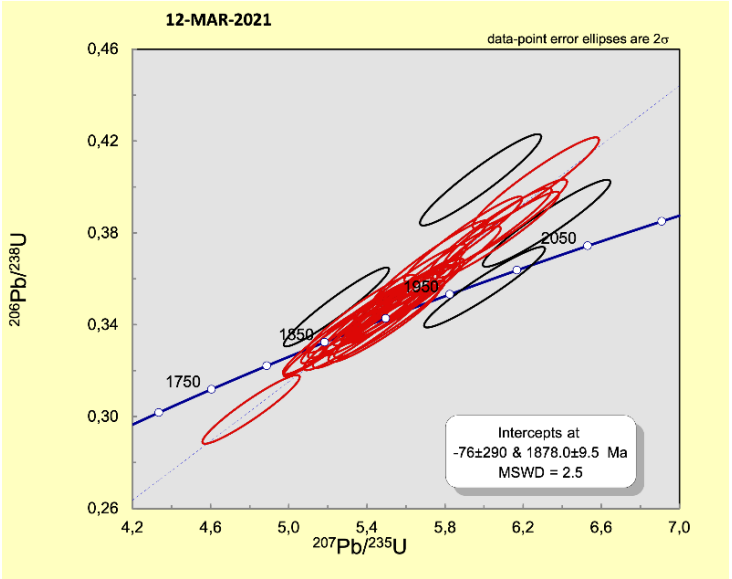

Figure 3. Concordia diagram showing the age of sample 12-MAR-2021.

References:

Hermansson, T., Stephens, M.B., Corfu, F., Page, L.M., Andersson, J., 2008. Migratory tectonic switching, western Svecofennian orogen, central Sweden: constraints from U/Pb zircon and titanite geochronology. Precambrian Research, 161, 250–278. https://doi.org/10.1016/j.precamres.2007.08.008

Hopgood, A., 1984. Structural evolution of Svecokarelian migmatites, southern Finland: A study of Proterozoic crustal development. Transaction of the Royal Society of Edinburgh: Earth Sciences, 74 (4), 229-264. https://doi.org/10.1017/S0263593300013675

Kara, J., Väisänen, M., Heinonen, J.S., Lahaye, Y., O'Brien, H., Huhma, H., 2020. Tracing arclogites in the Paleoproterozoic Era – A shift from 1.88 Ga calcalkaline to 1.86 Ga high-Nb and adakite-like magmatism in central Fennoscandian Shield. Lithos, Volumes, 372–373. https://doi.org/10.1016/j.lithos.2020.105663

Lahtinen, R., Korja, A., Nironen, M., 2005. Paleoproterozoic tectonic evolution. In: Lehtinen, M., Nurmi, P.A., Rämö, O.T. (Eds.), Precambrian Geology of Finland – Key to the Evolution of the Fennoscandian Shield. Elsevier B.V., Amsterdam, pp. 481-532. https://doi.org/10.1016/S0166-2635(05)80012-X.

Nevalainen, J., Väisänen, M., Lahaye, Y., Heilimo, E., Fröjdö, S., 2014. Svecofennian intraorogenic gabbroic magmatism: A case study from Turku, southwestern Finland. Bulletin of the Geological Society of Finland, 86, 93–112. https://doi.org/10.17741/bgsf/86.2.003

Stephens, M.B., Andersson, J., 2015. Migmatization related to mafic underplating and intra- or back.arc spreading above a subduction boundary in a 2.0-1.8 Ga accretionary orogen, Sweden. Precambrian Research, 264, 235-257. https://doi.org/10.1016/j.precamres.2015.04.019

Sederholm, J.J., 1926. On migmatites and associated pre-cambrian rocks of southwestern Finland. Part II: The region around the Barösundsfjärd W of Helsingfors and neighbouring areas. Bulletin nr 77, Geologiska kommissionen i Finland, Helsingfors

Väisänen, M., Eklund, O., Lahaye, Y., O'Brien, H., Fröjdö, S., Högdahl, K., Lammi, M., 2012. Intra-orogenic Svecofennian magmatism in SW Finland constrained by LA-MC-ICPMS zircon dating and geochemistry. GFF, 134 (2), 99–114. https://doi.org/10.1080/11035897.2012.680606

Lunar regolith as an archive of Solar System history

E. Salin[1,2]

[1]Åbo Akademi University, Turku, Finland
[2]Swedish Museum of Natural History, S-104 05 Stockholm, Sweden
E-mail: Evgenia.salin@abo.fi

Lunar glass beads are tiny particles which can be found in the lunar regolith (or "soil") covering almost the entire surface of the Moon. Glass beads can form due to volcanic eruption or be a result of impact flux, which defines two directions of the project. Volcanic glasses provide information about the lunar interior and the origin of mare basalts, mantle composition and its differentiation. Impact glasses aim to study compositional evolution of the lunar crust, regolith and impact processes. Investigation of glass beads will be help to decrease the ambiguity in the lunar chronology, providing precise U-Pb ages of the impact history.

Keywords: Moon, lunar regolith, lunar chronology

1. Introduction

Lunar science is a relatively young area of geologic investigation. Lunar return samples from known locations (and meteorites) allow us to directly investigate chemical and physical properties of our closest neighbour in detail. Less than a decade (1969-1976) of intense investigation, which started with six Apollo and three Luna sample-return missions, had changed a concept of the Moon as a simple planetary body to a highly differentiated one with a complex internal structure (e.g., Zubber et al., 1994) and unique crustal evolution (Hartmann and Davis, 1975).

2. Moon formation

It is generally thought that the Moon formed due to a collision of a Mars-sized body with the proto-Earth, which ejected hot material into the Earth's orbit, rapidly depleting in volatiles (e.g., Hartmann and Davis, 1975). Soon after planetesimal accretion, the Moon underwent extensive melting resulted in the lunar magma ocean (LMO), which was followed by the early differentiation and crystallization of the LMO completed by ~ 4.4 Ga (Nemchin et al., 2009). Fractional crystallization implies that the early lunar crust was produced by flotation of the plagioclase-rich crust formed by ferroan anorthosites and sinking of mafic cumulates (Shearer, 2006). Late stage precipitation of ilmenite led to formation of residual melt highly enriched in incompatible elements and referred to as KREEP (potassium, rare-earth elements and phosphorus rich), Figure 1A.

Based on textures and chemical composition, lunar rocks can be divided into 1. highland anorthosites and norites; 2. basaltic volcanic rocks or mare basalts; 3. polymict clastic breccias and impact melt rocks; and 4. lunar regolith or lunar "soil" (Figure 1B). The latter has been generated by impact "gardening" of the first three rock types and represents an unconsolidated fine-grained material with an average grain size of 60-80 μm, which covers almost the entire lunar surface. It is mainly composed of mineral and rock fragments, glass beads (volcanic and impact, Figure 1C) and agglutinates, which represent mineral and rock fragments welded by glass.

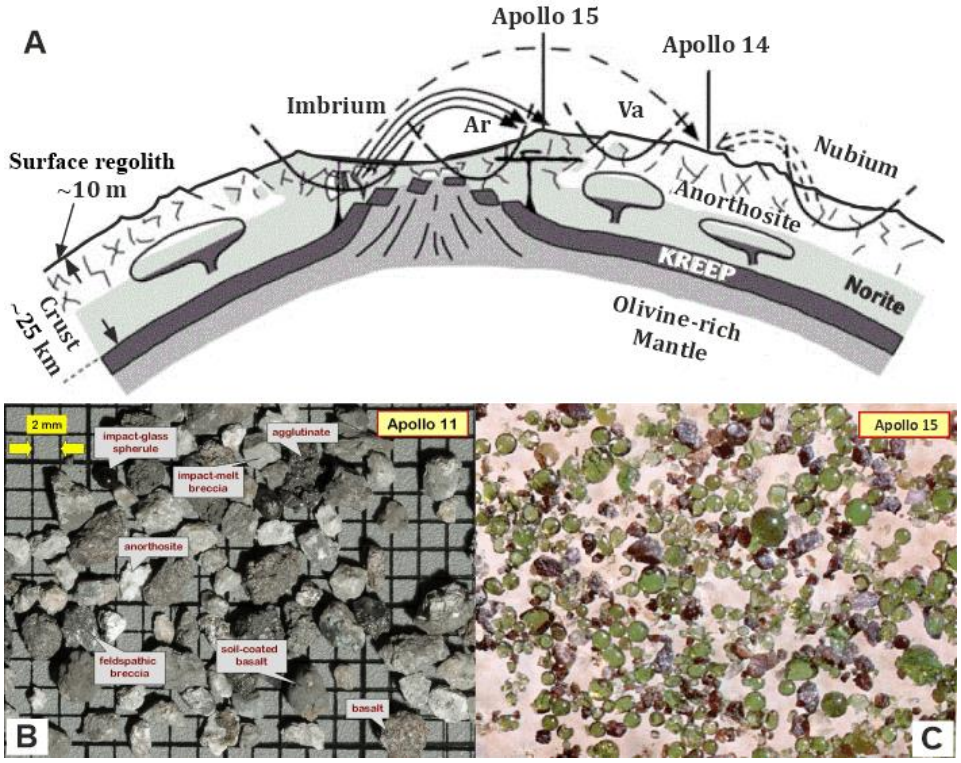

Figure 1. A. Simplified cross section of lunar crust and upper mantle at ~3.8 Ga after formation of Imbrium impact basin. Ar – Archimedes basin, Va – Vaporum basin. Modified after Stöffler (1990). B. Lunar regolith fragments from the Apollo 11. C. Green glass beads from Apollo 15 (40-250 μm-size fraction) from Carusi et al. (1972).

3. Lunar record

Compared to terrestrial planets, the Moon has a globally continuous lithosphere ("one-plate" planet), which has not been subject to plate tectonic processes. In turn, the most important process shaping the lunar surface after planetesimal accretion was projectile influx or "heavy bombardment", which was also responsible for impact-driven mixing and burial of the crust (Marchi et al., 2014). The existing model of the impact cratering history of the Moon suggests a rapid decline with a smaller or more prominent peaks between 3.5 and 4.2 Ga ago (Figure 2; Zellner, 2017; Hartmann et al., 2007). The hypothesis of a "terminal lunar cataclysm" at ~3.9 Ga leading to the formation of the most of the impact craters and thus the majority of lunar breccias and the impact melts (Tera et al., 1974; Stöffler and Ryder, 2001) is now largely abandoned due to possible sampling bias from Apollo 14 and 15 and thus a predominance of the Imbrium ejecta ages (Figures 1A and 2; Baldwin, 2006; Michael et al., 2018).

A later increase in the impact flux has been recorded within Apollo and Chang'e-5 landing sites with age peaks at ~2800 Ma (Zellner, 2017) and at < 1000 Ma and particularly predominant peaks at ~800 Ma and ~500-400 Ma (Culler et al., 2000; Long et al., 2022; Nemchin et al., 2022).

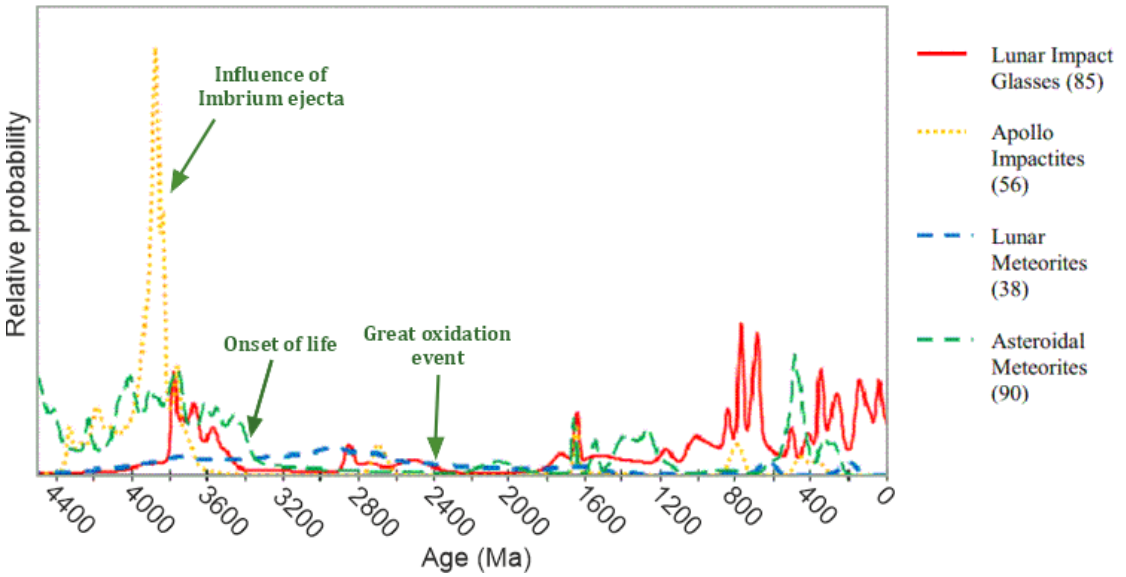

Figure 2. Relative probability of impact ages including important terrestrial biological events. Peak at ~3.9 Ga is probably due to influence of Imbrium ejecta. Modified after Zellner (2017).

4. Future work

In spite of more than fifty years of lunar exploration, the geochronological record of the early evolution of the Moon is still debated. Lunar chronology is dominated by $^{40}Ar/^{39}Ar$ ages, which often show around 300 m.y. younger ages compared to U-Th-Pb "chemical ages" (Zellner, 2019), this is not to mention the fact that the $^{40}Ar/^{39}Ar$ method is highly destructive. The purpose of the current project is to clarify the impact history of the Moon using *in situ* ion microprobe approach and providing absolute U/Pb ages of the impact and volcanic glass from the lunar regolith samples.

Furthermore, the project is aimed to study the Moon's interior through the volcanic eruptions (volcanic glass beads) and lunar crust through meteorite impacts (impact glass beads), which altogether will give a full image of the Moon's composition and processes involved into its formation.

Lack of plate tectonic recycling or exposure to any kind of weathering allowed lunar rocks to preserve a record of early (4.5-3.9 Ga) geological events and processes, for which we do not have evidence on the Earth. It is mostly agreed that the impact flux behaviour was the same throughout the inner Solar system, therefore clarifying the lunar record will not just define the early ages within the Moon, but also will shed the light on the impact regime under which life on the Earth became established and the rate at which volatiles and organic materials were delivered to the early Earth (Ryder, 2002; Zellner, 2017).

References:

Baldwin, R.B., 2006. Was there ever a Terminal Lunar Cataclysm? With lunar viscosity arguments. Icarus, 184, 308-318.

Carusi A. et al., 1972. Lunar glasses as an index of impacted sites lithology: The source area of Apollo 15 "green glasses". Geol. Romana, 11, 137.

Culler, T.S., Becker, T.A., Muller, R.A., Renne, P.R., 2000. Lunar impact history from $^{40}Ar/^{39}Ar$ dating of glass spherules. Science, 287, 1785-1788.

Hartmann, W.K., Davis, D.R., 1975. Satellite-sized platetesimals and lunar origin. Icarus, 24, 504-515.

Hartmann, W.K., Quantin, C., Mangold, N., 2007. Possible long-term decline in impact rates: 2. Lunar impact-melt data regarding impact history. Icarus, 186, 11-23.

Long et al., 2022. Science Advances 8, eabq 2542.

Marchi, S., Bottke, W.F., Elkins-Tanton, L.T., Bierhaus, M., Wuennemann, K., Morbidelli, A., Kring, D.A., 2014. Widespread mixing and burial of Earth's Hadean crust by asteroid impacts. Nature, 511, 578-582.

Michael, G., Basilevsky, A., Neukum, G., 2018. On the history of the early meteoritic bombardment of the Moon: Was there a terminal lunar cataclysm? Icarus, 302, 80-103.

Nemchin, A., Timms, N., Pidgeon, R., Geisler, T., Reddy, S., Meyer, C., 2009. Timing of crystallization of the lunar magma ocean constrained by the oldest zircon. Nature Geoscience, 2, 133-136.

Norman, M.D., Adena, K.J.D., Christy, A.G., 2012. Provenance and Pb isotopic ages of lunar volcanic and impact glasses from the Apollo 17 landing site, Australian Journal of Earth Sciences 59:2, 291-306.

Shearer, C.K., 2006. Thermal and magmatic evolution of the moon. *In*: New Views of the Moon, Rev. Mineral. Geochem. 60, 365-518.

Ryder, G., 2002. Mass flux in the ancient Earth-Moon system and benign implications for the origin of life on Earth. Journal of Geophysical Research: Planets, 107, E4, 6-1.

Stöffler, D., 1990. Die Bedeutung des Rieskraters für die Planeten- und Erdwissenschaften, *In*: Rieskrater-Museum Nördlingen, Hrsg. von der Stadt Nördlingen, Verlag F. Steinmeier, Nördlingen, 2. Auflage 1991, 97-114.

Tera, F., Papanastassiou, D.A., Wasserburg, G.J., 1974. Isotopic evidence for a terminal lunar cataclysm. Earth and Planetary Science Letters 22, 1-21.

Zellner, N.E.B., 2017. Cataclysm No More: New Views on the Timing and Delivery of Lunar Impactors. Origins of Life and Evolution of Biosphere, 47, 261-280.

Zellner, N.E.B., 2019. Lunar impact glasses: Probing the Moon's surface and constraining its impact history. Journal of Geophysical Research: Planets, 124, 2686-2702.

Magmas, metasomatism, and melting – the Svecofennian orogeny in southernmost Finland

A. Saukko[1], K. Nikkilä[1], S. Fröjdö[1], O. Eklund[1] and M. Väisänen[2]

[1]Geology and Mineralogy, Åbo Akademi University
[2]Department of Geography and Geology, University of Turku
E-mail: Anna.Saukko@abo.fi

The evolution of the Svecofennian crust in the Hanko-Ekenäs area in southernmost Finland was a nearly 100 myr-long process involving metamorphic, metasomatic, and magmatic processes. Supracrustal rocks deposited during the early Svecofennian were deformed, intruded by granitoids, and significantly altered by fluids. Both the supracrustals and the intrusive granitoids were partially melted during the late Svecofennian.

Keywords: Svecofennian orogeny, granite, migmatite, metasomatic alteration

1. Introduction

The Svecofennian orogeny at *ca* 1.9-1.8 Ga formed or modified most of the crust in southern and western Finland. In southern Finland, evidence of partial melting is abundant in the Late Svecofennian granite-migmatite (LSGM) zone, a WSW-ENE belt of psammopelitic, metapelitic, and metavolcanic migmatites and anatectic granites (Ehlers et al., 1993). Edelman and Jaanus-Järkkälä (1983) proposed that a tectonic boundary separates the southernmost directly observable part of the Svecofennian domain from the rest of Southern Finland. Thus, the Hanko-Ekenäs coast and archipelago may have formed in a different setting than the LSGM zone and contribute to a more detailed picture of the Svecofennian orogeny.

2. Methods and lithological materials

To investigate the crustal evolution in the study area we combine field observations, petrographic examination, major and trace element whole-rock geochemistry, and U-Pb in zircon radiometric dating. We have also identified shear zones in the field and in pre-existing aeromagnetic and bathymetric data to discuss the petrological data in a tectonic context.

The study area rock types are supracrustal metatexites, granitic metatexites, even-grained granodiorites, and different kinds of leucogranites. *The supracrustal metatexites* are compositionally varied migmatised metavolcanic and metasedimentary rocks, some of which contain conspicuous non-primary K-feldspar megacrysts. The megacryst-bearing supracrustal metatexites resemble deformed granites. *The granitic metatexites* also contain K-feldspar megacrysts and were migmatised, but in contrast to the protolith of the supracrustal metatexites, they were originally plutonic granitoids. They are near-parallel to the schistosity of the supracrustal metatexites but crosscut them in places. In both types of metatexites, leucosomes have diffuse boundaries to the host rocks and melanosomes are absent.

The even-grained granodiorites are deformed grey granodiorites that display preferred mineral orientation. At some locations, the grey granodiorite gradually transitions into pink, granitic stripes of varying width. In contrast, *the leucogranites* of the area are non-oriented granites containing partially assimilated paleosome rafts. The leucogranites appear as the major rock type in the central part of the study area, but similar granite also appears as leucosomes among the metatexites. The leucogranites vary in appearance between predominantly red and

predominantly grey variants with inconclusive relative ages. At one location, an *altered leucogranite* contains quartz-poor and K-feldspar rich altered stripes.

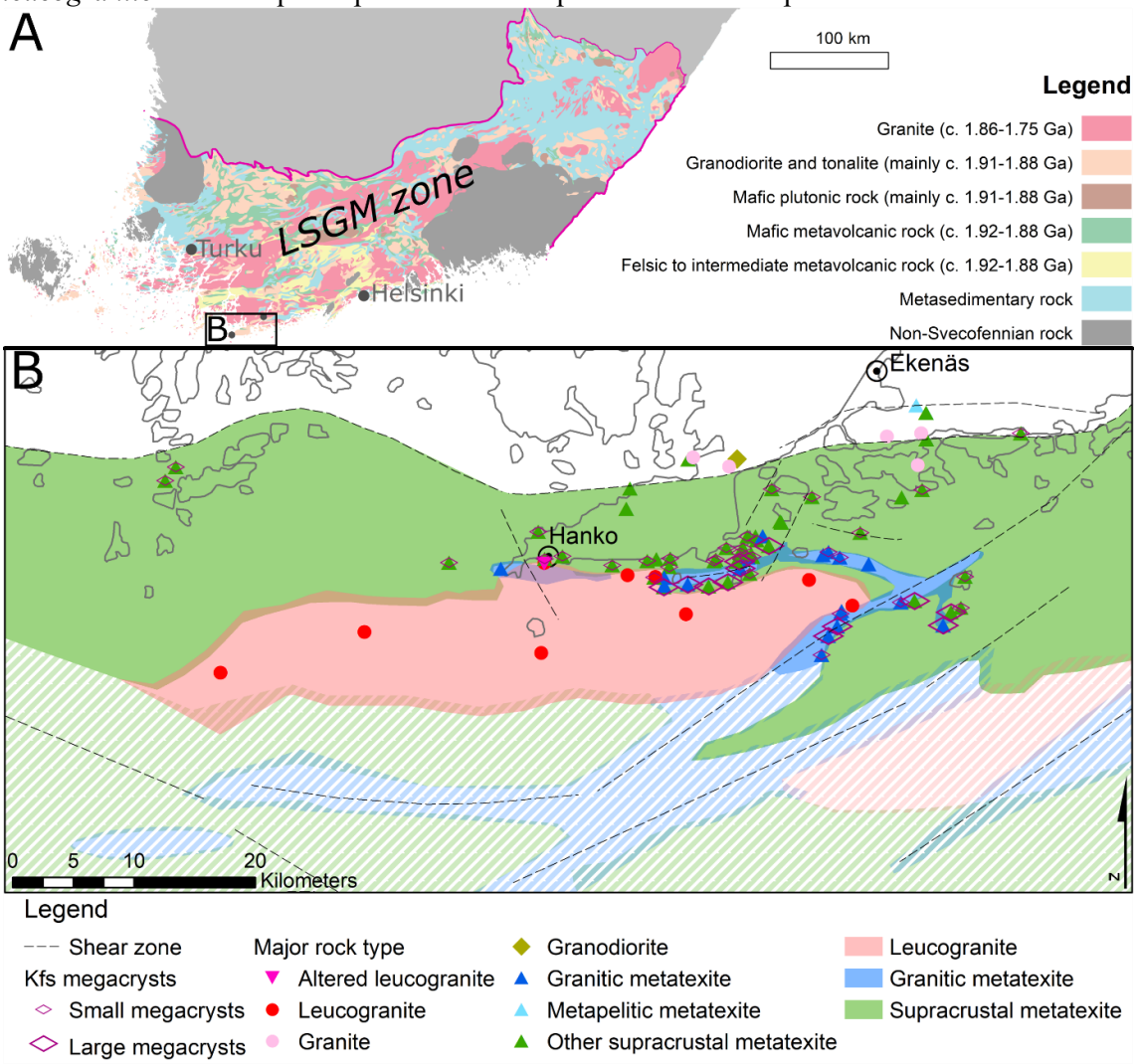

Figure 1. A) The Southern Svecofennian Subprovince. B) Map of the study area based on field observations, aeromagnetic maps, and previous lithological maps. To the North, the study area is bordered by the proposed tectonic boundary (Edelman & Jaanus-Järkkälä, 1983). The hatched filling indicates areas lacking any outcrops above the sea level.

3. Results

The U-Pb in zircon dating of migmatite samples reveals both protolith and migmatisation ages. The megacryst-bearing supracrustal metatexite source ages are around 1.89 Ga, whereas the granitic metatexite crystallisation ages are *ca.* 1.88 Ga. Leucosome crystallisation ages in both types of migmatites are *ca.* 1.82 Ga. The best estimate for the even-grained granodiorite crystallisation age is 1.87 Ga, although this age is only tentative due to large errors and small sample size. The leucogranite ages range from 1.85 to 1.82 Ga.

Geochemically, the granitic metatexites and leucogranites are mainly ferroan and calc-alkalic to alkali-calcic, whereas the even-grained granodiorites are mostly magnesian and distinctly calcic. The altered leucogranite is significantly more alkalic than any other rocks.

Apart from some of the even-grained granodiorites, which are metaluminous, all our analysed samples are weakly peraluminous. Even the leucogranites are only weakly peraluminous. Notably, the megacryst-bearing supracrustal metatexites are similar to the granitic metatexites in major element composition except for a wider variation in SiO_2-content.

The REE slopes of the even-grained granodiorites and granitic metatexites display similar basic shapes, but the granitic metatexites are more enriched in REE than the granodiorites. Compared to the even-grained granodiorites, the leucogranites are enriched in LREE but contain similar amounts of HREE. The altered leucogranite is heavily enriched in all REE except Eu and the heaviest REE (Er-Lu). The analysed supracrustal metatexites are different from each other and display different REE slopes than any of the granitoids.

P_2O_5, Zr, and Hf are mostly depleted in the leucogranites in comparison to the metatexites. These elements are significant constituents of apatite and zircon, the accessory minerals usually found as inclusions within biotite in our study area. As the leucogranites contain very little biotite compared to the migmatites, these mineral phases and elements are also depleted in them. Monazite is prevalent in leucogranites as well as in migmatites, and its compatible trace elements Rb, Th, U, and light REE are present in roughly similar quantities in these rock types, although the variation is a little higher among the leucogranites than among the metatexites.

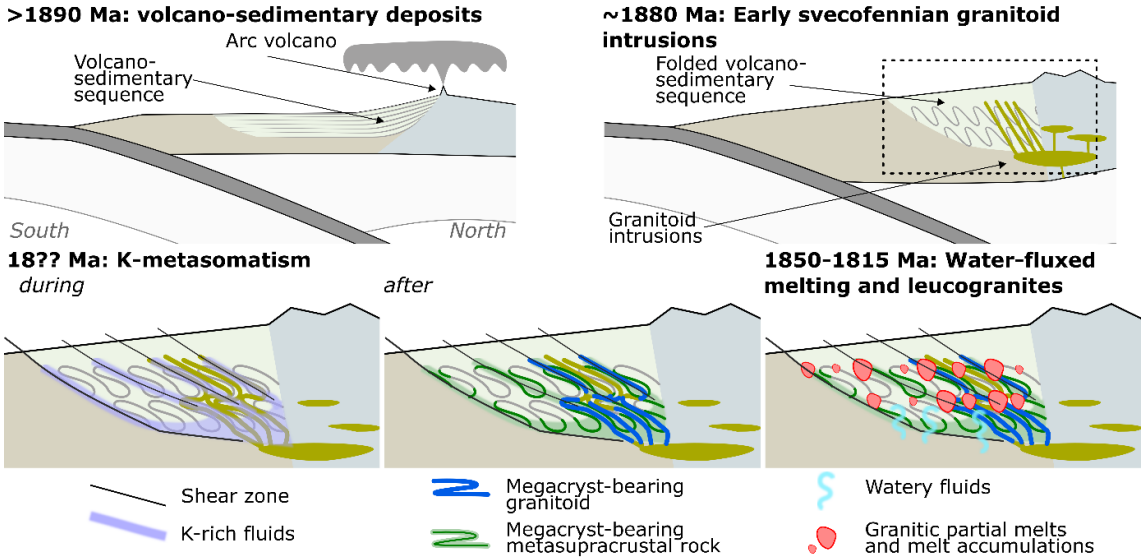

Figure 2. Schematic interpretation of the magmatic evolution in southernmost Finland. Present day north and south marked on the first picture.

4. Crustal evolution stages

I) Until ca 1.89 Ga: Volcano-sedimentary deposits

Supracrustals in the form of volcanic deposits interspersed by limestone and psammitic sediment layers. As pelitic sediments were rare during the deposition phase, and as very few zircons are older than 1.9 Ga, the supracrustal material likely came from the growing magmatic arc rather than an older craton.

II) Ca 1.88 Ga: Early Svecofennian granitoids

The early Svecofennian granitoid magmatism resulted in two different rock types: the even-grained granodiorites and the protolith of the granitic metatexites. As the dating results are not conclusive and no crosscutting relationships between the rock types were found in the

field, it is unresolved if they represent two distinct magmatic events with different sources, or if they share a common source but were altered in different ways during later processes. The protolith of the granitic metatexite intruded in folded supracrustal rocks through shear zones.

III) Metasomatic alteration

Non-primary K-feldspar megacrysts in originally supracrustal rocks are associated with the same shear zones where the protolith of the granitic metatexite intruded. The shear zones thus likely carried K-rich fluids that caused megacryst crystallisation in the hosts, resulting in granite-like composition in the originally supracrustal rocks. The timing of this metasomatic event is unclear: the fluids may have either originated in the granitoid magma that crystallized in the shear zones (meaning that the megacrysts in the granitic metatexite were a primary feature), or a later metasomatic event utilizing the same shear zones caused megacryst crystallisation in both the supracrustal and the granitoid rocks.

IV) 1.85-1.81 Ga: Water-fluxed melting and leucogranite formation

Fluid activity continued in the area during the late Svecofennian, as the mineral composition and leucosome morphology in the migmatites indicate water-fluxed melting (Weinberg & Hasalová, 2015). Although the age is concurrent with the migmatisation event in the rest of the southern Finland Subprovince (e.g. Huhma, 1986; Väisänen et al., 2002), dehydration melting was the main anatectic process in the LSGM zone (e.g. Andersen & Rämö, 2021).

The altered leucogranite was enriched in K_2O and depleted in SiO_2 in veinlike patterns. As the dated sample yields two non-overlapping zircon ages, it is possible that the older 1.84 Ga age represents the original crystallisation age of the leucogranite, and the younger 1.82 Ga age a later heat or melt pulse, possibly coinciding with the metasomatic alteration.

In the areas where the leucogranite is the major rock type, largely assimilated paleosome or residuum rafts are noticeably present within the leucogranite. The leucogranites may thus have stalled close to their source rocks rather than risen upwards in the crust. This stalling is consistent with previous work indicating that water-rich granitic magmas are not very mobile (García-Arias et al., 2015).

References

Andersen, T., Rämö, O.T., 2021. Dehydration Melting and Proterozoic Granite Petrogenesis in a Collisional Orogen—A Case from the Svecofennian of Southern Finland. Journal of Earth Science, **2**, 1289–1299. https://doi.org/10.1007/s12583-020-1385-8

Edelman, N., Jaanus-Järkkälä, M., 1983. A Plate tectonic interpretation of the Precambrian of the Archipelago of southwestern Finland. Geological Survey of Finland, Bulletin, *325*, 33. https://tupa.gtk.fi/julkaisu/bulletin/bt_325.pdf

Ehlers, C., Lindroos, A., Selonen, O., 1993. The late Svecofennian granite-migmatite zone of southern Finland-a belt of transpressive deformation and granite emplacement. Precambrian Research, 64 (1–4), 295–309. https://doi.org/10.1016/0301-9268(93)90083-E

García-Arias, M., Corretgé, L. G., Fernández, C., Castro, A., 2015. Water-present melting in the middle crust: The case of the Ollo de Sapo gneiss in the Iberian Massif (Spain). Chemical Geology, *419*, 176–191. https://doi.org/10.1016/j.chemgeo.2015.10.040

Huhma, H., 1986. Sm-Nd, U-Pb and Pb-Pb isotopic evidence for the origin of the Early Proterozoic Svecokarelian crust in Finland. Geological Survey of Finland, Bulletin, 337, 48 p. https://tupa.gtk.fi/julkaisu/bulletin/bt_337.pdf

Väisänen, M., Mänttäri, I., Hölttä, P., 2002. Svecofennian magmatic and metamorphic evolution in southwestern Finland as revealed by U-Pb zircon SIMS geochronology. Precambrian Research, 116 (1–2), 111–127. https://doi.org/10.1016/S0301-9268(02)00019-0

Weinberg, R. F., Hasalová, P., 2015. Water-fluxed melting of the continental crust: A review. Lithos, 212–215, 158–188. https://doi.org/10.1016/j.lithos.2014.08.021

Geochemical features of the felsic and intermediate igneous rocks in Pasalanmäki area in Archean Proterozoic boundary

A. Savakko[1], P. Mikkola[2] and E. Heilimo[1]

[1] Department of Geography and Geology, University of Turku, Finland
[2]Geological Survey of Finland, P.O. Box 1237, 70211 Kuopio, Finland
E-mail: aino.t.savakko@utu.fi

This study focuses on the felsic and intermediate plutonic rocks in Pasalanmäki area in Leppävirta, Eastern Finland. The bedrock in this area is part of the Archean–Proterozoic boundary in the Raahe-Ladoga shear zone. Whole rock geochemistry, especially REE-compositions revealed new views for the bedrock in this area as some of the rocks have chemical composition similar to adakites with low HREE-patterns.

Keywords: Fennoscandia, Svecofennia, Proterozoic, bedrock, geochemistry, Archean-Proterozoic boundary, Raahe-Ladoga shear zone

1.Introduction

Bedrock in Pasalanmäki area in Leppävirta has been a field of interest for many decades. Outokumpu Ltd studied the bedrock during the 1970s, but mostly from an economical point of view. The Outokumpu Ltd was interested in mafic and ultramafic intrusions found in the area and their possible economical potential related to nickel mineralizations (Parkkinen, 1974). Detailed field description of the bedrock in the area, let alone petrography, geochemical classification and the age of the rocks have remained unresolved.

In 2021 Geological Survey of Finland started a joint project with University of Turku, University of Oulu, and University of Helsinki, to study the bedrock in Pasalanmäki with modern methods. This part of the project focuses on the geochemical properties of felsic to intermediate plutonic rocks and gneisses, here we publish our preliminary results. Data are used to describe their petrological characteristics and to discuss their possible sources.

2. Geological background

The study area is located close to Raahe-Ladoga shear zone, on the Svecofennian side of the Archean and Paleoproterozoic boundary (DigiKP). The bedrock in the Pasalanmäki area and broader in Leppävirta was at least during the time when Outokumpu studied the area thought to be a part of the dome and keel structure (Parkkinen, 1974).

The key part of the currently favoured tectonic model for to the region is a continent-arc collision, in which Paleoproterozoic arc collided with the Archean craton at around 1.91 Ga ago (e.g. Lahtinen et al., 2015). The study area is currently considered as part of the colliding arc, and thus it should represent the older Svecofennian magmatism (1.93–1.91 Ga, DigiKP).

3. Methods

Samples used for this study were collected by two trainees in 2021. Altogether, 65 samples of felsic- and intermediate plutonic rocks and gneisses were collected. Thin sections from the samples were made in Geohouse, University of Turku. Whole rock geochemistry measurements were made by ALS Global using X-ray fluorescence (XRF) and inductively coupled plasma mass spectrometry (ICP-MS).

4. Results

During the field work, the rocks and collected samples were divided to dikes, gneisses, and plutonic rocks, based on mode of occurrence, grain size and degree of deformation. Samples that had grain size of 1-2 mm were named gneisses and samples that had larger grain size were classified as plutonic rocks. The dikes were separated as their own group. This division was done due to field hypothesis, which was based on two different magma sources.

We propose for the same samples redivision into six groups: tonalites (n=26), gneisses (n=19), granodiorites (n=10), dikes (n=8), granite (n=1), and gabbro (n=1), based on the modal composition and field observations. On TAS diagram (Figure 1) most of the samples create a rather continuous trend in which SiO_2 contents vary between 54 wt.% and 76 wt.%, granodiorites and dikes forming the SiO_2 richest end of this trend. Some samples have a high $(La/Yb)_N$ with low $(Yb)_N$ ratios indicating TTG/adakite composition (Figure 2). Some of the tonalite, gneiss and granodiorite group samples display a distinct positive Eu-anomaly on the chondrite normalised REE-diagrams, setting them apart from the majority which either lacks the anomaly or displays weakly negative Eu-anomaly (Figure 3a-c). In the dike group two samples show a very strong negative Eu-anomaly (Figure 3d).

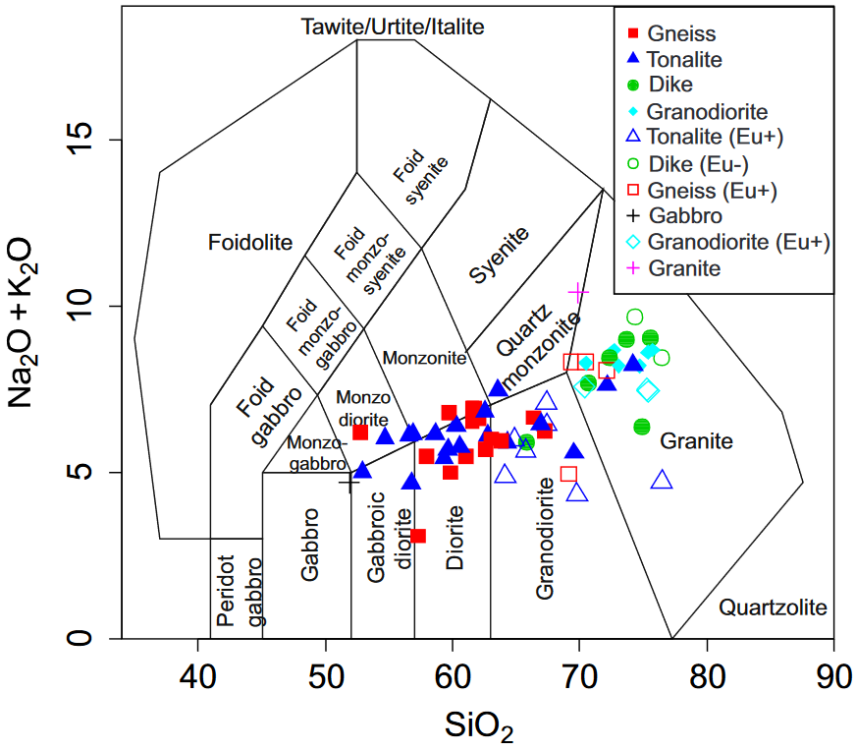

Figure 1. Total alkali versus silica (TAS) diagram for plutonic rocks (Middlemost, 1994) with the studied samples.

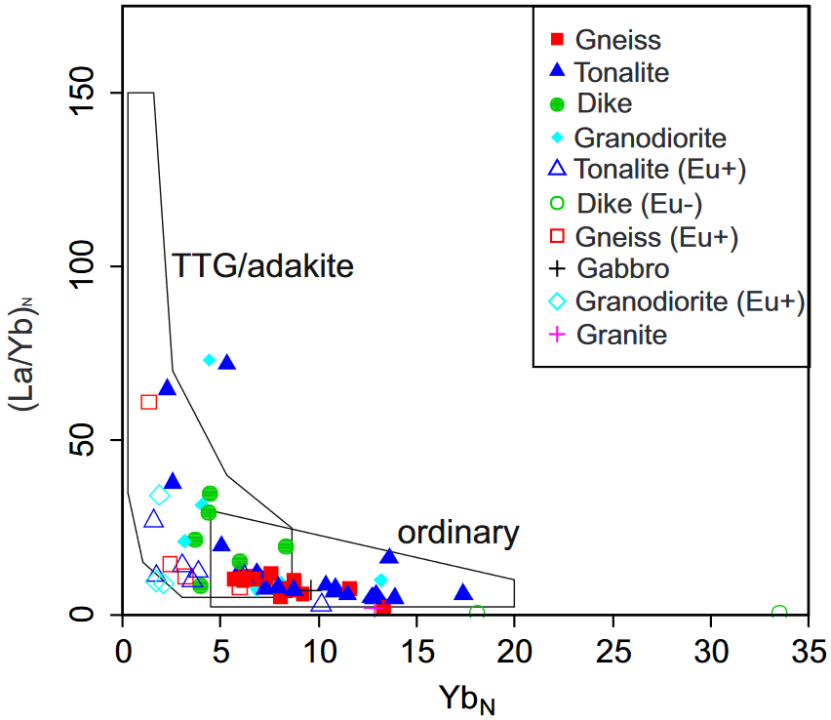

Figure 2. Diagram based on $(La/Yb)_N$ vs. $(Yb)_N$ for detecting TTG/adakite rocks by Martin (1986)

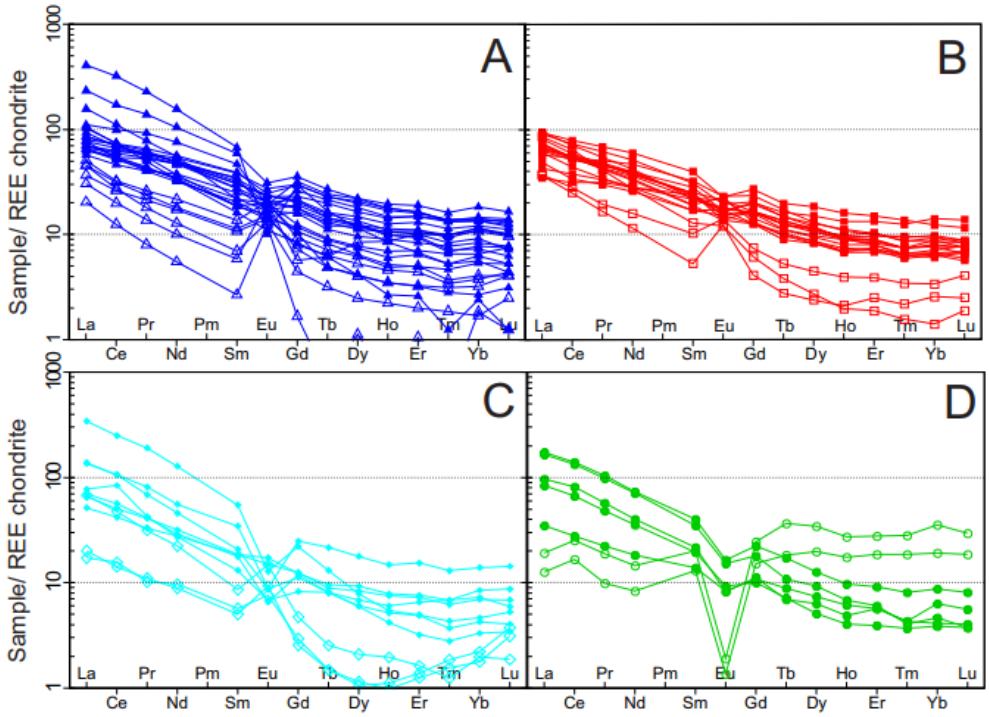

Figure 3. Chondrite normalised patterns of the Pasalanmäki samples. A) tonalite group, B) gneiss group, C) granodiorite group and D) dikes. REE-patterns are normalised after Boynton (1984) chondrite.

5. Discussion

After examining the whole rock geochemistry and revisiting the studied outcrops, the field hypothesis of two different magma sources, one for gneisses and another for plutonic units, has mostly been convert to hypothesis of single origin of the source magma due to similar geochemical characteristics. The elevated natrium contents might indicate similarities to 1.93-1.91 Ga older Svecofennian preorogenic plutonites (typically Na_2O > 3.0 wt. %). For the variable REE-patterns, two main hypotheses are considered.

In a study published by Mikkola et al. (2011) a possible cause for the type of REE-patterns where HREE content is low, was variable amounts of garnet in the residue where the parental magma originates from, as seen in some of the samples in tonalite, gneiss and granodiorite groups (Figure 3).

Origin of strong positive Eu-anomaly as seen in some of the samples in tonalite, gneiss and granodiorite group, could be related to rock forming minerals cumulation. Samples with positive Eu-anomalies could represent plagioclase cumulation and samples with negative Eu-anomalies rocks that originated from the remaining magmas (Mikkola et al., 2012; Mikkola et al., 2011). Furthermore, rocks that have negative Eu-anomaly and low in HREE contents could be derived from magmas generated from basaltic source in stability fields of both minerals, plagioclase, and garnet (Martin, 1986), which could be compatible explanation with the REE-patterns seen in tonalite, gneiss and granodiorite groups.

Some of samples in tonalite, gneiss, granodiorite, and dike groups, according to Figure 2, could be adakites. This is furthermore supported by the SiO_2 contents, which in these groups are over 56%, the calc-alkaline nature of the samples and the REE-patterns that are like adakites described by Martin (1999). Adakites have typically fractionated low HREE patterns, as seen in some of the samples in Figure 3a, 3b and 3c. This is due to garnet and amphiboles remaining in residual melts that generated adakites and they can show positive Eu-anomalies in REE-patterns as well (Martin, 1999).

References:

Boynton, W., 1984. Cosmochemistry of the Rare Earth Elements: Meteorite Studies. Developments in Geochemistry, Volume 2, 63-114.

Bedrock of Finland − DigiKP. Digital map database [Electronic resource]. Espoo: Geological Survey of Finland [referred 13.10.2022].

Lahtinen, R., Huhma, H., Lahayea, Y., Kousa, J., Luukas, J., 2015. Archean–Proterozoic collision boundary in central Fennoscandia: Revisited. Precambrian Research, vol. 261, 127–165.

Martin, H., 1999. Adakitic magmas: modern analogues of Archaean granitoids. Lithos, vol. 46, 411–429.

Martin, H., 1986. Effect of Steeper Archean Geothermal Gradient on Geochemistry of Subduction-Zone Magmas. Geology, vol. 14, 753-756.

Middlemost, E., 1994. Naming materials in the magma/igneous rock system. Earth-Science Reviews, vol. 37, 215-224.

Mikkola, P., Huhma, H., Heilimo, E., Whitehouse, M., 2011. Archean crustal evolution of the Suomussalmi district as part of the Kianta Complex, Karelia: Constraints from geochemistry and isotopes of granitoids. Lithos, vol. 125, 287–307.

Mikkola, P., Lauri, L., Käpyaho, A., 2012. Neoarchean leucogranitoids of the Kianta Complex, Karelian Province, Finland: Source characteristics and processes responsible for the observed heterogeneity. Precambrian Research, vol. 206–207, 72–86.

Parkkinen, J., 1974. Raportti Leppävirran aluetutkimuksesta 1968–73. Outokumpu Oy:n malminetsintä, raportti 020/3241,3242,3234/JYS/74. 296 p. (in Finnish)

Plans and Actions with FIN-GEO

M. Seitsamo-Ryynänen[1] and M. Kotilainen[1]

[1]University of Helsinki, PL 64, 00014 Helsingin yliopisto
E-mail: minja.seitsamo-ryynanen@helsinki.fi

Keyword: FIN-GEO Education Collaboration Network is a Ministry of Education and Culture funded joint project for 2021-2023. The project aims to improve and formalize Geoscience education collaboration between the partners.

Keywords: geoscience education, collaboration, Finland

1. General

Collaboration between geology and geoscience departments of the Finnish universities and the Geological Survey of Finland has a long tradition. Over the years this collaboration has enabled high tech research infrastructures and novel research projects as well as education for benefit to all parties. For instance, joint courses on advanced bedrock mapping or clastic sedimentology have been active over twenty years. So, when the Ministry of Education and Culture opened a special call for network-like development of higher education, Aku Heinonen saw the possibility for a new opening. Further co-operation on strengthening the level and scope of geoscience degrees in all Finnish universities.

FIN-GEO Education Collaboration Network is a joint project of five universities offering education in geoscience and adjacent fields in Finland: University of Helsinki, University of Oulu, University of Turku, Åbo Akademi University and Aalto University. The project is funded by Ministry of Education and Culture for three years (2021-2023) and aims to improve and formalize education collaboration between the partner universities.

The project is led by Mia Kotilainen from the Geosciences and Geography Department of the University of Helsinki. The other members of the steering group are Esa Heilimo (UTU), Kari Strand (OU), Olav Eklund (ÅA), and Jussi Leveinen (Aalto). The network's coordinator Minja Seitsamo-Ryynänen is responsible for the network's practical side. In addition to the steering group, a wider working group consisting of personnel from all partner universities is involved in the network's operations. The scope of the project also includes the entire staff and students participating in education in the field of Geosciences at the network universities.

2. Activities

FIN-GEO activities include developing joint teaching materials and courses, educational and pedagogical training for geoscience teachers, and improving the visibility of Geoscience education in Finland.

The first major task of the project was the national “Geo-Expert 2030” study of needs that was executed in late 2021. The survey was conducted to map out industry and stakeholder views on the geoscientific expertise required in the developing geoscience education on a 10- to 20-year timescale and to better prepare geoscience graduates who enter the work force in the future. The full results of the survey are posted on the website of the FIN-GEO network.

Several online and MOOC courses are being prepared, e.g. about Finnish bedrock, geochemistry, structural geology and geological sustainability. The network also offers

pedagogical support for the planning and implementation of joint teaching materials and online courses by organizing workshops a couple of times a year (Figure 1).

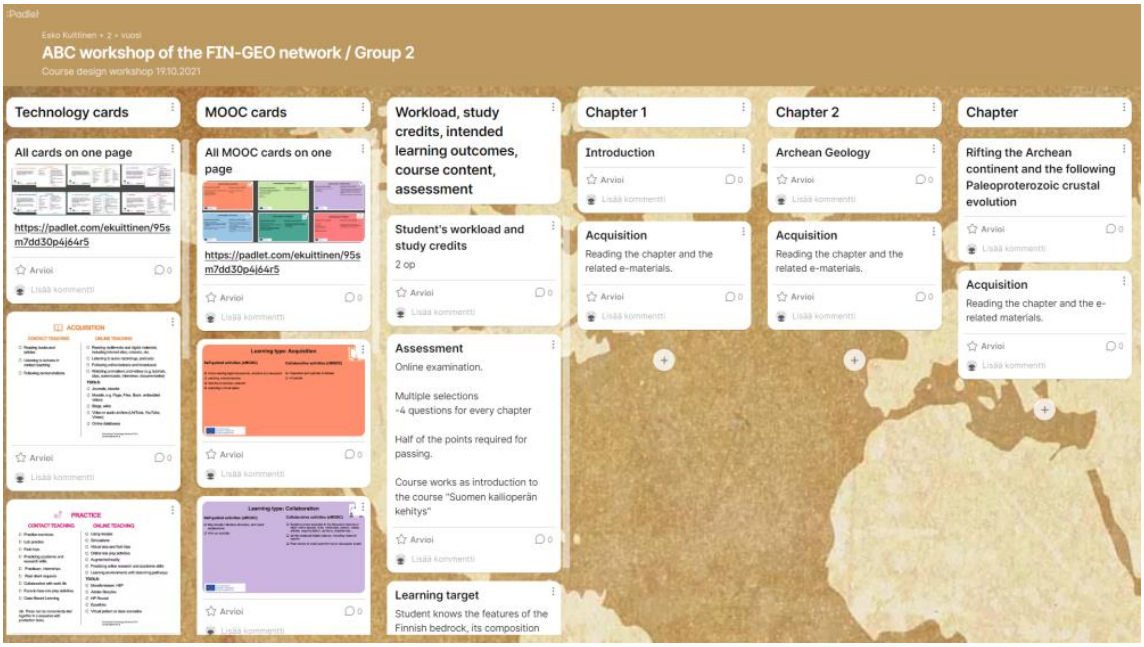

Figure 1. Pedagogical workshops and info sessions are organized to support development of joint teaching materials and online courses.

3. Today´s goal

In our presentation we present the current status of the project and invite discussions and ideas for the last 14 months of the FIN-GEO actions and future collaboration.

Additional information about the network activities and information on how to get involved are available from the authors and the website of the FIN-GEO network: https://fingeokoulutus.edublogs.org/

Introduction to project SEMACRET: Sustainable exploration for orthomagmatic (critical) raw materials in the EU: Charting the road to the green energy transition

S. Yang[1], E. Kozlovskaya[1] and SEMACRET consortium
[1] Oulu Mining School, University of Oulu, Oulu, Finland
E-mail: shenghong.yang@oulu.fi

Critical raw materials (CRMs) are fundamental to the EU industrial value chains and strategic sectors, particularly with regard to the green energy transition. Currently, the EU domestic supply of primary CRMs is below 3% for many important commodities. To obtain an improved understanding of the EU's critical raw materials potential, discover new ore deposits and thereby increase the internal sourcing of CRMs and secure its raw materials autonomy, the EU aims to boost the exploration and production of CRMs. This project is designed to develop socially and environmentally sustainable means of exploration for orthomagmatic CRMs. We will generate improved ore models for orthomagmatic mineral deposits which will be translated to mappable exploration criteria to delineate areas of high exploration potential, from regional scale to local scale. Through collaboration between geosciences and social sciences the project will also develop methods to promote social awareness of the importance of responsible exploration and mining. Further, we will map the exploration and production potential of CRM in the EU and key CRM supplier countries.

Keywords: exploration, green transition, critical raw material, orthomagmatic ore deposit

1. Introduction

To reduce the amount of drilling the efficiency of the exploration method needs to be maximised while improving the discovery rate. One way to achieve this is to improve the understanding of ore formation. A major advance in understanding ore deposits has been made with the application of the Minerals Systems Approach. Different from traditional exploration, this acknowledges that the formation of ore deposits is dependent on the interplay of several critical geological components, namely the presence of a metal source, a fluid pathway and a metal sink. If an area lacks one of these components, an ore deposit cannot form. In theory, this allows distinguishing prospective from non-prospective areas, making targeting more efficient. However, there remains controversy about the specific nature of the source, pathway and sink components (Barnes et al., 2016). In addition, it has proven challenging to translate the three components to exploration criteria that can guide explorers at both the regional scale (so-called greenfield exploration) and the local deposit scale (so-called brownfield exploration). There are several additional challenges for the exploration industry and governmental decision-makers in the EU: The social awareness of the significance of raw materials and their sustainable sourcing in the EU is relatively low and heterogeneous, which hampers the implementation of efficient exploration. Also, the amount of information on mineral resources and mineral potential in the EU is limited, and the currently reported resources are following different standards, making it difficult to integrate the data. The overarching goal of this project is to provide a clearer understanding of the EU's mineral potential, and to develop sustainable exploration techniques for green transition (critical) raw materials hosted in orthomagmatic ore deposits, thereby bridging this gap between academic research and the mineral exploration industry.

2. Project objectives and approach

Ore model refinement following the Mineral Systems Approach (WP1-OB1)

It was proposed several decades ago that the formation of orthomagmatic ore deposits is largely understood, yet the recent discovery of major ore deposits downdip of existing deposits in the

Bushveld Complex of South Africa, with a history of exploration and mining dating back a century, proves that this view was overly optimistic. The uncertainty in geological models results in serious limitations to our predictive capabilities for the exploration of critical metals, increasing the environmental footprint of exploration. A major advance has been the development of the Mineral Systems approach considering fundamental source-pathway-sink processes to identify regions of high exploration potential. However, there remains considerable controversy for each component. In this project we will refine the ore formation models using geochemistry, computational modelling and high temperature experimental study.

Developing methods for regional-scale exploration targeting (WP2-OB2)

Regional-scale (greenfield) exploration is particularly challenging as it usually is entirely conceptual, i.e. it cannot rely on historical discoveries. McCuaig et al. (2010) translated critical ore-formation factors defined under the scope of the Mineral Systems Approach to mappable proxies using multiple geoscience datasets including geophysics, geology and geochemistry. The multiple data layers can then be integrated on a GIS platform to generate prospectivity maps distinguishing areas of low and high exploration potential. In the present project, based on the refined ore model (see above section), we will define proxies reflecting all the components of the Mineral Systems Approach including 'source', 'pathway' and 'sink' to guide regional exploration targeting for orthomagmatic deposits.

Developing methods for brownfield exploration targeting (WP3-OB3)

Because ore deposits typically occur in clusters, explorers can assume that areas surrounding existing ore deposits are relatively prospective. They can use existing geodatabases as a starting point to develop refined ore models, and they can use the existing infrastructure to access deeper portions of the crust. Also, the Mineral Systems Approach is easier to apply as the 'source' component is not relevant, and research can focus on the 'pathway' and 'sink' components. For these reasons, brownfield exploration is often considered less challenging and more fruitful. However, as in the case of greenfield exploration, there is ample room for increasing efficiency. In this study, we will improve existing techniques (notably surficial geochemistry) and develop new techniques (notably 3-D modelling and inversion of ground and airborne geophysics), and introduce new machine learning tools for 3D prospectivity modelling using random forest methods.

Surficial geochemical exploration (upper soil, plant chemistry) allows to delineate geochemical domains and anomalies with low to zero environmental impact. It can be applied as well in agricultural used areas as in environmental protection areas. In this study, the focus lies on testing under different surface conditions with different host rocks how the use of surface media can be calibrated to find hidden mineralization of Ni-Cu dominated sulphide deposits and Cr-V-PGE dominated deposit. We will develop new data analytical tools and improve existing concepts, codes and guidelines to better filter relevant information for exploration from the highly variable surface geochemical data. The approach includes how to implement information about the mineral system, geology, geophysics and knowledge about the surface media to provide statistical models for target determination.

Traditionally, resource estimation has relied on intensive drilling. The main challenge is to predict metal grade in three dimensions, especially in complex ore bodies, where the continuity of mineralization is not always guaranteed. Supervised machine learning (ML) methods have been successfully applied to resource modelling, increasing the accuracy of resource estimation compared to the traditional geostatistical methods (e.g., kriging), but the

method has not yet been applied to orthomagmatic deposits. In this study, we will apply ML to improve resource estimation in ore deposits.

Promote social awareness (WP4-OB4)

Social awareness of the importance and ethical sourcing of raw materials is critical for the sustainable supply of CRMs. Because of the many negative environmental and social impacts, mineral exploration and mining have started to receive more attention from traditional and social media platforms. Social acceptance of exploration and mining has become the key challenge for the whole sector. Awareness plays an important factor in molding acceptance which depends on the perceived impacts at the regional and local levels, but it is also driven by broader societal trends, discourses, and narratives (Boutillier 2021).

Against this background, we aim to investigate the preconditions and practices for gaining social awareness and acceptance for exploration and mining for CRMs. The other aim is to promote awareness about the significance of CRMs to broader audiences. The work focuses on the elements of awareness and acceptance of mining activities at two levels: 1) at the level of local (community) stakeholders and 2) at the level of media, social media, and policy narratives. The main stakeholders are citizens, exploration and mining companies, environmental organizations and other NGOs, municipalities, local and regional environmental authorities, geologists, investors, and the media.

Exploration and production potential survey in the EU and globally (WP5-OB5)

The future metal needs of the EU are such that they are unlikely to be met entirely by internal production. Imports of CRMs will thus remain a key pillar of the EU's CRM strategy. This requires a reliable survey of the exploration and production potential for CRMs in the EU and globally. For mafic-ultramafic mineral systems, Mudd et al. (2018) have published a database of known mineral resources and ore reserves. However, this database is mainly based on the JORC code, and data on many historic and recent exploration projects have not been included. In the EU, the UNFC (United Nations Framework Classification for Resources) code is recommended to harmonize the mineral resource data. Horn et al. (2020) has been the first to apply UNFC to the of cobalt (Co) mineral resources in the EU. In this study, we will update the available mineral resource database related to key commodities of orthomagmatic ore deposits (Ni, Cu, PGE, V, Ti, Cr), in a harmonized form using UNFC and UNRMS (United Nations Resource Management System) (UNECE, 2019).

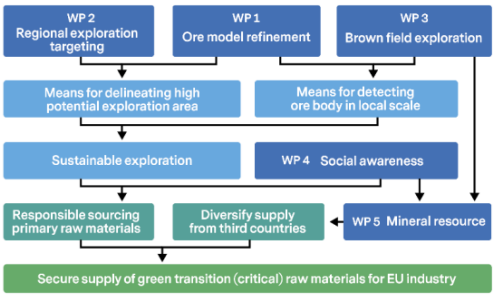

Figure. Structure of working packages and their links.

3. Reference sites

To address the objectives of the project, we have chosen several reference sites (Table 1). These include the most significant prospective regions in the EU: 1) Lapland Belt in Finland, 2) Variscan orogenic belt in Portugal, and less explored areas yet with all the hall marks of

enhanced orthomagmatic ore potential including, 3) Bohemian belt in the Czech Republic, 4) Suwalki anorthosite belt in Poland, and 5) Sleza ophiolite in Poland. In addition, the chosen reference sites represent different tectonic settings, including continental rift zones, orogenic belts and ophiolites, and different mineralization styles varying from Ni-Cu-(Co-PGE) deposits in magma conduits (Ransko, Czech Republic) to sulphide-poor V-PGE-Cr-(Ni-Cu-Co) deposits in layered intrusions (Akanvaara/Finland, Beja/Portugal) and V-Ti-dominated oxide deposits in transitional (partly massive-type, partly layered) anorthosite complexes (Suwalki/Poland) (Table 1). The reference sites represent areas of variable exposure, different social and cultural environments.

Table 1. reference sites of regional metallogeny and key deposit in local scale

Site	Metallogeny	Tectonic setting	Key deposit in WP3	Country	Exploration maturity	Exploration potential
1	Lapland	Rifting	Akanvaara V-Cr-PGE	Finland	Relatively high	Highest
2	Variscan	Orogeny	Beja V-Ti	Portugal	Moderate	High
3	Bohemian	Orogeny	Ransko Ni-Cu-(Co-PGE)	Czech	Low	High
4	Suwalki	Post collision	Suwalki (Ti-V)	Poland	Low	Medium
5	Sleza	Ophiolite	Strzegomiany-Kunów V-Ti	Poland	Low	Medium

4. Expected result

Using Mineral Systems Approach in exploration for orthomagmatic ore deposits, comprehensive mineral resource mapping of exploration and production potential of (critical) raw materials in orthomagmatic ore deposits in EU and third countries, in harmonized with UNFC and UNRMS reporting standards. Low environmental impact geophysical and geochemistry exploration methods, 3D prospectivity modelling and resource modelling using machine learning. Development of sustainable exploration solution, promote social awareness of exploration and mining. The long-term impact would be efficient exploration targeting resulting in new discoveries in the EU, and diversify supply of critical raw materials from third countries. Transparency and improved comparability of assessments of mineral resource exploration and production potential; Better policymaking for raw materials supply in EU. Resilient, sustainable and secure (critical) raw mate-rials value chains for EU industrial ecosystems, in support of the twin green and digital transformations.

Acknowledgements: The SEMACRET project number is funded by Horizon Europe and UKRI during 6/2022-5/2025.

References:

Barnes, S.J., Cruden, A.R., Arndt, N. et al., 2016. The mineral system approach applied to orthomagmatic Ni–Cu–PGE sulphide deposits. Ore Geol. Rev., 76, 296-316.

Boutilier, R.G (2021) From metaphor to political spin: Understanding criticisms of the social license. Extr. Ind. Soc., 8, 100743.

Horn, S., Gunn, A.G., Petavratzi, E., Shaw, R., Eilu, P., Törmänen, T., Bjerkgård, T., Sandstad, J.S., Jonsson, E., Kountourelis, S., Wall, F., 2020. Cobalt resources in Europe and the potential for new discoveries. Ore Geol. Rev., 103915.

McCuaig, T.C., Beresford, S., Hronsky, J., 2010. Translating the mineral systems approach into an effective exploration targeting system. Ore Geol. Rev. 38, 128–138.

UNECE. 2019. United Nations Framework Classification for Resources, Update 2019. UNECE Energy Series 61. 20 pages.

Fracture-controlled glacial erosion - using outcrops analogues to model the erosional signature of unexposed faults

P. Skyttä[1], E. Ruuska[1], T. Lindqvist[1,2], K. Ahlqvist[1]

[1]Department of Geography and Geology, FI-20014 University of Turku, Finland
[2] Geological Survey of Finland, P.O. Box 96, FI-02151 Espoo, Finland
E-mail: Pietari.skytta@utu.fi

This paper presents the structural evolution of the Siilinjärvi carbonatite complex from the initial ultramafic magma intrusion through.

Keywords: fault, fracture, glacial erosion, topography, digital elevation model

1. Introduction

Areas of aerial scour are characterized by rugged and uneven bedrock surfaces that received contributions from glacial abrasion, quarrying and glacial ripping (e.g. Glasser et al., 2020; Hall et al., 2020). The style and effectivity of erosion is controlled by the lithological (e.g. Sugden, 1978) and structural properties of the bedrock. Foliation and other anisotropies have been recognized to provide some contribution towards the character of the developed erosional features (Glasser et al., 1998). However, brittle structures are even more important as they are utilized by glacial quarrying that leads to overall higher erosion rates and distinct topographic signatures such as elongate depressions along the bedrock surface that result from syn-glacial removal of preferentially weathered domains of bedrock (Krabbendam & Bradwell, 2014). In this work we address how the fracture type (e.g. joint, extension fracture, shear fracture, fault) affects the erosion style and effectivity, and how this understanding could be used to model the erosion signatures, and indirectly, the size and architecture of unexposed faults. The results will provide input into regional lineament interpretations and compilation of scaling laws for faults occurring within the crystalline rocks.

2. Data and methods

We used field mapping and orthophotography the from the Geta area, Åland Islands. We classified the fractures and evaluated their significance for the developed erosion surfaces (Figure 1C) and summarized the findings into conceptual models over fracture-control in glacial quarrying.

3. Results and discussion

The result indicate that indivual fractures or fracture swarms will not lead to the formation of laterally continuous elongate topographic depressions. By contrast, larger shear fractures that are linked (e.g. step-over fractures) and distinct faults with gouge-bearing core domains lead to the generation of distinct valleys along the bedrock surface, and the character of these valleys can be linked to the architecture of the fault (comprising core and damage zones). Future work aims at generating a catalogue of the properties of the faults and the associated erosion surfaces for well-outcropping areas, and using this understanding as guidelines for interpreting the unexposed faults. This involves assessments about e.g. the width of the core and the damage zone, topographic signatures of the erosion surface (rougness, asymmetry) and the thickness of the overburden (Figure 1B).

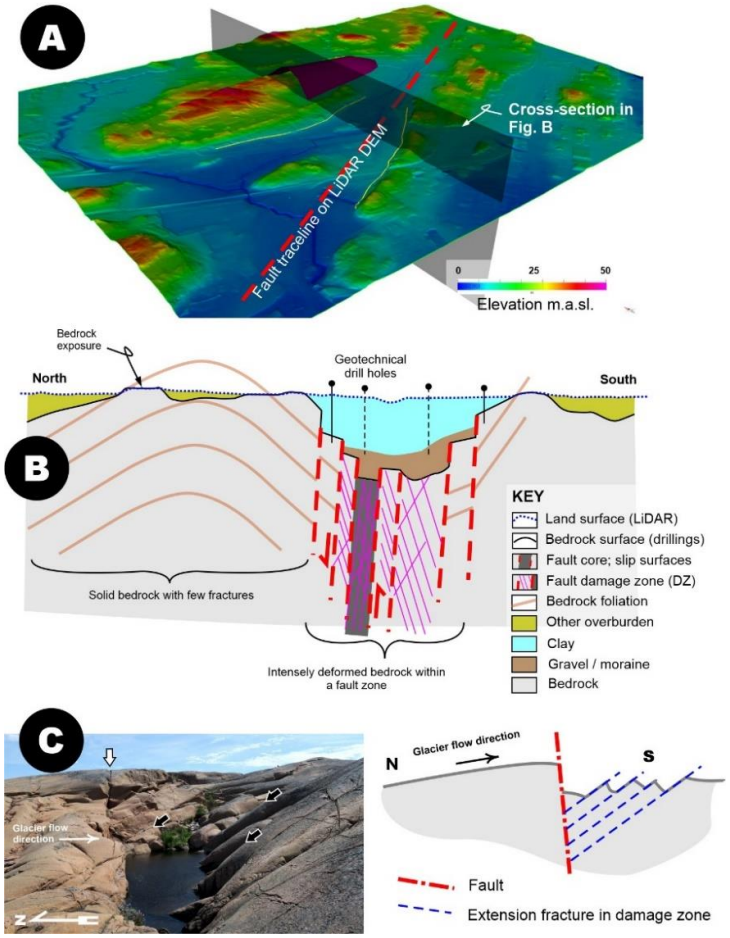

Figure 1. A: Lineament interpreted form LiDAR data (National Land Survey). B: A cross-sectional view over the lineament in A, showing the inferred architecture of the fault and the surrounding damage zone, and their influences over the morphology of the topographic depression, and thickness of the overlying sedimentary material. C: A field photo and corresponding line drawing illustrating how an indivivual fault surface and the associated extension fractures control the glacial erosion processes and the bedrock surface morphology.

References:

Glasser, N. F., Crawford, K. R., Hambrey, M. J., Bennett, M. R., Huddart, D., 1998. Lithological and structural controls on the surface wear characteristics of glaciated metamorphic bedrock surfaces: Ossian sarsfjellet, svalbard1. Journal of Geology, 106 (3), 319–329. https://doi.org/10.1086/516025

Glasser, N. F., Roman, M., Holt, T. O., Žebre, M., Patton, H., Hubbard, A. L., 2020. Modification of bedrock surfaces by glacial abrasion and quarrying: Evidence from North Wales. Geomorphology, 365. https://doi.org/10.1016/j.geomorph.2020.107283

Hall, A., Krabbendam, M., van Boeckel, M., Goodfellow, B., Hättestrand, C., Heyman, J., Palamakumbura, R., Stroeven, A., Näslund, J., 2020. Glacial ripping: geomorphological evidence from Sweden for a new process of glacial erosion. Geografiska Annaler, Series A: Physical Geography, 102(4), 333–353. https://doi.org/10.1080/04353676.2020.1774244

Krabbendam, M., Bradwell, T., 2014. Quaternary evolution of glaciated gneiss terrains: Pre-glacial weathering vs. glacial erosion. Quaternary Science Reviews, 95, 20–42. https://doi.org/10.1016/j.quascirev.2014.03.013

Sugden, D.E., 1978. Glacial Erosion by the Laurentide Ice Sheet. Journal of Glaciology, 20(83), 367–391. https://doi.org/10.3189/s0022143000013915

Critical Earth Resources: an Estonian Contribution

A. Soesoo[1]

[1]Tallinn University of Technology, Ehitajate tee 5, Tallinn 19086, ESTONIA
E-mail: alvar.soesoo@gmail.com

In this article I describe the occurrences and types of the main Earth resources of Estonia: oil shale, phosphorite, iron sulphide ore, black shale, limestone and dolostone.

Keywords: Earth resources, iron ore, phosphorite and rare earth elements, oil shale, carbonate rocks, black shale, Estonia

1. Introduction to the Concept

A good question is – what is a critical resource at the moment in the Nordic and Baltic region? It depends on what kind of the world's political-economic-technological architecture we are living now and what are our (country's) needs for the coming future. There are very different options – both country-wise and regionally. Generally, a country will not accept changes diminishing the present lifestyle and economy. This itself is the biggest limitation for the current way of global development.

Earth resources criticality is the concept that mainly evaluates economic and technological dependency on a certain raw material or element. Commonly it also includes a variable which assesses the probability of supply for a defined region, stakeholder group and in many cases the timeframe. However, in most of the Earth resources criticality concepts, not enough focus has been set on the present environmental-social-economic situation where people have confronted with environmental and climate changes, fast-growing population in a number of regions, shortage of food/good soil, drinking water and raw materials in general, rising pandemic and military issues. The very late history has already shown that several international agreements may not hold, and resources have become central for national development and they are survival indicators in some niches of present life. In this respect, a new approach is needed to map, assess, and develop country's resources for overall good.

The European Green Deal (GD) is just an example of a New Era in development of the sustainable environmental-social-economic realm of the planet, but also the region. If taken separately, GD is a challenge to change historical way of using energy resources. However, at present, import and export trajectories of the classical energy resources have changed, at least for some periods of time. So, the concept of raw material criticality is changing too by giving it much broader definition, but at the same diminishing the size of region.

Historically, very little attention has been put on the raw material criticality of small counties, where the EU CRM list may have even minor relevance in some countries. For example, Estonian economy and social-environmental development is vastly dependent on raw materials like gravel, sand, carbonate rocks for construction sector, and it has been dependent recently on oil shale in the power generation. In rebuilding these and other sectors in a more sustainable way in a small country, the geomaterial criticality concept needs to be re-addressed in Nordic and Baltic countries and available supply lines defined in the region for available geomaterials.

Estonia is rich in mineral resources. For example, oil shale usage has over 100 years of history and Estonia has the biggest phosphate resources in Europe. Some resources are known, some are not so well known presently. Oil shale was just a few months back regarded as one of

the most polluting energy resources in the country. However, the present accumulated crises (in plural) will change the view on local resources in most of the countries in Europe. So, let's map better our available resources!

2. Basics of Geology of Estonia

Estonia is situated in the central part of the Baltica paleocontinent, so being a part of the East European Craton. The crust consolidated during the Svecofennian Orogeny in the Paleoproterozoic. The crystalline rocks are covered by Late Proterozoic (Ediacaran) to Lower Paleozoic (Cambrian to Devonian) sedimentary rocks, with thicknesses from 100 m (in the north) to 800 m (in the South and SW Estonia; Soesoo et al., 2004). Precambrian rocks do not outcrop anywhere in Estonia but are present in the subsurface. The surface of the crystalline basement dips gently to the south. The boundary between the Neoproterozoic to Paleozoic sedimentary sections of Baltica and the Precambrian Fennoscandian Shield extends along the seabed of the Finnish Bay of the Baltic Sea in northern Estonia.

3. Energy resources

Probably the most important resource in Estonia at the moment is oil shale. Estonian oil shale – kukersite - with mining history over 100 years, is a Late Ordovician (deposited some 460 Million years ago) organic-rich sedimentary rock. The kukersite deposits are possibly the world's second highest-grade (after the Australian torbanite) oil shale deposits with its organic content from 15% to 55% (calorific value is 15 MJ/kg (3,600 kcal/kg) and its Fischer Assay oil yields of 30 to 47%. The largest kukersite deposits in Estonia – the Estonian and the Tapa – cover about 3,000 km^2. The mined kukersite resource is more than 1,2 Billion tons, while the total kukersite resource is estimated about 4.63 Billion tons. So, the Estonian kukersite represents about 1.1% of global and 17% of European oil shale resources. Even the direct combustion of oil shale in power plants is not economically and environmentally plausible in the future, the Estonian oil shale has been the ground for Estonian energy independence for years. A new technological breakthrough is needed in the oil shale sector to support energy independence during long years before Estonia and Europe, and most of the world are achieving better and greener energy sources to support everyday's life.

Estonian Ordovician black shale (graptolite argillite) and Cambrian–Ordovician shelly phosphorite are also the sources for uranium and thorium (Soesoo et al., 2020). The Estonian black shale contains 5.667 million tons of U and about 0.5 Mt of Th. The phosphorites contain about 150 to 180 thousand tons of uranium. The Sillamäe (NE Estonia) radioactive waste depository contains about 1200 tons of U and 800 tons of Th.

4. Metal and other critical elements and raw material resources in the Lower Paleozoic sedimentary rocks

Phosphorus and REE: Estonia holds, the largest in Europe, unused sedimentary phosphate rock reserves about 3 Billion metric tons. These sediments with Brachiopod shells deposited approximately 488 million years ago. The shells and detritus contain up to 35–37 wt% P_2O_5. Present studies have revealed relatively enriched, but variable content of rare earth elements (REE) in phosphate shells. For example, La in single shells ranges 50 to 600 ppm, Ce – 40–1300, Pr - 4–170, Nd – 20–850, Sm – 3–200 and Gd – 4–155 ppm. The total REEs can reach 3600 - 4000 ppm, ranging in average from 1000 to 2600 ppm (Soesoo, present studies, 2022). Today, the Estonian phosphorites were regarded as economically not yet feasible for REE production, but considering REEs as a co-product of phosphorous production, it may economically be well feasible in the present development of the World political-technological

architecture.

Relying on the vast phosphorite reserves in Estonia, the critical nature of both the phosphorus and REEs for the European economy and security, this may be an important economical tool for the Nordic – Baltic region in coming years. Bearing in mind the classical mining operations with an annual production of 5 Mt tons of ore, the estimated annual total REE amounts will be 720 tons at REE^{tot} = 1200 ppm, or 900 tons at REE^{tot} = 1500 ppm (Soesoo et al., 2020). In addition, about 120 tons of uranium and 27 tons of thorium can be extracted each year. Most likely the annual production in future can be much higher.

Carbonate rocks: Carbonate sedimentary rocks – limestones and dolomites (dolostones) – are widespread within the rock sections of the Estonian Paleozoic basement. These carbonate sediments were deposited about 470-360 Million years ago. Dolomite as well as limestone has been and still is an important raw material in Estonia and it is used for different purposes locally and abroad. Historically, these carbonate rocks were used in construction. In medieval ages the usage of carbonate rocks increased remarkably, and they became the main construction material in castle and town building. The carbonate rocks from coastal quarries and stone quarries were exported to Germany, Russia, Latvia and Nordic countries. The dolostone (total of technological, construction, filling and other exploitation groups) was mined in 2021 in 37 mines as total of was 834 thousand m^3. Most of mined dolostone was used in building construction activities. The active resources of the Estonian dolostones (@ 31.12.2021) are as high as 100 940 thousand m^3, while active reserves are 199 647 thousand m^3 and passive reserves are about 83 230 thousand m^3 (Estonian Land Board: www.maaamet.ee). The limestone was mined in 2021 in 61 mines. Total amount of mined limestone was about 2491 thousand m^3. Vast amount of the mined limestone was used in building construction activities. The active resources of the Estonian limestone (@ 31.12.2021) are as high as 245 310 thousand m^3, while active reserves are 309 606 thousand m^3 and passive reserves are about 494 126 thousand m^3 (Estonian Land Board: www.maaamet.ee).

Metals in black shale: Although Estonian kukersite is low in metals, there is another type of oil shale known as black shale (graptolite argillite). The graptolite argillite is of sapropelic origin and is characterized by high concentrations of a number of metals, for instance: U (up to 1200 ppm), Mo (1000 ppm), V (1600 ppm), Ni and other heavy metals, and the rock is rich in N, S and O. The calorific value of the rock ranges from 4.2–6.7 MJ/kg and the Fischer Assay oil yield is 3–5 %. During the Soviet era, the graptolite argillite was mined for uranium production at Sillamäe, NE Estonia.

Between 1964 and 1991, approximately 73 million tons of graptolite argillite was mined and piled into waste heaps from a covering layer of phosphorite ore at Maardu, near Tallinn. The calculated reserve of the Estonian graptolite argillite is about 65-70 Billion tons (Hade and Soesoo, 2014). The calculated tonnage of zinc is 16.5330 Mt (20.5802 Mt as ZnO), vanadium - 47.7538 Mt and molybdenum - 12.7616 Mt (19.1462 Mt as MoO_3). Western Estonia has the highest potential for these elements, especially for U and Mo production. It is important to note that due to the neighboring geological positions in cross-section of the graptolite argillite and phosphate ore, the future mining activity can be complex.

5. Metal resources in the Lower Proterozoic rocks

The Estonian Precambrian basement can be considered as a southern continuation of the Fennoscandian Shield rock complexes. Magnetite-gneisses (Fe_2O_3 ranges from 21.0 to 57 wt%.), sometimes rich in manganese (up to 6 wt%) are found in Jõhvi complex, NE Estonia and in several locations in northern Estonia. In the older literature, these Mt-gneisses were named as “magnetite-quartzites”, however, the matrix rock for magnetite is garnet-pyroxene or

garnet-amphibole-biotite gneiss and not quartzite. Historical drillings have shown that the complex of magnetite-rich rocks is about 100 m thick, and the reserves of iron ore (Fe over 25%) are about 355 Million tons (calculated to depth of 500 m), 629 Million tons if calculated to the depth of 700 m and 1500 Million tons if calculated to the depths of 1000 m (Soesoo et al., 2004). These estimates, however, are based on very limited data and need to be assessed by drilling in the future. The new drillings during 2018-2020 were not able to provide better understanding on the size of the deposit.

The mineralized beds have a complicated structural outline and provide a large range of rock varieties. Magnetite and sulphide minerals can be found sporadically in all rock types. Large scale mineralization is related to certain rock types e.g., garnet-pyroxene, pyroxene-garnet, pyroxene gneisses or garnet-amphibole, amphibole-garnet and biotite-amphibole gneisses (Soesoo et al., 2021; Nirgi and Soesoo, 2021).

Sulphide mineralization as a pyrite/pyrrhotite association and minor chalcopyrite, arsenopyrite and iron arsenide - loellingite, galena and sphalerite indicate a complex, possibly multiphase mineralization history of these rocks. While the chalcopyrite appears together with pyrite and pyrrhotite, loellingite and arsenopyrite seem to be commonly related to quartz-feldspar veining, which sometimes also contain gold and silver (Nirgi and Soesoo, 2021). These Jõhvi rocks are similar to Bergslagen in Sweden and possibly to Orijärvi in Southern Finland. Significant anomalies of sidero-chalcophile sulphide-graphite-bearing gneisses also occur in other regions in Northern Estonia (Cu, Pb and Zn can be in places as high as 5.6 %).

6. Conclusions

Estonia holds the largest in Europe, unused sedimentary phosphate rock reserves, about 3 Billion metric tons ore. The ore is relatively enriched by rare earth elements, where the total rare earth metals reach up to 3600 ppm.

The phosphates are overlain by metal-enriched black shale – graptolite argillite. The shale can be the source for a number of critical elements.

The Estonian oil shale resources are estimated about 4.627 Billion tons.

Several metal occurrences are known in the Paleoproterozoic crystalline basement. In NE Estonia, magnetite-gneisses and gneisses enriched in Mn (up to 6 wt%) are found in Jõhvi complex and in several locations elsewhere. Historical reserve estimates provide tonnages above 300 Million tons.

The carbonate rocks are largely used in Estonia. Dolostone mining in 2021 was about 834 thousand m^3. The limestone was mined - 2491 thousand m^3.

Acknowledgements: This study was supported by ERDF and Estonian Research Council via project RESTA20 to TalTech.

References:

Hade, S., Soesoo, A., 2014. Estonian graptolite argillites revisited: a future resource? Oil Shale, 31, 1, 4-18.

https://geoportaal.maaamet.ee/docs/geoloogia/koondbilanss_2021.pdf?t=20220605194101; Estonian Land Board, 2021.

Nirgi, S., Soesoo, A., 2021. Geology and geochemistry of a Paleoproterozoic iron mineralization in North-Eastern Estonia. Proceedings of the Karelian Research Centre of the Russian Academy of Sciences, 10, 25–43.

Soesoo, A., Puura, V., Kirs, J., Petersell, V., Niin, M., All, T., 2004. Outlines of the Precambrian basement of Estonia. Proceed Estonian Acad Sci Geol 53, 149–164.

Soesoo, A., Vind, J., Hade, S., 2020. Uranium and thorium resources of Estonia. Minerals, 10, 798.

Soesoo, A., Nirgi, S., Urtson, K., Voolma, M., 2021. Geochemistry, mineral chemistry and pressure–temperature conditions of the Jõhvi magnetite quartzites and magnetite-rich gneisses, NE Estonia. Estonian Journal of Earth Sciences 70, 2, 71–93.

New insights of the crustal structure across Estonia using satellite potential fields derived from WGM-2012 gravity data and EMAG2v3 magnetic data

J.D. Solano-Acosta[1], A. Soesoo[1] and R. Hints[1]

[1] Tallinn University of Technology, Ehitajate tee 5, Tallinn
E-mail: jusola@ttu.ee

Global WGM-12 gravity data and EMAG2v3 magnetic data were used to give new information of the Estonian crust. The Estonian Precambrian crystalline basement, composed of Paleo-Meso Proterozoic metamorphic and igneous rocks, is covered by a Palaeozoic sedimentary rock deposit 100 – 800 m thick. To visualise crustal layers of the Estonian basement, we employed spectrum analysis of magnetic and gravity data. The gravimetric data was used to identify the depth of the Moho and Conrad discontinuities. The magnetic data has been evaluated to calculate the Curie point depth (CPD), which was then utilized to predict heat flow values over the study area. The subsurface of Estonia is divided into six petrological-structural zones: Tallinn, Alutaguse, Jõhvi, West-Estonian, Tapa and South-Estonian. Potential lineaments in each zone delineates a NW-SE trend. In order to assess the structural variations of the crust over Estonia, different profiles are presented showing contrasting values of potential field, CPD and heat flow, particularly in the Precambrian Rapakivi granitic plutons and the Paldiski-Pskov deformation zone. The depth of the Curie point reveals a mean value of 15 km, while the depth of the Moho suggests a mean value of 60 km, while the mean depth of the Conrad discontinuity is around 18 km.

Keywords: Estonian crust, Precambrian basement, gravity and magnetic potential fields, geophysical modelling, Moho and Conrad discontinuities, Curie depth point (CPD), structural lineaments

1. General

In this research, we provide new insights on the Estonian crust tectonic. To achieve these results, we used magnetic (EMAG2v3) and gravimetric (WGM-12) satellite data. The Estonian Precambrian crystalline basement, composed of Paleo-Meso Proterozoic metamorphic and igneous rocks, is covered by a Paleozoic sedimentary rock deposit 100 – 800 m thick. The main features of the regional crustal structure were formed during the Svecofennian orogeny. Estonia is situated on a moderately thick crust (46–51 km, dropping to 41–44 Km in Saaremaa). Most of the crystalline basement comprises the Palaeoproterozoic (1.8 – 1.9 Ga) Svecofennian orogenic complex, subjected to high-grade metamorphism. The gneisses of amphibolite facies in northern Estonia represent an extension of the major structural units of southern Finland (All et al., 2004; Soesoo et al., 2020). Tallinn, Alutaguse, Jõhvi, West-Estonian, Tapa, and South-Estonian structural-petrological zones constitute the division of the basement (Figure 1).

The main goal of this work is to detail the magnetic and gravity signatures and structure of the Estonian crust (i.e., Curie depth point, Moho and Conrad discontinuities, and shallow potential spectra), also enhancing the structural divisions of the Estonian basement. Potential anomaly processing and matching filters are used in this research, allowing the shallow and deep geophysical responses of these structures and domains to be compared.

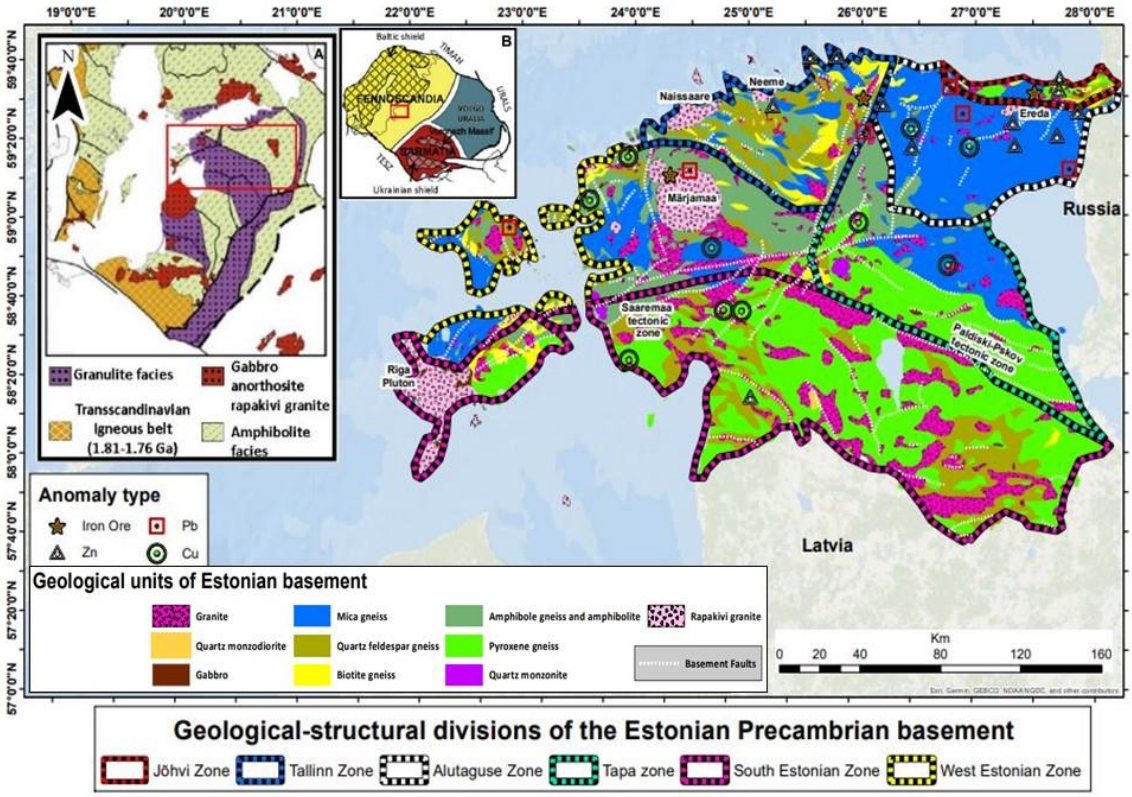

Figure 1. Geological map scheme of the Precambrian basement of Estonia, showing geochemical anomalies according to Soesoo et al. (2020). A) Major Palaeoproterozoic tectonic domains in the Baltic Sea area (modified after Bogdanova et al., 2015); B) Crustal segments of the East European craton (modified after Gorbatschev and Bogdanova, 1993).

We also want to account for geological structures retained on basement rocks as main features or those connected to subsequent metamorphic/igneous overprints. The geophysical modelling and interpretations provided here will help to better understand the geological formation of the Estonian basement and the possible overprinting of the Svecofennian orogeny in Estonia, as well as contribute to the debate on tectonic amalgamation theories (Bogdanova et al., 2015).

We provide the structural variations of the crust over Estonia (Figure 2), different profiles are presented showing contrasting values of potential field, Curie point depth (CPD) and heat flow (Figure 3), particularly in the Precambrian Rapakivi granitic plutons and the Paldiski-Pskov deformation zone. The CPD reveals a mean value of 15 km, while the depth of the Moho suggests a mean value of 60 km, while the mean depth of the Conrad discontinuity is around 18 km (Figure 3). Predominant NW-SE lineament trends from the potential anomalies are observed, supporting the theory of tectonic block convergence derived from the Svecofennian orogeny.

2. Methodology

To utilise the aforesaid data to understand the nature of the Estonian crust, regional-residual anomaly separation techniques must be used to extract gravity and magnetic anomalies attributable to crustal density and/or magnetic susceptibility sources (Omietimi et al., 2021).

By distinguishing anomalies associated to shallowest (residual) and deeper (regional) components of subsurface structures, these comprehensive interpretations aid in the identification of subsurface structures (see Nasuti et al. (2012) and Saada et al. (2021)). Due to the tiny density/magnetic susceptibility disparity between most crustal units, this is frequently a tough operation. The regional anomalies were estimated using derivatives, wavelength, and phase match filtering are used to accomplish the anomaly separation. In this research a wavelength-cut was done by using the High/Low pass filter of MAGMAP tool of Geosoft Oasis Montaj software.

The residual grids for gravity/magnetic data were obtained by removing the regional field from the filtered data, and allow to represent the crustal density sources (Fairhead, (2012)). To obtain the values of deep distance of the Moho and Conrad discontinuities, as well as the shallowest recorded signals, the Complete Bouguer Anomaly (CBA) data was used. For the magnetic data, the reduction-to-pole (RTP) transformation was implemented prior to the separation of the regional and residual field.

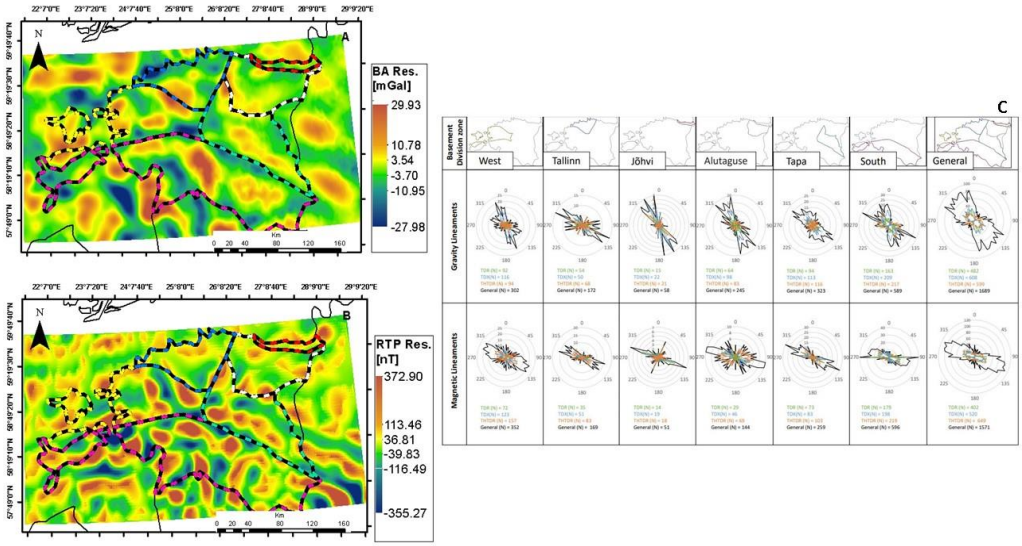

Figure 2. A) High-pass gravity (residual) anomaly map. B) High-pass filtered RTP magnetic (residual) anomaly map. C) Rose diagrams from potential data, subdivided into the geological-structural divisions of the Estonian Precambrian basement.

3. Conclusions

- According to the base potential data, the largest gravitational and magnetic values may be found in the Saaremaa and Paldiski-Pskov tectonic zones. It is also easy to see that those values are more significant in areas with more granulite facies.
- It has been discovered that using residual data, the Tallinn and Alataguse areas enhance several zones with high values, which match with zones with metal anomalies, particularly in the Alataguse zone. Johvi zone has high and increased residual potential values, which are most likely related to the existence of iron ores.
- Detailed power spectrum analysis of the CBA a Conrad discontinuity map (an average depth 17.8 km), and the Mohorovic discontinuity map (an average depth 60.45 km) in the study region.
- Previous research on the elastic thickness and seismic anisotropy backs up the crust thickness result (Moho boundary).

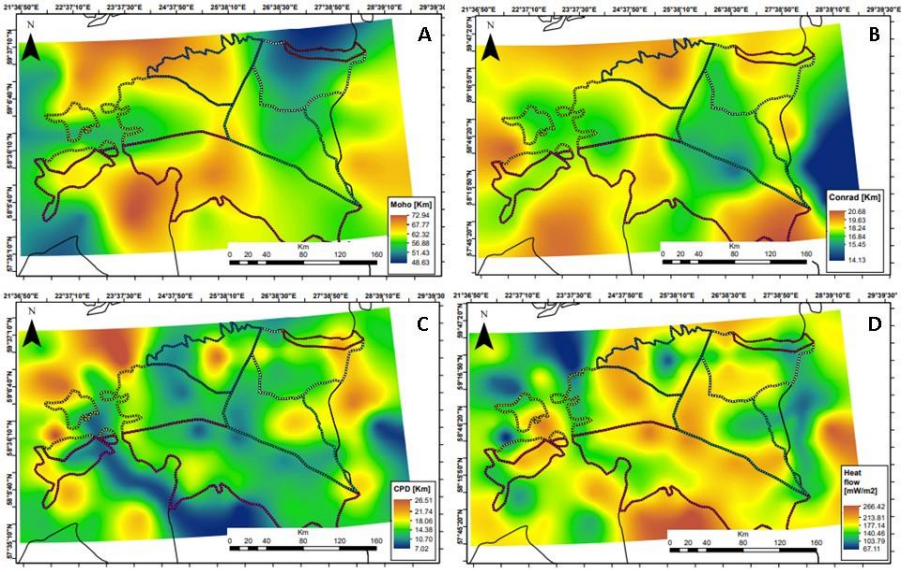

Figure 3. A) Moho discontinuity depth map from the power spectrum analysis of the residual gravimetric data. B) Conrad discontinuity depth map from the power spectrum analysis of the residual gravimetric data. C) CPD map estimated from the power spectrum analysis of the RTP residual magnetic data. D) Heat flow map estimated from the typical CPD analysis.

- CPD values are slightly shallow (at a depth similar to that of the Conrad discontinuity). The lowest CPD values are found in the Paldiski-Pskov tectonic zone and near the Marjamaa rapakivi pluton, in contrast to the heat flow, which has its highest values in these zones.
- The Moho-Curie difference shows that mantle magnetization is irrelevant in our research region since the magnetization is limited to the crust
- Predominant NW-SE lineament trends are observed, supporting the theory of tectonic block convergence derived from the Svecofennian orogeny**.**

References:

Nasuti, A., Pascal, C., Ebbing, J., 2012. Onshore–offshore potential field analysis of the mųre–trųndelag fault complex and adjacent structures of midnorway. Tectonophysics, 518, 17–28.

Omietimi, E.J., Chouhan, A.K., Lenhardt, N., Yang, R., Bumby, A.J., 2021. Structural interpretation of the south-western flank of the anambra basin (nigeria) using satellite-derived wgm 2012 gravity data, Journal of African Earth Sciences, 104290.

Fairhead, J.D., 2012. Regional tectonics and basin formation: The role of potential field studies, Regional Geology and Tectonics: Principles of Geologic Analysis, 1, 331.

Gorbatschev, R., Bogdanova, S., 1993. Frontiers in the Baltic shield. Precambrian Research, 64 (1-4), 3-21.

Saada, S.A., Mickus, K., Eldosouky, A.M., Ibrahim, A., 2021. Insights on the tectonic styles of the Red Sea rift using gravity and magnetic data. Marine and Petroleum Geology, 133, 105253.

Bogdanova, S. Gorbatschev, R. Skridlaite, G. Soesoo, A. Taran, L. Kurlovich, D., 2015. Trans-baltic palaeoproterozoic correlations towards the re1100construction of supercontinent Columbia/Nuna. Precambrian Research, 259, 5–33.

Soesoo, A., Nigri, S., Plado, J., 2020. The evolution of the Estonian Precambrian basement: geological, geophysical and geochronological constraints.

All, T., Puura, V., Vaher, R., 2004. Orogenic structures of the precambrian basement of Estonia as revealed from the integrated modelling of the crust. In:Proceedings of the Estonian Academy of Sciences, Geology, Estonian Academy Publishers, volume 53, pp. 165–189.

Relation between rare element pegmatites and post-collisional magmatism in the Svecofennian domain

O. Teräs[1], K. Nikkilä[1] and O. Eklund[1]

[1]Geology and Mineralogy, Åbo Akademi University, 20500 Turku, Finland
E-mail: oliver.teras@abo.fi

Post-collisional granitic magmatism is common in the Svecofennian domain. Studying these rocks is important for a better understanding of the processes that took place during the end of the Svecofennian orogeny. The age determinations and geochemistry of the granites and pegmatites belonging to the post-collisional event are crucial in constraining timing and tectonic interpretations of orogenic events, crustal melting, deformation and post-collisional pegmatites formation.

Keywords: granite, pegmatite, post-collisional magmatism, Fennoscandia

1. Introduction

After the collision of the arcs in the end of Paleoproterozoic growth and crustal thickening (1.9–1.83 Ga), the crust became intruded by rare element pegmatites and post-collisional granites at roughly 1.80 Ga ago. At present, common interpretation of rare element pegmatites is that they originate from host granites and represent the last melts of crystallization. However, host granites rarely exist in the same area as the rare element pegmatites. The interpretation of the origin of post-collisional magmatism varies depending on the composition of formation. Example, in northern Finland the Nattanen-type granites are derived mostly from an Archaean tonalite–trondhjemite–granodiorite (TTG) source via dehydration melting involving breakdown of amphibole (Heilimo et al., 2014). In the other hand, in southern Finland, high Ba-Sr granites are suggested to represent a high-level expression of the mantle magmatism that was derived from depleted mantle source, which where enriched during a previous subduction episode (Eklund et al., 1998; Rutanen et al., 2011). Whatever the interpretations, there is a temporal overlapping between rare element pegmatites and post-collisional rocks in the Svecofennian domain. This indicates a common tectonic setting for the rare element pegmatites and post-collisional magmatism.

2. Origin of the rare element pegmatites

A common way to explain the origin of pegmatites and why some of them are enriched in rare elements is that pegmatites represent fractionated melts derived from a host granite source. These melts become enriched in certain rare elements depending on their distance from the host granite. With decreasing temperature, the composition of the melt is changing. This is called regional zoning first described by Černý (1991). The model is based solely on a crystallizing granite host and the composition of the pegmatites are dependent on the granite type of the host. Two principal pegmatite families, NYF- and LCT-type pegmatites are formed depending on the host granite. NYF stands for elements Nb, Y and F; and LCT for elements Li, Cs and Ta. In this study we will focus on LCT-type of pegmatites only.

Recently, the model by Černý (1991) has been concurred by the idea that pegmatites can be formed by partial melting of any type of protoliths. Simmons et al. (2016) suggested that bulk chemical evidence supports the formation of an LCT-type pegmatites by partial melting of metapelitic rocks in the northern Appalachians. Moreover Müller et al. (2017) report that in the

Sveconorwegian pegmatite province, there are thousands of pegmatites without parental granites. They state that pegmatites are not related to a parental granite, but to high grade metamorphism with leucosome formation and local melt collection.

3. LCT-type pegmatites in the Svecofennian domain

According to Alviola (2012), there are about 50 rare element pegmatites groups in Finland. Of these 37 are supposed to be LTC-type pegmatites. They mainly appear in southern Finland and in western Finland (Figure 1). However, the granites of the same ages are lacking. Peak metamorphism in western Finland took place at 1.87 Ga ago (Chopin et al., 2020) and the age of the LCT-type pegmatites are around 1.80–1.79 Ga (Alviola et al., 2001), indicating age difference between 80 Ma and 70 Ma. The age of the peak metamorphism in southern Finland was between 1.83 Ga and 1.82 Ga (Mouri et al., 2005), while the age of the pegmatites are 1.80 Ga in Kemiö (Lindroos et al., 1996) and 1.77 Ga in Kitee (Nykänen, 1975). Again, indicating an age difference between 20 Ma and 60 Ma. These time lags between peak metamorphism/granite formation and appearance of pegmatites makes it difficult to understand the hypothesis that LCT-type pegmatites are late fractionates from a host granite. However, if we consider formation of pegmatites as a consequence of direct products of anatexis, we still need a heat source that generate the anatexis. A good candidate for this heat source is the post-collisional rocks appearing over extensive areas in Finland (Figure 1).

4. Post-collisional magmatism in the Svecofennian domain

At 1.81–1.75 Ga, Svecofennian domain experienced voluminous granitic magmatism: Nattanen-type granites intruded in northern Finland at 1.79–1.76 Ga (Heilimo et al., 2014); parts of the Central Lapland granitoid complex intruded around 1.81–1.76 Ga (Ahtonen et al., 2007; Lauri et al., 2012) and southern Finland experienced post-collisional bimodal granitic magmatism at 1.81–1.76 Ga (Eklund et al., 1998; Rutanen et al., 2011). Moreover 1.80 Ga carbonatites and lamprophyres are also intruded throughout southern Finland (Woodard and Huhma, 2015). Simultaneously, the coastal batholith, Transscandinavian Igneous Belt (TIB) was active in the western part of the newly formed Svecofennian domain (Högdahl et al., 2004). There are several genetic models to explain the post-collisional magmatism in Svecofennian domain. For example, post-collisional magmatism has been explained in terms of their relationship to supercontinents (Heilimo et al., 2014 and references therein).

5. Connection with post-collisional magmatism, pegmatites and tectonic setting

It is known that pegmatites are formed at a late stage of plutonic activity depending less of the tectonic setting of the pluton. However, the recent literature report more and more examples of rare element pegmatites formed in a post-collisional setting in orogenies. For example, Yan et al. (2022) reports a 600 km long rare element pegmatite belt associated with post-collisional granitic rocks in the Kunlun orogenic belt in western China. This is the situation also in the Svecofennian domain where rare element pegmatites are situated in southern and western Finland and geochronology indicate the tectonic setting was post-collisional. The anatexis could be generated by mantle delamination or slab break-off at the end of the Svecofennian orogeny. An analogue to this scenario was presented from the Chinese Altay orogenic belt by Zhang et al. (2016).

6. Summary

Pegmatites are generally acknowledged to form by a process of fractional crystallization of a granitic composition melt. In many cases the connection of pegmatites with a parent granite is

obvious from spatial relationships, age determinations and chemical characteristics. However, it also has been proposed that it may be possible to form pegmatites as a consequence of direct products of anatexis. With this new way to look at pegmatites, the prospection of rare elements may take a new direction. One should not look for the parental granite, but for any suitable fertile protolith. Thus, the hypothesis is that a big part of LCT-type pegmatites in Svecofennian domain are generated as a consequence of direct products of anatexis from various sources.

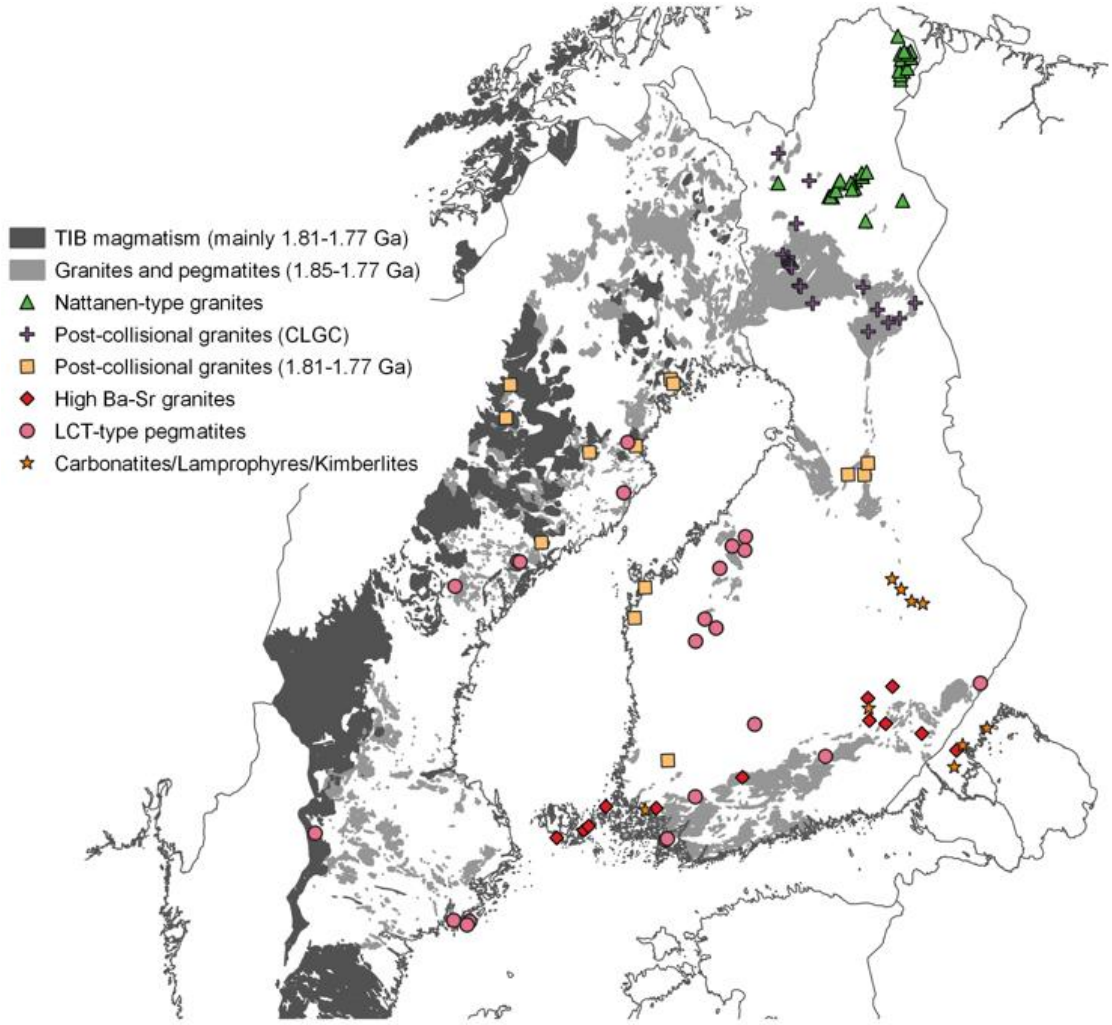

Figure 1. Post-collisional magmatism in Svecofennian domain during 1.81–1.75 Ga. Nattanen-type granites shown by triangle (Heilimo et al., 2014) and post-collisional granites intruded in CLGC shown by cross (Ahtonen et al., 2007). CLGC = Central Lapland granitoid complex. Other post-collisional granites throughout Sweden and Finland shown by square (SGU database and DigiKP (2022)). High Ba-Sr granites shown by diamond (Eklund et al., 1998; Rutanen et al., 2011) and LCT-type pegmatites shown by circle (Gourcerol et al., 2019). Carbonatites and lamprophyres shown by star (Woodard and Huhma, 2015). Sources for TIB granitoids are from

SGU database. Granites and pegmatites are also from SGU (2022) and from DigiKP (2022). TIB = Transscandinavian igneous belt.

References:

Ahtonen, N., Hölttä, P., Huhma, H., 2007. Intracratonic Palaeoproterozoic granitoids in northern Finland: prolonged and episodic crustal melting events revealed by Nd isotopes and U-Pb ages on zircon. Bulletin of the Geological society of Finland, 79 (2), 143-174.

Alviola, R., 2012. Distribution of rare element pegmatites in Finland. In: Lithosphere 2012: Seventh Symposium on the Structure, Composition and Evolution of the Lithosphere in Finland. Programme and Extended Abstracts, p 1-4.

Alviola, R., Mänttäri, I., Mäkitie, H., Vaasjoki, M., 2001. Svecofennian rare-element granitic pegmatites of the Ostrobothnia region, western Finland: their metamorphic environment and time of intrusion. Geological Survey of Finland, Special Paper, 30, 9-29.

Černý, P., 1991. Rare-Element Granitic Pegmatites. Part I Anatomy and Internal Evolution of Pegmatitic Deposits. Geoscience Canada, 18, 49-67.

Chopin, F., Korja, A., Nikkilä, K., Hölttä, P., Korja, T., Abdel Zaher, M., Kurhila, M., Eklund, O., Rämö, O.T., 2020. The Vaasa Migmatitic Complex (Svecofennian Orogen, Finland): Buildup of a LP-HT Dome During Nuna Assembly. Tectonics, 39 (3), e2019TC005583.

DigiKP, 2022. Digital map database. Geological Survey of Finland, Espoo. Page visited 20.9.2022. https://hakku.gtk.fi/fi/locations/search

Eklund, O., Konopelko, D., Rutanen, H., Fröjdö, S., Shebanov, A.D., 1998. 1.8 Ga Svecofennian post-collisional shoshonitic magmatism in the Fennoscandian shield. Lithos, 45 (1-4), 87-108.

Gourcerol, B., Gloaguen, E., Melleton, J., Tuduri, J., Galiegue, X., 2019. Re-assessing the European lithium resource potential–A review of hard-rock resources and metallogeny. Ore Geology Reviews, 109, 494-519.

Heilimo, E., Elburg, M.A., Andersen, T., 2014. Crustal growth and reworking during Lapland–Kola orogeny in northern Fennoscandia: U–Pb and Lu–Hf data from the Nattanen and Litsa–Aragub-type granites. Lithos, 205, 112-126.

Högdahl, K., Andersson, U.B., Eklund, O., 2004. The Transscandinavian Igneous Belt (TIB) in Sweden: a review of its character and evolution. Geological Survey of Finland, Special Paper, 37, 123 p.

Lauri, L.S., Andersen, T., Räsänen, J. and Juopperi, H., 2012. Temporal and Hf isotope geochemical evolution of southern Finnish Lapland from 2.77 Ga to 1.76 Ga. Bulletin of Geological Society of Finland 84, 121-140.

Lindroos, A., Romer, R.L., Ehlers, C., Alviola, R., 1996. Late-orogenic Svecofennian deformation in SW Finland constrained by pegmatite emplacement ages. Terra Nova, 8 (6), 567-574.

Mouri, H., Väisänen, M., Huhma, H., Korsman, K., 2005. Sm-Nd garnet and U-Pb monazite dating of high-grade metamorphism and crustal melting in the West Uusimaa area, southern Finland. GFF, 127(2), 123-128.

Müller, A., Romer, R.L., Pedersen, R.B., 2017. The Sveconorwegian pegmatite province–thousands of pegmatites without parental granites. The Canadian Mineralogist, 55 (2), 283-315.

Nykänen, O., 1975. Geological map of Finland 1: 100 000. Explanation to the maps of Precambrian rocks. Sheets 4213 Kerimäki and 4231 Kitee. Precambrian rocks of the Kerimäki and Kitee map-sheet areas. Geological Survey of Finland, Espoo, 43 p.

Rutanen, H., Andersson, U.B., Väisänen, M., Johansson, Å., Fröjdö, S., Lahaye, Y, Eklund, O., 2011. 1.8 Ga magmatism in southern Finland: strongly enriched mantle and juvenile crustal sources in a post-collisional setting. International Geology Review, 53 (14), 1622-1683.

SGU database, 2022. Geological Survey of Sweden, Upsala. Page visited 20.9.2022. https://apps.sgu.se/kartvisare/kartvisare-bergets-alder.html

Simmons, W., Falster, A., Webber, K., Roda-Robles, E., Boudreaux, A.P., Grassi, L.R., Freeman, G., 2016. Bulk composition of Mt. Mica pegmatite, Maine, USA: Implications for the origin of an LCT type pegmatite by anatexis. The Canadian Mineralogist, 54 (4), 1053-1070.

Woodard, J., Huhma, H., 2015. Paleoproterozoic mantle enrichment beneath the Fennoscandian Shield: Isotopic insight from carbonatites and lamprophyres. Lithos, 236, 311-323.

Yan, Q.H., Wang, H., Chi, G., Wang, Q., Hu, H., Zhou, K.,Zhang, X.Y., 2022. Recognition of a 600-km-long late Triassic rare metal (Li-Rb-Be-Nb-Ta) pegmatite belt in the western Kunlun orogenic belt, western China. Economic Geology, 117 (1), 213-236.

Zhang, X., Zhang, H., Ma, Z.L., Tang, Y., Lv, Z.H., Zhao, J.Y., Liu, Y L., 2016. A new model for the granite–pegmatite genetic relationships in the Kaluan–Azubai–Qiongkuer pegmatite-related ore fields, the Chinese Altay. Journal of Asian Earth Sciences, 124, 139-155.

Exploring the effects of continental collision obliquity and temperature on orogeny evolution and *P-T-t* paths

L. Tuikka[1], B. Cateland[1], D.M. Whipp[1] and M. Häkkinen[2]

[1]Institute of Seismology, Dept. of Geosciences and Geography, University of Helsinki
[2]Geology and Geophysics Research Programme, Dept. of Geosciences and Geography, University of Helsinki
E-mail: leevi.tuikka@helsinki.fi

The Paleoproterozoic era probably acted as a transition period between different modes of plate tectonics, due to secular cooling of Earth. One of the remarkable orogens of the Paleoproterozoic was Svecofennian orogeny, collision of a craton and several microcontinents. We explore by using 3D thermo-mechanical geodynamic models, how different collision angles and temperature scenarios, ranging from Paleoproterozoic to modern one, affect on the orogeny evolution and metamorphic environment. *P-T-t* paths are extracted from the models as well, to allow comparison to metamorphic rock samples.

Keywords: geodynamic modelling, Svecofennian orogen, continental collision, *P-T-t* paths

1. Introduction

When did plate tectonics begin on Earth? A major question in geosciences but particularly geodynamics, along with the evolution and different modes of plate tectonics. Heat budget of Earth has been decreasing at least since the Hadean-Eoarchean transition (ca. 4 Ga ago), controlling Earth's large-scale rheological behaviour via mantle potential temperatures, and further the style of plate tectonics. Based on geodynamic modelling (e.g. Fischer and Gerya, 2016a) and metamorphic (e.g. Brown, 2007) studies, it is thought that the Paleoproterozoic Era (2.5-1.6 Ga ago) acted as a transition period from plume-lid (Fischer and Gerya, 2016b) tectonics to behaviour like modern plate tectonics. Metamorphic rocks from the Paleoproterozoic generally lack a record of UHP conditions but indicate higher temperatures, which may be related to different mode of plate tectonics at that time. However, time poses a unique challenge. Paleoproterozoic rocks that can be accessed easily today have been exhumed as a result of deep levels of erosion. We aim to address this challenge using pressure-temperature-time (*P-T-t*) paths extracted from generic continent-continent collision models and comparing them to *P-T-t* paths from metamorphic minerals.

1.92-1.77 Gyr ago, the Svecofennian orogeny produced the majority of the bedrock in southern Finland. Svecofennian orogeny is well studied by number of geological and geophysical means, but physics-based geodynamic models of it are still lacking. For example, extraordinary thick Svecofennian crust and gravitational collapse of the orogen (e.g. Korja et al., 2006) can be investigated by using geodynamic continental collision models. In terms of mountain building, the most important phase of Svecofennian orogeny was microcontinental collisions (Korja et al., 2006), first on the edge of Archean cratons and later on, between several microcontinents.

Assuming that these collisions were strictly perpendicular, would be rather redundant conclusion, so we test how obliquity of collision angle in Paleoproterozoic temperature conditions affects on the structure of orogen and metamorphism. This would be necessary to properly investigate tectonic settings in e.g. Svecofennian orogeny. Additionally, metamorphic samples will be collected from vicinity of the continent-continent collision zones in southern Finland to allow comparison between the models and nature.

2. Methods and model design

The models were run using the 3D thermo-mechanical, geodynamic modelling software DOUAR (Braun et al., 2008). It uses the finite element method (FEM) and the landscape evolution model FastScape (Braun and Willett, 2013), which builds realistic topography and also results in exhumation to produce the *P-T-t* histories. DOUAR has demonstrated its capabilities when combining surface dynamics with lithospheric dynamics (Nettesheim et al., 2018) to model rock exhumation, for example. Basis of DOUAR lies on solving laminar viscous flow equation (Stokes equation) for flow velocity and heat equation for temperature distribution in time and space. Also, other quantities, such as strain rate and pressure are computed in the models. In DOUAR, *P-T-t* paths are extracted from Lagrangian particles, which track pressure, temperature and velocity throughout a simulation.

Our work is exploring the effects of various continental collision obliquity angles and temperature conditions in a set of nine different models. We assume that in the Svecofennian orogeny, continent-continent collision was an event between colder and hotter continental blocks (material geometry shown in Figure 1.), which is implemented in the models by having a temperature difference of 100 °C on the model base at 70 km. Along this boundary, heat production is varied laterally in three different temperature scenarios, ranging from colder, modern-day temperatures to hot, Paleoproterozoic temperatures (see geotherms in Figure 2.). Convergence obliquity angle is varied between 0°, 30° and 60°, while subduction dip angle is 45°. In Table 1. other important model parameters are reported.

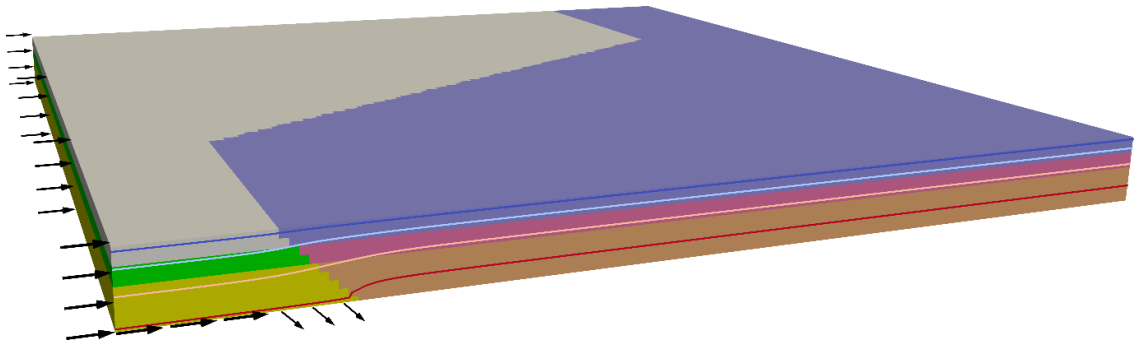

Figure 1. Example material, velocity and temperature models, with θ=60° and high temperature case. Isotherms range from 200 °C to 800 °C, with 200 °C contour interval.

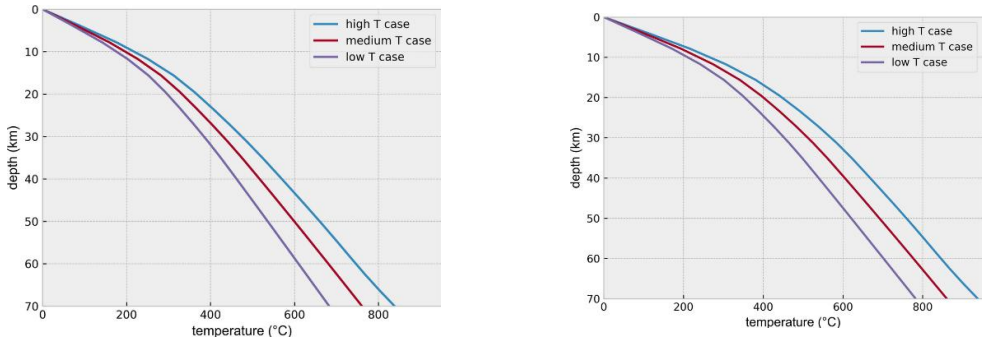

Figure 2. Geotherms of the colder sides (left) and the hotter sides (right) of the models. All three temperature cases presented.

Table 1. DOUAR model parameters.

parameter	value
model dimensions	1000×1000×70 km
resolution	7.8125×7.8125×3.90625 km
time step length	75 ka
layer thicknesses	20, 15, 35 km
convergence obliquities θ	0°, 30°, 60°
subduction dip angle	45°
convergence rate	10 cm/a
layer densities	2700, 2800, 3300 kg·m^{-3}
strain softening φ_s	15°→ 5°
layer viscosity prefactors B^*	2.92·10^6, 3.08·10^4, 1.90·10^5 Pa·s^{-n}
layer exponental factor n	4.0, 4.2, 3.5
layer viscosity coefficients	5.0, 3.0, 3.0

3. Preliminary results

Models show orogeny build-up for ca. 5 Ma in the beginning, until erosion processes and boundary mass fluxes are in balance. Slight difference in dynamics and structure of the models can be seen between different temperature scenarios, such as in orogeny height and strain rate distribution (Figure 3.). As expected according to (Whipp et al., 2014), orogen-parallel mass transport velocities increase as a function of collision obliquity angle. *P-T-t* paths generally show distinction between temperature scenarios.

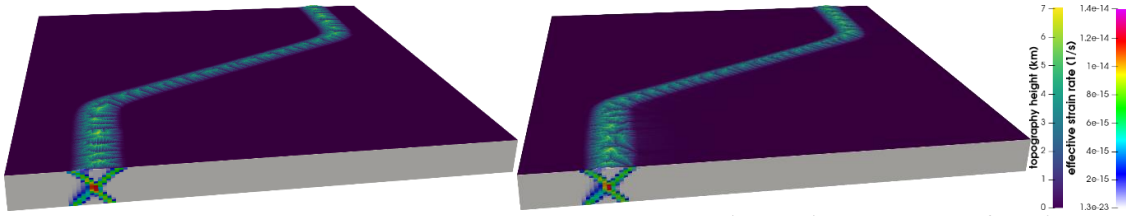

Figure 3. Example results at 16 Ma of strain rates, and topography built by continental collision. The model on the top is low temperature case with θ=60° and the model at the bottom is high temperature case with θ=60°.

4. Discussion and conclusions

Our preliminary results indicate that lithospheric temperatures are indeed important factors controlling orogen dynamics and *P-T* conditions of exhumed rocks. Hence, the Paleoproterozoic metamorphic environment in orogens was apparently different than today, and that should be perceived in rock sample data as well. On the contrary, change in collision obliquity express little or no influence on *P-T-t* paths.

However, our models serve rather as a starting point than versatile final product. Model thickness of 70 km limits incorporating some effect of mantle, such as more frequent slab breakoffs due to hotter, Paleoproterozoic temperatures. Also increasing spatial model resolution could help to capture effect of collision obliquity better. Further on, implementing phase changes as a result of changing model *P-T* conditions would improve coupling of different geological processes.

References:

Braun J., Thieulot C., Fullsack P., DeKool M., Beaumont C., Huismans R., 2008. DOUAR: A new three-dimensional creeping flow numerical model for the solution of geological problems, Physics of the Earth and Planetary Interiors, 171(1-4), 76-91.

Braun J., Willett, S. D., 2013. A very efficient O(n), implicit and parallel method to solve the stream power equation governing fluvial incision and landscape evolution, Geomorphology, 180–181, 170-179.

Brown M., 2007. Metamorphic Conditions in Orogenic Belts: A Record of Secular Change, International Geology Review, 49(3), 193-234.

Fischer R., Gerya T., 2016a. Regimes of subduction and lithospheric dynamics in the Precambrian: 3D thermomechanical modelling, Gondwana Research, 37, 53-70.

Fischer R., Gerya T., 2016b. Early Earth plume-lid tectonics: A high-resolution 3D numerical modelling approach, Journal of Geodynamics, 100, 198-214.

Korja, A., Lahtinen, R., Nironen, M., 2006. The Svecofennian orogen: a collage of microcontinents and island arcs, European Lithosphere Dynamics, 32, 561-578.

Nettesheim M., Ehlers T.A., Whipp D.M., Koptev A., 2018. The influence of upper-plate advance and erosion on overriding plate deformation in orogen syntaxes, Solid Earth, 9, 1207-1224.

Whipp, D.M., Beaumont, C., Braun, J., 2014. Feeding the “aneurysm”: Orogen-parallel mass transport into Nanga Parbat and the western Himalayan syntaxis, Journal of Geophysical Research: Solid Earth, 119 (6), 5077-5096.

New U-Pb age data from Pasalanmäki in Leppävirta, central Finland – older Svecofennian magmatism or not?

M. Tuppurainen[1], P. Mikkola[2] and M. Kurhila[3]

[1]University of Oulu, P.O. Box 8000 Oulu, Finland
[2]Geological Survey of Finland, P.O. Box 1237, 70211 Kuopio, Finland
[3]Geological Survey of Finland, Vuorimiehentie 2 K, 02150 Espoo, Finland
E-mail: markus.tuppurainen@outlook.com

This study provides new age data from previously poorly studied "hornblende gneisses" and granitoids occurring in Pasalanmäki in Leppävirta, Central Finland. The gneisses have been tentatively interpreted as part of the older Svecofennian magmatism (1.93–1.91 Ga), but no age data from them exists. This study provides a brief summary of the different rock types, their mutual relationships and single grain zircon U-Pb ages obtained from them. Based on the results, it is clear that there are no Archean rocks in the area. However, data from individual samples display significant scatter with spot ages typically varying between 1.94 and 1.84 Ga. Thus, calculation of exact ages and linking the rocks to a specific magmatic event is extremely difficult.

Keywords: U-Pb, absolute age, zircon, bedrock, Leppävirta, Finland

1. Background

Pasalanmäki area is located in central Finland, within the Raahe-Laatokka suture zone which forms the boundary zone between two major geological domains; the Archean Karelian domain, and the Svecofennian Domain (Kähkönen, 2005). Because of its location within the highly deformed suture zone, practically all primary structures have been destroyed. Currently the "hornblende gneisses" of the study area have been regarded as part of the older Svecofennian magmatism (1.93–1.91 Ga, DigiKP; Figure 1).

Previous studies have focused on the ore potential of the area (e.g., Parkkinen 1974) and petrographical or geochemical description of these rocks have received very little attention. Purpose of this study is to determine the age of the hornblende gneisses; are they part of older or younger Svecofennian magmatism, or Archean. The latter possibility must also be considered due to the proximity of Archean Kotalahti domes and field appearance closely resembling Archean gneisses.

Altogether seven samples representing the various observed rock types were taken for single grain zircon U-Pb dating. All analyses were performed at the Geological Survey of Finland in Espoo using Nu Plasma AttoM single collector ICP-MS connected to Photon Machine Excite laser ablation system.

2. Field observations

The main rock types in the study area are heterogeneous tonalites and finer grained, often banded, biotite-hornblende gneisses (Figure 2). Main minerals in both are plagioclase, quartz, hornblende and, in some cases, biotite.

Structurally the tonalites vary from nearly unoriented igneous texture to strongly oriented gneissic texture. Intensity of the deformation is linked to the proximity of shear zones transecting the area.

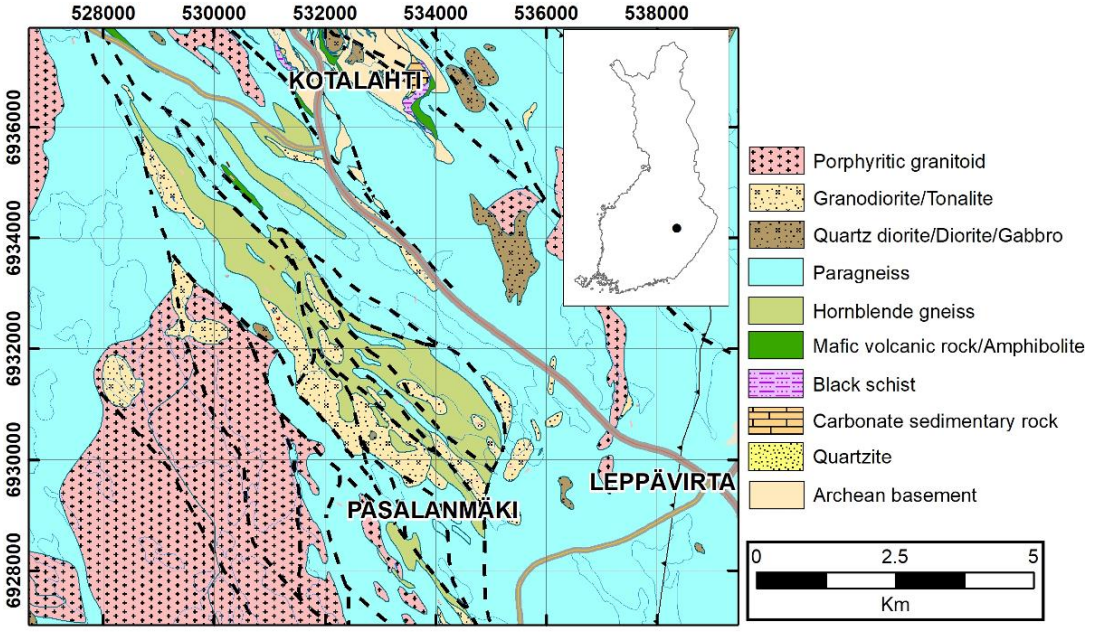

Figure 1. Bedrock map of the study area, modified form DigiKP. In inset location of the study area. Basemap ©National Land Survey.

Biotite-hornblende gneisses are variably migmatized and moderately to strongly oriented. Banding is the most typical migmatitic structure. In most locations the migmatite neosome resembles the tonalites in appearance, thus it seems possible that the tonalites represent partial melts separated from the gneisses.

Figure 2. Outcrop pictures. On the left fine-grained biotite-hornblende gneiss, with pegmatitic veins. On the right typical heterogeneous tonalite with felsic veins. Length of the compass 10 cm.

Hornblende-rich gabbro fragments and inclusions (5–70 cm across) are present throughout the study area in the tonalite and hornblende-biotite gneiss. Also, a small (<200 m across) gabbro intrusion occurs in the area.

Voluminous paragneisses surrounding the studied units occur also as lenses of variable size within the tonalite and hornblende-biotite gneisses. They are heterogenous, quite

intensively migmatized, sometimes garnet bearing and contain characteristic calc-silicate-concretions, setting them apart from the hornblende gneisses. As the paragneisses have been dated before (Mikkola et al., 2022), no age sample from them was included in this study.

Crosscutting felsic veins are present throughout the study area, cutting all the aforementioned rock types. Orientation of the veins varies, and they also crosscut each other. The veins seem to postdate the main deformation event(s) as they are usually unoriented or weakly orientated, equigranular and rather homogenous. Grain size varies from small to coarse, pegmatitic. Mineralogically these veins are very quartz and feldspar rich. On some outcrops accessory magnetite was observed in the pegmatite.

3. Results and discussion

None of the analysed seven samples included a clear magmatic population, instead all of them displayed a continuum of $^{207}Pb/^{206}Pb$ ages from ca 1850 to 1940 Ma (Figure 3), with small number of older ages (1960–2810 Ma) observed. Ages do not correlate significantly with neither zircon composition (U, Pb, Th) nor morphology (oscillatory zoned, homogeneous). Ages spanning from older Svecofennian magmatism to younger Svecofennian magmatism have two possible end member solutions:

1) the rocks are part of the older Svecofennian magmatism, i.e. 1.93–1.91 Ga and they have been heavily influenced by peak metamorphic lead-loss, examples of which are abundant in the area, see Mikkola et al. (2022) for examples and references
2) the rocks are part of the younger Svecofennian magmatism, i.e. 1.89–1.87 Ga and the older ages present either inherited or detrital grains

Some constraints can be conducted from the field observations. The felsic veins postdate both the migmatization event and the main deformation, both which have taken place close to 1880 Ma ago (Mikkola et al., 2022). Thus, in the case of these veins the older zircons must be inherited from either their source or represent contamination during emplacement. It is worth mentioning that the only Archean zircons were found in one of the dyke samples.

In case of the biotite-hornblende gneisses the same argumentation can be used to rule out at least the youngest obtained ages as result of lead loss or metamorphic overgrowth. The fact that volcanic and plutonic samples representing the younger Svecofennian magmatism rarely contain significant amounts of inherited zircons from older events (e.g., Mikkola et al., 2018), supports the lead loss explanation for the observed spread of $^{207}Pb/^{206}Pb$ ages. Thus, we tentatively interpret the gneisses as part of the older Svecofennian magmatism. In any case it is clear that the gneisses represent a different geological unit as the surrounding paragneisses, which always contain abundant Archean and ~2.0 Ga detrital zircons, which are not present here in studied gneisses.

If the field interpretation, that the tonalites are segregated melts from the biotite-hornblende gneisses, is correct, the observed spread of ages in these tonalites would be due to both inheritance from the source and post-crystallisation lead-loss. Further consideration of this possibility will be possible later based on geochemical data, which allows evaluation of the partial melting hypothesis.

In the case of the gabbro, its relation with tonalites of the area seems rather complex. The one intrusion present seems to be deformed by the tonalites, which would make the gabbro older. On the other hand, all of the gabbro fragments found do not seem to be only pieces of country rock but could very well be parts of deformed veins. We hope that geochemical results give some information whether these rocks belong to the Kotalahti type magmatism or not. Gabbros being Kotalahti type would age them at 1.88Ga (Peltonen, 2005).

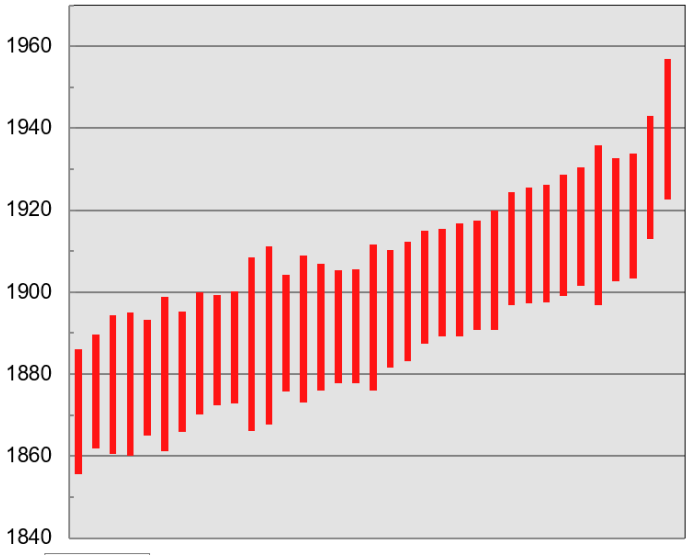

Figure 3. Typical plot of $^{207}Pb/^{206}Pb$ ages for an individual sample from Pasalamanmäki heterogenous tonalite.

4. Conclusions

Our results show that it is unlikely that Archean rocks are present in Pasalanmäki. Also, the gneisses belong to different system than the surrounding paragneisses. This is based on the distribution of both Archean and ~2.0 Ga zircons, which are abundant in the paragneisses, but are missing from the rocks studied here.

However, categorizing the studied rocks to either older Svecofennian magmatism or to younger Svecofennian magmatism is difficult due to scattering of the zircon ages obtained from individual samples. Both scenarios are possible: populations with significant inherited component, or significant lead loss due to associated high grade metamorphism. We hope to clarify the question later when our age data is combined with a geochemical data set of the same rocks.

References:

Bedrock of Finland – DigiKP. Digital map database [Electronic resource]. Espoo: Geological Survey of Finland [referred 10.10.2022]. Version 2.1.

Kähkönen, Y., 2005. Svecofennian supracrustal rocks. In: Lehtinen, M., Nurmi, P., Rämö, O.T. (eds.) The Precambrian Bedrock of Finland—Key to the evolution of the Fennoscandian Shield. Elsevier Science B.V., Developments in Precambrian Geology, 14, 343–405. doi:10.1016/S0166-2635(05)80009-X

Mikkola, P., Aatos, S., Halkoaho, T., Heinonen, S., Hietava, J., Hietala, S., Kurhila, M., Jäsberg, J., Laine, E.-L., Luukas, J., Niskanen, M., Nousiainen, M., Nygård, H., Piispanen, A., Pirinen, H., Rantanen, H., Romu, I. 2022. Geological evolution and structure along the western boundary of the Outokumpu allochthon. Geological Survey of Finland, Open File Research Report, 23/2022.

Mikkola, P., Mönkäre, K., Ahven, M., Huhma, H., 2018. Geochemistry and age of the Paleoproterozoic Makkola suite volcanic rocks in Central Finland. In: Mikkola, P., Hölttä, P., Käpyaho, A. (eds) Development of the Paleoproterozoic Svecofennian orogeny: new constraints from southeast boundary of the Central Finland Granitoid Complex. Geological Survey of Finland, Bulletin, 407, 85–105. Available at: http://doi.org/10.30440/bt407.5

Peltonen, P., 2005. Svecofennian mafic-ultramafic intrusions. In: Lehtinen, M., Nurmi, P., Rämö, O T. (eds.) The Precambrian Bedrock of Finland—Key to the evolution of the Fennoscandian Shield. Elsevier Science B.V., Developments in Precambrian Geology, 14, 407–442. doi:10.1016/S0166-2635(05)80010-6

Correlation of bedrock outcrop structures with subsurface data – with emphasis on the need of geoenergy research

E. Virta[1], T. Lindqvist[1,2], P. Skyttä[1] and S. Mustonen[3]

[1]University of Turku
[2]Geological Survey of Finland
[3]Helen Oy
E-mail: elmvir@utu.fi

This article presents structural geological features found from bedrock outcrops that may affect negatively to the proper working of geothermal well located in the study area. More inexpensively and easily collected surface data will be correlated to subsurface data which is typically collected using more expensive and arduous methods. If correlation can be proven, the uncertainty related to placement of geothermal wells may be significantly decreased by structural mapping in the future.

Keywords: geothermal energy, geothermal well, bedrock outcrop, bedrock mapping, field observation, structural geology, fault

1. Introduction

The demand of energy is increasing in this rapidly developing world day by day. Energy production has favored effective yet contaminant fossil fuels for a long time. Cleaner future and response to the increasing demand of energy can be achieved by using renewable energy sources such as geothermal energy. Great geothermal potential and constantly developing technology are making this progress possible, although expenses are still relatively high. In favorable regions, where natural steam or hot water reservoirs are existing, expenses are reasonable thus in areas where reservoirs require technical enhancement, the situation is the opposite (Clauser and Ewert 2018). This significant disadvantage needs to be solved so that geothermal energy can be used as a competitive source to produce energy along other renewable energy sources (Clauser and Ewert 2018).

Until now, research related to building of geothermal wells such as site selection and risk surveying has mainly been based on subsurface data. Subsurface studies are certainly effective, however, used methods are typically expensive and arduous, while surface data is accessible with more ease. Structural geological features such as fractures and faults may cause the malfunction of the geothermal well if the drilling site is located unfavorably with respect to this kind of features. Possible negative consequences are, for example, the entrance of cold water into, or the collapse of the system or difficulties in drilling. If correlation between subsurface and surface data can be proven, the uncertainty regarding the suited placement geothermal wells may reduce through structural mapping. This work further links to increase the production of geothermal energy by providing an easily approachable guideline for well drilling in the future. This guideline will point out risks and possible failures that should be taken into consideration when drilling site of the well is selected.

In this study, we will be collecting data from surface level which will be correlated to the subsurface data. Surface data is collected by bedrock mapping on the study area, where structural geological features may be identified. The main aim of the work is to compile as structural model of the site, including fold patterns, geometry of a larger fault observed north of the drilling target, and its subsurface extension, lithological variation and their bearing of the

fracture systems. The study area is located in Ruskeasuo, Helsinki, Finland, which is the site of energy company Helen Oy's geothermal well. The drilling process started in September 2021. The main part of drilling, which was done by using 12-inch hammer, started in November 2021. The drilling stopped in the beginning of May 2022.

2. Materials and methods

The drilling site is located in Ruskeasuo, Helsinki, in the Helen Oy's site, near a linking point of busy roads. Typical rock types in the area are Svecofennian gneisses and granites. The well was drilled to the southern side of a large bedrock outcrop, which rises to a height of about 20 meters. Drilling started before the bedrock mapping was done. Planned depth of the well was 2,5 kilometers. In the beginning of the drilling, the borehole was filled with rock material that was mixed in to the water, making it appear totally brown. Cleaning the water was challenging. The well had casing which reached the depth of 648 meters. At this point there was fractures that made drilling more difficult. At the depth of 804 meters, a large fracture which continued all the way to the depth of 865 meters, was detected. This fracture could have been penetrated with drill, however, expenses per drilled meter would have increased excessively. Cementing was considered and partly done, but there was no guarantee that it would have been beneficial enough. This led to the decision that drilling stopped permanently in the depth of 865 meters.

This study uses both subsurface and surface datasets. On surface level, the main focus was on the site-scale bedrock mapping. The site-scale structural observations included field mapping which reveals typical rock types and directions of structures such as faults, fractures, foliations, and folds. All the measurements were done by using a compass. Based on all of this information, a bedrock map was created. This data will be supported by photogrammetric models that are drone-derived. Together these methods will give information about the nature of ductile and brittle structures. More comprehensive understanding of the geology of the area was achieved by including regional structural interpretation based on LiDAR and bedrock mapping from surrounding areas, and through a review of pre-existing publications and other information.

Most important data from subsurface was collected by distributed temperature sensing (DTS), temperature probing and pumping tests. DTS-measurements were made by using optical fibre method, which scatters optical rays of light in optical fibre and scattered photons return to the device that calculates temperatures to each depth. This was done in the whole depth of the borehole and spacing of measurements was 25 centimeters. DTS-measurements were calibrated by using ice-water mixture. The used cable was not reaching the bottom of the hole since there was a risk that it would get stuck to the drilling soy. Pumping test was done by inserting water to the borehole. During this, temperature changes were monitored. Also, some geophysical measuring such as high resolution optical (OBI) and acoustic (ABI) images were done although results did not give any desirable results.

All of the site-scale, regional and drill hole data will be correlated. Correlation will detect possible false assumptions and to find similarities between the results achieved from using different methods.

3. Results

The main structural feature of the study area is an E-W trending, steeply S-dipping fault, which occurs on the northern side of the main road (Fig.1 A). The fault is characterized by homogeneous grey quartz-k-feldspar-gneiss where the core of the fault is incoherent and broken, and the fault wall is quite coherent and smooth. The dip of the fault is approximately 80^{o} towards south and projected downwards (Figure 1 B). It intersects vertical geoenergy drill

hole at the same depth (804-865 meters) where large fracture was detected during drilling process.

Figure 1 A shows the bedrock map from the Ruskeasuo area. This area is composed of granite, pegmatite, gneiss, mica gneiss and quartz-k-feldspar-gneiss, which is the most typical rock type in the area. Foliation of the area (Figure 1 C) is subvertical. The ductile foliation defines open asymmetric folds (s-shaped); statistical axes (beta-axes) plunge steeply E (appr.). Fractures (Figure 1 D) follow the ductile foliation (clusters 1-3), with additional gently-dipping fractures with dominantly 50-10° dipping orientations (cluster 4). Fracturing is most intense in granitic and quartz-k-feldspar-gneiss lithologies, whereas in in gneisses and mica gneisses the intensity is the lowest. Different fracture sets can be observed in both sides of the road, and fracturing is typically quite dense.

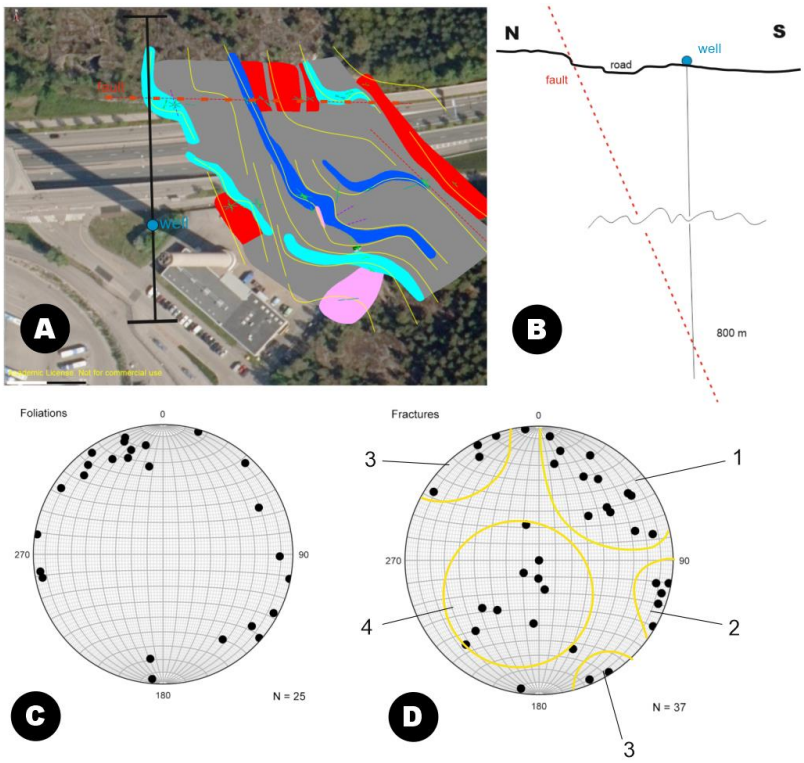

Figure 1. A) bedrock map from the study area, which includes faults (red dashed lines), ductile curves (yellow lines), fractures (green lines), folds (purple dashed lines) and main lithologies of quartz-k-feldspar-gneiss (grey), granite (red), pegmatite (pink), gneiss (light blue) and mica gneiss (dark blue). The location of cross-section (1 B) is on the left side of the map. B) A sketch of cross-section illustrating the main E-W trending, steeply S-dipping fault that penetrates through the well at about 800 meters, where the drilling ultimately stopped. At 600 meters there is also some fractures that affected negatively to the drilling process. C) Foliations on the stereogram which are all mainly steeply dipping. D) Fractures that can be divided into 4 clusters based on their dips.

4. Conclusions

The main E-W trending steeply (about 80°) S-dipping fault on the northern side of the street is going to penetrate well in the depth of 800 meters which is the same depth were the drilling had to be stopped completely. Main reason for this is that the fault has strong fracturing and rock is

not cohesive. Dense fractures can be observed in multiple rock types on the surface level, as well as the incoherent nature of the rock which can be observed in the core of the fault.

Ductile structure and changes in lithologies were possible to be observed quite effortlessly although subsurface studies such as geophysical measurements failed. Results from OBI and ABI were mostly useless since the water in the hole remained unclear. Based on DTS-measurements, temperatures were rising according to the geothermal gradient and the temperature of the water on the bottom of the well was 17,4°. This test did not point out any distinct fractures that would have inserted cold water to the system. Correlation between surface observations and subsurface geophysical methods cannot be proven in this case.

This study can still be used as an example for geological characterization in future sites where ductile structure, features and changes in lithologies are taken into a consideration. By executing bedrock mapping before starting of drilling process, it is more reliable to estimate the occurrence and variation of fracture systems in the study area.

References:

Clauser, C., Ewert, M. 2018. The renewables cost challenge: Levelized cost of geothermal electric energy compared to other sources of primary energy – Review and case study. Renewable and Sustainable Energy Reviews, volume 82, part 3, p. 3683-3693.

Quantifying crustal evolution using low-temperature thermochronology and numerical modelling

D. Whipp[1] and D. Kellett[2]

[1]Institute of Seismology, Department of Geosciences and Geography, University of Helsinki, Finland
[2]Geological Survey of Canada – Atlantic, Natural Resources Canada, Dartmouth, Canada
E-mail: david.whipp@helsinki.fi

This abstract presents: (1) a short overview of low-temperature thermochronology and some current challenges related to thermochronology data, (2) an overview of a new, open-source thermal and thermochronometer age prediction model (T_c1D), and (3) an example of how model results can be used as a guide for data interpretation.

Keywords: thermochronology, crust, exhumation, tectonics, numerical modelling

1. Introduction: What is thermochronology and what does it measure?

Thermochronology is a radiometric dating method in which the measured ages typically reflect the time elapsed since the dated mineral cooled below a system-specific temperature, known as the effective closure temperature (e.g., Reiners and Brandon, 2006). The closure temperatures vary depending on the mineral and daughter product measured, but applications of this method to study processes in the upper and middle crust have closure temperatures of ~50-400 °C (i.e., low-temperature thermochronology). Typical target minerals for thermochronology include apatite, zircon, and micas. A common challenge for interpreting low-temperature thermochronology data is linking the effective closure temperatures to corresponding depths in the crust to be able to calculate long-term rates of rock exhumation that can be related to tectonic and surface processes. Estimation of the depths of effective closure temperatures normally requires some type of model, as both heat transfer processes and crustal rock composition/thermal properties will affect the crustal thermal field.

However, a second set of challenges emerge when applying thermochronological methods to slowly cooled regions such as Fennoscandia, where ages are typically quite old (hundreds of Ma). First, in some cases the accumulation of the daughter products of decay will reach high enough levels that they may be difficult to measure. Fission tracks, the damage trails left by spontaneous fission of ^{238}U in the host mineral's crystal lattice, can accumulate in minerals such zircon in such high numbers that their density cannot be measured using the typical approach of counting etched tracks using an optical microscope. Second, the decay of parent isotopes alone can produce damage zones within crystals that can alter the retention of the daughter products used for measuring radiometric ages. This issue, which can also affect younger and more rapidly cooled minerals, is generally more challenging for older and slowly cooled rock samples as its effects influence the effective closure temperature (Figure 1). Although models exist to assist with interpreting mineral ages that have been affected by radiation damage (e.g., Flowers et al., 2009; Guenthner et al., 2013), the effects of radiation damage produce dispersion in ages from bedrock samples that can make it difficult to link these ages to meaningful geological events and estimate long-term rates of rock exhumation.

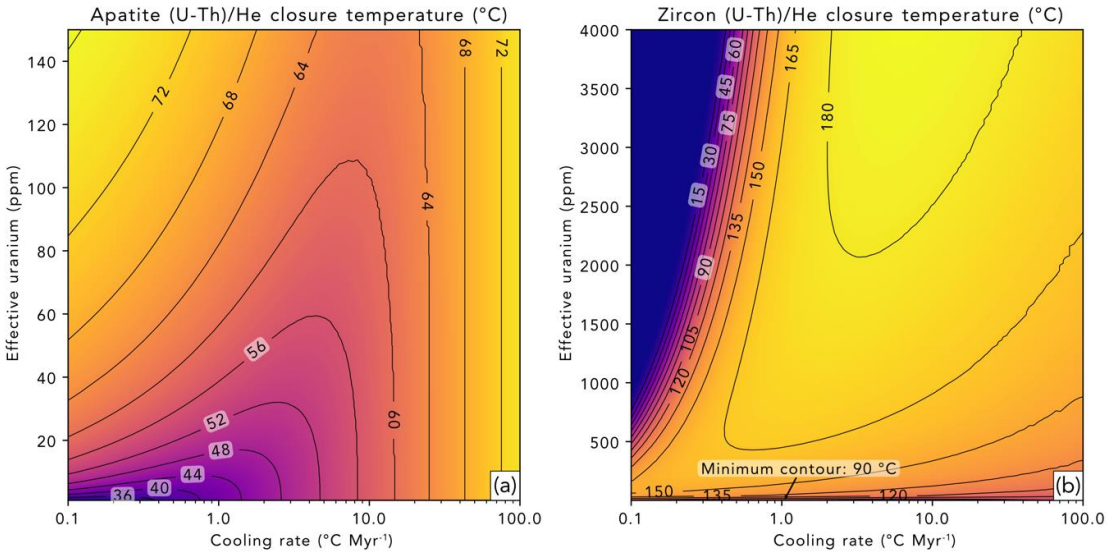

Figure 1. Predicted effective closure temperatures for the apatite and zircon (U-Th)/He thermochronometer system for a range of cooling rates and parent isotope concentrations. Modified from Whipp and Kellett et al. (2022).

2. Numerical model overview

Here we present results produced using T_c1D (Whipp, 2022), a new, open-source thermal and thermochronometer age prediction model for simulating the effects of tectonic and surface processes on thermochronometer ages. The T_c1D software is written in Python and allows for the simulation of heat transfer processes in 1D to simulate the effects of heat conduction, advection (e.g., erosion, sedimentation), and radiogenic heat production on the thermal profile. The thermal model uses the finite difference method to solve the heat transfer equation, making the software flexible to be applied to a varied of geological processes, including magmatic intrusion and lithospheric delamination, for example. Thermochronometer ages are predicted by tracking the thermal history of rock particles in the model as they travel from depth to the surface during their exhumation history. The thermal histories are input to age prediction algorithms, including algorithms that account for the effects of radiation damage in minerals (e.g., Flowers et al., 2009; Guenthner et al., 2013), making the software applicable to thermochronometer age interpretation in a wide variety of geological settings. It is also possible to run the software in batch mode to explore the effects of variations in the input model parameters on predicted ages.

3. Example result

An example of the thermal and exhumation history, and predicted ages calculated using T_c1D can be found in Figure 2. In this case, the rate of exhumation increases from 0 to 3 mm/yr from 16-0 Ma in the model. In this scenario cooling begins around 15 Ma and accelerates until 0 Ma, producing very young predicted ages (<5 Ma). This example is based on a hypothesised increase in the rates of rock exhumation in the Southern Alps of New Zealand and differences in the ages measured in various thermochronometers from that region (e.g., Lang et al., 2020).

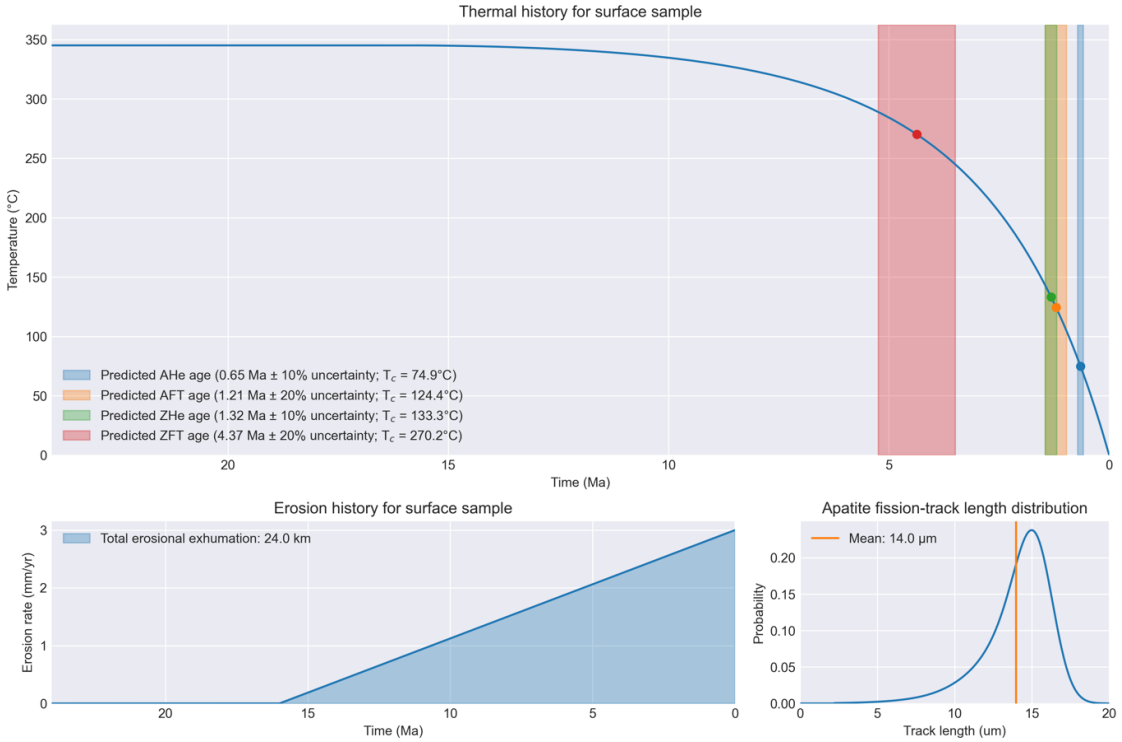

Figure 2. Thermal and exhumation histories, and predicted thermochronometer ages for a numerical simulation using T_c1D.

4. Future work

Current work applying Tc1D is exploring how thermochronometer ages vary across a set of generic tectonic scenarios, including variable rates of surface erosion, sedimentary burial followed by exhumation, burial by overthrusting of nappes, and lithospheric delamination. Software development is focussed on implementation of inverse modelling using the Neighbourhood Algorithm (Sambridge, 1999), creating a graphical user interface to the software, and porting the C and C++ age prediction algorithms to Python.

References:

Flowers, R.M., Ketcham, R.A., Shuster, D.L., Farley, K.A., 2009. Apatite (U–Th)/He thermochronometry using a radiation damage accumulation and annealing model. Geochimica et Cosmochimica acta, 73(8), pp. 2347-2365.

Guenthner, W.R., Reiners, P.W., Ketcham, R.A., Nasdala, L., Giester, G., 2013. Helium diffusion in natural zircon: Radiation damage, anisotropy, and the interpretation of zircon (U-Th)/He thermochronology. American Journal of Science, 313(3), pp.145-198.

Lang, K.A., Glotzbach, C., Ring, U., Kamp, P.J., Ehlers, T.A., 2020. Linking orogeny and orography in the Southern Alps of New Zealand: New observations from detrital fission-track thermochronology of the Waiho-1 borehole. Earth and Planetary Science Letters, 552, p.116586.

Reiners, P.W., Brandon, M.T., 2006. Using thermochronology to understand orogenic erosion. Annual Review of Earth and Planetary Sciences, 34 (1), pp. 419-466.

Sambridge, M., 1999. Geophysical inversion with a neighbourhood algorithm—I. Searching a parameter space. Geophysical journal international, 138 (2), pp.479-494.

Whipp, D.M., 2022. T_c1D: A 1D thermal and thermochronometer age prediction model. doi: http://doi.org/10.5281/zenodo.7124271.

Whipp, D.M., Kellett, D.A., Coutand, I., Ketcham, R.A., 2022. Modeling competing effects of cooling rate, grain size, and radiation damage in low-temperature thermochronometers. Geochronology, 4 (1), pp.143-152.

Tektonika: A new diamond open-access journal for the structural geology and tectonics community

D. Whipp[1] and K. Cutts[2]

[1]Institute of Seismology, Department of Geosciences and Geography, University of Helsinki, Finland
[2]Geological Survey of Finland, P.O. Box 96, 02151 Espoo, Finland
E-mail: david.whipp@helsinki.fi

Tektonika is a new community-led, diamond open-access journal for research in structural geology and tectonics. As a diamond open-access journal, there are no fees for authors or readers. Tektonika opened for submissions in May 2022, and we encourage all researchers within its scope to submit their work to this new journal and support the journal by serving as reviewers.

Keywords: structural geology, tectonics, open-access publishing, open science, equity

1. The need for open-access publishing

Open-access publishing is an increasingly important part of our research, and now even required in projects funded by the Academy of Finland. Unfortunately, while open access to research articles is of benefit to both researchers and society in general, the fees for publishing works in an open-access form can be unaffordable to some researchers (e.g., Brainard, 2021) and potentially prevent them from being able to contribute their research (e.g., Alperin, 2022). There are several tiers of open-access publication (Figure 1), and diamond open-access journals (DOAJ) aim to provide researchers with a means to publish their work with no submission fee, and for readers to access that work without a cost. In other words, free to publish and free to read.

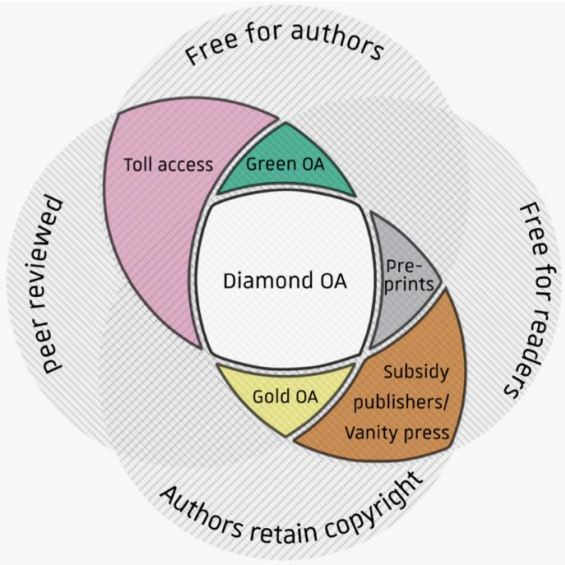

Figure 1. Elements of various open-access (OA) publishing models from Farquharson (2018).

2. Tektonika: A new DOAJ for structural geology and tectonics

Tektonika (http://tektonika.online; Figure 2) is a new DOAJ for publishing work broadly in the fields of structural geology and tectonics that began accepting submitted articles in May 2022. As of October 2022, 17 articles have been submitted, 13 are currently under review, and a first issue is expected in the near future. The journal has been developed from within the structural geology and tectonics community, mainly by a team of early career researchers, and is part of a growing number of DOAJs in the geosciences, including Volcanica, Seismica, Sedimentologika, and Geomorphica. The aim of the journal and other DOAJs in the geosciences is simple: to reduce barriers for publication and access to geoscience research, while maintaining a high level of scientific quality and author copyrights.

Figure 2. General information and web links for Tektonika.

3. How to contribute

We request the Finnish geoscience community consider contributing to this new journal in two ways: submitting your research for publication and serving as a reviewer. Articles are already being accepted for review, and details about how to prepare an article and templates for article submission can be found on the journal website. It is also possible to register on the journal website to be part of the reviewer pool, which will be essential for ensuring high standards for research in geological settings within and similar to the Baltic Shield. Any questions about how to submit research, register as a reviewer, or other aspects of Tektonika can be directed to the authors of this abstract, who are part of the editorial team.

References:

Alperin, J.P. 2022. Why I Think Ending Article-Processing Charges Will Save Open Access. *Nature,* 610 (7931), 233–233. https://doi.org/10.1038/d41586-022-03201-w.

Brainard, J. 2021. Open Access Takes Flight. *Science,* 371 (6524), 16–20. https://doi.org/10.1126/science.371.6524.16.

Farquharson, J.I., Wadsworth. F.B., 2018. Introducing Volcanica: The First Diamond Open-Access Journal for Volcanology. *Volcanica,* 1, (1): i–ix. https://doi.org/10.30909/vol.01.01.i-ix.

ISSN 0357-3060
ISBN 978-952-10-9610-5 (Paperback)
Grano Print
Turku 2022
ISBN 978-952-10-9611-2 (PDF)